INCREASING ALUMINUM LEVELS IN SOUTHWESTERN NOVA SCOTIA RIVERS

by

Sarah MacLeod

Submitted in Partial Fulfillment of the Requirements for the degree of
Master of Science

at

Dalhousie University
Halifax, Nova Scotia
December 2016

Dedication Page

To Taylor, who has been dealing with my chaos since day one. Thank you for putting up with me after many sleepless nights and breakdowns, and for always supporting me. You have been my rock and I am forever grateful. I love you.

To Shannon, for taking me under your wing and guiding me. Thank you for being so patient and kind to me during this process; I've learned so much from you!

To my wonderful family, both MacLeod/Gouthro and Rombaut, who've encouraged me throughout this process. Thank you for being my cheerleaders, my coaches and my audience. I could not have done this without you.

And to my friends, who've kept me sane. Thank you for reminding me of my blessings, distracting me, and making me take a break every once and awhile.

Table of Contents

List of Tables

List of Figures

Abstract

Declines in Atlantic salmon populations in Nova Scotia (NS) may be linked with aluminum, a known toxin to aquatic organisms; however, aluminum trends in NS have not been assessed. Here we analyze water chemistry from 1980-2014 in 65 NS rivers and lakes; 35% have significantly increasing aluminum. We propose a new acidification recovery model, incorporating the effects of organic acids on chemical recovery in regions with high dissolved organic carbon (DOC). 67% of ionic aluminum (Al_i) samples collected between April 2015 and July 2016 in two rivers were above 15 µg/L, the 5.0< pH <6.0 threshold for Atlantic salmon. Al_i predictive equations were created using water chemistry parameters, and back-cast to >20-year water chemistry data; back-cast trends show increasing Al_i in the spring/summer seasons. Following reductions in acid deposition, it appears that increased aluminum, a direct effect of acidification, poses a threat to aquatic life in regions with high DOC.

List of Abbreviations Used

AAS	Atomic Absorption Spectroscopy
Al	Aluminum
ALET	Atlantic Laboratory for Environmental Testing
Al_i	Ionic Aluminum
Al_o	Organic Aluminum
Al_t	Total Aluminum
ANC	Acid Neutralizing Capacity
BC	Base Cations
CAPMON	Canadian Air and Precipitation Monitoring Network
CEC	Cation Exchange Capacity
CSRS	Canadian Spatial Reference System
CV	Covariance
DEM	Digital Elevation Model
DOC	Dissolved Organic Carbon
EC	Environment Canada
EIFAC	European Inland Fisheries Advisory Council
GIS	Geographical Information Systems
HERC	Health and Environment Research Center
HESS	Hydrology and Earth System Sciences
HTC	High Temperature Combustion
ICAP	Inductively Coupled Argon Plasma
ICP-MS	Inductively Couples Plasma-Mass Spectrometry
ICP-OES	Inductively Coupled Plasma-Optical Emission Spectroscopy
ICPWaters	International Cooperative Programme on Assessment and Monitoring of Acidification of Rivers and Lakes
ICS	Ion-Chromatography System
JTU	Jackson Turbidity Unit
KCC	Kejimkujik Calibrated Catchments
LS	Least Squares
MAGIC	Model of Acidification of Groundwater In Catchments
MET	Measurement Tower
miRNA	Micro Ribonucleic Acids
MPB	Moose Pit Brook

MR	Mersey River
MS	Mass Spectrometry
NAD	North American Datum
NAO	North American Oscillation
NS	Nova Scotia
NSE	Nova Scotia Environment
NSERC	Natural Sciences and Engineering Research Council
NSS	Non-Sea Salt
PMB	Pine Marten Brook
RQ	Research Questions
SD	Standard Deviation
SIC	Suppressed Ion Chromatography
SMK	Seasonal Mann Kendall
SWNS	South Western Nova Scotia
TOC	Total Organic Carbon
UK	United Kingdoms
US	United States
USA	United States Environmental Protection Agency
US EPA	United States of America
UTM	Universal Transverse Mercator
UK	United Kingdom
UV	Ultra Violet

Acknowledgements

Thank you to Denis Parent, and Guy Leger for providing the Environment Canada data, and for updating our database and answer all questions regarding; and to Debbie Veinot for showing us the sample sites. Thank you to Chris McCarthy at Parks Canada for helping me sort out sampling permits.

Thank you to our funders, who made the study of aluminum in Nova Scotia possible: Shell, The Salamander Foundation, The Nova Scotia Museum Grant, Natural Sciences and Engineering Research Council (NSERC), Nova Scotia Department of Fish and Aquaculture, and The Atlantic Salmon Conservation Foundation.

Thank you to Lobke Rotteveel and Marley Geddes for their help with GIS analyses, in addition to sample collected. Kai Bogglid, Taylor Rombaut, Helen, Tim and Beth MacLeod, Sean McOuat, Shannon Sterling, Tom Clair, Jillain Haynes, and Rob Varcoe also assisted with sample collection. Thank you to Dr. Nicholas Howden for providing valuable advice on statistical analyses using the R-software.

Thank you to Norma Keeping and the lovely ladies in the Dalhousie Earth Science's main office for helping with payments, ordering, registration, deadlines, and so much more. Your help is greatly appreciated!

Chapter 1 Introduction

1.1 Problem Statement

Aluminum is a known toxin to aquatic life in its ionic form; in Nova Scotia (NS), a region with high DOC, Southern Upland Atlantic salmon populations have declined by 88-99% in four rivers (Bowlby et al., 2013), and chronic freshwater acidification and high aluminum concentrations are suggested factors in the declines of the NS Atlantic salmon populations (Dennis and Clair, 2012). Aluminum (Al) trends and acidification recovery in regions with high dissolved organic carbon (DOC, >10 mg/L) have not been assessed. Without knowledge on acidification recovery and aluminum trends in high-DOC regions, the threat of aluminum concentrations to Atlantic salmon populations in NS remains unclear and mitigation studies to promote healthy habitats for salmon may fail if toxic aluminum concentrations are not addressed.

1.2 Background

The release of pollutants to the atmosphere from industrial emissions resulted in widespread acidification of surface waters in Europe and North America by the 1970s (Likens et al., 1972, Lükewille et al., 1997). Industrial emissions contain gaseous sulfur and nitrogen oxides, which can be transported in the atmosphere and interact with water vapour to form sulfuric and nitric acid, which are deposited as acid deposition (Singh and Agrawal, 2007). Acid deposition occurs as both wet (during precipitation events) and dry (settles out from the atmosphere) deposition, and can increase soil and freshwater acidity. Across North America, the United Kingdom and Scandinavia, a paleoecological study of lakes reported pH decreases between 0.5 to 1.5 pH units since atmospheric deposition post 1850 (Charles, et al., 1990A). Alkalinity in twelve lakes in the Adirondack Mountains of New York, USA dropped between 2 and 34 ueq/L from 1920 to 1970, based on diatom assemblages (Charles et al., 1990B). Increased SO_4 acid deposition was recorded between 1981-1989 in mountainous sites in the Adirondack Mountains compared to river bottom

sites (Gilliam and Adams, 1996). In Canada, sediment cores from 51 NS lakes used to estimate trends from ~150 years before present had pH declines up to 0.4 pH units, with the largest pH declines occurring in Kejimkujik National Park, Southwestern Nova Scotia (SWNS; Ginn et al., 2007).

Climate change events can increase acidification of freshwater catchments. Increased temperatures are linked to increased decomposition of soil organic matter (Friedlingstein et al., 2006); a Model of Acidification of Groundwater In Catchments (MAGIC) model of 14 Scandinavian, UK and North American lakes showed increased organic acids in soil pore water decreased the base cation saturation in soils (Wright et al., 2006). Climate change increases storm occurrences and severity (Laudon, 2008); 25 modelled Swedish streams between the 1980s to 2000s demonstrated that excess sea salt introduced by storms alters the net charge of soils, increasing ion exchanges and flushes hydrogen ions from the soils, resulting in increased freshwater acidity (Laudon, 2008). The North American Oscillation (NAO) is also correlated to increased storm events and flow (Hurrell and Deser, 2009), and found to increase the effects of acidification by further depleting base cations and increasing the concentrations of Al during storms from anion (Cl^-) inputs (Hindar et al., 2004).

Using the MAGIC model, Cosby et al. (1985) predicted the timeline of the acidification recovery steps of freshwaters to reductions in acid deposition proposed by Galloway et al. (1983). Acidification recovery refers to the return of ecosystems to their pre-acidified chemical and biological conditions (Skjelkvale et al., 2003); for the purpose of this thesis, we refer to recovery as the return to pre-acidified chemical conditions only. A classic acidification recovery model ("classic model") theorized the response of freshwaters to reduced acid deposition (Galloway et al., 1983, Cosby et al., 1985). The classic model predicted freshwater pH would increase in response to reduced acid deposition, with nonlinear and nonstationary decreases in base cations during soil replenishment. The exponential decay trend in acid deposition predicted by the classic model during acidification recovery controls the

nonlinear and nonstationary trends of base cation replenishment in soils. Although the classic model considers anthropogenic acid inputs, the model does not consider the input of acids from DOC sources. Without the DOC components, pH recovery would occur more rapidly, as the presence of organic acids buffer pH changes (Evans et al., 2008). Hruska et al. (2009) incorporated DOC into their MAGIC model simulations, and found that DOC dampened the predicted recovery of pH, due to increases in organic acids.

Anthropogenic and organic acids increase the acidity of NS freshwaters (Kerekes et al., 1986); due to high concentrations of DOC in NS freshwaters (average of 49 uEq/L of organic anions in 234 NS lakes compared to <8 mg/L DOC measured across 22 European streams from 2003-2008; Gorham et al., 1986, Monteith et al., 2014), acidification recovery may diverge from the classic model. High DOC concentrations in NS may be buffer pH changes, resulting in increased aluminum Al concentrations in rivers of South Western NS (SWNS); a response not consistent with the classic model.

Possible divergence of NS from the classic model poses a threat to Atlantic salmon populations, as ionic Al (Al_i – positively charged species of Al), a toxin to aquatic organisms, increases with decreased freshwater pH (Poleo, 1995); if high concentrations of DOC maintain low pH levels, Al can be increasingly mobilized in soils and speciate into Al_i, increasing Al_i concentrations. Al_i levels surpassed 15 µg/L, a toxic threshold for Atlantic salmon suggested by Howells et al. (1990), in a survey of Al_i in the fall of 2006 in NS (Dennis and Clair, 2012). Current levels of Al_i are unknown in NS; however, if their concentrations are similar to those in 2006, Al_i in NS may be one of the factors causing the decline of NS Atlantic salmon populations.

1.3 Knowledge Gaps

High organic acidity in NS freshwaters may be buffering pH increases, and potentially increasing Al and toxic Al_i concentrations; however, the role of organic

acids on chemical freshwater acidification recovery in high-DOC regions is unknown. No surveys of Al and Al_i in NS have been done since 2006 (Dennis and Clair, 2012), and Al trends in NS, during peak acid deposition and following acid deposition reductions, have not been quantified. The accuracy of Al_i equations proposed in the literature as alternatives to Al_i field measurements has not been tested. Without knowledge of the role of DOC on acidification recovery in high-DOC regions, and no information on the current status and trends of Al in NS freshwaters, it is unclear whether toxic levels of Al and Al_i in NS rivers could be factors in the declines of Atlantic salmon populations.

1.4 Objectives

To determine if NS freshwaters follow the classic recovery model, with increases in pH and decreases in Al following acid deposition reductions, and if Al_i concentrations in NS are currently above the toxic threshold for salmon, this thesis answers the following research questions (RQs):

RQ 1 **Do water chemistry trends in SWNS match the recovery stages of the classic model? Addressed in Chapter 2.**

RQ 2 **Do changes in flow, DOC and temperature correlate to changes in Al_t concentration in NS rivers? Addressed in Chapter 2.**

RQ 3 **Are Al_i concentrations above toxic levels (>15 µg/L) in SWNS from 2015-2016? Addressed in Chapter 3.**

RQ 4 **Are DOC, pH and flow variables required for an Al_i prediction equation with 95% significance? Addressed in Chapter 3.**

RQ 5 **Are Al_i concentrations increasing in SWNS from 1980-2014? Addressed in Chapter 3.**

Chapter 2 Increasing Aluminum Levels in Streams Recovering From Acidification

2.1 Preamble

Shannon Sterling, Sarah MacLeod, Lobke Rotteveel, Tom Clair

This chapter comprises a manuscript to be submitted to a journal in winter 2017. I am co-author on the paper; I conducted all statistical data analyses, provided the idea for a monthly analysis of concentrations via boxplot, created all figures except the spatial GIS map of chemistry trends in NS, wrote the introduction and methods, with shared writing credits for the results and discussion. My writing focus was on divergence of SWNS lake and river chemistry trends from the classic model, the role of DOC on recovering watersheds, and suggested revisions for the model. Dr. Sterling provided the idea for studying aluminum trends in Nova Scotia (NS), the study design, the idea to analyze chemical cumulative mass exports, the idea for comparison of recovery of NS to the classic recovery model and shares partial writing credits for the results and discussion. Dr. Sterling's writing focus was on the role of dissolved organic carbon (DOC) and climate change on SWNS rivers' chemistries. Lobke Rotteveel provided GIS map of SWNS river chemistry trends, and Tom Clair provided the idea for combining Al trends with other cation concentration trends in one graph, in addition to providing background on the sampling sites and knowledge on Environment Canada sampling and laboratory methods.

2.2. Problem Statement

Increased aluminum (Al) is known to be caused by increased freshwater acidity, and can be toxic to aquatic organisms. In Europe and North America, Al declines have coincided with acid deposition reductions, reducing the possible stresses of acidification on fish, vegetation and other organisms; however, regions with high DOC may be an exception to acidification recovery and reductions in Al, due to

maintained freshwater acidity, and may be negatively affecting the diversity of life in these regions.

Regions with high DOC concentrations may not be recovering from acidification in the same ways as low DOC regions. The presence of DOC adds a source of organic acidity, which has been known to buffer pH changes in freshwaters (Evans et al., 2008); chronic acidification of freshwaters results in increased aluminum (Al), which can be toxic for certain species of aquatic life (Nilsen et al., 2010). The role of DOC has not been considered in freshwater acidification recovery models with low base cation inputs from bedrock; therefore, the recovery process and Al trends for freshwaters with high DOC concentrations and low-bedrock weathering rates are unknown following decreased acid deposition.

In NS, declines in the Southern Upland Atlantic salmon populations by 88-99% in four NS rivers are linked to chronic acidification, as estimates of juvenile salmon densities from 2008/2009 electro-fishing surveys had a 95% reduction in rivers with pH between 4.7-5.0 compared to the same rivers monitored in 1936-1953 (Bowlby et al., 2013, Watt, 1986); declines of the Atlantic salmon populations may be indirectly affected by acidification due to increases in Al. Increased acidification in soils mobilizes and releases Al from soils into rivers; concentrations of Al in SWNS doubled between 1945 and 1981, concurrent with acid deposition (Watt et al., 1983). The current trends of Al in NS freshwaters are unknown, and the potential threat of Al to salmon populations is unclear.

The purpose of this study is to determine if freshwater regions with high-DOC follow the recovery stages summarized in a 'classic' acidification model following acid deposition reductions, by comparing trends of >20-year water chemistry data in freshwaters in NS. I analyze surface water chemistry data from NS, a region with chronically acidified watersheds and high DOC, to determine if acid deposition is decreasing in NS, if high DOC concentrations are correlated to decreased pH values, and if Al concentrations are increasing.

2.3. Introduction

2.3.1. Mobilization of Aluminum

Soil acidification across North America and Europe has resulted in increased aluminum in freshwaters (refer to Chapter 1). During acid deposition on soils, hydrogen ions exchange with cations (Ca, Na, Mg, K, Fe, and Al) from cation exchange sites in soils, thereby buffering rivers from the effects of acid deposition. The number of sites where cations can be exchanged is called the Cation Exchange Capacity (CEC; Seybold et al., 2005). Cations usually exchange in the order of Ca<Na<Mg<K<Fe<Al from soils (Schlesinger and Bernhardt, 2013), where heavier cations tend to exchange when the lighter, base cations (Ca, Na, Mg, K) in the soils are depleted (Watt et al., 2000). Further, at low pH (pH<5), fulvic acid dominates DOC fractions (You et al., 1999), which contributes to soil acidity, further depleting the soil CEC and can result in Al mobilization and leaching into streams due to lighter cation depletion (Drever and Vance, 1994, Bache, 1985). A paleolimnological study in the Adirondack Mountains found that naturally acidified freshwaters can mobilize aluminum, as the chemistry of diatoms and chrysophytes in lake sediments of the Adirondack Mountains had monomeric Al concentrations up to 7 µmol/L since 1900 (Kingston et al., 1992).

2.3.2. Global Acidification Recovery

Global initiatives to reduce industrial emissions have been implemented across North America, Europe and Asia. Upon identification of the environmental effects of acidification due to industrial emissions, governments introduced policies to mitigate the acidification problems: the United States (US) adopted the Clean Air Act Amendments in 1990 to reduce sulfur and nitrogen emissions (Likens et al., 2001), Canada and the US signed an air quality agreement in 1991 to reduce industrial emissions and transboundary pollutant transport, and between 1979 and 1990, over 30 governments, including the US, Canada and the European Union, signed the Economic Commission for Europe Convention of Long-range Transboundary Air Pollution (Menz and Seip, 2004).

Following the implementation of the Economic Commission for Europe Convention of Long-range Transboundary Air Pollution and the Clean Air Act Amendments, recovery of watersheds from acidification has been recorded since 1980 across Europe and North America. Reductions in sulfate and nitrate concentrations in freshwaters, along with increases in pH, have been documented in North Eastern United States (Warby et al., 2005). Skjelkvale et al. (2005) recorded a decrease in hydrogen ions within lakes and rivers between 1990-2001 by -0.19 meq/L/year in the Adirondacks of New York, -0.08 meq/L/year in the Appalachian Plateau, and -0.05 meq/L/year for Vermont and Quebec. Increases in pH have also been documented in a Norway lake from 1990-2008 (Hesthagen et al., 2011), across the United Kingdom by up to 0.043 pH/year from 1988-2008 (Monteith et al., 2014), and from 1980-1999 in the Czech Republic by 0.011 meq/L/year and 0.013 meq/L/year in Slovakia (Evans et al., 2001).

Recovery in freshwaters from acidification has been linked to increases in DOC in Europe and North America. In 2007, Monteith et al. found that the reductions in sulfate deposition caused a concurrent increase in DOC steam concentrations for lakes and streams in North America and northern Europe from 1990-2004; increases in DOC are believed to be associated with the return of waters to natural concentrations, after sulfate anthropogenic acidity sources suppressed natural organic acidity from DOC (Krug and Frink, 1983, Davis et al., 1985, Driscoll et al., 1989). Monteith (2007) proposed that ionic strength and declines in SO_4 deposition concentrations were the primary mechanisms controlling DOC concentration increases. Pre-acidification concentrations of DOC influence the status of freshwater acidification, as only 24% of lakes with higher natural DOC in Sweden were considered acidified compared to the 47% if the same lakes had lower initial DOC concentrations (Erlandsson et al., 2011).

Concurrent with acidity declines since 1990 in Europe and North America, total aluminum (Al_t) concentrations are decreasing. Using the long-term monitoring

datasets from International Cooperative Programme on Assessment and Monitoring of Acidification of Rivers and Lakes (ICPWaters), Evans et al. (2001) assessed the trends of Al_t across Europe between 1980-1999: Italy experienced a drop of 1.4 mg/L/year, the Czech Republic saw a -20.5 mg/L/year trend, and Germany had a decrease of 4.2 mg/L/year. Between 1988-2000, Al concentrations in rivers of Slovakia and the UK increased by +0.1 mg/L/year due to continued acidic input into the rivers, and may indicate a possible shift in Al species away from the toxic inorganic forms (Evans and Monteith, 2001). For North America, Ohio's Raccoon Creek was monitored from 1975-2013 and showed a -0.247 mg/L/year (-247 mg/L/year) trend of Al_t (Underwood et al., 2014).

2.3.3. Classic Acidification Recovery Model

In 1983, Galloway et al. proposed an acidification and recovery model for watersheds exposed to acid deposition (hereby known as the 'classic recovery model' or 'classic model'); Cosby et al. (1985) used the Model of Acidification of Groundwater In Catchments (MAGIC) computer model to estimate the timeline of each recovery stage in freshwaters. The model has seven stages: stage one consists of the catchment conditions prior to any acid deposition. Stage two defines the beginning of acid deposition, where soils' acidity increases and cations increasingly leach into nearby waters during high flow; the length of time and amount of cations leached depends on the catchment's soil CEC. Low base cation saturation of soils' CEC and decreases in cations in freshwaters occur in during stage three; an acidified, cation-depleted steady-state is reached by stage four. Acid deposition decreases in stage five, resulting in a slow recovery of soils in stage six, where pH increases and cation concentrations within rivers decrease. Stage six initially occurs rapidly, becoming increasingly slower over time; stage six recovery of cations is nonlinear and nonstationary. Stage seven defines the return to pre-acidification conditions. The classic recovery model is referenced for recovering catchments in Swedish lakes (Futter et al., 2014). As the classic model does not account for acid inputs from organic matter, and since increases of DOC have been linked to declines in sulfate deposition (Monteith et al., 2007), the model may not apply to regions with high

DOC concentrations. Hruska et al. (2009) included increased DOC trends when predicting acidification recovery using the MAGIC model; they ran two different models and found that the pH recovery was dampened due to organic acidity inputs between 1970 and 2030. Hruska et al. (2009) also recorded decreases in Al concentrations from 1992-2008 in two Czech Republic streams.

2.3.4. Freshwater Chemistry Trends in SWNS

No pH recovery from acidification has been observed in NS following decreased acid deposition (Clair et al., 2011). Lake data analyzed for 68 lakes in NS show significant decreases in sulfate concentrations, in addition to decreases in wet atmospheric deposition sulfate concentrations between 1983 and 2007 (Clair et al., 2011), with decreased sulfate acid deposition in NS from 1983-1997 (Clair et al., 2002); however, no significant regional change in pH and acid neutralizing capacity (ANC) was observed in 18 Atlantic Canada/Maine freshwater sites from 1990-2001 (Skjelkvale et al., 2005). Between 1989 and 1997, 53 of 64 NS lakes had no significant H^+ trend, and nine sites had significant increases in H^+ (Clair et al., 2002). No change in pH for two rivers in NS from 1983 to 1998 was observed during baseflow (Laudon et al., 2002).

Ca concentrations are decreasing in SWNS following acid deposition reductions, indicating depletion of SWNS' soil base cations. Decreasing Ca concentrations in 68 Nova Scotian lakes from 1983-2007 was recorded (Clair et al., 2011). Decreases in base cations in Maine/Atlantic Canada from 1980-1995 are attributed to greater declines in base cation than sulfate concentrations (Stoddard et al., 1999). No base cation recovery is expected for the next 100 years, based on a MAGIC model of 35 Nova Scotian rivers (Clair et al., 2004).

2.3.5. Knowledge Gaps

The role of organic acidity in regions with high-DOC on acidification recovery is unknown. Recovery trends predicted by the classic acidification model may not apply for regions with high-DOC, as Hruska et al. (2009) have found that organic acidity buffers pH recovery; trends of Al in high-DOC regions recovering from

acidification are not quantified. In SWNS, the trend of acid deposition reductions have not been assessed since 2007, and the acidification recovery stages for SWNS rivers are unknown; the linearity and stationarity of long-term trends of cations are unknown. It is unclear if SWNS rivers follow the classic model for chemical acidification recovery.

2.4. Objectives and Research Questions

To examine whether the classic acidification recovery model applies to highly acidified rivers that have naturally high DOC levels, this study will investigate the following research questions (RQs) and hypotheses (Hs):

RQ 1 Do water chemistry trends in SWNS match the recovery stages of the classic model?

H1.1. Wet and dry acid deposition in SWNS decreased from 1980-2014, consistent with the proposed decreasing depositional trend in stage five of the classic model.

H1.2. Ca, Mg, and Al_t trends in Mersey River (MR) and Moose Pit Brook (MPB) from 1980-2014 decreased, consistent with the proposed decrease in cations in stage six of the classic model.

H1.3. Cation concentration trends in MR and MPB from 1980-2014 are nonlinear and nonstationary, consistent with the nonlinear and nonstationary trends of cations predicted in stage five of the classic model.

RQ 2 Do monthly changes in flow, DOC and temperature drive changes in monthly Al_t concentrations in NS rivers?

H2.1. Al_t seasonality coincides with peaks in flow during the winter and spring seasons in MR and MPB from 1980-2014.

H2.2. DOC is positively correlated to Al_t concentrations in MR and MPB from 1980-2014.

H2.3. Increased air temperatures are correlated to increasing Al_t concentrations in MR and MPB, from 1980-2014.

To answer the above RQs, this study investigates trends of long-term water chemistry data obtained by Environment Canada (EC) for rivers and lakes across NS, in addition to atmospheric deposition and climate data. Trends for water chemistry and climatic data are analyzed for statistically significant slopes and seasonality.

2.5. Methods

2.5.1. Experimental Design

Water chemistry and acid deposition trends from Southwestern NS (SWNS) are compared to each stage of the classic recovery model to demonstrate if the classic model applies to high-DOC regions. Wet and dry acid deposition trends are compared to the expected declines in sulfate acid deposition concentrations in stage five of the classic model (H1.1). Trends of Ca, Al_t, H^+ and TOC are quantified for lakes and rivers in NS. Ca, Mg, and Al_t in SWNS rivers are assessed for slope direction, stationarity and linearity to compare to the nonlinear and nonstationary decreases expected for stage five; values of chemical ('x') concentrations exceeded 95% of the time (x_{95}) and 5% of the time (x_{05}) are compared between the 1980s and 2000s to determine if the majority (x_{95}) and outlier (x_{05}) values have decreased following decreased acid deposition (H1.2 and H1.3). Al_t seasonality and time-series are compared to flow, DOC and air temperature to determine if correlations indicate possible drivers of Al_t (H2.1, H2.2, and H2.3).

2.5.2. Study Sites

2.5.2.1. Location

The study area is South West Nova Scotia, which is underlain by base cation-poor slates and granites. Long-term water chemistry data of lakes and rivers in NS from 1980-2014 were obtained from EC. Water chemistry slopes and seasonal trends were analyzed for two rivers located in SWNS: MR and MPB.

MR and MPB sites are two of the Kejimkujik Calibrated Catchments (KCCs); MR and MPB have been monitored since the 1980s. These two KCCs are located in SWNS (Figure 2.1), with MR running through the Kejimkujik National Park. Moose Pit Brook is located 15 km to the north east of the MR sampling site. Mersey River has an area of 297 km², while MPB is 17 km² (Clair et al, 2008).

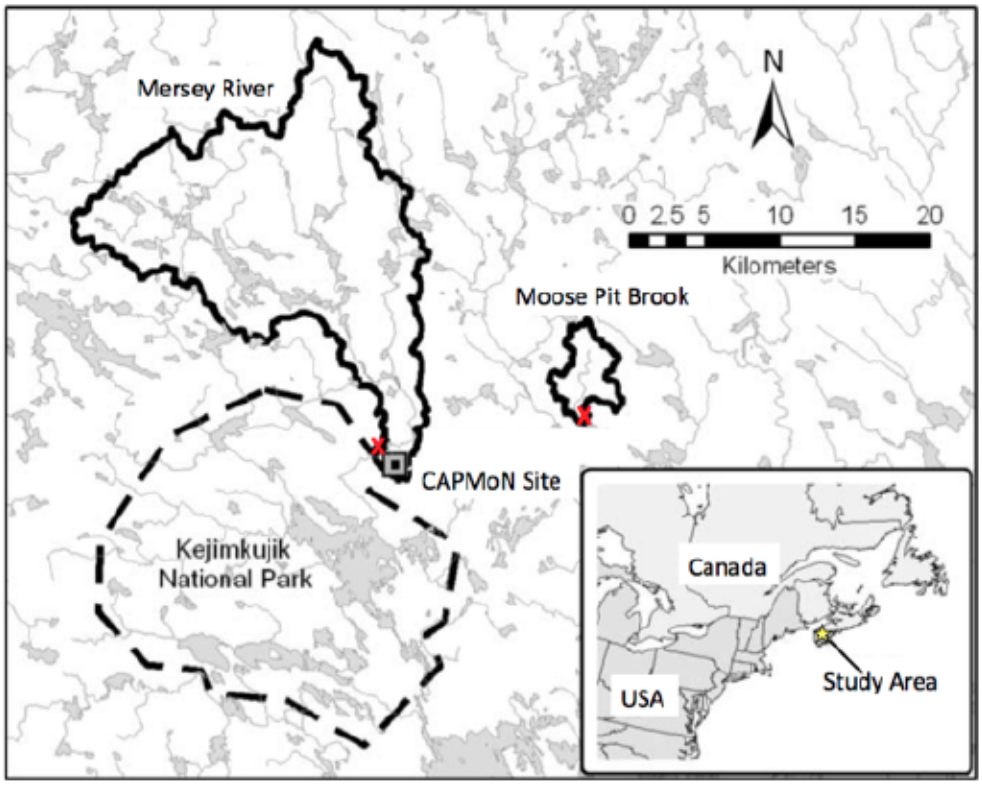

Figure 2.1: The Mersey River and Moose Pit Brook study areas, with sampling sites denoted with a red 'X', with the inset indicating the location of our study sites (yellow star) on the Eastern Coast of North America. Modified from Clair et al. (2008).

2.5.2.2. Geology

The two KCCs are underlain by Halifax slates with quartzite materials and Goldenville greywacke and by Devonian granite (Rencz et al., 2003, Bobba and Lam, 1989). Previous glaciation in the region has left moraines and tills, primarily consisting of granite, gneiss and quartz materials (Freedman and Clair, 1987). Due to the slow weathering of the tills and bedrocks, the sandy-loam/loamy-sand soils in the region are thin, and, due to their low acid neutralizing capacities from chronic acidification (Whitfield et al., 2006), have a low Cation Exchange Capacities (CEC) (Yanni et al., 2000, Clair et al., 2008).

2.5.2.3. *Vegetation and Land Use*

A mixture of soft and hardwoods dominate the KCCs. The forests are dominated by white pine (*Pinus strobus*), eastern hemlock (*Tsuga Canadensis*), white birch (Betula papyrifera) and red maple (*Acer rubrum;* Rencz et al., 2003). The KCCs also include bogs and swamps, with up to 6.5% of the Mersey, and 0.15% of Moose Pit Brook covered in wetlands (Department of Natural Resources, 2005). DOC concentrations in the region have exceeded 10 mg/L and contribute to the waters' tea color (Ginn et al., 2007). Both MR and MPB have had 15% of forests' clear-cut between 1992 and 2005 (Table 2.4, Department of Natural Resources' Forest Inventory, 2005), which may have increased Al mobilization due to decreased pH, as reduced nitrate uptake in harvested regions results in the increase of nitric acids in soils (McHale et al., 2007); however, detailed information on clear-cutting history in the region is not available (Department of Natural Resources' Forest Inventory, 2005).

2.5.2.4. *Environment Canada Monitoring*

Water chemistry data from 58 lakes and seven rivers in NS, which contained major ions, base cations, pH, and organic carbon data from 1980-2014 were obtained from Environment Canada. All study lakes are monitored by the Nova Scotia Environment (NSE) and Environment Canada (EC), with a sampling frequency of two times per year at spring and fall turn-over up to and including 2011, after which the lake sampling program was reduced to once per year at either spring or fall turnover. The study rivers include three rivers monitored as part of the Kejimkujik Calibrated Catchments: the 291 km^2 MR, the 17 km^2 MPB, and the 1.3 km^2 Pine Marten Brook (PMB) (Figure 2.1); for these three, the sampling schedule for stream chemistry measurements is weekly or better up to 2012 after which the sampling frequency was reduced to biweekly. Water chemistry monitoring was started in 1980 for MR, 1983 for MPB, and in 1991 for PMB. Discharge is monitored continuously under the Canadian National hydrometric monitoring program at Mersey River below Mill Falls (station 01ED0007, 1968-2014), and Moose Pit Brook at Tupper Lake (station 01EE0005, 1981-2014).

2.5.3. Water Chemistry Analysis

2.5.3.1. Lake and River Water Grab Samples

Lake and stream water grab samples were collected by EC. Using a metal clasper, a plastic bottle was immersed into the water and rinsed three times. The bottle was then filled with sample water and the lid is placed underwater, to ensure no air bubbles are within the sample. The samples collected were stored in a cooler, surrounded by ice packs, and transported to the Environment Canada Atlantic Laboratory for Environmental Testing (ALET) in Moncton, New Brunswick.

All lake and river samples were analyzed in the ALET, with methodology changes occurring for each chemical throughout the sampling period. For total (extractable) Al concentrations, flame Atomic Absorption Spectroscopy (AAS) was used in 1980, then the analysis switched to flameless AAS from 1980-1996 and to Inductively Coupled Argon Plasma (ICAP) from 1996-1999. Between 1999 and 2008, Al concentrations were measured using in-bottle digestion, followed by ICAP in 2008, Inductively Coupled Plasma Optical Emission Spectrometry (ICP-OES) from 2008-2011 then finally back to in-bottle digestion with ICP-OES from 2011-present. Total iron was measured using directed aspiration AAS from 1980-1996, ICAP from 1996-1997, AAS with solvent extraction from 1997-1999, ICP Mass Spectrometry (MS) from 1999-2008, ICAP from 2008-2011 and in-bottle digestion with ICP-OES from 2011-present. Dissolved Cl concentrations were measured using a chloride specific electron from 1980-1986, and ion chromatography from 1986-present. Dissolved Ca concentrations were measured using AAS in 1980, automated AAS from 1980-2001, Suppressed Ion Chromatography (SIC) from 2001-2007, following 2007, Ca was measured as total Ca (unfiltered), using ICAP from 2007-2011 and in-bottle digestion with ICP-OES from 2011-present. Dissolved Mg concentrations were measured using direct aspiration AAS from 1974-1983, automated AAS from 1983-2001, and SIC from 2001-2007; following 2007, Mg was measured as total Mg using ICAP from 2007-2011 and in-bottle digestion with ICP-OES from 2011-present. The Total Organic Carbon (TOC) parameter incorporates lab fluctuations between

filtering and not filtering samples. From 1980-1982, TOC was measured using infrared analysis, then the lab filtered samples to analyze DOC from 1982-1993 using colourimetry, and Ultra Violet (UV) digestion with colourmetry from 1993-1995; sample filtration was stopped and TOC was measured using high temperature combustion (HTC) from 1995-present. As particulate matter was <5% of TOC in MR and MPB (Clair et al., 2008), little difference is assumed between the dissolved and total concentrations for Mg, Ca, and DOC/TOC, and therefore the parameters are known as 'total' to include all filtration changes. For the results, we discuss TOC instead of DOC, as to remain consistent with EC analytical techniques. ANC was measured as the difference between base cations (BC – Ca, Mg, N and K) and anions (A – SO_4, NO_3 and Cl) from 1980-present; turbidity was measured in Jackson Turbidity Units (JTU) between 1972-2013 in MR, and 1983-2013 in MPB, with a sampling gap from 1992 to 2008 at both sites. pH values were analyzed via electrometric method in the EC lab, with H^+ concentrations calculated as the 10^{-pH}.

2.5.3.2. River Flow Representation

Flow was calculated using a calibrated comparison between known stage and flow values; the flow calibration equation is assessed yearly. As flow was measured more frequently than water samples, histograms were created to ensure the water samples represented the total distribution of discharges within the rivers.

2.5.3.3. Atmospheric Deposition

The Canadian Air and Precipitation Monitoring Network (CAPMoN) monitors atmospheric deposition chemistry at Kejimkujik National Park; wet deposition is collected through precipitation, and dry deposition collected via atmospheric particles. Precipitation is captured in buckets and collected daily for analyses, while atmospheric particles are captured daily in a 47 mm filter based using a 17 L min^{-1} flow rate. Cations and anions are measured using ion chromatography, with non sea-salt sulfate concentrations derived by EC as the difference between measured sulfate and the sea-salt sulfate contributions. Total sulfate, non sea-salt sulfate, nitrate and chloride values are calculated as the sum of wet and dry deposition

amounts. Kejimkujik CAPMoN station is 0.6 km away from MR sampling site and 13.6 km away from MPB sampling site.

2.5.4. Mass Export Estimation

Using MR and MPB water chemistry data from Environment Canada, flow values and concentrations of Ca, Na, Mg, K, Fe, Al_t, TOC, H^+, and SO_4 are interpolated and converted to obtain monthly and yearly masses. As the flow and chemical data sets do not have the same time intervals, the datasets are combined as to have daily time series for both, with "Not Available" placed where there are no data. The combined dataset is then cropped to start when there is simultaneous flow and chemistry data. Each chemical concentration is then converted into a mass by multiplying by the corresponding flow for that day and converting from g/s to g/day. Flow is converted from m^3/s to L/day by multiplying by 86,400,000 sL/m^3day. The mass for water chemicals, and flow, are then linearly interpolated, to ensure that each day has an estimated value. Cumulative mass exports are calculated as the sum of the previous value and the present value.

2.5.5. Statistical Analysis

2.5.5.1. 95% and 5% Exceedance Threshold Calculation

To determine if the majority of water chemistry values (95%) and extreme values (5%) changed over time, the Al, Ca, TOC, and flow (Q) threshold values that exceeded 95% and 5% of the time, respectively, were calculated. Thresholds exceeded 95% and 5% of the time for each water chemical ('x') are referred to as x_{95} and x_{05}, respectively. To calculate the 95% and 5% threshold values per water chemical, the water chemistry data are organized in descending order (for 95% threshold) and ascending order (for 5% threshold). The values are ranked, and then their probabilities calculated; the value with the probability closest to 95 is then selected as the 95% or 5% threshold value.

2.5.5.2. R-Software Commands

To plot data and calculate statistical significances, daily concentrations and mass export time-series were analyzed using the R statistical software (version 3.1.0).

The time-series were converted from uneven to daily time intervals, interpolated to remove missing values and decomposed using the 'decompose' trend in R to obtain the general trends. The decompose command separates the trend from observations using a symmetrical, equal-weight moving average; the trend is then subtracted from the observations and seasonality is obtained using averages for each time unit (R command: 'decompose'). The cumulative mass exports were calculated using the command 'cumusum', and boxplots with error lines created with the 'boxplot' command. R-scripts used for data analyses are available in Appendix A.1.

2.5.5.3. Regression Statistics

All slope trends are tested for a significance of 95% confidence ($p < 0.05$). Regressions and regression significances in the data are quantified using the Least Squares Test (LS). The significance of the regression slopes is determined by their p-value, where $p > 0.05$ is not significantly different from zero. Regressions and their significances for lakes and rivers are calculated using LS and plotted using ArcGIS. Mean Al_t concentrations are calculated per month of the year, then each month plotted yearly values, with a LS regressions, to determine the monthly 1980-2014 trends. Overall increasing or decreasing trends are also tested using the non-parametric Seasonal Mann Kendall (SMK) test, with significant trends indicated by p-values <0.05. Welch Two Sample T-test is used to compare means of different groups, as done with turbidity and chemical trends before and after 2003 (due to a large apparent slope change in water chemistry data at 2003), with $p>0.05$ indicating no difference between the means.

2.5.5.4. Arc GIS Maps

To determine spatial water chemistry trends in SWNS, LS water chemistry trends for lakes and rivers in NS since the 1980s are plotted using ArcGIS v.10.1. Water chemistry trend slopes from 1980-2014, for all rivers and lakes with data from the 1980s, are exported from the R software with their respective latitudes and longitudes. The resulting excel sheet was input into ArcGIS, with the coordinates reprojected using the Transverse Mercator and applying the North American Datum

(NAD) 1983 Canadian Spatial Reference System (CSRS) UTM (Universal Transverse Mercator) Zone 20N datum. A 1:10,000 NS digital elevation model (DEM) raster with 20-m grid resolution, from the Nova Scotia Department of Natural Resources, is used, in conjunction with the ArcHydro GIS addition to ArcGIS, to delineate watersheds corresponding to each river and lake sampling point. Points, and the watersheds represented by the points, are coloured based on trend direction if trends were significant; non-significant trends are coloured grey.

2.5.6. Quality Assurance

2.5.6.1. Outliers Tests

The Grubb's Test (R command: 'grubbs.test') was applied to all time series to find and remove extreme outliers that may skew water chemistry trends. A one-sided Grubb's Test compares the maximum value to the mean and largest standard deviation, to determine if the maximum value in the time series is an outlier. If the Grubb's Test finds an outlier, the value is removed. For MPB, no outliers were removed, whereas MR has the maximum value for Al and Fe removed and the Medway River had the max Al value removed.

2.5.6.2. Duplicate Data

As the EC river water chemistry data contained several concentrations for the same day, duplicate dates were removed. Using the 'duplicate' command in R, only the first row of repeated days was kept, with the remaining duplicated removed from the time-series to avoid skewing statistical tests.

2.6. Results and Discussion

2.6.1. Acid Deposition Trends in SWNS

Acid deposition CAPMoN data in Kejimkujik show that Atlantic Canada has received a declining rate of wet and dry acid deposition from atmospheric emission sources (Figure 2.2), consistent with stage five of the classic model, where, following emission reductions, there is a reduction in sulfate concentrations for acid deposition. Total (addition of wet and dry deposition concentrations) sea-salt

corrected (Non-Sea Salt – NSS) sulfate depositions halved from 0.11 gm^{-2} in 1990, to 0.05 gm^{-2} by 2014. The overall total NSS sulfate trend shows a decrease in deposition since implementation of controls in the US and Canada, with a significant decrease between 1980-2014 of $7.9*10^{-6}$ $gm^{-2}mo^{-1}$. Total nitrate deposition is significantly declining, from 0.15 $g*m^{-2}$ in the early 1990's, to less than 0.010 $g*m^{-2}$ by 2014. The $7.9*10^{-6}$ $gm^{-2}mo^{-1}$ slope of NSS sulfate provides a slope value which confirms the general decreasing acid deposition SO_4 direction observed by Clair et al. (2011) from 1983-2007, and shows a reduction in sulfate deposition compared to the $3.1*10^{-2}$ $gm^{-2}mo^{-1}$ slope (calculated as the difference of 324 Eq SO_4 in 1983 and 214 Eq measured in 1997, per ha, per year, per month) of sulfate monitored at Kejimkujik by Clair et al. (2002) from 1983-1997. Acid deposition declines from 1908-2014 in SWNS agree with the decreases in SO_4 deposition concentrations predicted in stage five of the classic recovery model.

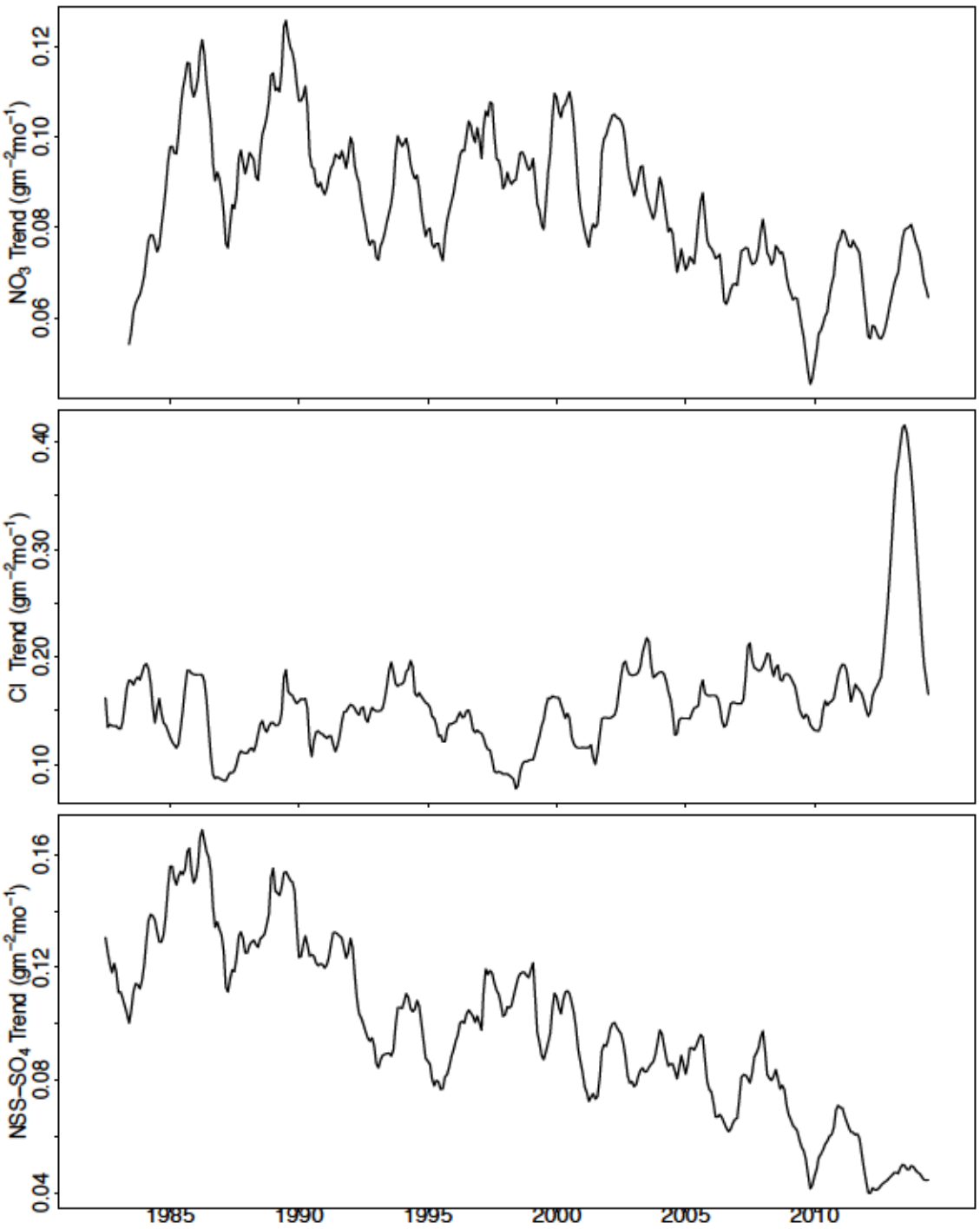

Figure 2.2: Decomposed trends for total wet and dry deposition of NO_3, Cl and NSS-SO_4 in Kejimkujik National Park, from 1980-2014.

2.6.2. Cation Concentrations Trends in SWNS

Long-term stream and lake chemistry data show that, in contrast to Europe and the U.S., the rivers and lakes of Nova Scotia do not follow the standard model of acidification recovery (Figure 2.3). After declining rates of wet and dry acid

deposition from 1985-2014 (Figure 2.2), pH of the surface waters is increasing (Figure 2.3C), as expected. However, instead of decreasing, Al levels in NS are significantly increasing in 35.4% of the lake and river stations, which represent 70% of the monitored catchment area (Figure 2.3A); the 29 remaining sites with increasing, but trend significances <95%, may be due to smaller time-series, as many sampling sites were added onto the EC sampling list in the 1990s (Appendix B). Only 1.54% of the area (1 station) has significantly decreasing Al concentrations (Table 2.1). TOC levels are high (mean value for all stations in 2010-2014 is 7.8 mg/L (SD 4.16)) and are increasing in 89.2% of stations (Figure 2.3D). Further, instead of increasing following reductions in sulfate deposition, the already low levels of calcium levels (mean value for all stations in 2010-2014 is 0.75 mg/L (SD 0.40)) continue to decrease in many parts of the province (Figure 2.3B). It appears that the sulfate deposition rates still exceed critical loads because base cations continue to decrease, while heavier metals (Fe and Al) are increasing. NS surface waters appear to diverge from the stage six classic recovery model; although base cations are decreasing, as predicted by the model, the model does not predict the increases in Al_t observed in NS.

Table 2.1: Water chemistry trend statistics for stations monitored across NS (lakes and rivers). Inc=Increasing, Dec.=Decreasing, Sig=LS statistically significant at 95%, #N= total samples.

	Al_t	Ca	Fe	TOC	pH	H^+
#N	65	65	65	65	65	65
# Inc.	52	19	54	58	55	14
# Dec.	13	46	11	7	10	51
% Inc.	80.0	29.2	83.1	89.2	84.6	21.5
% Dec.	20.0	70.8	16.9	10.8	15.4	78.5
#N Inc. Sig.	23	4	25	43	33	2
#N Dec. Sig.	1	25	4	1	2	30
% Inc. Sig.	35.4	6.15	38.5	66.2	50.8	3.08
% Dec. Sig.	1.54	38.5	6.15	1.54	3.08	46.2

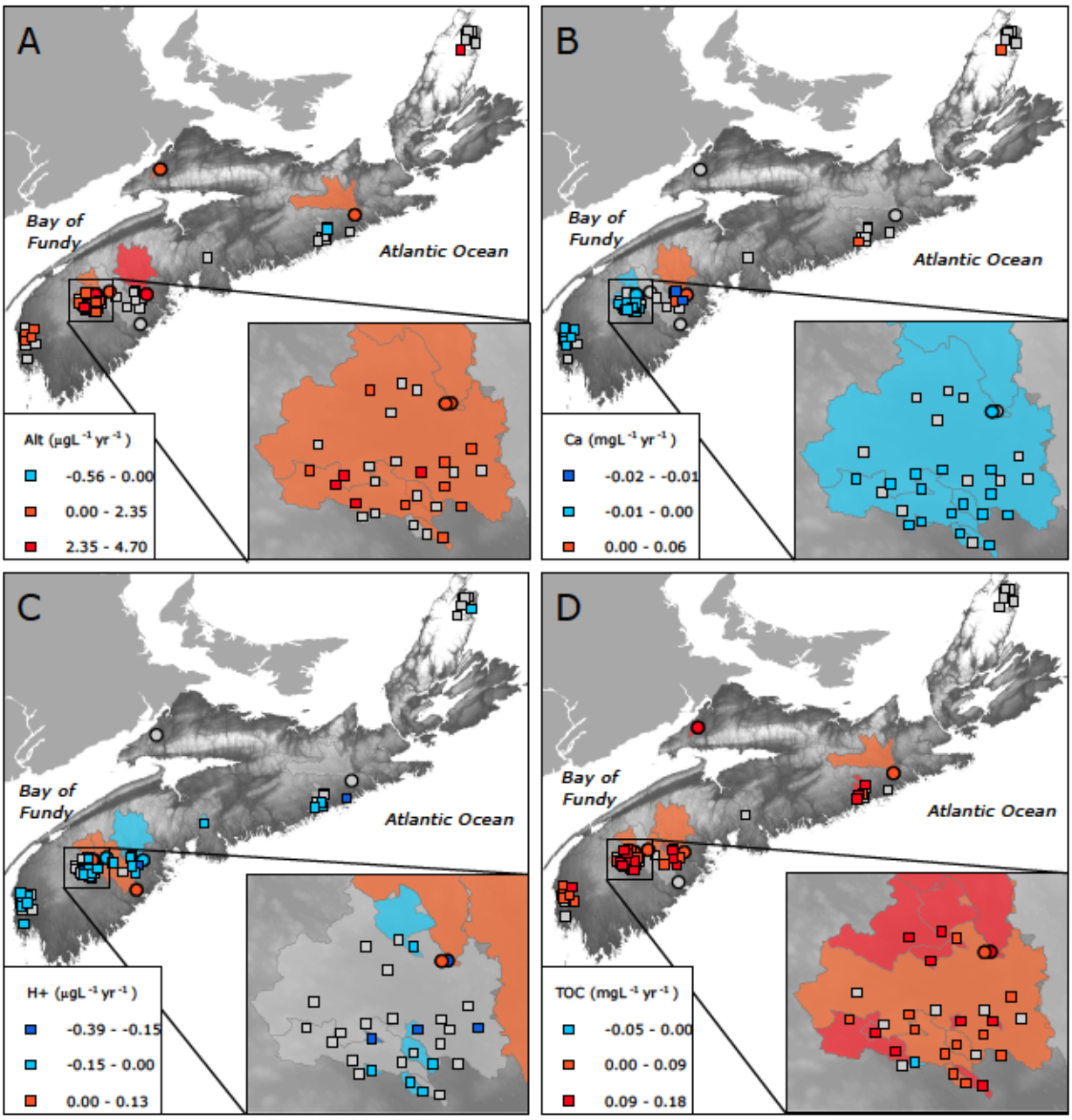

Figure 2.3: Trends in surface water chemistry from 1980 and 1990s to present in Nova Scotia. Coloured fill indicates a significant trend as calculated by Least of Squares test ($p < 0.05$); Grey fill indicates insignificant trend. Blue shades indicate decreasing concentrations, red shades indicate increasing concentrations. Circles represent rivers and squares represent lakes. A) Total aluminum, B), Calcium, C), H+, D) Total Organic Carbon (TOC). Years of sampling vary for rivers. Catchments of rivers stations are shown and coloured according to trends. Map produced of Lobke Rotteveel.

The longest and highest frequency stream chemistry records available in Nova Scotia (Mersey River 295 km² (MR) and Moose Pit Brook 17 km² (MPB)) detail divergence in NS from classic acidification recovery. Concentrations increased significantly from 2003 to 2014 (decomposed trends) for: Al (0.14 ugL^{-1} yr^{-1}, 0.05 ugL^{-1} yr^{-1}), Fe (0.16 ugL^{-1} yr^{-1}, 0.03 ugL^{-1} yr^{-1}), and TOC (0.0072 mgL^{-1} yr^{-1}, 0.0021 mgL^{-1} yr^{-1}) in MR and MPB, respectively (Figures 2.4 & 2.5; Tables 2.2 & 2.3). Decreases in Ca concentrations were significant in MR (-0.00028 mgL^{-1} yr^{-1}) and non-significant at MPB (-0.0000072 mgL^{-1} yr^{-1}). Mean Al_t concentrations increased from 180 µg/L between 1980-2003 to 230 µg/L from 2003-2014 in MR and 220 µg/L between 1980-2003 to 240 µg/L from 2003-2014 MPB (Table 2.4). Water chemistry samples are proportionally representative of all flow stages in MR and MPB (Figures 2.6 & 2.7), indicating trends are representative of all flow dynamics in the streams; water chemistry trends do not appear to be influenced by laboratory method changes, as no time-series inflections coincide with years with method changes.

The monitoring of lakes in SWNS confirms the divergence of NS surface waters from the classic model's stages five and six, with depletion of base cations and increase of metals in the region. Of 58 lakes, which were sampling biannually for >20 years, 42 had increasing trends of Al, with 16 increasing significantly with 95% confidence (Figure 2.3A). The lakes also had decreasing Ca concentrations, with Ca concentrations decreasing in 34 of the 58 lakes and six significantly decreasing (Figure 2.3B). As particulates settle to the bottom of lakes, lake trends are not influenced by clay particles or large sediment influxes, suggesting that increasing Al_t trends are not influenced by increases in clay concentrations.

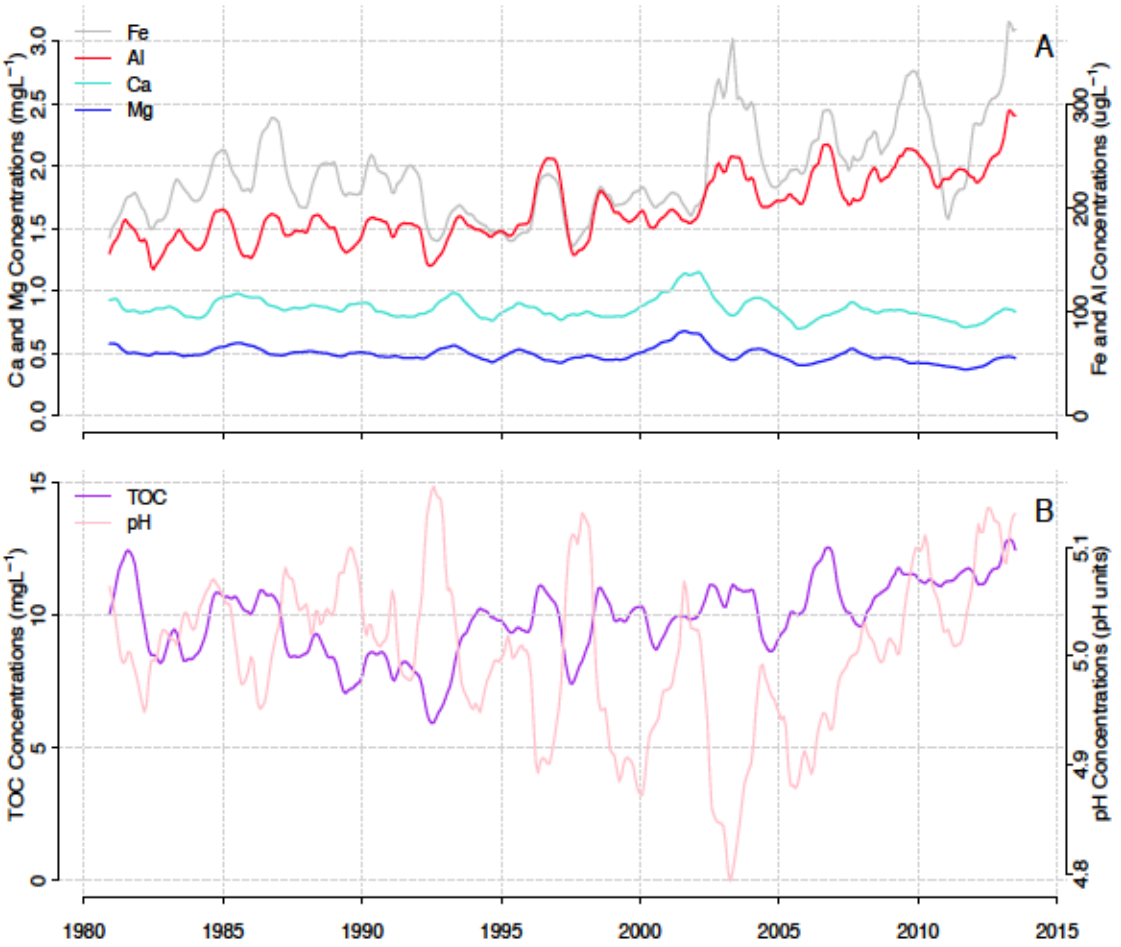

Figure 2.4: A) Decomposed trends of Ca, Mg, Fe and Al from 1980-2014 in the Mersey River, B) Decomposed trends of TOC and pH from 1980-2014 in the Mersey River.

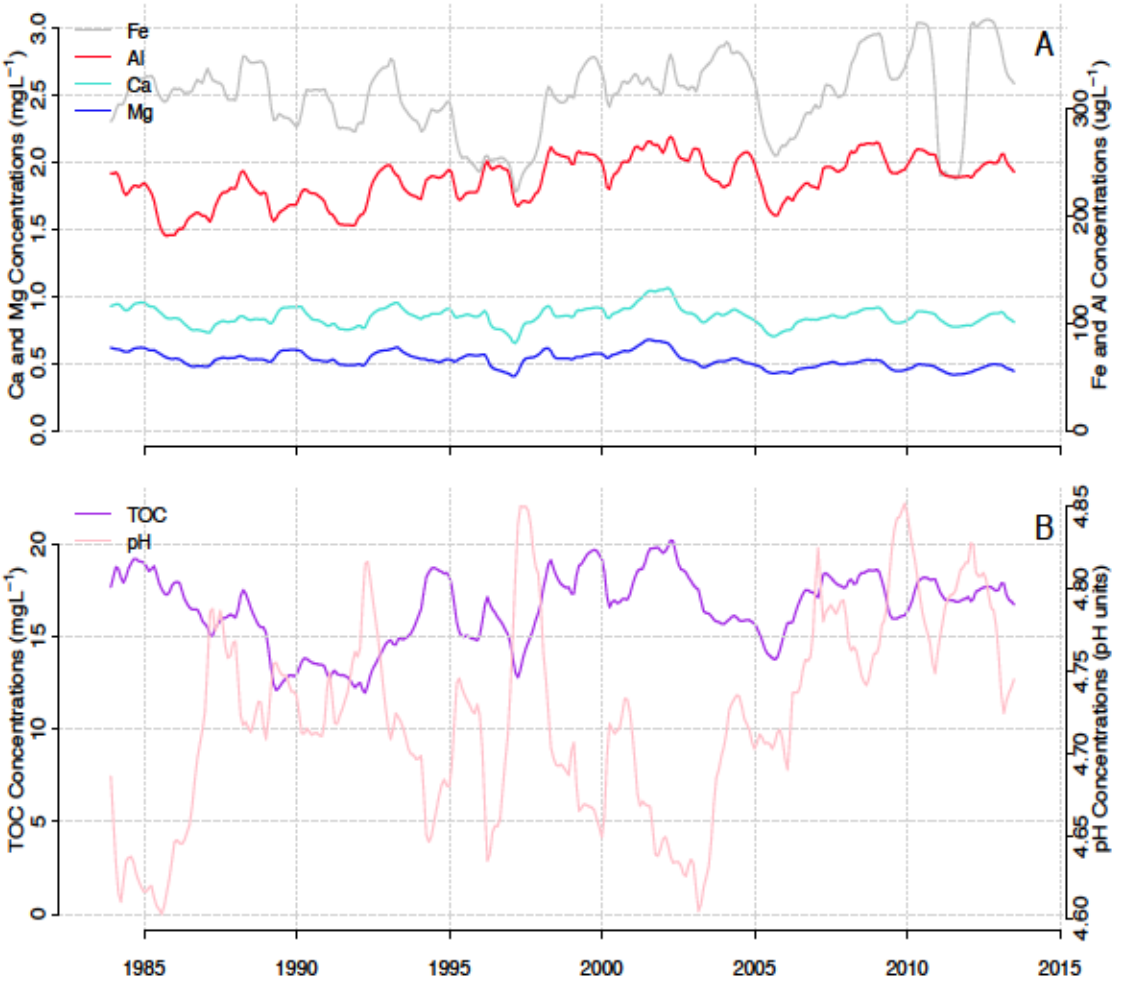

Figure 2.5: A) Decomposed trends of Ca, Mg, Fe and Al from 1983-2014 in Moose Pit Brook, B) Decomposed trends of TOC and pH from 1983-2014 in Moose Pit Brook.

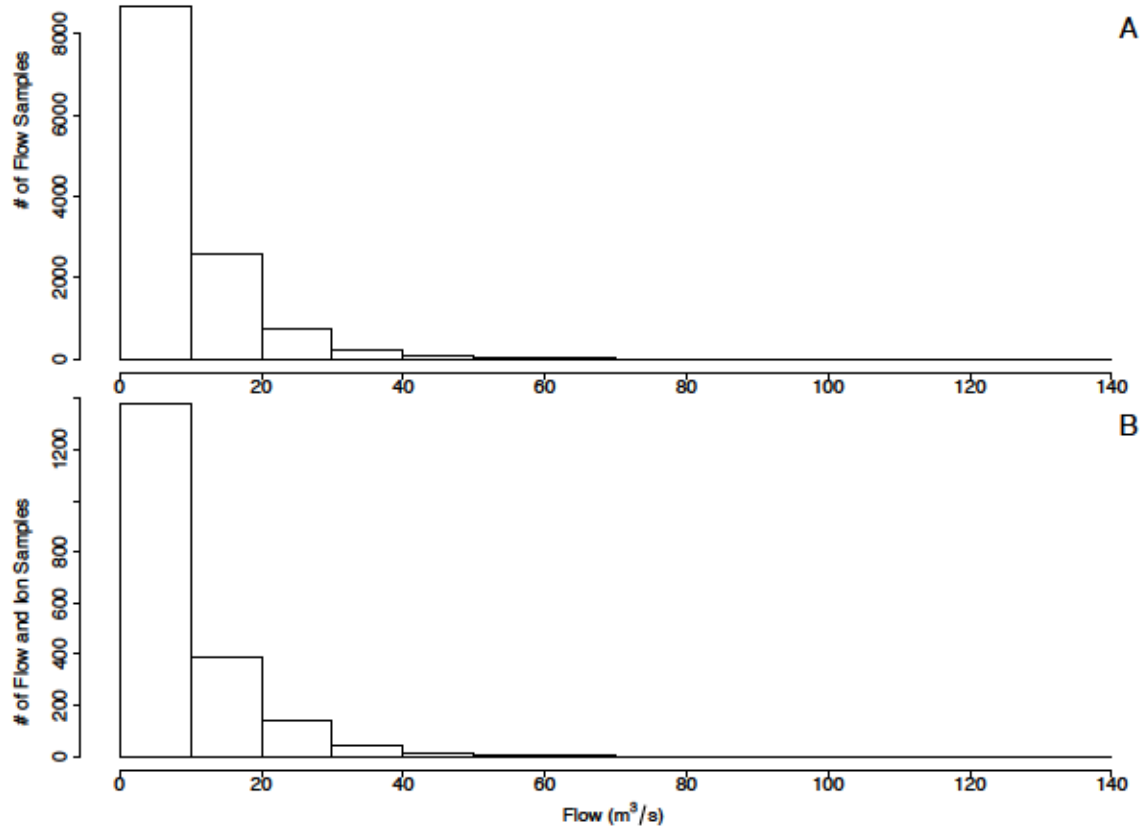

Figure 2.6: A) Histogram of flow values recorded in the Mersey River, from 1980-2014; B) Histogram of flow values recorded at the same time as water grab samples in the Mersey River, from 1980-2014.

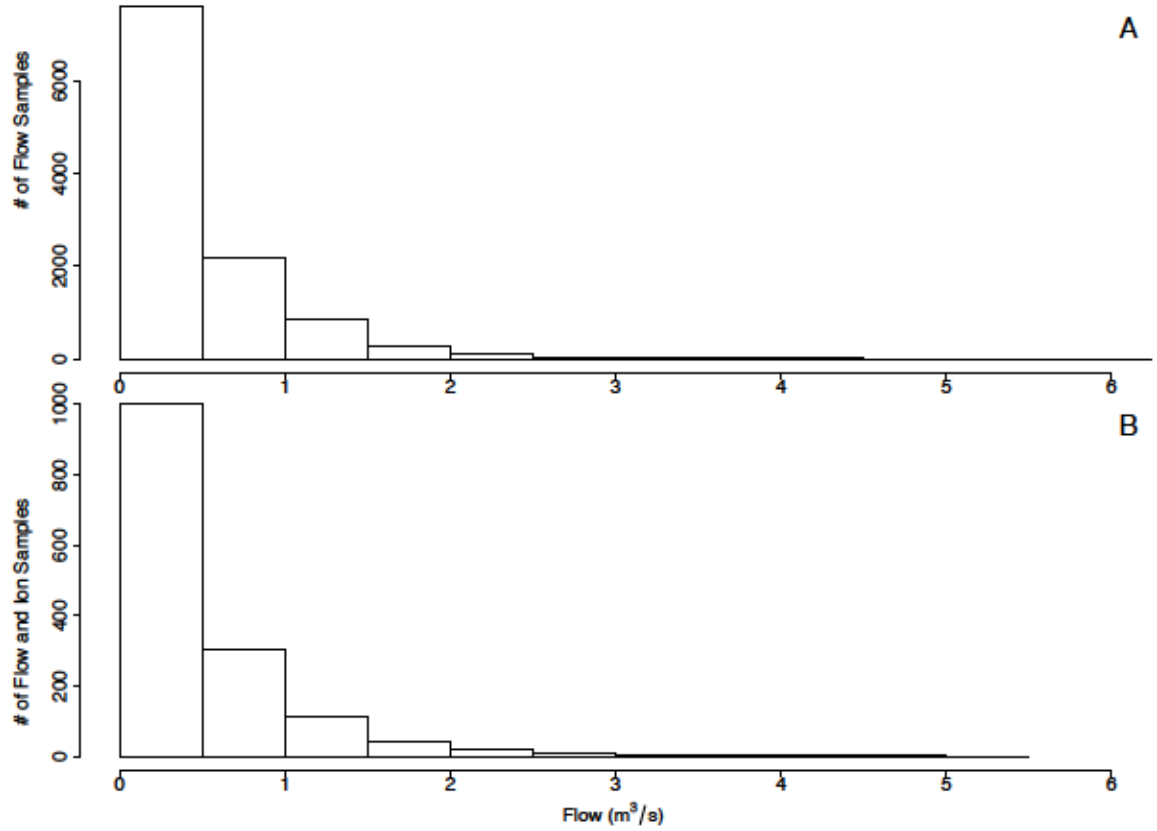

Figure 2.7: A) Histogram of flow values recorded in Moose Pit Brook, from 1983-2014; B) Histogram of flow values recorded at the same time as water grab samples in Moose Pit Brook, from 1983-2014.

Table 2.2: Water chemistry slopes for observed and trend data from the decomposed data for Mersey River from 1980-2014. Slopes and significances calculated with the Least Squares test; bold slopes indicate significance greater than 95%.

	Overall Observed (p-value)	Overall Trend (p-value)	Trend 1980-2003 (p-value)	Trend 2003-2014 (p-value)
Ca ($mgL^{-1}yr^{-1}$)	**-6.4E-05** (2.0E-02)	**-5.9E-05** (0.00)	**9.8E-05** (0.00)	**-2.9E-04** (0.00)
Na ($mgL^{-1}yr^{-1}$)	**5.8E-04** (0.00)	**6.4E-04** (0.00)	**1.6E-03** (0.00)	**-2.4E-03** (0.00)
Mg ($mgL^{-1}yr^{-1}$)	**-8.1E-05** (0.00)	**-7.6E-05** (0.00)	**2.9E-05** (8.0E-02)	**-2.8E-04** (0.00)
K ($mgL^{-1}yr^{-1}$)	**1.0E-04** (0.00)	**1.0E-04** (0.00)	5.5E-06 (5.7E-01)	**1.4E-04** (0.00)
Fe ($mgL^{-1}yr^{-1}$)	**9.1E-02** (0.00)	**7.5E-02** (0.00)	**-2.7E-02** (0.00)	**1.6E-01** (0.00)
Al ($mgL^{-1}yr^{-1}$)	**9.4E-02** (0.00)	**8.6E-02** (0.00)	**4.9E-02** (0.00)	**1.4E-01** (0.00)
TOC ($mgL^{-1}yr^{-1}$)	**2.5E-03** (0.00)	**2.4E-03** (0.00)	1.8E-05 (9.6E-01)	**7.2E-03** (0.00)
SO4 ($mgL^{-1}yr^{-1}$)	**-1.6E-03** (0.00)	**-1.5E-03** (0.00)	**-4.6E-04** (0.00)	**-2.5E-03** (0.00)
pH (pH $unityr^{-1}$)	-2.3E-05 (5.4E-01)	-2.2E-05 (8.0E-02)	**-1.0E-04** (0.00)	**7.4E-04** (0.00)
Cl ($mgL^{-1}yr^{-1}$)	**7.1E-04** (0.00)	**8.7E-04** (0.00)	**2.3E-03** (0.00)	**-6.4E-03** (0.00)
Flow ($m^3s^{-1}yr^{-1}$)	1.9E-03 (1.1E-01)	**9.6E-04** (0.00)	-9.3E-04 (4.0E-02)	-2.3E-03 (8.0E-02)

Table 2.3: Water chemistry slopes for observed and trend data from the decomposed data for Moose Pit Brook from 1983-2014. Slopes and significances calculated with the Least Squares test; bold slopes indicate significance greater than 95%.

	Overall Observed (p-value)	Overall Trend (p-value)	Trend 1980-2003 (p-value)	Trend 2003-2014 (p-value)
Ca ($mgL^{-1}yr^{-1}$)	-2.7E-05 (6.2E-01)	-7.2E-06 (6.1E-01)	**1.3E-04** (9.6E-06)	4.5E-05 (4.0E-01)
Na ($mgL^{-1}yr^{-1}$)	-1.2E-04 (1.7E-01)	-5.9E-05 (5.9E-02)	**1.5E-04** (9.6E-03)	**9.0E-04** (1.0E-09)
Mg ($mgL^{-1}yr^{-1}$)	**-1.2E-04** (3.1E-04)	**-1.1E-04** (8.4E-22)	**5.1E-05** (1.4E-02)	**-1.3E-04** (2.0E-04)
K ($mgL^{-1}yr^{-1}$)	-1.2E-06 (9.5E-01)	-5.7E-06 (6.3E-01)	**-2.0E-04** (3.5E-25)	-9.1E-05 (1.4E-01)
Fe ($mgL^{-1}yr^{-1}$)	2.4E-02 (5.1E-01)	**2.8E-02** (1.1E-04)	**-2.4E-02** (4.2E-02)	8.2E-02 (7.4E-02)
Al ($mgL^{-1}yr^{-1}$)	**4.1E-02** (2.2E-02)	**4.9E-02** (2.9E-35)	**9.4E-02** (6.9E-34)	**7.1E-02** (1.5E-05)
TOC ($mgL^{-1}yr^{-1}$)	1.7E-03 (2.5E-01)	**2.1E-03** (4.5E-08)	**3.6E-03** (6.6E-05)	**7.2E-03** (5.0E-10)
SO4 ($mgL^{-1}yr^{-1}$)	**-1.3E-03** (4.3E-14)	**-1.3E-03** (1.6E-67)	**-3.1E-04** (1.1E-02)	**-1.3E-03** (1.2E-16)
pH (pH $unityr^{-1}$)	**8.9E-05** (2.6E-03)	**1.0E-04** (5.2E-18)	2.1E-05 (3.3E-01)	**3.1E-04** (4.7E-15)
Cl ($mgL^{-1}yr^{-1}$)	**-5.1E-04** (5.8E-05)	**-4.7E-04** (1.5E-15)	**-9.3E-04** (1.3E-15)	-5.1E-04 (7.8E-02)
Flow ($m^3s^{-1}yr^{-1}$)	1.1E-04 (1.3E-01)	**7.2E-05** (3.0E-05)	**-7.5E-05** (1.8E-02)	**-2.9E-04** (5.7E-04)

Table 2.4: Catchment characteristics and stream chemistry values for Nova Scotian rivers with the longest complete data set. X95 is the value of the variable at which 95 percent of the measurements exceed that value. X5 is the value of the variable at which 5 percent of the measurements exceed that value. The separation of data ('breakpoint') in March 2003 is used to define the time periods. Bold indicates a 95% significant difference, using a t-test, between the means of 1980-2003 and 2003-2014.

a. Clair et al. (2008)
b. Department of Natural Resources NS, Geoscience and Mines Branch, NS DEM 2006, Version 2.
c. Calculated as the area of clear cut percentage over entire catchment area, using ArcGIS and forest cover layers from the Department of Natural Resources NS' Forestry Inventory GIS shapefile.
d. Calculated as the area of wetlands percentage over entire catchment area, using ArcGIS and forest cover layers from the Department of Natural Resources NS' Forestry Inventory GIS shapefile.

							Flow (m^3/s)			Al_t (ug/L)			Ca (mg/L)			TOC (mg/L)		
	Size (km^2)	Relief (m)	Forest Cover (%)	Harvested (%)	Wetland (%)	Sampling Period	Mean (CV)	Q_{95}	Q_{05}	Mean (CV)	Al_{95}	Al_{05}	Mean (CV)	Ca_{95}	Ca_{05}	Mean (CV)	TOC 95	TOC 05
Mersey River	291	103-250	Spruce, Maple, Pine, Hemlock	15	6.5	1980-2003	**7.9** (1.0)	0.32	24	**180** (0.31)	**100**	**280**	**0.91** (0.22)	0.63	**1.3**	**9.5** (0.32)	**5.0**	**15**
						2003-2014	**9.3** (1.1)	0.79	26	**230** (0.45)	**140**	**350**	**0.82** (0.19)	0.59	**1.1**	**11** (0.29)	**6.5**	**17**
Moose Pit Brook	17	103-207	Spruce, Fir, Pine	15	0.15	1983-2003	**0.45** (1.2)	0.011	1.5	**220** (0.42)	100	410	0.86 (0.37)	0.48	**1.5**	**16** (0.48)	6.0	31
						2003-2014	**0.54** (1.3)	0.031	1.7	**240** (0.45)	110	420	0.83 (0.33)	0.51	**1.3**	**17** (0.47)	7.3	31

To test whether suspended solids in river chemical concentrations are in part driving the trends, we examined trends in turbidity over the same time period, and the data showed no significant difference in mean turbidity over time for both MR and MPB (Figures 2.8 & 2.9); and therefore an increase in delivery in solid load is likely not responsible for the increasing Al_t trends observed here.

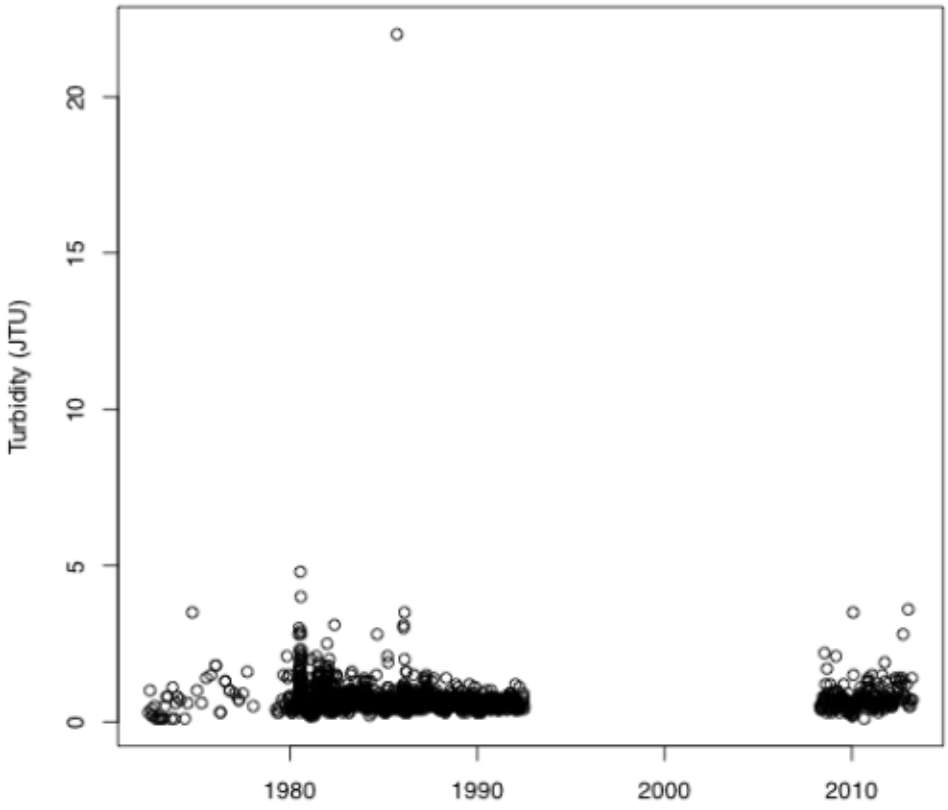

Figure 2.8: Turbidity from 1972-2013 in the MR.

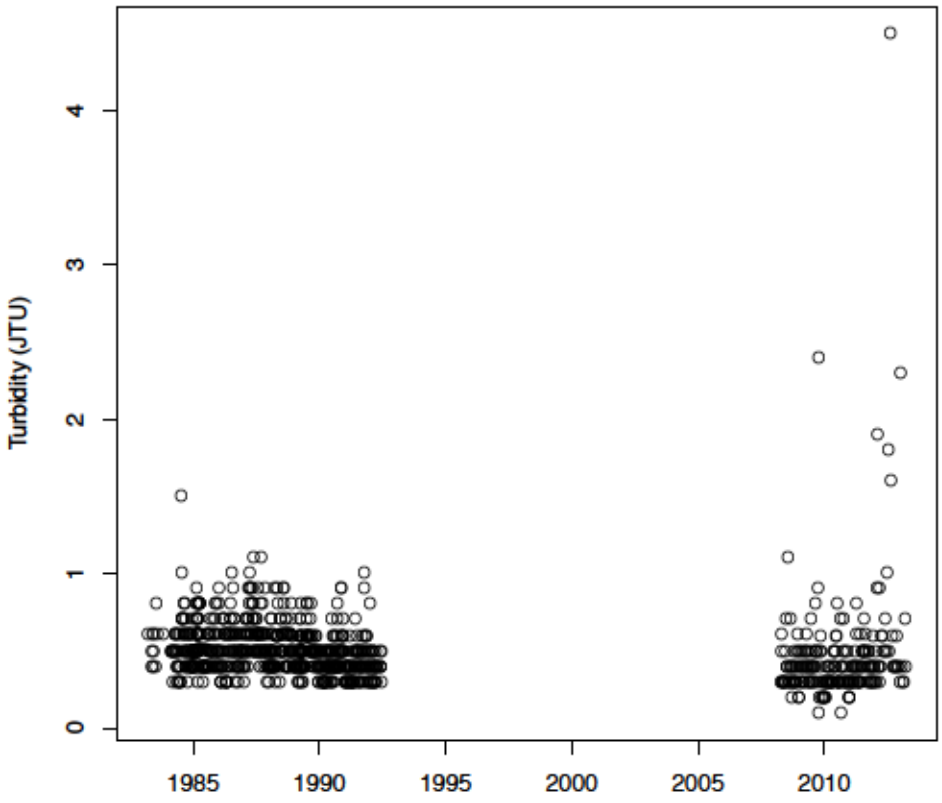

Figure 2.9: Turbidity from 1983-2013 in the MPB.

2.6.3. Trends' Stationarity and Linearity

Cation concentration trends in MR and MPB are nonlinear, nonstationary, and coincide with high flow events and SO_4 slope changes. Cumulative mass exports for MR and MPB have two close inflection points in the time-series for Al, Fe, Ca, TOC, H, Ca, Mg and SO_4 (Figures 2.10 - 2.15). Two inflection points in the MR and MPB water chemistry data are identified as specific dates that separate significantly different chemical slopes (Tables 2.5 & 2.6). The first inflection point occurs on March 26th, 2003, coinciding with the rising limb of the largest flow event recorded between 1980 and 2014, with the second inflection point occurring on the falling limb of the same flow event, on April 6th, 2003. Methodology changes do not appear to influence the slope changes, as no laboratory methodology changes for any water chemicals occurred during 2003 (refer to Chapter 2.5.3.1).

The two inflection points suggest an ecosystem shift due to extreme flow rates causing major soil cation flushing. The SO_4 slope changes after both inflection points; however, these changes may be due to continued decreases in SO_4 wet and dry deposition rates. As decreased SO_4 is linked with increases in pH in the classic model (Galloway et al., 1983), pH and SO_4 shifts should coincide in MR and MPB mass export trends; the lack of consistent pH shifts coinciding with SO_4 shifts in MR and MPB suggests a decoupling of SO_4 and pH, and therefore resulting in less of an influence of SO_4 on Al_t trends and a divergence from the classic model.

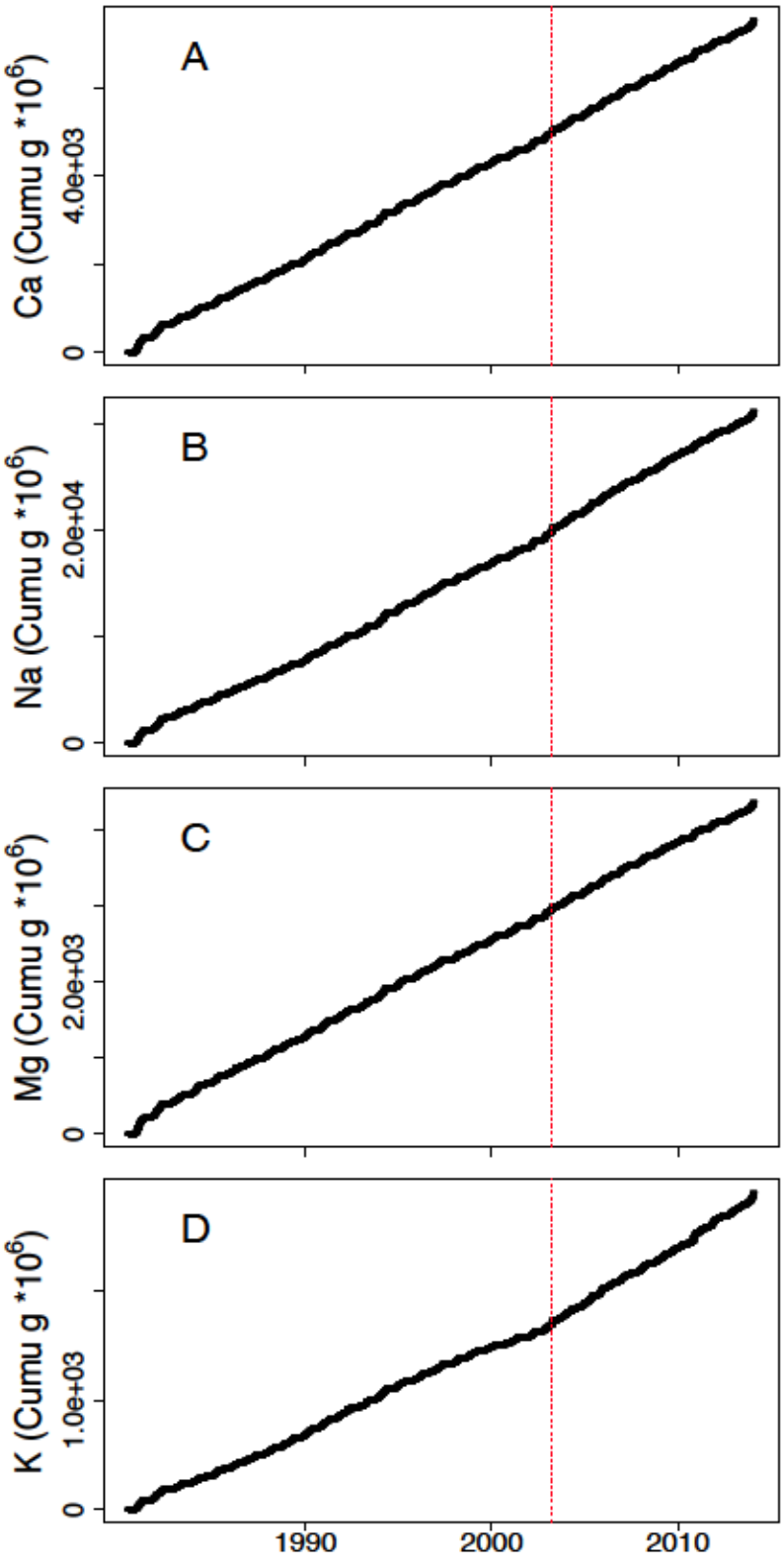

Figure 2.10: Cumulative mass exports for A) Ca, B) Na, C) Mg, D) K in MR from 1980-2014, with inflection points annotated with red dashed lines.

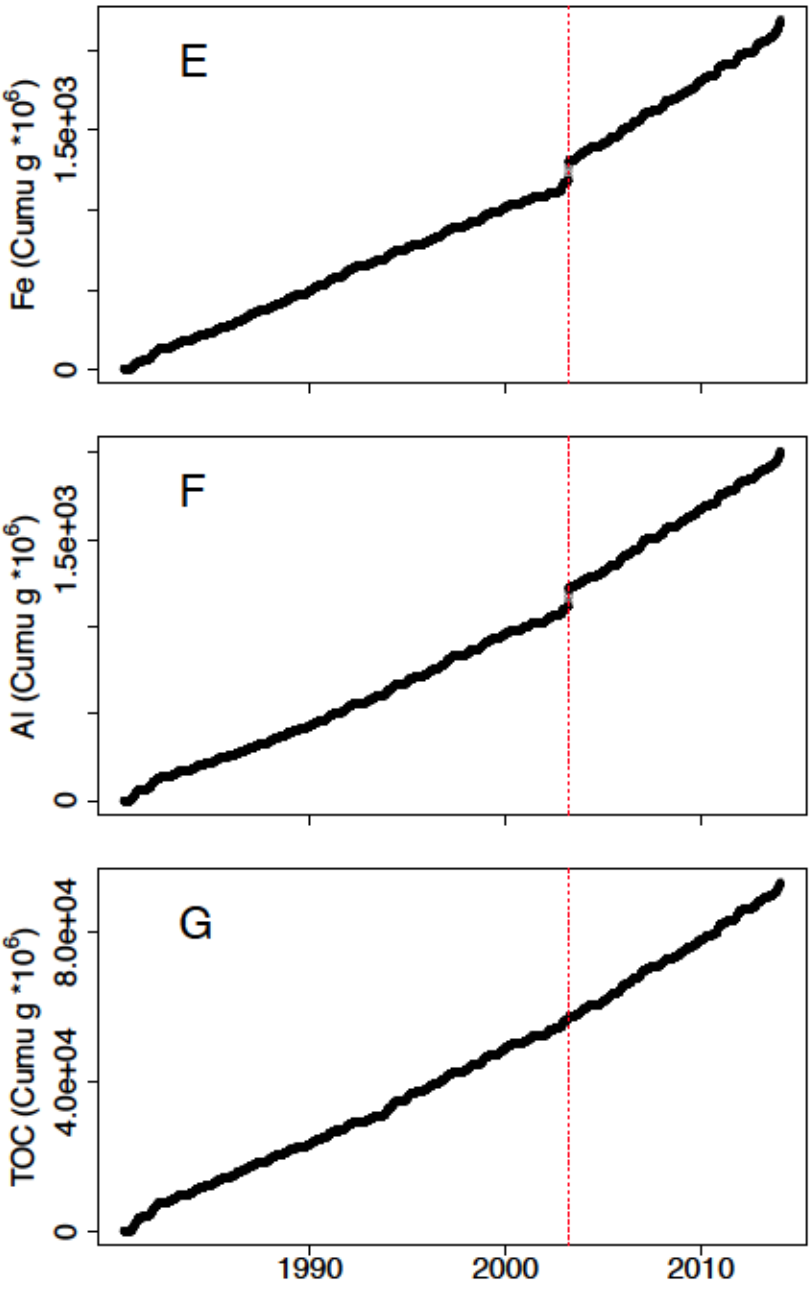

Figure 2.11: Cumulative mass exports for E) Fe, F) Al, G) TOC in MR from 1980-2014, with inflection points annotated with red dashed lines.

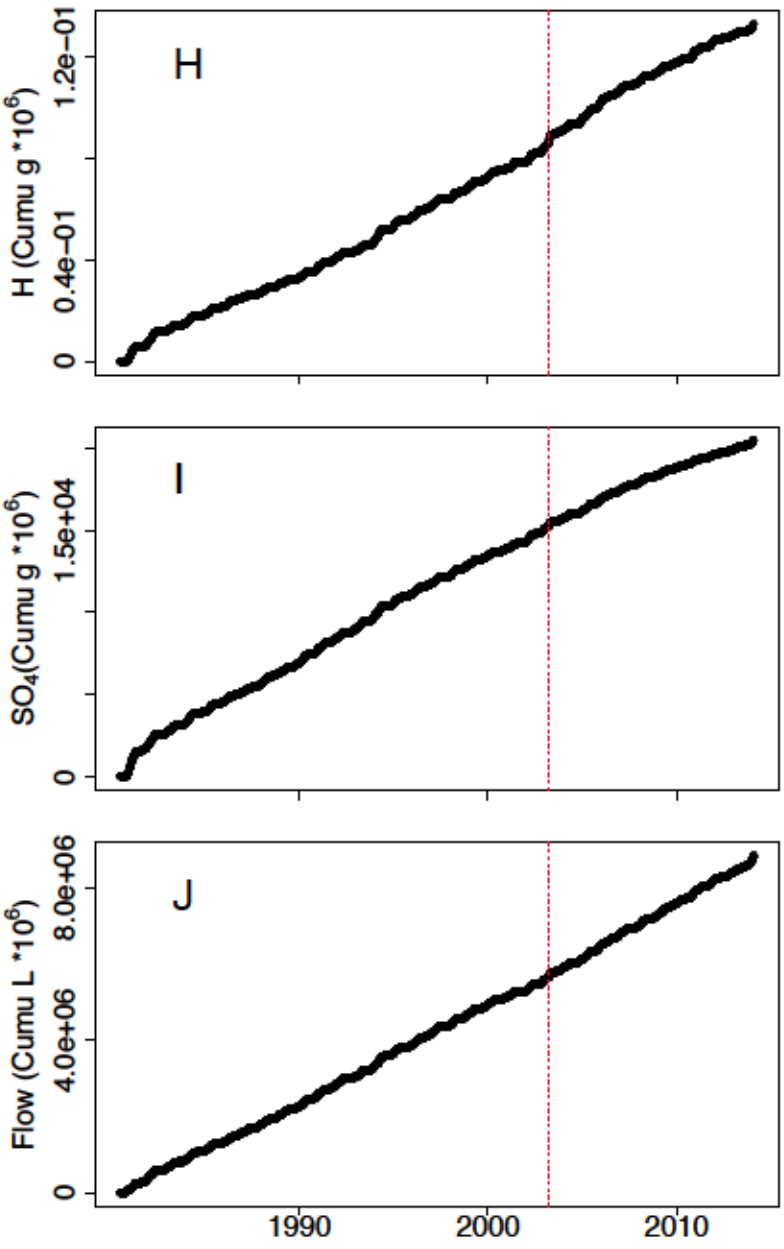

Figure 2.12: Cumulative mass exports for H) H, I) SO_4, and J) Flow in MR from 1980-2014, with inflection points annotated with red dashed lines.

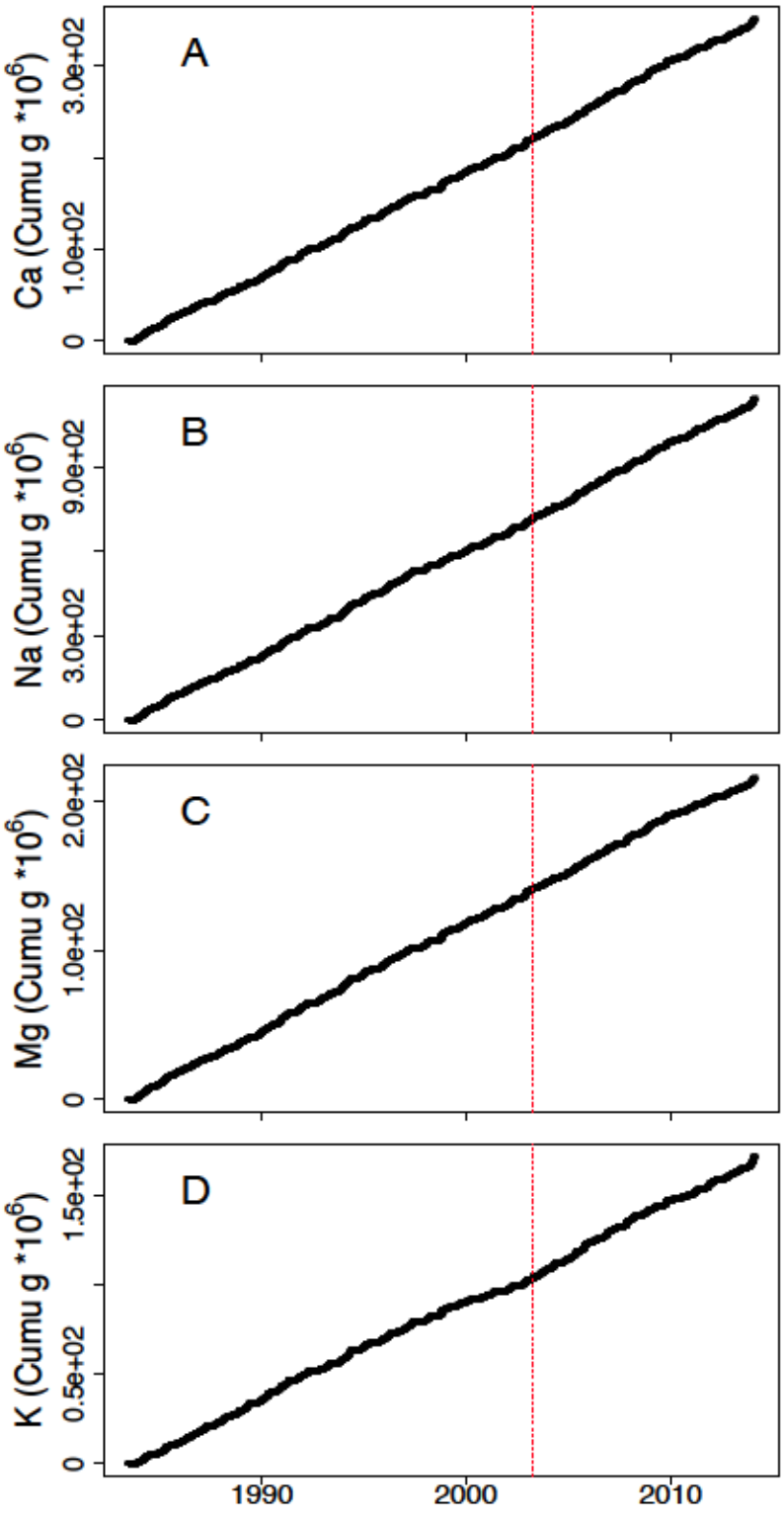

Figure 2.13: Cumulative mass exports for A) Ca, B) Na, C) Mg, D) K in MPB from 1983-2014, with inflection points annotated with red dashed lines.

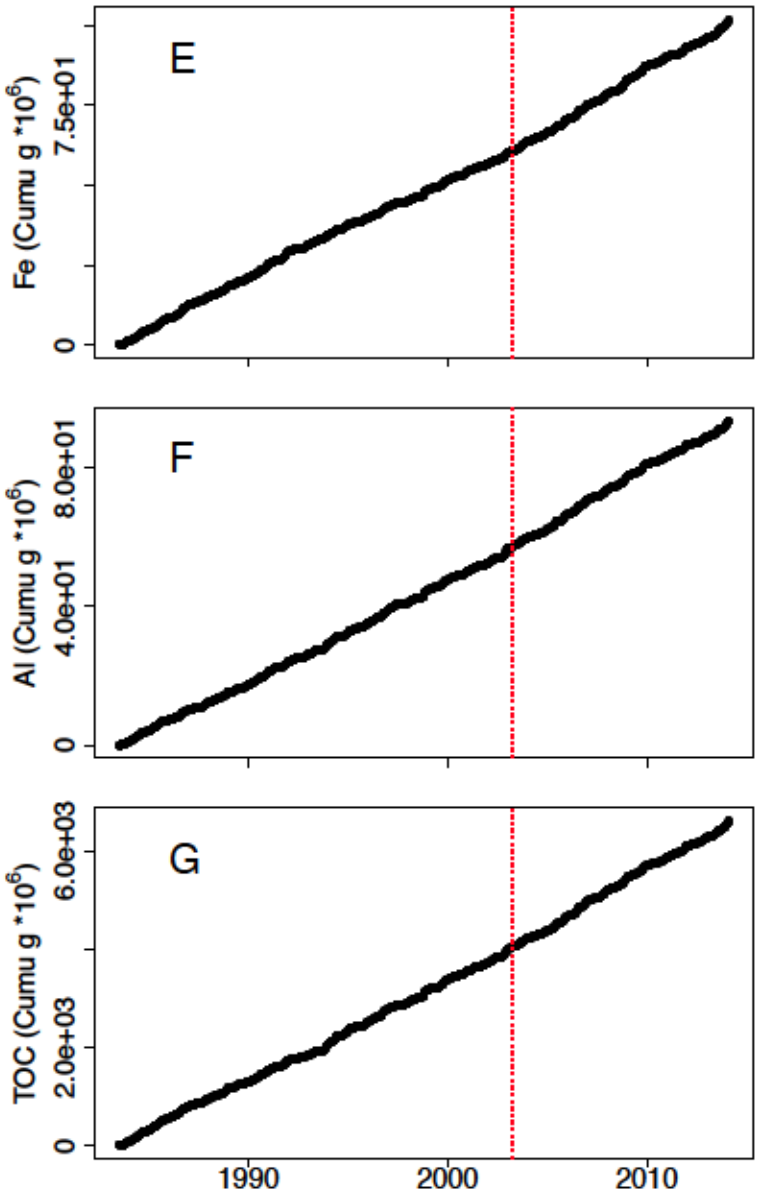

Figure 2.14: Cumulative mass exports for E) Fe, F) Al, G) TOC in MPB from 1983-2014, with inflection points annotated with red dashed lines.

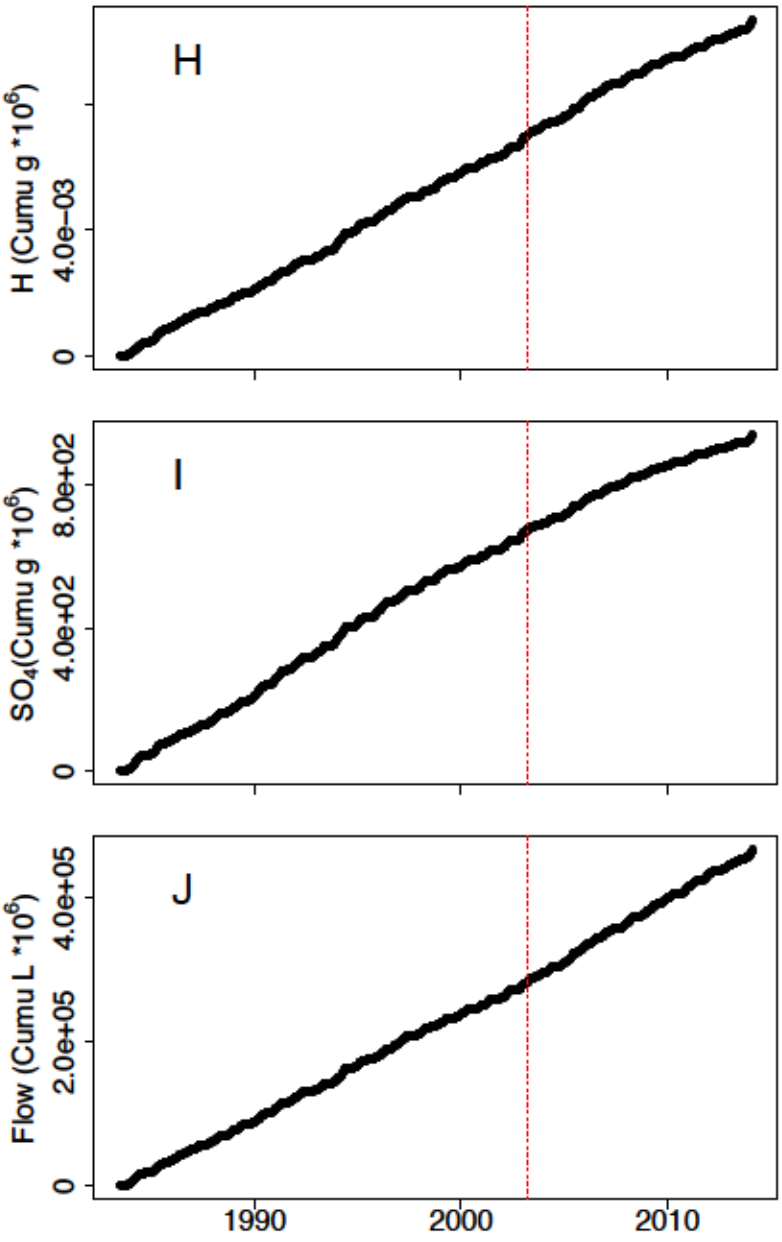

Figure 2.15: Cumulative mass exports for H) H, I) SO_4, and J) Flow in MPB from 1983-2014, with inflection points annotated with red dashed lines.

Table 2.5: Slopes and p-values for three periods for each cumulative mass export of flow values, and Ca, Na, Mg, K, Fe, Al, and TOC concentrations the Mersey River, determined by the Least Squares test; 95% significant trends are in bold. * indicates significant difference between 1980-2003 slope and 2003-2014; ^ indicates significant difference between 1980-2003 slope and 2003-2003 slope; ` indicates significant difference between 2003-2003 slope and 2003-2014 slope.

Water Parameters	Slopes		
	June 27/1980 – Mar 26/2003 (p-value)	Mar 26/2003 – Apr 06/2003 (p-value)	Mar 26/2003 – Mar 10/2014 (p-value)
Ca`	**$5.8*10^5$** (0.00)	**$5.4*10^6$** (0.00)	**$6.1*10^5$** (0.00)
Na`	**$2.3*10^6$** (0.00)	**$2.8*10^7$** (0.00)	**$2.7*10^6$** (0.00)
Mg ^`	**$3.4*10^5$** (0.00)	**$3.0*10^6$** (0.00)	**$3.4*10^5$** (0.00)
K`	**$2.1*10^5$** (0.00)	**$2.8*10^6$** (0.00)	**$2.9*10^5$** (0.00)
Fe`	**$1.4*10^5$** (0.00)	**$1.3*10^7$** (0.00)	**$2.1*10^5$** (0.00)
Al`	**$1.3*10^5$** (0.00)	**$1.1*10^7$** (0.00)	**$1.9*10^5$** (0.00)
TOC`	**$6.5*10^6$** (0.00)	**$5.1*10^7$** (0.00)	**$8.8*10^6$** (0.00)
Flow`	**$6.9*10^8$** (0.00)	**$6.3*10^9$** (0.00)	**$7.7*10^8$** (0.00)

Table 2.6: Slopes and p-values for three periods for each cumulative mass export of flow values, and Ca, Na, Mg, K, Fe, Al, and TOC concentrations in the Moose Pit Brook, determined by the Least Squares test; 95% significant trends are in bold. * indicates significant difference between 1980-2003 slope and 2003-2014; ^ indicates significant difference between 1980-2003 slope and 2003-2003 slope; ` indicates significant difference between 2003-2003 slope and 2003-2014 slope.

Water Parameters	Slopes		
	June 27/1980 – Mar 26/2003 (p-value)	Mar 26/2003 – Apr 06/2003 (p-value)	Mar 26/2003 – Mar 10/2014 (p-value)
Ca	**$3.1*14^5$** (0.00)	**$3.2*10^4$** (0.00)	**$3.2*10^4$** (0.00)
Na`	**$1.0*10^5$** (0.00)	**$1.4*10^5$** (0.00)	**$1.1*10^5$** (0.00)
Mg ^`	**$2.0*10^4$** (0.00)	**$2.0*10^4$** (0.00)	**$1.9*10^4$** (0.00)
K`	**$1.5*10^4$** (0.00)	**$2.4*10^4$** (0.00)	**$1.6*10^4$** (0.00)
Fe*	**$8.4*10^3$** (0.00)	**$4.9*10^3$** (0.00)	**$1.0*10^4$** (0.00)
Al	**$7.9*10^3$** (0.00)	**$7.7*10^3$** (0.00)	**$9.1*10^3$** (0.00)
TOC*	**$5.5*10^5$** (0.00)	**$4.9*10^5$** (0.00)	**$6.4*10^5$** (0.00)
Flow`	**$4.0*10^7$** (0.00)	**$3.0*10^8$** (0.00)	**$4.5*10^7$** (0.00)

2.6.4. Drivers Diverting Al_t from the Classic Model

The seasonality of Al_t concentrations in MR and MPB suggest positive correlations with TOC and flow (Figures 2.16 & 2.17). The seasonal highs during the summer and fall for Al correspond to highs in flow values and Fe, Ca, and TOC concentrations; following the 2003 breakpoint, Al and Fe increase in all months for MR and the summer and fall for MPB. The fall peak in Al concentrations moves from November to October in MR, and from October to September in MPB. The Al fall peak shifts correspond to shifts of TOC and flow into earlier parts of the fall. It is possible that the increase in flow may have resulted in flushing of cation-depleted soils, and TOC, resulting in the increase of Al_t and TOC, with the decrease of Ca and Mg concentrations in MR and MPB.

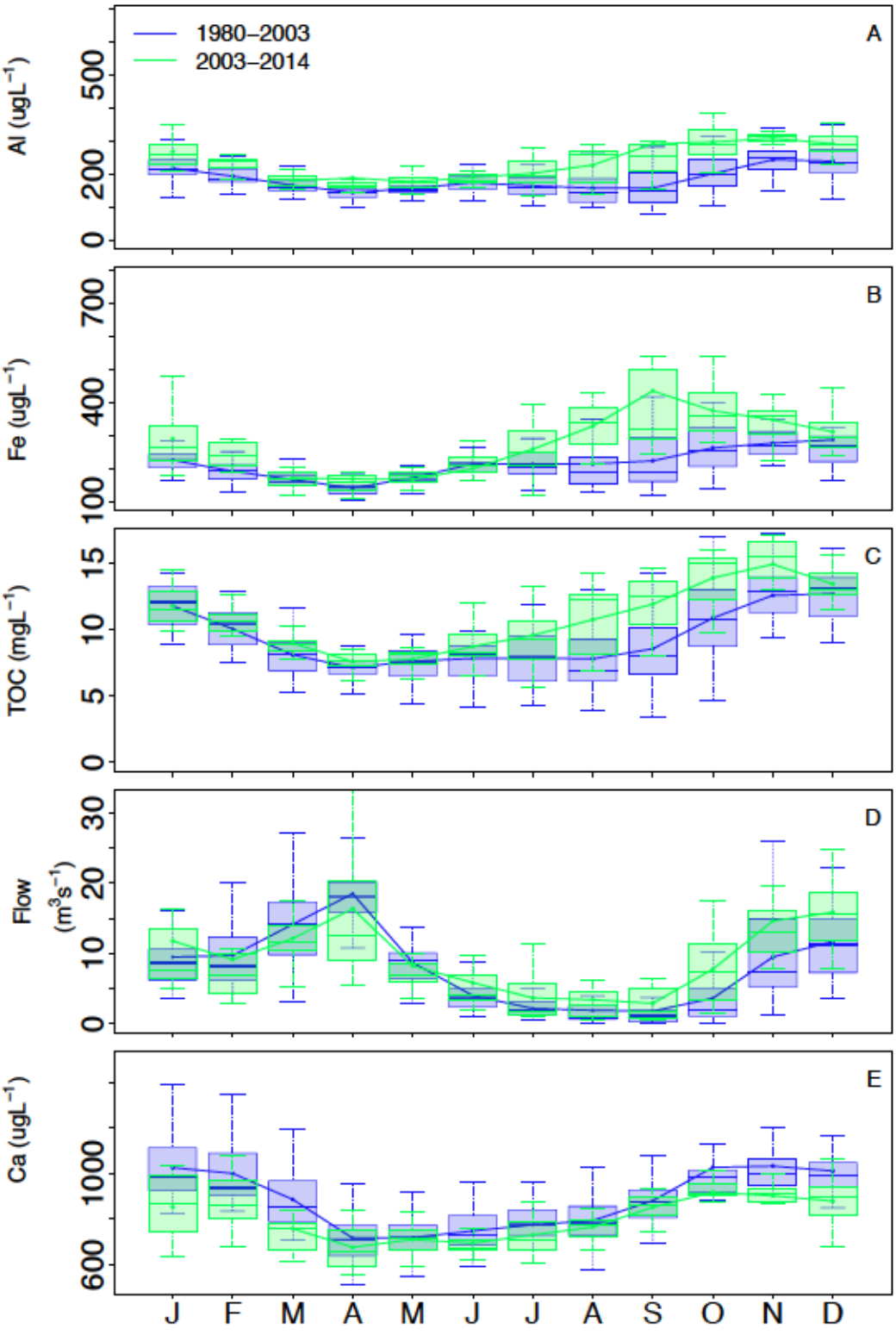

Figure 2.16: Monthly values for A) Al, B) Fe, C) TOC, D) Flow, and E) Ca in MR from 1980-2003 and 2003-2014.

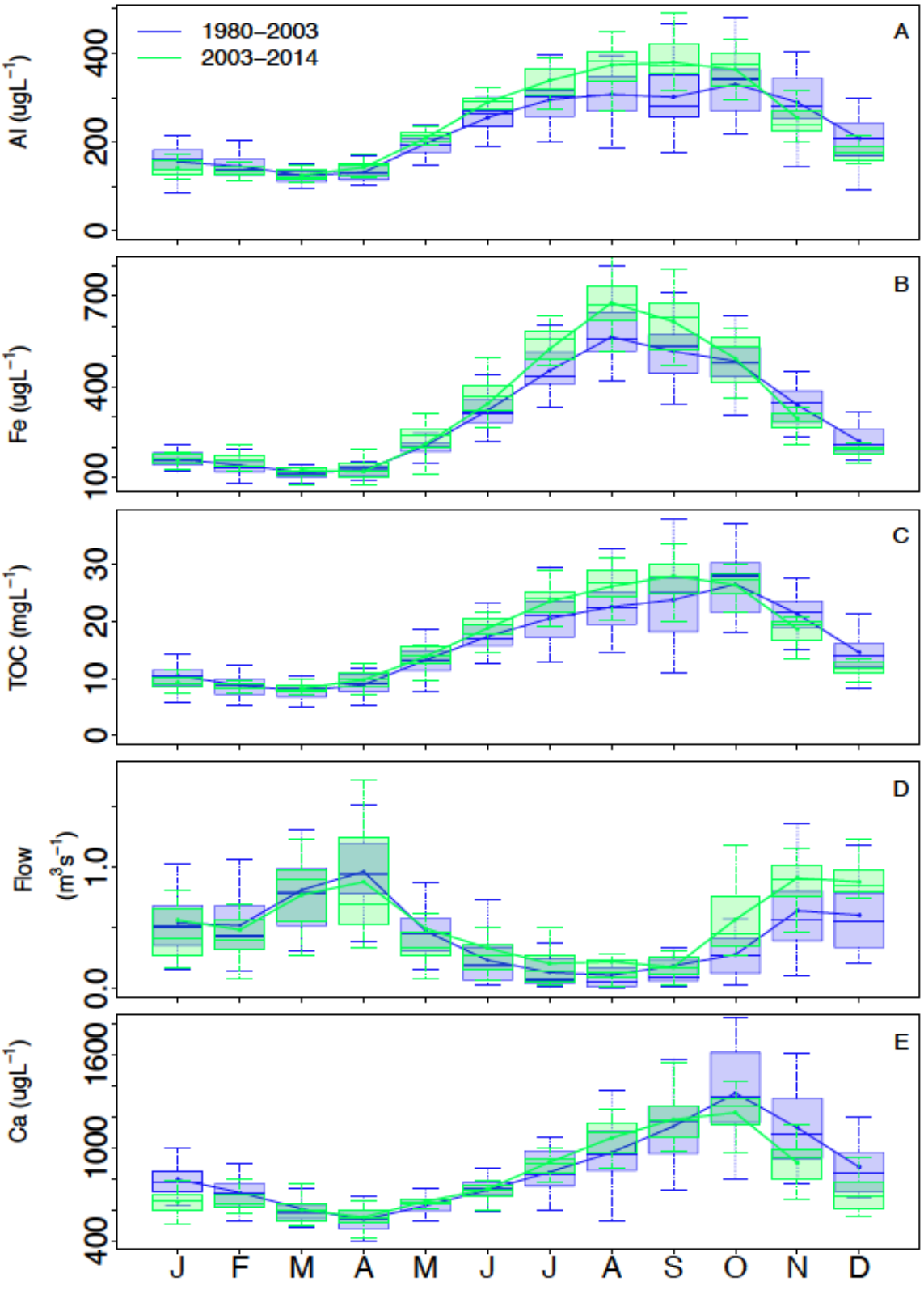

Figure 2.17: Monthly values for A) Al, B) Fe, C) TOC, D) Flow, and E) Ca in MPB from 1983-2003 and 2003-2014.

The presence of TOC and reduced soil base cation concentrations appear to drive the divergence of NS acidification recovery from the classic model. Increases in TOC concentrations in MR and MPB from 1980-2003 and 1987-2003, respectively (Figures 2.6 & 2.7) are consistent with the increasing DOC trends reported by Monteith et al. (2007) for North America and Northern Europe from 1990-2004. The increasing TOC concentrations in MR and MPB are concurrent with decreasing pH values in MR and MPB between 1980-2003; we hypothesize that organic acids from TOC delayed pH increases from reduced acid deposition in MR and MPB, as organic inputs are known to buffer changes in soil pH (Sullivan et al., 1996, Clair et al., 1992). Our findings of increased TOC concurrent with a lag in pH recovery confirm the findings of Hruska et al. (2009), where organic acidity buffers pH recovery; however, increases in NS Al_t concentrations conflict with the deceased Al_t concentrations reported by Hruska et al. I suggest that a combination of high TOC, and slow-weathering bedrock has resulted in the divergence of NS freshwaters from the classic, and Hruska et al.'s, models.

The lighter base cations (Ca and Mg) remain very low in MR and MPB (less than the 1.5 mg/L needed for the survival of aquatic invertebrates; Ashforth and Yan, 2008), and have decreased steadily since 1980 and 1983 (Figures 2.5 & 2.6; Tables 2.1, 2.3 & 2.4). The decreases in base cations may be due to reduced requirement for soil buffering from less acid deposition, or due to the low base cation saturation of soil CEC from continued acid inputs by TOC, with minimal base cation replenishment from slow-weathering bedrocks. The loss of base cations is known to coincide with soil acidification and increased Al concentrations, even after sulfate emission reductions (Larssen and Carmichael, 2000). Increases in Fe and Al for both rivers support the hypothesis of CEC low base saturation due to continued acid inputs; soils exchange heavier cations, such as Al and Fe, to buffer soil acidity as Ca and Mg concentrations decrease. The increase in Al and Fe concentrations for MR and MPB also corresponds with increased TOC concentrations from April until December between the 1980-2003 and 2003-2014 periods (Figures 2.16 & 2.17); as DOC

concentration increases have been reported in North America and Europe (Monteith et al., 2007), the continued organic acid inputs may continue to mobilize and increase Al concentrations in SWNS rivers. Stage six in the classic model predicts cation recovery in soils, with decreases in river cations due to less cation exchange from acid deposition; however, little cation replenishment, soil cation depletion, chronic soil acidity, and increased Al concentrations coincide with the poorly weathered bedrock and high TOC concentrations found in SWNS rivers.

Changes in climate may be exacerbating increases of Al_t in NS. The mean air temperature has increased in all months for the 2003-2014 period compared to the 1980-2003 period (Figure 2.18); increased temperature and decreased pH may increase Al mobilization from soils. Increased temperatures are linked to increased rates of microbial respiration, resulting in the rapid breakdown of detritus (dead organic matter) and increased release of TOC and organic acidity (Worrall et al. 2004). Mean flow values in the 2003-2014 period have exceeded the 1980-2003 period from June to January in MR and MPB (Figures 2.14 & 2.15). Precipitation, a possible cause of the increases in flow, has increased significantly since 1980 within the Kejimkujik region; a significant shift upwards, from $-2.42*10^{-4}$ to $7.81*10^{-3}$ mm/year, in precipitation occurred on the March 15th, 2003 inflection point (Table 2.7). The 2003 peak occurs during a positive NAO cycle (Climate Prediction Center Internet Team, 2012); a positive NAO index is linked to increased winter precipitation along Eastern NA, which may a factor in the March 2003 precipitation increase. The increased flow in MR, after the 2003 inflection points (Table 2.4), may be acting as possible sources for increases in Al due to flushing of ions from the soils and differences in flow partitioning. Decreased flow in MPB compared to MR (Table 2.4), may explain the smaller increase in Al_t in the MPB catchment.

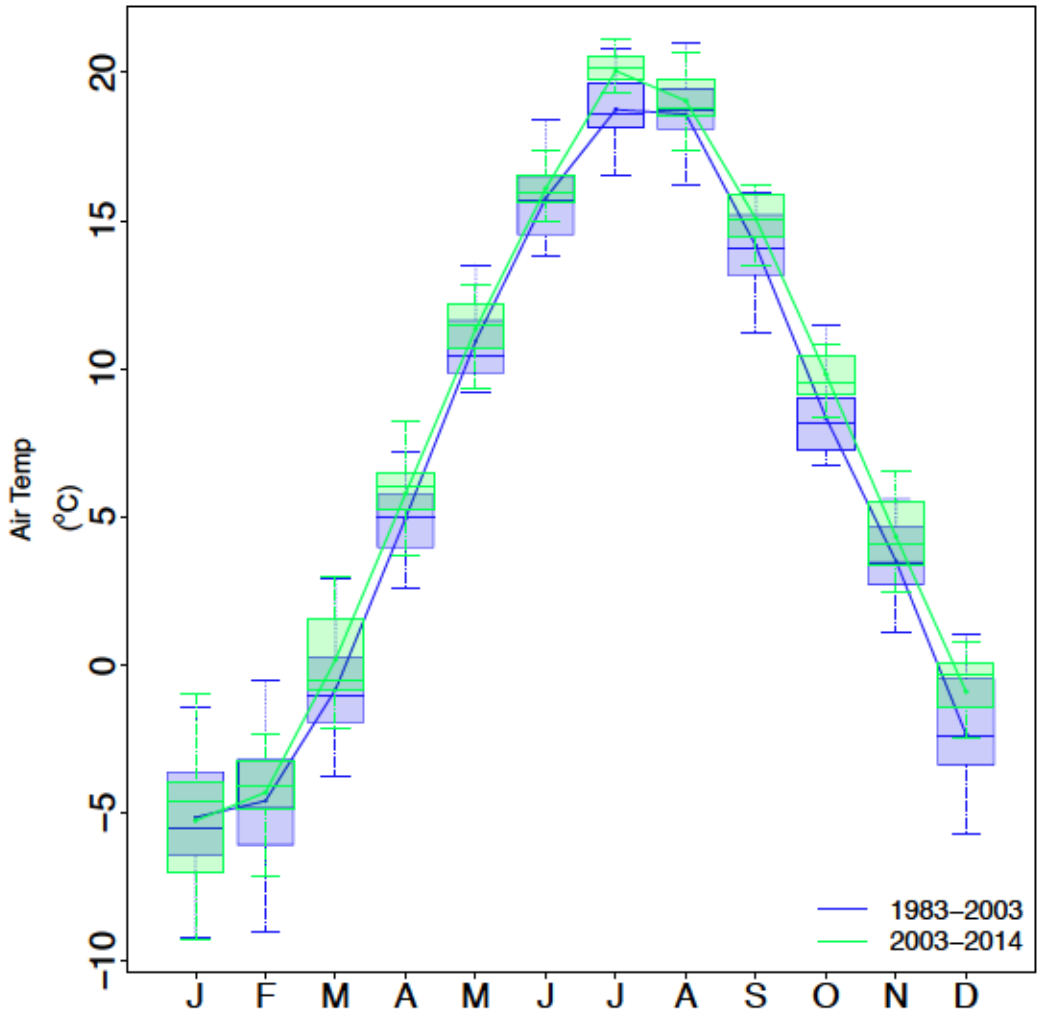

Figure 2.18: Monthly values for air temperature in Kejimkujik National Park from 1980-2003 and 2003-2014.

Table 2.7: Observed and decomposed (trend) collected precipitation measurement slopes (in mm/year) and p-values from 1980-2014, 1980-2003 and 2003-2014 in the Kejimkujik National Park.

	Observed Slope (p-value)	Trend Slope (p-value)	1983-2003 Trend Slope (p-value)	2003-2014 Trend Slope (p-value)
Precip	0.00199 (6.13E-06)	0.00169 (3.43E-30)	-0.000242 (0.0731)	0.00781 (1.68E-12)

2.6.5. Limitations and Recommendations for Future Work

Acid deposition trends reported by the CapMoN station are assumed to be representative of SWNS; however, deposition may vary spatially across NS. The MR may have received more acid deposition due to its higher elevation compared to MPB, similar to the increased SO_4 deposition in montane sites versus riverbottom sites in the Appalachian Mountains in 1981-1989 (Gilliam and Adams, 1996); however, only one acid deposition site (CapMoN) is located in SWNS, therefore no acid deposition comparison between sites was possible.

Due to the variability of metal concentrations in clay particles and sediments, the assumption that TOC is equivalent to DOC in SWNS may not apply to Al_t. Increasing total Al concentrations in SWNS from 1980-2014 may not be indicative of dissolved Al trends, as decreases in Al coincide with increases in non-labile Al for 22 lakes and streams from 1988-1999 (Evans and Monteith, 2001). In addition, methodology changes between 1980-2014 for the water chemistry parameters monitored by EC may increase uncertainty in trends presented in this study.

Soil acidity is assumed to be the cause of continued Al concentration increases in MR and MPB following increases in river pH after 2003; however, no soil chemistry samples have been analyzed to test this hypothesis. To test our hypotheses of depleted base cations and maintained acidity in soils, soil chemistry measurements in MR and MPB are required. We hypothesize that soil Al_t is the source of freshwater Al_t increases, and is mobilized due to low soil pH from high DOC concentrations; however, no soil chemistry tests have been done in SWNS to confirm these hypotheses. It would be beneficial for future studies to analyze soil metal and base cation concentrations at soil transects with varied concentrations of DOC, to investigate the role of DOC on Al soil cation exchange. Investigating the source of Al_t will help increase our understanding of acidification recovery trends in high-DOC regions.

The amount of time water chemistry was sampled in MR and MPB limits the conclusions we can draw regarding acidification recovery and the threat of Al to aquatic organisms. Water chemistry sampling for MR began during the 1980s, capturing the decline in acid deposition, but not capturing any trends before then. As the classic model follows acidification from beginning to end, the lack of data before 1980 limit whether we can say our system followed the classic model from stages one to four. In addition, it appears that there is recovery from acid deposition in MR and MPB, as sulfate concentrations are decreasing; however, the continued increase in Al_t indicates a divergence from the classic model. Divergence from the classic model in MR and MPB suggests a hysteresis acidification recovery response in high-DOC rivers; however, we may just be observing a delayed response in pH and Al_t due to inputs from organic acids buffering acidity changes. Further monitoring is required to determine if the freshwater acidification recovery divergence continues, or whether Al_t decreases and the freshwater trends converge with those expected from the classic model.

Increased Al monitoring is required at more sites across NS to quantify spatial trends and determine if the divergence of the classic model is a regional phenomenon. Although MR and MPB Al trends were quantified in this study, and appear to diverge from the classic model, no Al trends have been assessed for other regions in NS, therefore it is unclear whether the Al trends in MR and MPB are a localized event or regional phenomenon. Al trends should also be investigated in other regions of the globe that share low weathering bedrock and high-DOC freshwaters, to determine if the classic model fails to predict chemical acidification recovery in other high-DOC regions.

It would be beneficial for EC to include the filtration of samples in their sampling methods to reduce trend uncertainties associated with clay particles and to monitor trends of dissolved chemicals. Unfiltered samples include concentrations of elements bound to clay particles; these particles may be due to flood events or high

sediment influx and are not necessarily representative of the long-term trends of dissolved chemicals.

Aqueous Al speciation is known to be highly variable in aquatic environments, with variable effects on fish (Driscoll et al., 1980). The KCC record includes Al_t; however, the speciated forms of Al were not measured. With regards to the toxic forms of Al_t, Al_i, Dennis and Clair (2012) show that these non-complexed Al_i concentrations are indeed above the threshold to protect aquatic life. Without speciated forms of Al being monitored by EC or other groups, current levels of toxic Al_i are unknown. If Al_i levels mimic Al_t concentrations, we can assume that Al_i concentrations are increasing, and may be posing a threat to salmon and other aquatic populations, now or in the near future.

2.6.6. Revised Acidification Recovery Model

The increase in Al and lack of base cation replenishment, after >20 years of decreased acid deposition, was not predicted by classic recovery model, indicating a new model is required for regions with high organic acid concentrations, with the inclusion of TOC in the model. Here we propose a new recovery model, which considers the role of TOC in low-bedrock weather freshwater systems (Figure 2.19). Stages one to four of the classic model remain consistent, indicating a pre-acidified state followed by increases in sulfate deposition, cation depletion and a new acidified steady state. Added into the stages two to four is the inverse relationship between TOC and SO_4 noted by Monteith et al. (2007). Expected in stages three and four are increases in heavier cation concentrations in freshwaters, such as Fe and Al, due to base cation depletion in soils. In stage five, consistent with the classic model, acid deposition will reduce, decreasing sulfate concentrations; however, the new model includes increases in TOC and the continued increases in Al_t due to the continued presence of acidity. In stage six, the TOC concentration increases maintain freshwater acidity and result in a lag in pH recovery. As pH increases in stage six, base cations increase inversely with Al_t decreases. The rate of increase in base cations is dependent on soil replenishment through bedrock weathering.

Decreases in Al_t should coincide with increasing soil CEC base saturation, as lighter base cations will be available for acidity buffering instead of Al ions, and increases in soil pH will result in reduced Al mobility. The return to a pre-acidified steady state in stage seven may take much longer than in low-TOC regions due to the delay in pH recovery and soil cation replenishment.

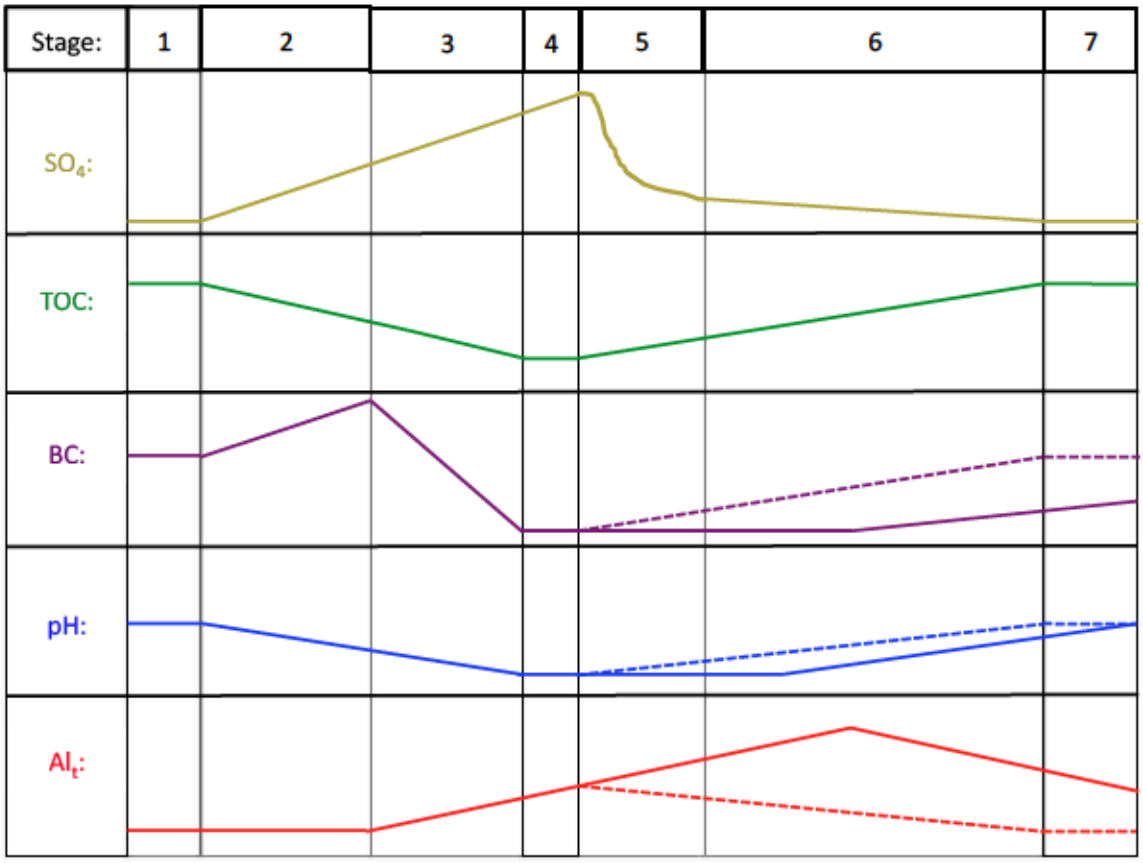

Figure 2.19: Predicted response of SO_4, TOC, Base Cations (BC), pH, and Al_t in high-DOC regions before (stage 1), during (stages 2-4), and after (stages 5-7) acid deposition, with dashed lines indicating response predicted by the classic model solid lines indicating the response predicted by the revised model.

2.7. Conclusion

Al is a toxin to organisms and is mobilized due to chronic acidification of soils and freshwaters. pH and aluminum concentration increases in freshwaters have been recorded across Europe and North American since the 1990s (Skjelkvale et al., 2005); however, in regions with high organic acids, acidification recovery is unclear.

A computer model predicted the chemical stages of recovery for freshwaters following reductions in acid deposition; however, this model did not include the impact of organic acids on acidification recovery. This study explores Al concentrations in high TOC rivers in response to reduced acid deposition. We asked: do the water chemistry trends in SWNS match the recovery stages of the classic model, and do monthly changes in flow, DOC and temperature drive changes in monthly Al_t concentrations in NS rivers?

Water chemistry trends in SWNS diverge from the recovery stages in the classic model. Reductions in sulfate acid deposition are consistent with the classic model; however, increases in Al concentrations suggest a divergence. Increases in Al concentrations coincide with decreases in Ca and sulfate, and increases in TOC and pH. Low soil base cation saturation explains the inverse trends of Al and Ca in SWNS rivers, with increased TOC buffering changes in soil pH. A new acidification recovery model is proposed for regions with high-TOC, incorporating the role of organic acids in buffering soil pH and increasing Al mobilization.

We measure a sudden upwards shift in 2003 in monthly Al concentrations, associated with increases in TOC, flow and air temperature. The 2003 shift is due to a high flow event; Al trends before and after the high flow event are significantly different, suggesting an ecosystem shift. Al concentration fall peaks in MR and MPB are concurrent with fall peaks in TOC; following the 2003 shift, autumn Al peaks appear to be occurring earlier. Drivers related to changes in the climate (increase in winter flows, and increased summer temperatures) coincide with the aluminum increases.

In high-DOC rivers, acidification recovery in NS rivers via reduced SO_4 concentrations from 1980-2014 and decreased SO_4 acid deposition have generated a new problem: increasing aluminum. We hypothesize that other acid sensitive (regions with thin soils, weathering-resistant bedrock, and low ANC) watersheds should also show aluminum increases, such as watersheds in Maine, USA, where

ANC and base cation concentrations have declined, and DOC concentrations have increased from 1990-2001 (Skjelkvale et al., 2005). In these acid sensitive rivers, emission reductions are not enough to address the problem of acidification, and on the ground mitigation via liming is known to be effective in addressing these serious consequences of chronic acidity and increasing aluminum (Lawrence et al., 2016, Sjöstedt et al., 2013).

This research has two important policy implications. Al should be monitored more extensively in freshwaters, in both NS and other high-TOC regions globally. For catchments that divert from the classic acidification recovery model and follow the "increasing Al risk" of acidification recovery, calcium should be added to the soils via liming (the application of base cations to soils). There is no sign of metal exports leveling off based on Al_t trends in MR and MPB, so for these types of catchments, standard emission reductions are not enough to achieve ecosystem recovery, and terrestrial liming is needed to avoid worsening Al conditions which pose a high threat to aquatic organisms.

Chapter 3 Estimated Ionic Aluminum Trends In South Western Nova Scotia From 1980-2014

3.1 Preamble

Sarah MacLeod, Shannon Sterling, Lobke Rotteveel, Tom Clair, Rob Jamieson

The majority of this chapter is composed of a manuscript in preparation for submission to a journal in winter 2017. I am primary author on the paper and this chapter, and created the primary study design, implemented the design, collected water samples, analyzed the data and wrote the introduction, methods, results, discussion and conclusion. Dr. Sterling provided the study idea and study design (including sampling sites, frequency and water chemicals monitored), in addition to suggestions on statistical methods for the ionic aluminum (Al_i) equations. Lobke Rotteveel prepared maps of the spatial trends of Al_i in NS and collected Al_i samples during spring and summer 2016. Tom Clair provided background knowledge on Al_i sampling techniques and in-stream chemical interactions. Dr. Jamieson provided information regarding regression types and statistical methods used for creating the Al_i equations.

3.2 Introduction

Increases in Al_i, a toxin to many aquatic organisms, are linked with chronic acidification; however, few studies have assessed Al_i trends in Nova Scotia (NS). In NS, a region highly affected by acid deposition (>0.16 g/m²/month of non-sea-salt SO_4 atmospheric deposition in Kejimkujik in 1986-refer to Chapter 2.6.1), declines of Atlantic salmon (*Salmo salar*) populations may be due to toxic levels (> 15 µg/L according to Howells et al. 1990) of Al_i. In a fall 2006 survey of NS freshwaters, toxic Al_i concentrations were measured in seven of 43 sites examined (Dennis and Clair, 2012). No survey has been conducted since the 2006 study; however, total Al (Al_t) has significantly increased (with 95% confidence) in two rivers in SWNS from 1980-2014 (refer to Chapter 2.5.2). Increases in Al can pose a risk to the health aquatic organisms, by increasing the ratio of toxic Al_i species.

Chemical separation of Al species is required in the field to obtain the representative ratio of Al_i species from the freshwater site; however, the separation is costly and time consuming. To provide an alternative method for monitoring Al_i concentrations, Dennis and Clair (2012) created an equation to predict Al_i using water chemistry parameters that are more cost-effective. Their equation was based on field measurements of Al_i data collected across Canada's Atlantic provinces in the fall of 2006; however, their equation did not account for geological and seasonal variations of Al_i drivers, which vary spatially. A new, river-specific Al_i equation is required, with data derived from the watershed's geology, vegetation and chemistry, to provide reliable and accurate predictions. The river-specific equations are necessary if Al_i predictive equations are to provide cost-effective alternatives to field samples.

In this study, we measure Al_i concentrations in two rivers in Southwestern NS (SWNS) to determine if Al_i is above the 15 µg/L toxic threshold for Atlantic salmon. We also create a regression to predict Al_i concentrations based on water quality parameters (eg. pH, temperature and dissolved Al – parameters which do not require the separation of specific species).

3.2.1 Soil and Freshwater Acidification

Continued acidification from acid deposition results in the lowering of pH in soils and freshwater systems. Gaseous sulfur and nitrogen oxides released from industrial emissions combine with water vapour to form acidic solutions known as "acid rain" or "acid deposition". The peak of acid deposition occurred in the 1970s, with emissions and acid deposition being transported to NS from central Canada and Northeasthern USA sources towards Atlantic Canada provinces (Summers and Whelpdale, 1976). Although soils have base cations which exchange with hydrogen ions (H^+) to buffer pH changes in soils, the exceedance of critical loads for H^+ results in the depletion of base cation concentrations in the soils and the reduction in soil pH (Whitfield et al, 2006). The amount of negative sites, which can exchange cations

in soils are known as Cation Exchange Capacity (CEC); increased cation exchange results in the depletion of cation saturation in a soil's CEC, and the increase in H^+ bound to soil negative sites. With excess hydrogen ions, and reduced pH buffering, the soil pore water pH decreases. Leaching of SO_4 from soil waters into rivers, and decreased soil Acid Neutralizing Capacity (ANC), results in decreased river pH (Driscoll et al., 2001, Clair et al., 2011).

3.2.2. Acidification Recovery Trends

Although chemical acidification recovery is occurring in freshwater systems globally (Warby et al., 2005, Skjelkvale et al., 2005, Hesthagen et al., 2011, Monteith et al., 2014, Evans et al., 2001), reductions in acid deposition across NS have not been accompanied by freshwater recovery (Clair et al., 2011, Jefferies et al., 2003). Intergovernmental emission reduction agreements, like the 1991 Canada-US Air Quality Agreement, were created to promote the reduction of industrial emissions and decrease acid deposition (Butler et al., 2001). Decreases in freshwater acidity have been linked to reductions of acid deposition across Europe and North America (refer to Chapter 2.2.3); in NS, reductions in sulfur and nitrogen deposition rates to below the critical load is not expected (Whitfield et al, 2006) and pH measurements in NS rivers from 1982-1996 showed no significant trends (Watt et al., 2000). From 1990-2001 in Europe and North America, Atlantic Canada and Maine freshwaters were the only sites with continued significant acidification, reduced gran alkalinity (ANC_G – measured by titrating acid into a solution and linearly extrapolating H^+ concentrations from added acid), decreased SO_4 concentrations and decreased combined Ca and Mg concentrations (Skjelkvale et al., 2005). There have been no ANC_G increases in SWNS rivers (Clair et al., 2011).

Lack of pH recovery in SWNS rivers is attributed to high concentrations of organic acids (Clair et al., 2007). Increases in dissolved organic carbon (DOC) concentrations have been reported in the United Kingdom (Evans et al., 2005) and Eastern Canada (Couture et al., 2012) following acid deposition reductions; decreases in acid deposition SO_4 increase organic carbon solubility by increasing soil pH and

decreasing ionic strength in pore water (Monteith et al., 2014). DOC is the source of organic acidity, which buffers changes in pH and results in continued river acidity in regions with high-DOC (Clair et al., 1992). Although sulfate and nitrate deposition have decreased in SWNS (refer to Chapter 2.5.1), total organic carbon (TOC) concentrations are increasing in SWNS rivers and are positively correlated with increases in Al (refer to Chapter 2.5.4).

3.2.3 Al Mobilization

Increases in soil acidity can result in increases in Al mobilization. Clays, and other minerals, include Al in their chemical formulas, and can have Al ions electrostatically bound to the negative sites along their surfaces. Al can be released into soil pore water as acid inputs deplete the soil's base cation saturation (Fernandez et al., 2003). As the saturation of base cations and soil solution pH decrease, exchangeable cations available in the soil shift from Ca and Na towards soluble Al (Walker et al., 1990, Schlesinger and Bernhardt, 2013).

Increases in DOC are linked with increases in Al mobilization. High concentrations of organic acids in soil pore water can decrease soil pH, resulting in low CEC base cation saturation depletion and Al dissolution (De Wit et al., 2007). DOC can also complex with Al, which creates a chemical concentration gradient; DOC-Al complexation follows Le Chatelier's principle by further increasing Al concentrations and creating a new chemical equilibrium in the soil (Jansen et al., 2003).

3.2.4. Aluminum Speciation in Freshwater

Water chemistry controls aluminum speciation. The fraction of each positive ionic aluminum species in freshwaters is dependent on pH and temperature in the water column (Figure 3.1). Helliweli (1983) identified the speciation of Al in laboratory experiments at 25 °C across the pH spectrum: $[Al(OH)_4]$ peaks at pH 6.4 (at 25 °C) and precipitates out; the positive Al_i (Al^{3+}, $Al(OH)_2^{1+}$, $Al(OH)^{2+}$ and $Al_{13}(OH)_{32}^{7+}$) dominate Al species at 4.0 <pH< 6.0 (Figure 3.1). Lydersen (1990) found that Al_i dominates Al fractions at pH<6 at temperatures of 2 °C, and pH<5.5 at temperatures of 25 °C.

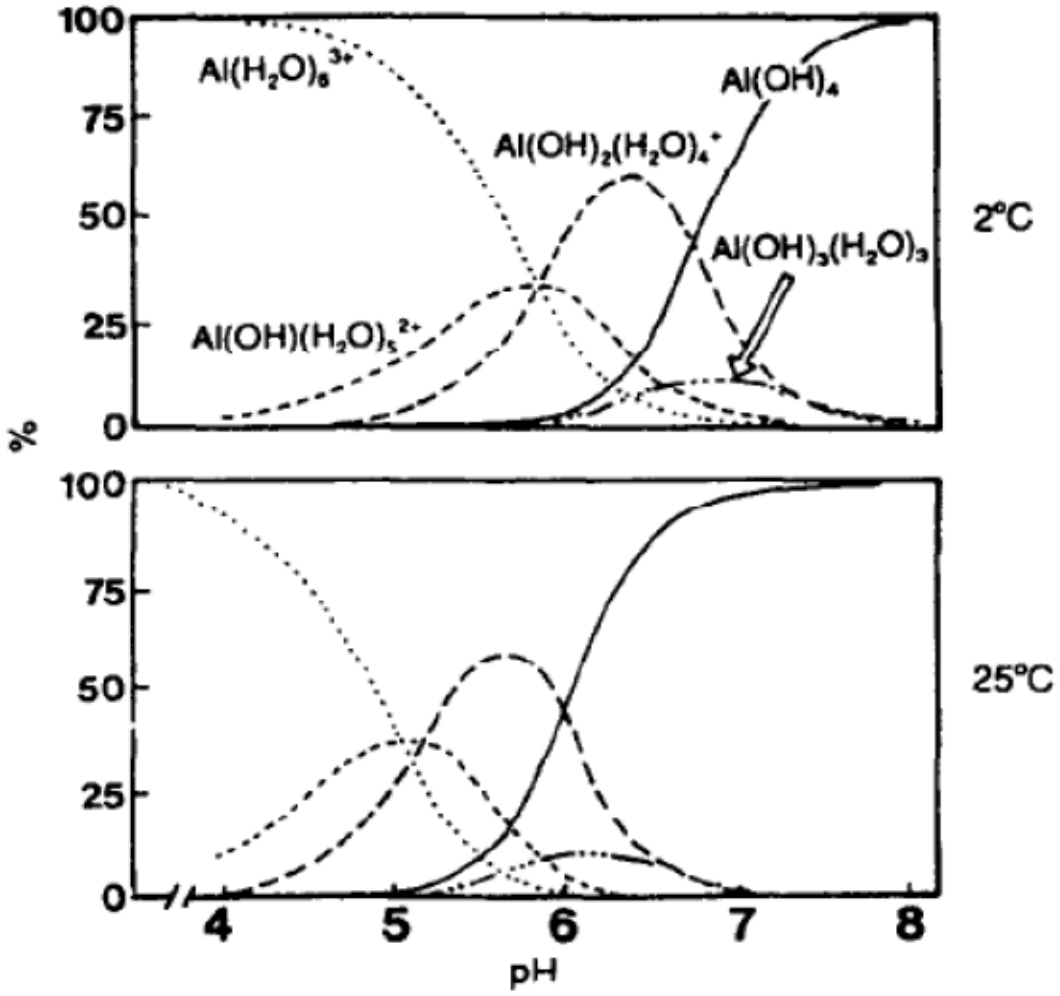

Figure 3.1: Distribution of Al species (as a percent of total Al) over a pH range from 4-8 at 2 °C and 25 °C. (after Lydersen, 1990).

Freshwater Al species fractions are controlled by the complexation of Al_i and DOC, which form organoaluminum complexes (Al_o). Al_o will either remain in solution or precipitate; however, not all Al_i are bound to DOC, resulting in some free Al_i particles (Tipping et al., 2002). At pH <6, Al^{3+} are the dominant Al forms included in Al_o complexation, with $Al(OH)^{2+}$ dominanting forms of Al in Al_o at pH >6, based on an experimental humic ion binding model (Tipping et al., 2002). Although Al_o particles are nontoxic to fish, as their neutral charge doesn't bind with the negatively charged fish gills, high concentrations of Al_i can be toxic to several freshwater organisms (Wauer and Teien, 2010).

3.2.5. Ionic Aluminum Toxicity

Al_i toxicity thresholds for Atlantic salmon vary between 5-50 µg/L. The binding of Al_i to fish gills can cause suffocation and mortality (Exley et al., 1991); Al also damages the gills and affects fish plasma by reducing nutrient intake by gills (Nilsen et al., 2010). Freshwaters in Norway with Al_i levels between 5-10 µg/L can cause up to 50% mortality in salmon smolt (Kroglund et al., 2007B); however, a study in Nova Scotia, Canada of the response of salmon to pH and Al_i concentrations used 50 µg/L as their threshold (Lacroix and Townsend, 1987) based on the reductions in salmon growth at 50 µg/L in Nova Scotia rivers identified by Peterson et al. (1989) in August 1987. An investigation of salmon marine survival rates after exposure to Al_i concentrations in Norway used 28 µg/L as their "low" concentration and 48 µg/L has their "high" exposure concentration (Thorstad et al., 2013).

The toxicity of Al_i on organisms is pH-dependent. The European Inland Fisheries Advisory Council (EIFAC) suggests an Al_i toxic threshold for Atlantic salmon in freshwaters of 15 µg/L at pH between 5.0 and 6.0, and 30 µg/L in pH <5 (Howells et al., 1990) based on geochemical and toxicological studies regarding Al_i and Atlantic salmon; in pH between 5.0 and 6.0, the $Al(OH)_2^+$ and $Al(OH)^{2+}$ species dominate, which are more toxic to organisms than Al^{3+} (which dominates at pH<5), as the lower ionic charges allow for greater amounts of Al_i to bind to negative sites, compared to the Al^{3+} ion (Helliweli et al., 1983). At pH >6, the toxic effects of Al_i to salmon are considered negligible, due to the low solubility of Al at pH>6 (Dennis and Clair, 2012). For this study, we use the Howells' (1990) Al_i 15 µg/L concentrations, to allow comparison with the Dennis and Clair (2012) survey, where more NS rivers had pH between 5.0 and 6.0, than pH<5.0.

The effects of aluminum concentrations vary with the lifestages and lifestage transitions of the salmon. Atlantic salmon transition from eggs to parr, then to smolt before maturing into adults; however, smolts are the most sensitive lifestage to acid and aluminum exposure (Monette and McCormick, 2008). Increased sensitivity of the smolt lifestage is attributed to increased environmental stressors during

transition from parr to smolt (smoltification), and the delayed impact of Al accumulation on gills during seawater entry (Kroglund et al., 2007A). The smoltification transition stage occurs during the spring months when the parr undergo morphological and physiological changes in order to help the salmon survive in the ocean where they will mature into smolts (Nilsen et al., 2013). During smoltification, salmonids are most vulnerable to morphological and physiological changes from toxic Al_i accumulation on gills; increased exposure of salmonids to Al_i results in reduced marine and freshwater survival (Kroglund et al., 2007B).

In SWNS, the Southern Upland Atlantic salmon populations have decreased by 88-99 % in four rivers (Bowlby et al., 2013); Al_i levels may be a factor in these declines due to chronic acidification of NS rivers and increases in Al_t. Due to the high concentrations of DOC in SWNS rivers, it was believed that all available Al_i were bound to DOC, thereby fish gills were protected from adverse effects of Al (Lacroix et al., 1990); however, Dennis and Clair (2012) found Al_i concentrations for seven out of 43 rivers in NS were >15 µg/L in the fall of 2006, and therefore not all Al_i was complexed with DOC. If Al_i concentrations are concurrent with increases in Al in SWNS, Al_i concentrations may be influencing Atlantic salmon population declines.

3.2.6. Ionic Aluminum Trends

Following acid deposition reductions, decreasing Al_i concentration trends were reported in the USA and across Europe (Burns et al., 2006, Monteith et al., 2014). In New York State, USA, Al_i concentrations from 1992-2001 declined by 0.12 and 0.13 umol/L/year in the Catskill Park rivers and Adirondack Park lakes, respectively (Burns et al., 2006), and fell by 0.21-9.74 umol/L from 1991-1995 in the Neversink River in New York, USA (Baldigo and Lawrence, 2000). Al_i concentrations declined at 20 of 22 European rivers and lakes monitored by the UK Acid Waters Monitoring Network (AWMN) from 1988-2008 (Monteith et al., 2014); Al_i concentrations declined significantly in 10 AWMN sites, a trend concurrent with decreases in sulfate (Davies et al., 2005).

Monthly fluctuations in Al_i concentrations are positively correlated to DOC, and negatively correlated to pH (Kopacek et al., 2006, Campbell et al., 1992); however, the role of discharge on Al_i concentrations is unclear, as Al_i concentrations are positively correlated to discharge (Campbell et al., 1992) and negatively correlated to discharge (McKnight and Bencala, 1988). Along the Czech-German border, lake Al_i from 2000-2005 peaked in the winter to spring (Kopacek et al., 2006), while Al_i concentrations in surface waters monitored between 1990-1993 in the Kola Peninsula in Russia were highest in the month of May (Rodushkin et al., 1995). Both Kopacek et al. (2006) attributed the increases in Al_i to decreases in soil pH during increased rainfall, and Rodushkin et al. (1995) attributed increases in Al_i to increased discharge flushing Al_i from soils. Al_i concentrations were highest in the winter months compared to summer months in 1998 for the Plesne and Certovo Lakes, located in the Bohemian Forest along the Czech-German-Austrian border (Kopacek et al., 2000). Nitrate concentrations are attributed to the winter increase in Al_i concentrations in the Plesne and Certovo Lakes as nitrate is a source of acidity and a complexing agent for Al_i (Kopacek et al., 2000). Minimum Al_i concentrations for three Quebec rivers in 1986 occurred during the winter and summer months (Campbell et al., 1992); the peak in Al_i concentrations during the spring of 1986 in the three Quebec rivers coincided with spring melt, decreased pH and increased DOC and flow (Campbell et al., 1992). Weekly water chemistry samples from Snake River within the Colorado Rocky Mountains from 1980-1986 contradict Campbell et al., 1992 findings, as the spring melt floods in Snake River correlate to decreases in Al concentrations (McKnight & Bencala, 1988); McKnight and Bencala suggest flow dilutes Al.

The volume of water flushing a system, and the pathway of waters through soils affect Al concentrations. Al concentrations from 1980-1986 were lowest during spring months in the Snake River in Colorado, USA, due to dilution from spring melt (McKnight and Bencala, 1988); however, Al concentrations for the River Severn in Wales increased ten-fold during the stormflow peak (time of maximum flow) compared to the baseflow (time of natural flow levels maintained by the watershed

without storm influence) from 1983-1984 (Neal et al., 1986). Flow paths of water within soil columns are linked with seasonal changes in Al_i; Al_i concentrations are higher in the summer than spring in the White Oak Run in the Shenandoah National Park, Virginia, USA, as water flow paths in the summer occur in deeper, Al_i-rich soil horizons (Cozzarelli et al., 1987), and high organic and particulate Al concentrations during spring melt in Norway 1984-1985 are linked with lateral flow through shallow, Al_i-poor soil horizons (Sullivan et al., 1986). In SWNS, seasonal variations in river discharge are inversely related to pH changes (Watt et al., 1983); however, Al_i seasonal trends have not been assessed in SWNS. The variability of seasonal Al_i trends in the literature makes estimating seasonal trends in NS unreliable, requiring ground-truthing of Al_i concentrations in NS to understand the temporal trends.

Physical watershed characteristics control spatial variations in water chemistry. Watersheds with weathering-resistant bedrock, such as granites and slates, have lower ANC than regions with limestone or calcareous conglomerates due to limited nutrient replenishment from bedrock to soils (Bricker and Rice, 1989). Modelled streamwater chemistry in the Duddon River, England includes bedrock weathering rates, dissolution rates of $Al(OH)_3$ in mineral soils and catchment size to accurately estimate river chemistry trends (Tipping, 1989). Al_i concentrations increase with decreased watershed sizes (<500 ha) in Swedish catchments (Lofgren et al., 2010).

Dennis and Clair (2012) and Lazerte (1984) created empirical models for Al_i concentration estimation using TOC and dissolved Al concentrations; however, neither the Dennis and Clair model, nor Lazerte model can be applied to SWNS with certainty, as watershed-specific characteristics were not accounted for in the models. Using Al_i concentrations from 2006 across Atlantic Canada, Dennis and Clair (2012) created an empirical equation for Al_i, which included total Al (Al_t), TOC and pH; however, the data used to create the model was from various watersheds with different geological properties, and river-specific characteristics were not accounted for. The Dennis and Clair Al_i equation has not been validated using Al_i concentrations in SWNS. Lazerte (1984) determined Al_i could be best predicted

using fast-reacting Al concentrations (Al species which react with oxine within 15 seconds at pH>8.3) and TOC, using laboratory and field data in two Ontario watersheds from February to May, 1982; however, the Lazerte Al_i equation requires adjusting the water sample to pH>8.3 to measure the fast-reacting Al concentrations. A pH value of 8.3 is beyond those found in SWNS, therefore the fast-reacting Al concentration measurements do not represent *in-situ* river chemistry and would provide inaccurate Al_i estimates in SWNS.

3.2.7. Knowledge Gaps

As Al_i monitoring is expensive, due to the requirement of separating Al species in the field (to ensure measured Al_i values are representative of the river chemistry), little research has been done on Al_i concentrations trends in SWNS. Current Al_i concentrations have not been assessed in SWNS since Dennis and Clair (2012) surveyed Al_i concentrations across Atlantic Canada in the fall of 2006; no studies have identified long-term trends or the seasonality of Al_i in SWNS rivers. Al_i concentration trends are variable, Al_i concentrations have decreased in two sites and increased in 20 sites in the AWMN from 1988-2008 (Monteith et al., 2014); seasonal Al_i peaks vary spatially: from spring Al_i peaks in Quebec rivers in 1986 (Campbell et al., 1992), to winter Al_i peaks in Russia in 1998 (Kopacek et al., 2000). In addition, there are no river-specific Al_i equations that have been validated with Al_i concentrations in SWNS. In NS, where Atlantic salmon populations approach extirpation, Al_i may be a factor in the declines, as Al_i concentrations measured for seven of 43 NS river during the fall of 2006 were greater than the 15 µg/L toxic threshold for Atlantic salmon (Dennis and Clair, 2012); without knowledge on current Al_i levels and trends, and with no reliable alternative way to monitor Al_i, the threat of Al_i to Atlantic salmon and other aquatic organisms in SWNS remains unclear.

The Al_i definitions and methods used to measure Al_i vary in the literature. Studies have defined Al_i as inorganic Al, inorganic monomeric Al, labile Al, or cationic Al (Table 3.1). Terminology differences coincide with methodology differences, as Al

species being measured may differ (eg. solely Al^{3+}, or all positive Al_i species). Reported Ali concentrations range from 10 to 72 µg/L due to inconsistencies between definitions and methods (Table 3.1). The 62 µg/L range between results can affect the toxicity status of rivers in relation to the 15 µg/L toxic threshold for Altantic salmon. In addition, definition and method inconsistencies result in the inability to compare measurements, thus limiting our general knowledge of the trends of Al_i globally. For the purpose of this study, we referred to Al_i as all positive ionic species of Al (Al^{3+}, $Al(OH)^{2+}$, and $Al(OH)_2^+$ based on Poleo, 1995).

Table 3.1: List of terminology, methodology and trends from various studies on Al species. Al_t=total Al, Al_o=organic Al, Al_{nl}=non-labile Al, Al_{tm}=total monomeric Al, Al_{om}=organic monomeric Al, Al_{tr}=total reactive Al, Al_{nlm}=non-labile monomeric Al, Al_m=monomeric Al. CEC= Cation Exchange Column, ICP-AES= Inductively Coupled Plasma-Atomic Emission Spectroscopy. AWNM= Acid Waters Monitoring Network.

Al Species	Definition	Analysis Method	Trend	Location	Reference
Al_i	Inorganic Al	Colourimetry (Al_t-Al_{nl})	Decreasing Al_i from 1988-2008	AWMN in UK	Monteith et al. (2014)
Al_{im}	Inorganic monomeric Al	Colourimetry (Al_{tm}-Al_{om})	Decreasing Al_i from 2001-2011	New York, USA	Josephson et al. (2014)
Al_i	Ionic Al	CEC (Al_t-Al_o)	Mean NS Al_i=25.3 µg/L Mean NB Al_i=31.0 µg/L	Atlantic Canada	Dennis and Clair (2012)
Al_i	Ionic Al	Colourimetry	Decreasing Al_i in lakes	Norway	Hesthagen et al. (2011)
LA1	Inorganic Al (sum of inorganic and monomeric Al species)	ICP-AES, Flow injection, Pyrocatechol violet, and CEC (Al_{tr}-Al_{nl})	15% of LA1 samples were >10 µg/L	Norway	Kristensen et al. (2009)
Al-l	Labile/cationic/inorganic monomeric Al	Colourimetry (Al_{tm}-Al_{nlm})	Decreasing Al-l across the UK	AWMN in UK	Evans & Monteith (2001)
Al_{im}	Labile Al (free and inorganically complexed Al)	Van Benschoten method	Mean Al_{im} of 72 µg/L from 2009-2010	China	Wang et al. (2013)
Al_i	Inorganic monomeric	Colourimetry and CEC (Al_m-Al_o)	Al_i fraction decreased in catchments between 1991 & 2007	Czech Republic	Kram et al. (2009)
Al_i	Inorganic Al	AAS	Decreasing Al_i from 1990-2010	Adirondack Mountains, USA	Strock et al. (2014)

3.3. Objectives and Research Questions

Although peak Al_i concentrations have been reported during the spring in Quebec (Campbell et al., 1992), and the winter in Russia (Kopacek et al., 2000), the seasonality of Al_i concentrations in SWNS is unknown; long-term trends of Al_i in high DOC, low-bedrock weathering watersheds were not found in the literature. We will identify current seasonal and long-term trends of Al_i in a DOC-rich (high DOC concentrations – ie >10 mg/L) catchment. In addition, as no study has provided a validated Al_i equation that is catchment specific for SWNS, this study will provide an Al_i equation tailored to SWNS, as an alternative to in-field Al speciation separation methods.

Our study sites are located in SWNS and were chosen due to their >20-year long-term water chemistry monitoring database and high DOC concentrations in freshwaters (Ginn et al., 2007). In SWNS, Environment Canada (EC) has been monitoring Mersey River (MR) and Moose Pit Brook (MPB) since 1980 and 1983, respectively. Continuous hydrological data was collected at MR and MPB since 1968 and 1980, respectively. The acidity of the SWNS freshwaters is due to the combination of acid deposition and organic acid sources originating from wetlands in the region (Gorham et al., 1986, Kerekes et al., 1986, Clair et al., 2008). Insight on how Al_i concentrations are influenced by pH and DOC can be gained by monitoring seasonal and long-term Al_i concentrations.

To identify current trends of Al_i in SWNS and provide a SWNS-specific alternative method to field Al separation for Al_i monitoring, we asked the following research questions (RQs) and proposed hypotheses (Hs):

RQ 1 Are Al_i concentrations in MR and MPB currently (2015-2016) above the 15 µg/L toxic threshold?

H1.1. Based on field samples from 2015-2016 in MR and MPB, Al_i concentrations are above 15 µg/L.

H1.2. Al_i concentrations peak during the fall months, correlating to increased flow and decreased pH.

RQ 2 **Are DOC, flow and pH variables required to make an Al_i equation with 95% significance in MR and MPB?**

H2.1. Al_i can be estimated in MR and MPB with 95% significance, using DOC, flow and pH parameters.

RQ 3 **Are Al_i concentrations increasing in SWNS from 1980-2014?**

H3.1. Using the Al_i equations for MR and MPB on long-term EC water chemistry data for MR and MPB, Al_i concentrations are increasing in MR and MPB, concurrently with known increases in Alt and TOC (refer to Chapter 2.5.2).

RQ 4 **Can an Al_i equation predict within 20% of known Al_i concentrations for other NS rivers?**

H4.1. Al_i equations can predict within 20% of known Al_i concentrations for other NS rivers.

To answer the above hypotheses, water samples from two rivers in SWNS were collected weekly/monthly from April 2015-July 2016 and water chemistry parameters are measured. Dissolved Al (Al_d) and organic Al (Al_o) measurements are used to indirectly estimate Al_i ($Al_{i\text{-}direct}$, Equation 1) for the 2015/2016 water samples.

$$Al_{i-direct} = Al_d - Al_o \quad \textbf{(1)}$$

$Al_{i\text{-}direct}$ concentrations exceeding 15 µg/L will be assessed for the 2015 $Al_{i\text{-}direct}$ concentrations, and the seasonality and correlations of $Al_{i\text{-}direct}$, flow and DOC concentrations in SWNS in 2015 will be determined. Sampling events were separated into three hydrograph components (baseflow, falling limb-time period where flow returns to baseflow from stormflow peak, and rising limb-time period

where flow increases in response to increased water inputs) to assess the role of storms on water chemistry in SWNS rivers. Al_i predictive equations for two rivers were created using water chemistry parameters monitored by EC. The use of EC parameters increased the applicability of the Al_i equations to all EC water chemistry databases; a standard water sampling parameters list is used for all EC freshwater samples in NS. The calculated Al_i values estimated from the equations (referred to as $Al_{i\text{-}c}$) were then validated using data from 2016 to assess accuracy of the MR and MPB equations. $Al_{i\text{-}direct}$ measurements were also obtained from other regions in NS to validate and assess the extrapolation of the Al_i equations. To quantify Al_i trends between 1980-2014, the MR and MPB Al_i equations were back-cast using the >30-year water chemistry databases from EC. The 20 most extreme outliers from the Al_i estimates of MR and MPB between 1980-2014 are plotted against the parameters used in the Al_i-predictive equations to understand which parameters are controlling Al_i extreme estimates.

3.4. Methods

3.4.1. Study Sites and Sampling Frequency

MR and MPB were chosen as the sampling sites to monitor Al_i in SWNS. MR and MPB are two of the Kejimkujik Calibrated Catchments (KCCs), where water chemistry and hydrological data have been collected for >30 years by EC. The two sites are underlain by slow weathering granites and slates, contributing few nutrients, such as Ca and Mg, to their thin soils, and have been affected by acid deposition since the 1980s (refer to Chapter 2.4.1). The MR catchment is 291 km^2, and the MPB catchment is 17 km^2.

Over 2015-2016, weekly water samples were collected, and *in-situ* data measured in MR and MPB by the Dalhousie Hydrology Research Group during each visit to the rivers (hereby referred to as a "sampling event"). Water chemistry data from MR and MPB were collected at the same locations used by EC to allow future comparisons between EC samples and the samples from this study. Samples were collected weekly from MR and MPB between April 22, 2015 – October 28, 2015 and

April 22, 2015 – October 14, 2015, respectively. The weekly intervals were chosen to capture short-term changes, while ensuring independence of observations. Sample independence was based on the assumptions that the MR and MPB catchments were small, and that the influence of individual storm events on hydrological and hydrochemical conditions did not last longer than a week. Due to limited funding, sampling was reduced from weekly to monthly from November 4th, 2015 – April 28th, 2016 in MR. As the road to the MPB site is not maintained in the winter season, no samples were collected until April 28th, 2016 in MPB due to limited winter access.

3.4.2. Climate Monitoring

For all field-sampling dates, the sampling event crew recorded climate data (air temperature, precipitation, cloud cover, last rainfall) for MR and MPB during sample collection. For both sites, the Kejimkujik 1 weather station (Climate ID: 8202592; 44.24'11.020" °N, 65.12'11.070" °W; Figure 3.2))was used to collect air temperature data for each sampling event; the Kejimkujik 1 weather station is run by the Government of Canada and is 3.5 km from the MR site, and 13 km from the MPB site. Missing air temperature data were replaced with air temperature data monitored from the Dalhousie University Hydrology Research Group's Measurement Tower (MET) located one kilometer to the Northwest of the MPB site (Figure 3.2). The Canadian Air and Precipitation Monitoring Network (CapMoN) Kejimkujik station collected total shortwave radiation (direct and scattered) every 15 minutes with a pyranometer (Figure 3.2); the radiation data is assumed to be representative of both sites.

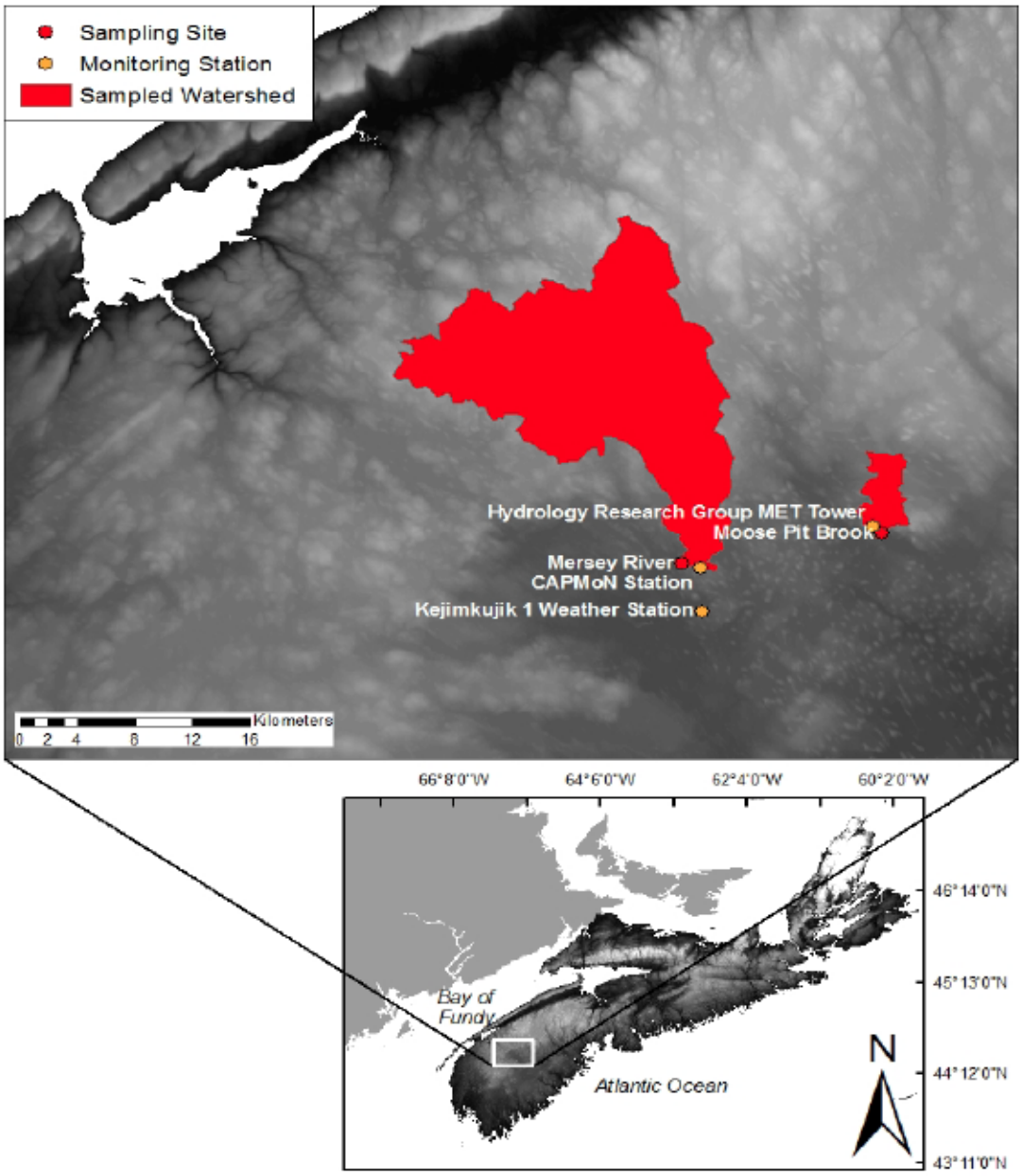

Figure 3.2: Climate monitoring sites in SWNS used to record air temperature and precipitation data for all 2015-2016 sampling events. Dalhousie Hydrology Research Group Measurement Tower (MET), CAPMoN=Canadian Air and Precipitation Monitoring Network. Map courtesy of Lobke Rotteveel.

3.4.3. Water Chemistry Analysis

3.4.3.1. *In-Situ* Water Chemistry Analysis

Water temperature, pH and conductivity were measured *in-situ* during each sampling event. Two instruments, a handheld multi-parameter pH meter and a YSI

sonde were used for the *in-situ* measurements to ensure data collected by the instruments was repeatable. The handheld pH meter was chosen due its portability and low-cost, while the YSI was used due to its high precision and accuracy. A polyethylene bottle was rinsed three times with river water, to ensure no prior contaminants remained in the bottle, then filled halfway with river water. The handheld pH meter was then placed into the bottle and continuously moved until the temperature reading remained constant. Continuous movement of the water ensured the water did not develop a thermocline, and that the pH reading was representative of the entire container. Once the temperature was constant, the pH meter was stopped so the pH could adjust. Once pH has adjusted, the time, pH and water temperature were recorded. The YSI sonde was removed from its case and its electrodes were covered with a metal cap containing holes for protection and water through-flow. The electrodes were then placed into the river and the instrument was given five minutes to adjust. When the temperature was stable, the time, water temperature, pH and specific conductivity were recorded. As the data from the sonde and pH meter deferred up to 1 pH unit at some points, only the sonde data was used during analyses, as its readings were obtained directly from the river and did not require water to be collected and tested in a separate container, therefore the sonde readings were more representative of the river.

3.4.3.2. Grab Samples

To assess water chemistry parameters related to Al_i, five grab samples per sampling event were obtained: DOC, pH, SO_4, Dissolved Metals (DM), and Total Digest (TD) of metals. The pH, and SO_4 samples are placed within polyethylene bottles, after being rinsed out with sample water three times down stream. For TD, DOC and DM, a clean 30 mL syringe is rinsed out three times downstream with river water; the syringe fills a polyethylene bottle for the TD sample, and is attached to a 0.45 um filter and collected in a polyethylene bottle for DM and an amber glass bottle for DOC. The DOC sample was collected in an amber glass to reduce microbial breakdown of organic matter in the sample due to increased temperature from light. In the DOC bottle, there is sulfuric acid preservative used to preserve the sample and

to eliminate the interference from inorganic carbon. A nitric acid preservative was added to the bottles prior to use by the Maxxam Analytical Laboratory; the Maxxam Lab provided the sampling bottles and is used for sample analyses. The acid is used to stabilize the trace metals in the sample. Grab samples were stored in a covered cooler with ice, to maintain river-representative sample temperatures and reduce microbial activity, while transporting samples to the Maxxam Analytics lab (for DOC, pH, DM and TD) and the Health and Environments Research Center (HERC; for SO_4) within three hours. The Maxxam Analytics lab was chosen due to its low prices, inclusion of sampling bottles, and quick turn-around time. The HERC lab was chosen to analyze sulfate concentrations, due to a lower limit of detection for the sulfate instrument compared to Maxxam Analytics.

3.4.3.3. Organic Metals Extraction

To measure organic metal complexes (including Al_o; sample referred to as Organic Metals), we use the methods for organic metal extraction by Dennis and Clair (2012). 28 mL of 0.4 M ammonium acetate buffer is passed through a clean 30 mL syringe and 0.45 um filter into a 3 cm, negatively charged cation exchange column (Bond Elut Jr. Strong Cation Exchange Column). A negatively charged column is chosen as to bind with all positive ions and only allow neutral (organic) compounds to pass. The buffer is passed through the column drop-wise at a rate of 28 drops/min; the buffer shifts the column pH towards that more common of Al_i speciation, to ensure more sample ions are bound to the column and better represent the river conditions. The buffer syringe and filter are removed, while a new syringe is rinsed three times with river water down stream, then filled to 28 mL and attached to a new 0.45 um filter. The syringe is attached to the column and the water is passed drop-wise at a rate of 28 drops/min. The eluate of the water passing through the column is not collected, as it is rinsing the column of the buffer solution. Once the 28 mL of water are passed through the column, the syringe is refilled and passed through the filter and column at 28 drops/min. Fifty milliliters of river water are passed through the column and collected in a polyethylene bottle. For Organic Metals, nitric acid preservative is added to stabilize the trace metals in the sample.

Solutions with known chemistry (blanks) were used to assess contamination during the Alo extraction procedure. Triply deionized water was collected before passing through the filter and column ('Blank Before'), and after ('Blank After'); as the triply deionized water would have traces of chemicals below the detection limits of our Laboratories, which would provide 'Not Detectable' results in our Blank Before sample, the presence of chemicals in the Blank After sample indicates leaching of chemicals from the column. Blanks were collected on 10% of samples and taken on randomly chosen sampling events, to ensure methodology techniques were consistent and column leaching was continually monitored.

3.4.3.4. Environment Canada Samples

EC has monitored water chemistry at MR and MPB since 1980 and 1983, respectively. EC collected grab samples for chemical analyses bimonthly to monthly at the Mersey River below Mill Falls (station 01ED0007) and Moose Pit Brook at Tupper Lake (station 01EE0005) (refer to Chapter 2.4.1.4 and 2.4.2). As the 2015-2016 samples had not been analyzed or quality checked, the EC database used for back-casting $Al_{i\text{-}c}$ stops at 2014.

Canadian National hydrometric monitoring program continuously monitored stage at MR below Mill Falls (station 01ED0007, 1968-2014), and MPB at Tupper Lake (station 01EE0005, 1981-2014). Stage data for MR and MPB were collected at 15-minute intervals by EC, then converted to flow using a river-specific stage-flow conversion created by EC. The stage and flow data are calibrated for instrument error and drift each year; however, as the 2015-2016 data collected were not calibrated due to a lag in processing, the stage and flow data presented in this study are considered preliminary and subject to change following calibration. The stages that coincided with sampling events were also categorized into hydrograph components.

3.4.4. Laboratory Analysis

3.4.4.1. Metals

The filtered and unfiltered metal grab samples from the field are analyzed at the Maxxam Analytics Laboratory in the Bedford, Nova Scotia. The samples are refrigerated at 1-6 °C until analysis. Maxxam protocols follow the approved methods of the U.S. Environmental Protection Agency (US EPA) for identifying trace elements in water (Method 200.8- EPA, 1994) and analyzing samples using Inductively Coupled Plasma-Mass Spectrometry (ICP-MS; Method 6020A-EPA, 1998).

Filtered samples, labeled DM and Organic Metals, follow the US EPA sample preparation for dissolved analytes in Method 200.8 (EPA, 1994). Each DM and Organic Metals sample has a 20 mL aliquot taken and is placed in a polypropylene centrifuge tube to be adjusted with nitric acid to a 1% (volume/volume) nitric acid solution before analysis. The samples are analyzed using ICP-MS (EPA, 1998).

Unfiltered samples labeled TD follow the US EPA sample preparation protocol for total recoverable analytes in Method 200.8 (EPA, 1994). The samples must undergo total digestion before they can be analyzed by an ICP-MS, as the grab samples may contain particles > 45 um, which can clog up the instruments. To prepare the samples, a 100 mL aliquot of each TD sample is transferred to a 250 mL Griffin beaker, then 2 mL of nitric acid and 1 mL of hydrochloric acid are added to the beaker. The beaker is then covered with an elevated watch glass and placed on a hot plate at 85 °C for approximately 2 hours to reduce the volume of the sample to 20 mL. The watch glass should then be lowered directly onto the beaker, and the sample should be gently reflux for 30 minutes then removed from the hot plate to cool. The solution is then completely transferred to a 50 mL volumetric flask, then deionized water is added until the solution is at 50 mL and mixed. The sample is left to settle overnight and any remaining suspended solids are filtered with a 0.45 um filter. A 20 mL aliquot of the solution is pipetted into a 50 mL volumetric flask, and

diluted with deionized water to adjust the chloride concentrations. An internal standards solution, 10 mL of scandium, yttrium, indium, terbium and bismuth diluted to 100 mL with deionized water is added to the sample before analysis. The prepared solution is then analyzed using ICP-MS (EPA, 1998).

Duplicates of metal samples were analyzed for 10% of samples for quality assurance and quality control. On randomly chosen sampling events, Al_o and one of TD or DM, were analyzed twice, independently, by the laboratory. Duplicates were requested to ensure results were precise and accurate. The laboratory also conducts duplicates, blanks, reference materials, matrix spikes, instrument calibrations and standards for quality control and quality assurance. Standards in the lab did not have matrices matched to the matrices of samples.

3.4.4.2. DOC

Samples labeled DOC are analyzed using a Continuous Flow Analyzer at Maxxam. Inorganic carbon is removed from samples using an automated pretreatment system, which acidifies the sample with sulfuric acid, then bubbles a high velocity nitrogen gas through the sample. The sample stream is transformed into a thin turbulent liquid film, which is transported through a multi-turn glass coil, which removes carbon dioxide. Inorganic carbon is removed at a purge rate of 600 mL/min. An aliquot of the carbonate-free sample is mixed with a stream of 1 M sulfuric acid and 4% potassium persulfate, then subjected to UV radiation. To reduce chlorine, 10% ascorbic acid is added to the sample. The sample is then dialyzed through a silicon rubber membrane and mixed with phenolphthalein indicator before being analyzed by a spectrometer at a wavelength of 550 nm. Maxxam uses a second source standard to analyze instrument calibration, and a same source standard to analyze for instrument drift. In addition, duplicates, spiked blanks and standards are analyzed in each batch of 20 samples for quality assurance and control.

3.4.4.3. pH

A pH meter, using a standard hydrogen electrode and reference electrode, is used to measure samples labeled pH at Maxxam. Before analyses, samples are refrigerated with lids sealed on the containers. Upon analysis, the pH meter electrodes are immersed into the sample. To ensure accuracy, a second source standard is analyzed to accept the instrument calibration, and after 20 samples, a same source standard is analyzed for instrument drift. Analysis is duplicated for one sample in each batch of 20 samples. There is also a laboratory controlled spiked blank analyzed in each batch of 20 samples. The pH meter will automatically adjust, to provide pH values normalized to 25 °C, for temperature differences between samples.

3.4.4.4. SO_4

Sulfate samples are analyzed at the Health and Environments Research Center (HERC) in Halifax, Nova Scotia due to the lower detection limits of their instruments compared to the Maxxam Laboratories. Samples are filtered in the lab with a 0.45 um filter, and refrigerated at 4 °C while awaiting analyses. Each sample is placed into an automated sample, where 25 uL of sample is used for analysis. Using a Ion-Chromatography System (ICS) 5000 Dionex detector, a blank is run through the machine, followed by external standards composed of 7 anions ranging from 4-4000 ppb to create a standard curve. A sulfate standard of 1000 ppb is analyzed by the detector, followed by 25 uL of the water sample. A second sulfate standard of 1000 ppb is analyzed after the sample to ensure reproducibility.

3.4.5. Al_i Calculation

Ionic aluminum is indirectly sampled, and therefore, we calculate $Al_{i\text{-direct}}$ based on the methods by Dennis and Clair (2012). Ionic aluminum is calculated as the difference between Al_d and Al_o (Equation 1), with Al_d concentrations from the DM sample, and Al_o from the Organic Metals sample. The difference between the two samples indicates how many positively charged ions were left on the column. Al_o and Al_d are comparable using this method, as their field sampling techniques and

laboratory analyses were identical except the use of the column. Data obtained during the 2015/2016 sampling events are available in Appendix C.

3.4.6. Al_i Prediction Equations

Using the weekly and monthly $Al_{i\text{-}direct}$ samples collected from MR and MPB, multiple linear regressions were created for MR and MPB to estimate Al_i (referred to as $Al_{i\text{-}c}$). The multiple linear regression method was chosen, as it incorporates multiple parameters into the model and it maintains simplicity. The regressions were created using the R statistical software (v. 3.1.0); using the least squares multiple linear regression ('lm') command available in R, parameter combinations were included in the regressions using trial and error to obtain the best R^2 possible.

3.4.6.1. Seasonality

The $Al_{i\text{-}direct}$ data were divided into seasons in order to account for changes in $Al_{i\text{-}direct}$ drivers due to changes in discharge and DOC (refer to Chapter 3.2.6). The 2015/2016 data were divided into three seasons, with date boundaries determined by dates with the highest $Al_{i\text{-}direct}$ to Al_d relationship. Season one (referred to as Spring/Summer) included data from April 1st-August 5th, season two was from August 12th-October 31st (referred to as Fall), and season three included November 1st to March 31st (referred to as Winter).

3.4.6.2. Regression Parameters

The $Al_{i\text{-}c}$ equations were created based on parameters that are known drivers of $Al_{i\text{-}direct}$ concentrations (Table 3.2). Several $Al_{i\text{-}c}$ equations were created, with specific equations tailored to the EC sampling program, ensuring only EC water chemistry parameters were included in these equations. Total and dissolved Al were included as possible parameters in the $Al_{i\text{-}c}$ equations as they indicate the amount of unspeciated Al in a water sample. The DOC parameter was chosen as a possible parameter due to its two effects on Al_i: a source of acidity and a complexing agent (Dennis and Clair, 2012). pH was included as a possible parameter due to the role water acidity plays in Al speciation (Poleo, 1995), while SO_4 was included as a source of acid that can be attributed to acid deposition in the region, as few SO_4

sources are naturally found in SWNS (Clair et al., 2011) . Discharge was included as a possible parameter, as it is linked to the seasonal changes in Al_i (refer to Chapter 3.2.6). Water temperature was considered a possible parameter to be included in the $Al_{i\text{-}c}$ regressions, as the ratio of positive Al_i increase with decreased temperature (Poleo, 1995); air temperature was included as a proxy to water temperature. Finally, total calcium was included as a possible parameter for the $Al_{i\text{-}c}$ regressions, as it is associated with ion exchange in soils (Schlesinger and Bernhardt, 2013).

Table 3.2: Parameters included in the $Al_{i\text{-}c}$ equations for MR and MPB.

Parameter	Parameter Abbreviation	Units
Total Al	Al_t	µg/L
Dissolved Al	Al_d	µg/L
Dissolved Organic Carbon	DOC	mg/L
pH	pH	pH units
Sulfate	SO_4	µg/L
Discharge	Dis	m^3/s
Water Temperature	T_w	°C
Air Temperature	T_a	°C
Total Calcium	Ca_t	µg/L

3.4.6.3. Parameter Proxies and Conversions

Seasonal and river-specific parameter conversions and proxies were created using the 2015-2016 field data. As some water chemistry parameters measured during the 2015-2016 field sampling were not measured by EC, similar parameters that were found in both the EC database and the 2015-2016 field samples were used as proxies; the initial 2015-2016 parameter was converted to the proxy based on a best-fit linear trendline between the two 2015-2016 parameters' data. The linear relationship was chosen as it maintains conversion simplicity. Conversions were separated by season and river, as we assumed that the chemical relationships were regionally- and seasonally-dependent (Appendix D).

For application of the Al_i equations to EC data, a conversion was required for Al_d; EC measured total Al (Al_t), the sum of Al_d, organic Al (Al_o) and particulate matter, but Al_d had a better correlation to Al_i (R^2 of 31% for Al_d vs. $Al_{i\text{-}direct}$, and 0.05% for Al_t vs. $Al_{i\text{-}direct}$, for combined seasonal samples in MR from April 22nd, 2015 to March 29th, 2016). Seasonal and river-based Al_d conversions were created for the EC equations, based on a quantified linear relationship between the Al_d and Al_t 2015-2016 field measurements. To apply the $Al_{i\text{-}c}$ equations to the EC database, the EC Al_t concentrations were converted into Al_d concentrations using the season- and river-specific conversions.

Linear conversions per season and river were also created to convert lab pH to *in-situ* pH. EC measured pH in the lab; lab samples may be less representative of river chemistry than *in-situ* data, as samples' chemistries may have shifted during travel. Increases in sample water temperature due to exposure to warmer air temperatures can decrease the sample acidity, as less CO_2 can dissolve in solutions at higher temperatures, resulting in chemical concentration differences compared to those in the river. *In-situ* pH are defined as river pH, as there is no travel time for measuring *in-situ* pH, water chemistry values would not contain errors due to extrapolation of data over time, but only possible equipment errors. To apply the $Al_{i\text{-}c}$ equations to the EC database, the EC lab pH values were converted into *in-situ* pH values using the season- and river-specific conversions.

We used DOC as a proxy for TOC. EC monitors TOC; however, only DOC was collected during the 2015-2016 sampling events. DOC was considered an appropriate proxy for TOC in this study, as Clair et al. (2008) tested particulate matter in SWNS rivers and found that organic carbon was <5% of particulate matter, suggesting that DOC and TOC concentrations in SWNS rivers are approximately equivalent.

3.4.6.4. Missing Data

Not all data were included in the creation of the MR and MPB Al_i equations, due to missing data. Rows with missing values were removed, to ensure all measured parameters were included for each Al_i measurement used in the creation of the Al_i equations. The amount of data used to create each equation differs among seasons based on which parameters are included in the equations, and how many values are missing. No conversion or Al_i equations were created for MPB winter (season three), as no data was collected during this period.

3.4.6.5. Statistical Outputs

The R statistical software was used to provide statistical outputs for each multiple Al_i linear regression. The outputs from the Least Squares (LS) statistical test (R command 'lm') determined the fit of the regression to the data (R^2), and whether the regression slopes were significantly different from zero with 95% confidence (p-value < 0.05). In addition, the regression residuals were tested for normal distributions (R command 'shapiro.test'); normal distribution was determined by a p-value > 0.05, and the random pattern of residuals was verified visually. R-scripts used for statistical analyses are available in Appendix. A.2.

3.4.6.6. Validation

Sampling events between April 28th, 2016 to Jun 27th, 2016 in MPB and MR were used to validate the best MR and MPB Al_i regressions. The best MR and MPB equations were validated due to their reasonable $Al_{i\text{-}c}$ estimates (majority of $Al_{i\text{-}c}$ estimates within the 0-200 µg/L Al_i concentration range found in Atlantic Canada rivers by Dennis and Clair, 2012) in the $Al_{i\text{-}c}$ time-series. Direct measurements from the 2015-2016 sampling events in MR and MPB were input into the best MR and MPB spring/summer Al_i equations, as all sampling events obtained for validation occurring during the spring/summer season. Differences between the $Al_{i\text{-}direct}$ concentrations from the April-June, 2016 samples and $Al_{i\text{-}c}$ estimates for the two equations indicated how well the equations estimated Al_i concentrations beyond parameter values used to create the equations. Using a range of $Al_{i\text{-}direct}$ value ±20%,

$Al_{i\text{-}c}$ values were compared to the $Al_{i\text{-}direct}$ range to assess the accuracy of $Al_{i\text{-}c}$ values during validation.

The two best MR and MPB equations were applied to data from seven streams across NS, to assess how well the equations can be extrapolated. Water chemistry data were collected from Pine Marten Brook (PMB), Brandon Lake Brook (BLB), Keef Brook (KB), West River Sheet Harbour Lime Doser (LD), Maria Brook (MB), Colwell Creek (CC) and the Sackville River (SKV) (Table 3.3). PMB was chosen due to its proximity to MR and MPB, while MB was chosen due to the continuous water chemistry monitoring that has been occurring in the brook since 2010. BLB, KB, LD and CC were chosen to obtain an Al_i concentration baseline before watershed liming occurs in the area. Finally, SKV was chosen due to its proximity to Halifax and urban areas. Water samples for the nine sites were collected during baseflow, to avoid complications from high flow events; to capture seasonal Al_i changes, samples were collected every two weeks. The Halifax and Goldenville Formations (both apart of the Meguma Supergroup) underlie the PMB, SKV, BLB, LD, CC, and KB catchments; the MB watershed, traverse granitic intrusive plutons (Figure 3.3). Differences between $Al_{i\text{-}direct}$ and $Al_{i\text{-}c}$ indicated how well the equations could be extrapolated from their region and known parameter ranges. A 20% range of $Al_{i\text{-}direct}$ measurements was used to assess the accuracy of $Al_{i\text{-}c}$ values during extrapolation.

Table 3.3: Dates sampled for each NS site used to validate MR and MPB $Al_{i\text{-}c}$ equations.

Site	Latitude	Longitude	Dates Sampled
PMB	44.4264	-65.2128	May 27th, 2015 June 3rd, 2015 April 28th, 2016 May 27th, 2016 June 15th, 2016 June 27th, 2016 July 14th, 2016
MB	44.7790	-64.4137	May 27th, 2016 June 15th, 2016 June 27th, 2016 July 14th, 2016
BLB	45.0210	-62.6900	April 29th, 2016 June 3rd, 2016 June 16th, 2016 June 28th, 2016 July 15th, 2016
CC	45.0280	-62.7129	June 3rd, 2016 June 16th, 2016 June 28th, 2016 July 15th, 2016
KB	45.0266	-62.7137	April 29th, 2016 June 3rd, 2016 June 16th, 2016 June 28th, 2016 July 15th, 2016
LD	45.0541	-62.8004	April 29th, 2016 June 3rd, 2016 June 16th, 2016 June 28th, 2016 July 15th, 2016
SKV	44.7315	-63.6604	April 22nd, 2016

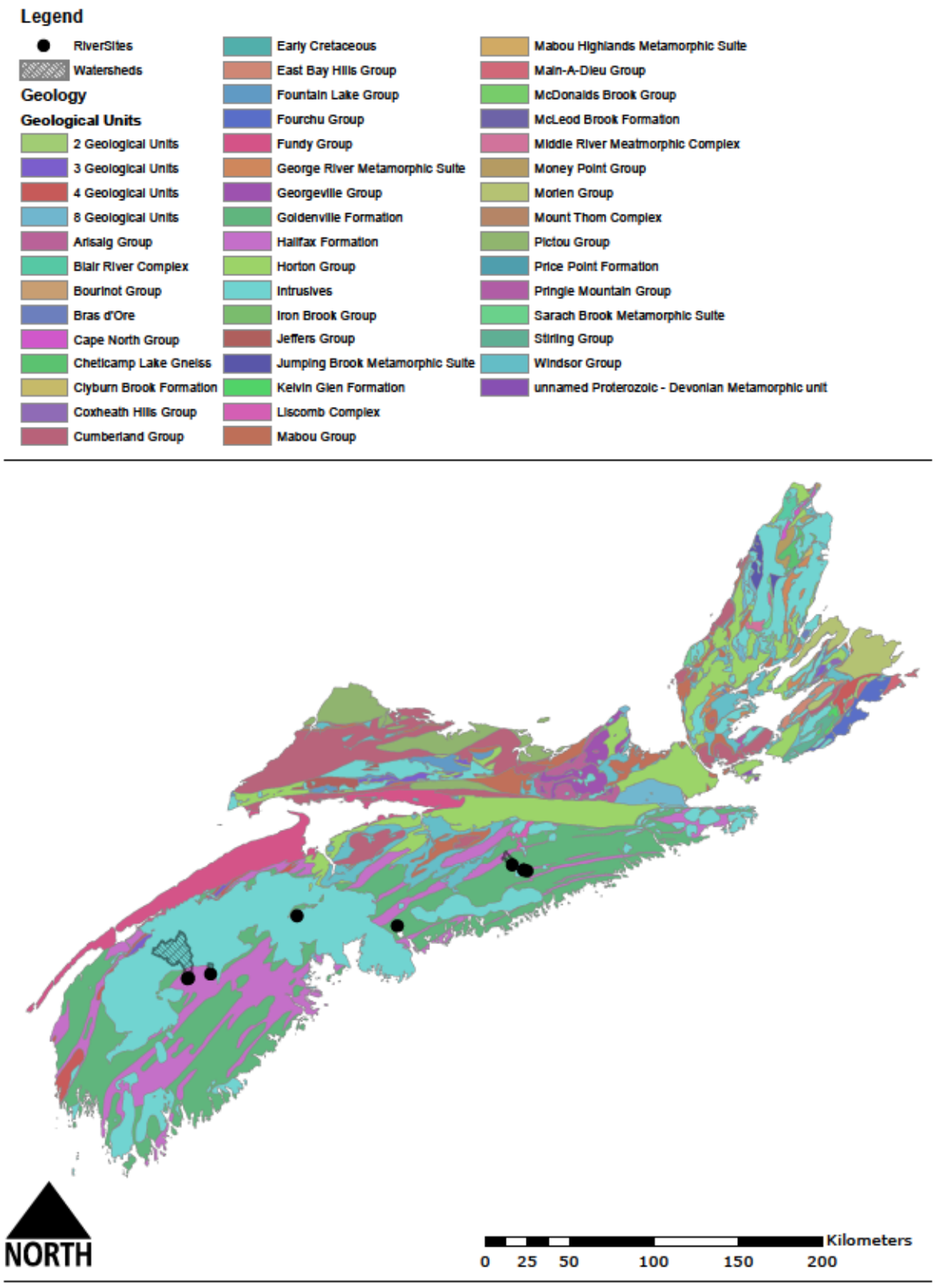

Figure 3.3: Geology of Nova Scotia, with the nine Al_i sampling sites for 2016. Map courtesy of Lobke Rotteveel.

3.4.7. Estimated Long Term Al_i Time-series

Using the 34 and 31-year water chemistry data from EC for MR and MPB, respectively, along with the best Al_i equations (river- and season-specific $Al_{i\text{-}c}$ equations with $Al_{i\text{-}c}$ estimates within known Al_i ranges and fewer required parameter conversions), Al_i time-series were estimated. The EC data were separated by river, then by the three Al_i seasons. Using R, the EC parameters were included in the equations, with conversions for Al_d and *in-situ* pH calculated if required, and Al_i was estimated from MR and MPB from 1980-2014 and 1983-2014, respectively. Al_i trends were quantified using the Least Squares (LS) statistical test, and trend significances determined with the LS and Seasonal Mann Kendall (SMK) test, with $p < 0.05$ indicating trend significance at 95% confidence.

3.5. Results and Discussion

3.5.1. Current Al_i Concentrations

3.5.1.1. MR and MPB Al_i Concentrations

$Al_{i\text{-}direct}$ concentrations exceed the 15 µg/L toxic threshold in the summer and fall seasons for MR and MPB between 2015 and 2016 (Figure 3.4). In MR, $Al_{i\text{-}direct}$ concentrations exceed the toxic threshold between June 3rd, 2015 and February 2nd, 2016, with the exceptions of August 12th and September 23rd; MR Al_i concentrations also exceed 15 µg/L on June 27th, 2016. MPB samples are under the 15 µg/L toxic threshold from April 22nd, 2015 until June 3rd, 2015; $Al_{i\text{-}direct}$ exceeds 15 µg/L on June 10th, 2015 and samples do not return below 15 µg/L for the remainder of the 2015 year. Al_i concentrations exceed 15 µg/L in MPB for 2016 on May 27th, 2016, June 27th, 2016 and July 14th, 2016; MPB 2016 Ali concentrations are below 15 µg/L on April 28th, 2016 and June 15th, 2016. 64.1% of the 39 samples obtained in MR were above the toxic threshold; 53.8% of the 31 MPB samples were above the 15 µg/L toxic threshold. Covariances of Al_t (8.0%) and Al_d (1.0%) concentrations, based on duplicates measured for 30% of the 2015/2016 sampling events, suggest laboratory methods are not a major source of error in water chemistry concentrations. Blanks

measured using the field-Al speciation method had concentrations below detection limits, suggesting that $Al_{i\text{-}direct}$ and Al_o concentrations are not affected by field speciation techniques. However, water sample matrices were not matched in the lab, therefore, there may be error associated with dissolved metal concentrations from water samples with complex matrices.

Fall concentrations of $Al_{i\text{-}direct}$ in MR are less than the 2006 survey by Dennis and Clair. Dennis and Clair measured the concentration of $Al_{i\text{-}direct}$ in MR on November 3rd, 2006, with a value of 39 µg/L; in 2015, on November 4th, $Al_{i\text{-}direct}$ in MR was 25 µg/L. The potential decrease in the fall $Al_{i\text{-}direct}$ concentrations from 39 µg/L to 25 µg/L may be due to the doubling of organic carbon (from 7.6 mg/L of TOC in 2006, to 14.4 mg/L of DOC in 2015); DOC is known to complex with Al_i to form biologically unreactive particles (Lacroix et al., 1990); however, we may also be observing interannual variability, therefore further monitoring is necessary to assess long-term Al_i trends.

$Al_{i\text{-}direct}$ concentrations in MR and MPB are highest during the fall season, concurrent with the seasonal peak in Al_d for MR and MPB (Figure 3.4). $Al_{i\text{-}direct}$ concentrations in MR rise from 12 µg/L on April 22nd to a peak of 42 µg/L on August 12, 2016, then decline throughout the late fall and winter months (from September 2nd, 2015-March 29th, 2016). Al_d concentrations in MR also increase throughout the spring, summer and fall seasons, with a peak in concentrations on November 2nd, 2015 and a decline in concentrations throughout the winter season (Figure 3.4). MPB $Al_{i\text{-}direct}$ concentrations follow a similar seasonal trend to MR, with a rise in concentrations in the spring and summer, with the peak of $Al_{i\text{-}direct}$ occurring in the fall (48 µg/L on October 7th, 2015); the peak in MPB $Al_{i\text{-}direct}$ concentrations on October 7th, 2015 coincides with the peak Al_d concentrations (Figure 3.4). No data were collected in MPB during the winter due to lack of access to the site.

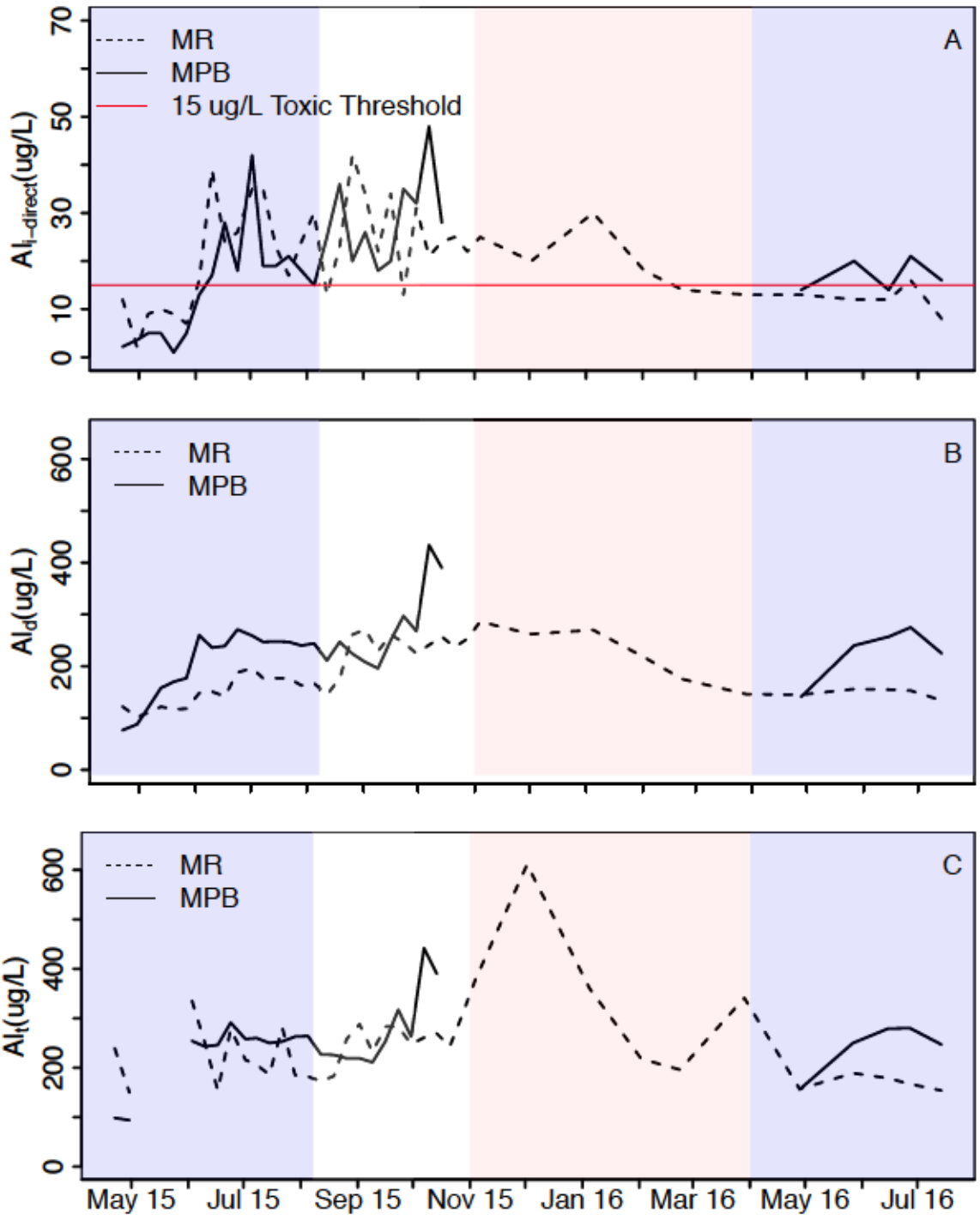

Figure 3.4: Time-series for A) Al_i, B) Al_d, and C) Al_t for MR and MPB from April 2015-July 2016. Background colours indicates a change of seasons, with season one (April 1st to August 5th) in blue, season two (August 12th to October 31st) in white, and season three (November 1st to March 31st) in pink. 14% error associated with $Al_{i\text{-}direct}$ concentrations, and 10% error associated with Al_d and Al_t measurements due to lab instruments.

Seasonality of $Al_{i\text{-}direct}$ in MR and MPB does not agree with the literature. Spring melt was attributed to the spring peak of Al_i concentrations in Rodushkin et al. (1995) and Campbell et al. (1992); however, no spring $Al_{i\text{-}direct}$ peak was observed at MR or MPB (Figure 3.5). The summer and fall peaks of $Al_{i\text{-}direct}$ for MR and MPB, respectively, contrast of Al_i winter peaks observed by Kopacek et al. (2006) and Kopacek et al. (2000). Kopacek et al. (2000) associated Al_i peaks with nitrate peaks (up to 5704 µg/L), as nitrate may act as a carrier of Al_i from soils; however, concentrations of nitrate in MR and MPB are much lower (10.0 - 25.5 µg/L) than those along the Czech-German border, limiting the role of nitrate as a carrier and indicating another driver may be causing the summer and fall $Al_{i\text{-}direct}$ peaks in MR and MPB, respectively. In addition, Al_i concentrations increase with decreased temperatures, therefore, Al_i concentrations would be highest in the winter months (Lydersen, 1990); however, 2015-2016 Al_i samples in MR and MPB indicate the opposite, with highest concentrations occurring in the summer and fall.

Correlations among $Al_{i\text{-}direct}$ and other water chemistry parameters are seasonally dependent (Table 3.4, Figure 3.5, Appendix D & E). In the spring/summer season, $Al_{i\text{-}direct}$ has a strong positive correlation with Al_d and DOC in MR (61.8% and 41.3%, respectively) and MPB (52.1% and 51.7%, respectively). Al_d and DOC remain correlated to $Al_{i\text{-}direct}$ in MPB during the fall season; however, Al_d and DOC correlations decrease (22.9% and -0.59%, respectively) in MR during the fall. The correlation of Ca_t and $Al_{i\text{-}direct}$ increases to 32.2% in the fall for MPB, but remains low (9.46%) in MR; Ca_t may be coupled with discharge (as Al_t variability coincides with Cat), with the smaller watershed size of MPB compared to MR resulted in no lag between discharge and chemical responses during the fall (Figures 3.4 & 3.5). It appears that $Al_{i\text{-}direct}$ is driven by an unknown water chemistry parameter during the fall in MR, as no other water chemistry parameter has a strong correlation with $Al_{i\text{-}direct}$ (Table 3.4). In the winter season, the correlation of Al_d and DOC with $Al_{i\text{-}direct}$ increases for MR (71.8% and 43.8%, respectively). For the winter in MPB, the correlation of $Al_{i\text{-}direct}$ and Al_d decreases slightly (46.9%), while the $Al_{i\text{-}direct}$ correlation with DOC increases (60.3%). We hypothesize that the difference

between the strong correlations between $Al_{i\text{-}direct}$ and dissolved chemicals (DOC and Al_d) in the fall for MPB and the weak $Al_{i\text{-}direct}$ to dissolved chemical correlations in MR are due to size of watersheds, where lower flows in MPB may result in higher particulate and dissolved matter, while higher flow in MR may be diluting any driving signal from dissolved matter.

Table 3.4: Correlations between $Al_{i\text{-}direct}$ 2015-2016 measurements in MR and MPB with Al_d, Al_t, Ca_t, SO_4, DOC, pH, and discharge for three seasons in MR and two seasons in MPB. Season one (S1 – Spring/summer) is from April 1st to August 5th, season two (S2- fall) includes data from August 12th to October 31st, and season three (S3- winter) is from November 1st to March 31st. 2 pH, 4 Al_t and 4 Ca_t data are missing from S1 for MR and MPB due to instrument malfunction, with no missing data for MR and MPB S2, and 1 pH data point missing for MR S3 due to instrument malfunction.

	Mersey River			Moose Pit Brook	
	S1 R^2 % (#N)	S2 R^2 % (#N)	S3 R^2 % (#N)	S1 R^2 % (#N)	S2 R^2 % (#N)
Al_d	61.8 (16)	22.9 (12)	71.8 (6)	52.1 (16)	46.9 (10)
Al_t	-9.94 (12)	1.13 (12)	-13.1 (6)	36.5 (12)	43.1 (10)
Ca_t	1.48 (12)	9.46 (12)	-15.4 (6)	17.9 (12)	32.2 (10)
SO_4	10.8 (16)	5.29 (12)	-22.7 (6)	41.4 (16)	-8.99 (10)
DOC	41.3 (16)	-0.593 (12)	43.9 (6)	51.7 (16)	60.3 (10)
pH	19.4 (14)	-9.7 (12)	22 (5)	-8.2 (14)	42.4 (10)
Discharge	12.3 (16)	-8.9 (12)	33.9 (6)	7.41 (16)	-13.7 (8)

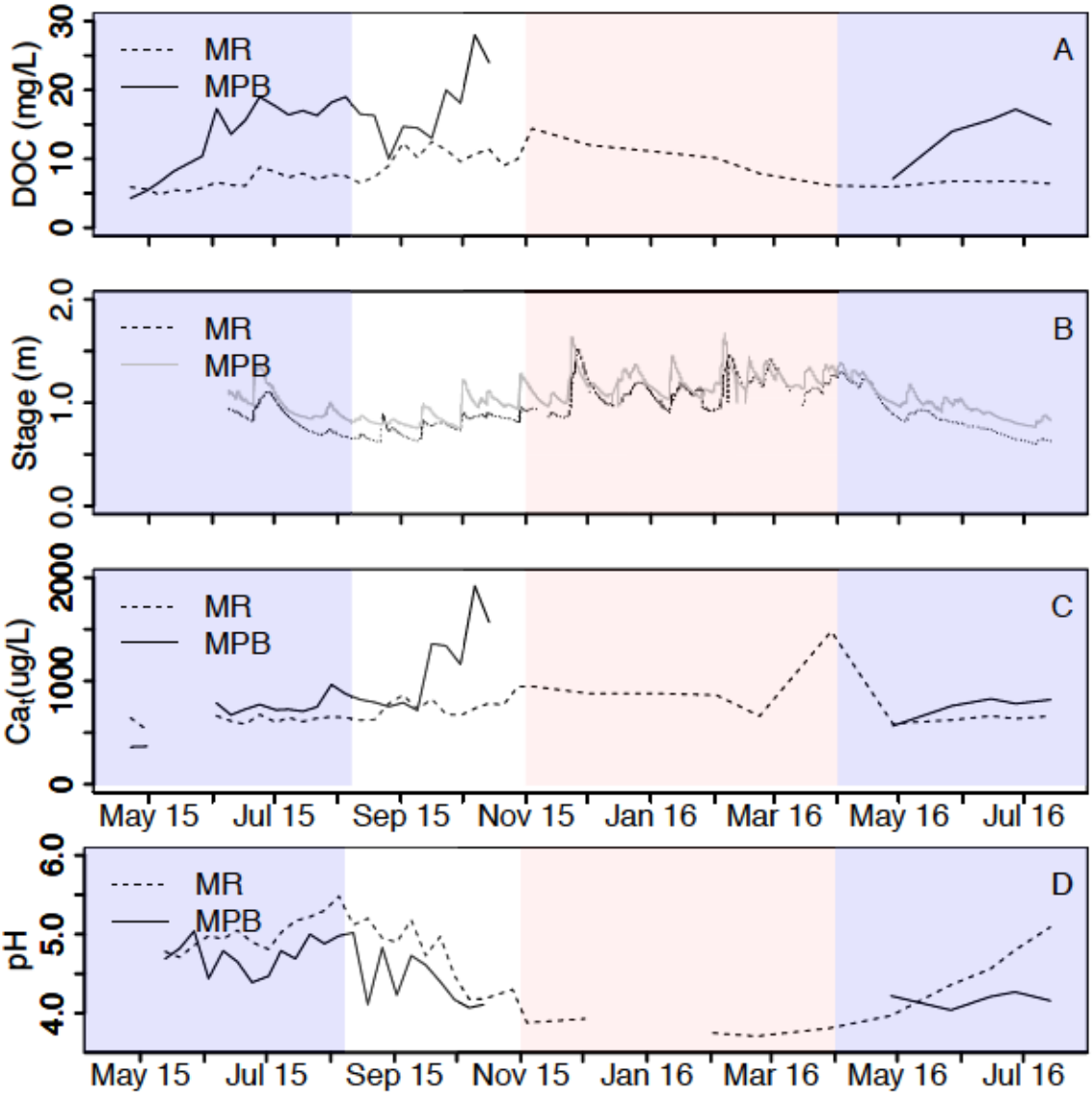

Figure 3.5: Time-series for A) DOC, B) Stage, C) Ca_t, and D) pH for MR and MPB from April 2015-July 2016. Background colours indicates a change of seasons, with season one (spring/summer- April 1st to August 5th) in blue, season two (fall- August 12th to October 31st) in white, and season three (winter- November 1st to March 31st) in pink. 10% error associated with DOC, Ca_t and pH measurements due to lab instruments, and 0.01 precision of Stage measurements.

Changes in DOC are concurrent with changes in $Al_{i\text{-}direct}$ concentrations during the spring/summer and winter seasons for MR, and spring/summer and fall seasons for MPB (Table 3.4). Peaks in MR DOC correspond to peaks in $Al_{i\text{-}direct}$ during the spring/summer and winter; however, the peaks in $Al_{i\text{-}direct}$ during the fall for MR have a lag before we observe peaks in DOC (eg. $Al_{i\text{-}direct}$ peaked on August 28th, 2016

and DOC did not peak until September 2nd, 2016), which may explain why the correlation between these two chemicals is low during the fall (-0.59%). During the spring/summer and fall seasons for MPB, variations in $Al_{i\text{-direct}}$ concentrations consistently match with variations in DOC (Figures 3.4 & 3.5). We hypothesize that DOC is complexing Al and increasing Al in solution, while also maintaining soil acidity which increases the solubility and mobilization of Al. Positive correlations between Al_d and DOC are found within the literature, as organic matter is known to control the solubility of Al in mineral soils (Mulholland et al., 1981, Berggren & Mulder, 1995). The positive relationship between DOC and $Al_{i\text{-direct}}$ conflicts with Lacroix and Townsend (1987), who proposed Al_i were being complexed with DOC; here, we agree with Dennis and Clair (2012), that $Al_{i\text{-direct}}$ concentrations are still at measureable levels near thresholds known to cause harm to aquatic organisms, regardless of the high DOC concentrations in MR and MPB.

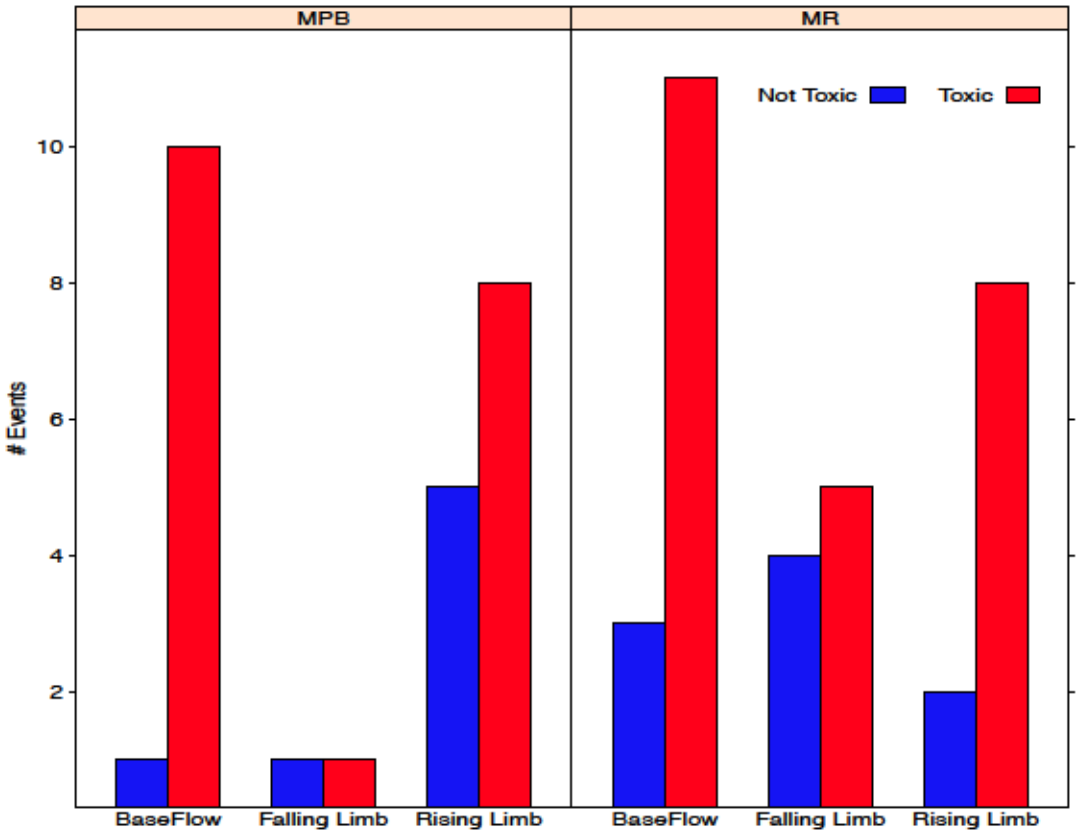

Figure 3.6: Distribution of toxic and non-toxic $Al_{i\text{-direct}}$ concentrations for baseflow, falling limb and rising limb events in Moose Pit Brook (MPB) and Mersey River (MR).

$Al_{i\text{-}direct}$ concentrations exceed the toxic threshold in baseflow, rising limb and falling limb hydrograph components (Figure 3.6). Most $Al_{i\text{-}direct}$ concentrations that exceed the toxic threshold occur during baseflow (21 out of 25 events); however, the rising limb also has more events exceeding the toxic threshold (16 out of 24 events) than below the threshold (eight out of 24 events). The falling limb is evenly distributed between exceeding and being below the toxic threshold: six and five events, respectively.

Two mechanisms appear to be controlling the inverse relationship between available Al_d concentrations and discharge (Figures 3.4 & 3.5, Appendix E): volume of water and flow pathway through soil. The dilution of $Al_{i\text{-}direct}$ and Al_d concentrations in the spring 2015 and 2016 for MR and MPB during high flow (Figure 3.4, Figure 3.5, Appendix E) support the findings of spring Al dilution due to an increased volume of water (McKnight and Bencala, 1988). Our results also suggest that shallow flow paths may be resulting in the low Al_i concentrations during high discharges, as flow does not penetrate past the organic (O) horizon where Al_o is the dominant Al_d species, resulting in reduced export of Al_i concentrations during high flow (Figure 3.7, Sullivan et al., 1986). Lateral flow along shallow organic soil horizons increases particulate Al concentrations (Mulholland et al., 1981); I hypothesize that the peaks of Al_t concentrations during the high flows in the winter and spring months for MR and MPB in 2015 and 2016 are limited to shallow flow paths (Figure 3.4). We also hypothesize that frozen soils during the winter months limit flow transport to the organic horizon. The peaks in Al_i and Al_d concentrations for MR and MPB are concurrent with the maximum Al concentrations measured in the White Oak Run soils in Virginia, USA during the summer of 1984 (Cozzarelli et al., 1987). Kopacek et al. (2000) found that Al_i decreased in the summer due to low nitrate concentrations; our findings contradict the findings of Kopacek et al., as Al_i concentrations increase in MR and MPB during the summer and fall months. More soil and river water sampling is required in MR and MPB to understand how flowpaths contribute to Al_i seasonality.

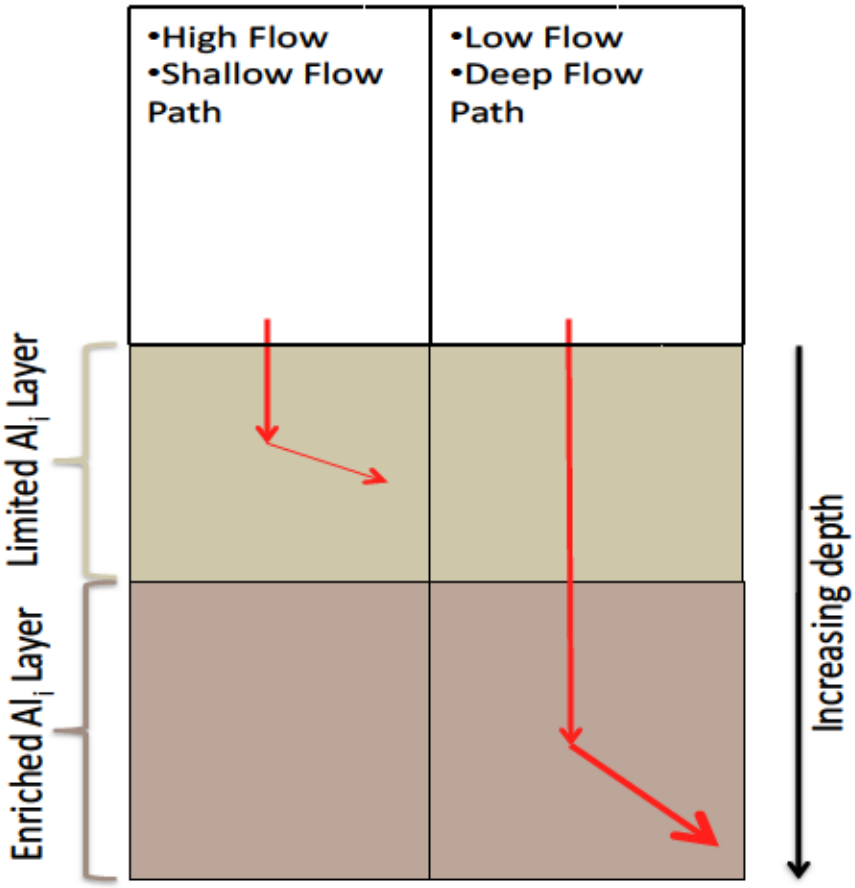

Figure 3.7: Flow paths (red arrows) of water at different soil depths throughout four seasons. The concentration of Al in flow passing through a soil layer is denoted by the size of the arrow, with increased size showing increased Al_i concentrations.

3.5.1.2. Other NS Rivers' Al_i Concentrations

$Al_{i\text{-direct}}$ concentrations measured across NS between April-July, 2016 exceed the toxic threshold of Al_i for Atlantic salmon (Figure 3.8). Field samples of $Al_{i\text{-direct}}$ along the Eastern Shore (ES) of NS (including BLB, CC, KB and LD) are above the 15 µg/L toxic threshold for Atlantic salmon (Figure 3.8). One sample out of five from KB was below the threshold; all four samples from CC doubled the threshold, with one in end of July more than seven times the toxic threshold, at 107 µg/L. In central NS, the one $Al_{i\text{-direct}}$ measurement SKV was above the toxic threshold. In southwestern NS, one sample in MR (out of five), one in PMB (out of seven) and three in MPB (out of five) were above the toxic threshold.

The measureable levels of $Al_{i\text{-direct}}$ concentrations above the 15 µg/L toxic threshold across NS suggest that regional high levels of DOC (>10 mg/L) and low weathering rates from bedrock may be influencing NS water chemistry. All nine NS sites measured in 2015/2016 are underlain by slates, sandstones or plutonic intrusives – these bedrocks have low weathering rates and are found in regions with low buffering capacities of soils (Langan & Wilson, 1992, Tipping, 1989). I hypothesize that the input of base cations from bedrock weathering into soils is less than the exchange of ions from acidification, resulting in base-cation-depleted soils, thereby increasing the exchange of Al, which is transported into freshwater rivers and streams. In addition, DOC concentrations commonly exceed 10 mg/L in MR and MPB throughout 2015/2016 (Figure 3.5). DOC is known to decrease soil pH due to the increase in organic acids (Driscoll, 1985); I hypothesize that the maintained soil acidity from DOC, following reduced acid deposition, has enhanced the mobilization Al (Figures 3.4 & 3.5), which increase the concentrations of Al_d available for speciation. I hypothesize that high organic acidity, and low base cation replenishment due low weathering rates from bedrock have resulted in the toxic concentrations of Al_i across NS, and may be driving Al_i concentrations in watersheds with similar bedrock and DOC concentrations to NS.

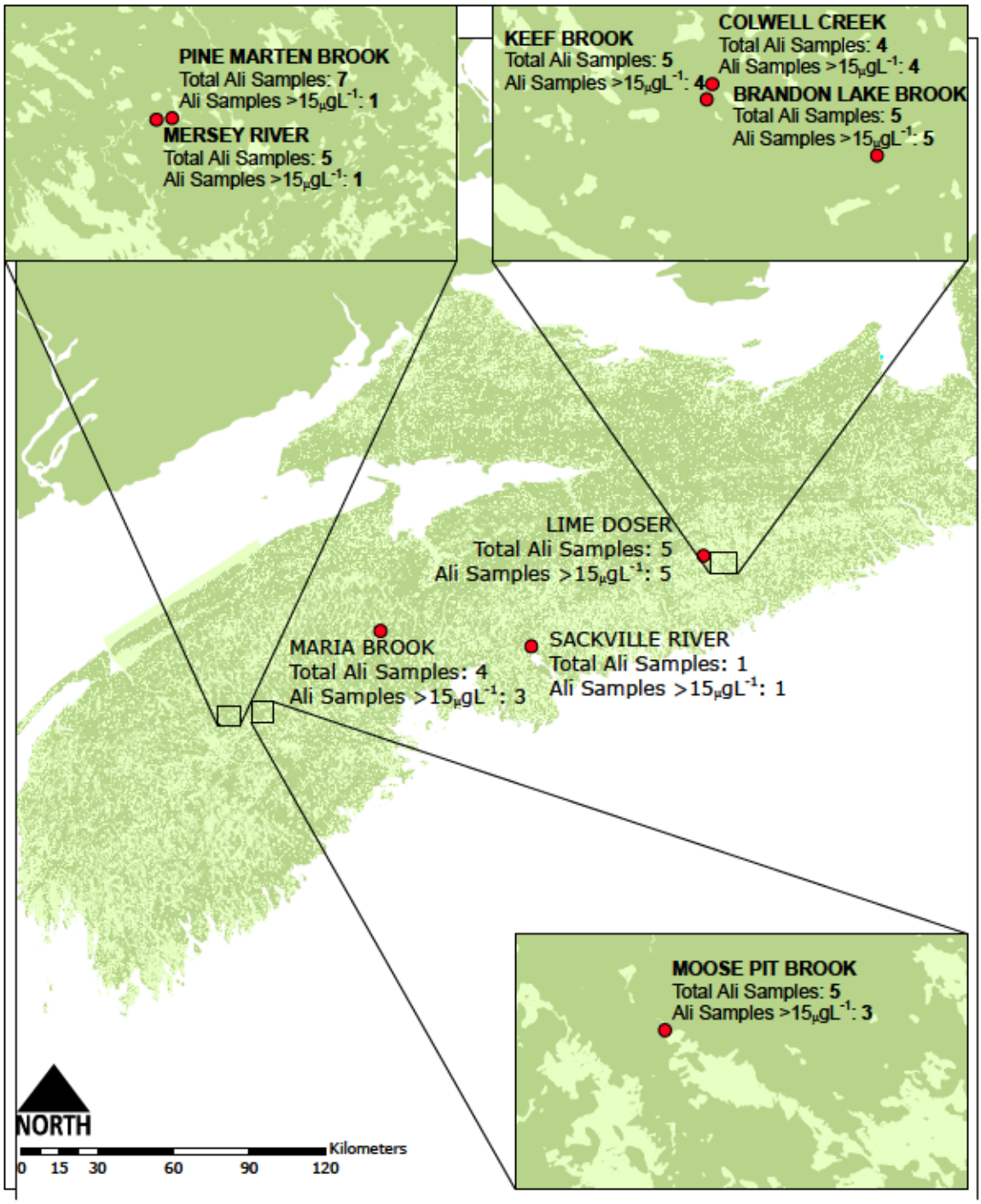

Figure 3.8: Locations and statistics for Al_i samples collected by the Hydrology Research Group at Dalhousie University during the spring and summer, 2016 in Nova Scotia. Rivers and lakes are in light green.

3.5.2. Al_i Equations

3.5.2.1. Mersey River Al_i Equations

Al_i concentrations in MR can be predicted with R^2 between 22-100%; however, parameters included in the MR $Al_{i\text{-}c}$ equations vary (Table 3.5). For all 2015 MR equations (spring/summer, fall and winter), either Al_t or Al_d were included (Table 3.5). Equations had higher R^2 values when the Al_d parameter was included compared to the Al_t parameter, this may be due to variability in Al_t due to the role of larger particles, as Al_t samples were not filtered. The DOC parameter appears to be an important parameter in predicting Al_i, as it is included in all equations for each season, except MRS1Ald1 (Table 3.5). The winter Al_i equations had high R^2 values (99% and 100% for MRS3Alt1 and MRS3Ald1, respectively); however, these equations were created using data from only six sampling events and may be artificially high. All MR Al_i equations had normal residuals (normality p-value > 0.05), and random distributions of residuals (Appendix F.1).

Table 3.5: Equations to predict Al_i for three seasons of Mersey River (MR). #N indicates sampling points included in the creation of the equation, R^2 (%) indicates regression fit, p-value <0.05 are significant regressions at 95% using the Least Squares statistical test, Norm=Normality p-value, with p <0.05 indicating normal residuals, and Appl.=Possible applications for the equations. An asterisk indicates the requirement of a conversion before application to the EC Database.

Name	*Season*	*Equation*	*R^2 (%)*	*P-value*	*Norm.*	*Appl.*
MRS1Ald1	1	$Al_i = -1.30*10^2 - 8.53pH + 1.33*10^1\sqrt{Al_d} + 2.30*10^{-8}SO_4{}^3$	79	0.00	0.999	Lakes, Rivers, EC Database*
MRS1Alt1		$Al_i = -42.8 + 19.4\sqrt{DOC} + 0.106\sqrt{Al_t} + 0.110pH^3$	22	0.60	0.457	Lakes, Rivers, EC Database*
MRS1Ald2		$Al_i = -1.49*10^2 + 1.68*10^1\sqrt{Al_d} - 3.08*10^{-1}DOC^2 + 2.19*10^{-8}SO_4{}^3 - 9.98pH$	82	0.00	0.119	Lakes, Rivers, EC Database*
MRS1Alt2		$Al_i = 21.7 - 14.7\sqrt{DOC} + 1.43\sqrt{Al_t} - 0.0295pH^3 + 1.59T_a$	42	0.43	0.149	Lakes, Rivers
MRS2Ald1	2	$Al_i = 5.07*10^1 - 1.35*10^1\left(\frac{Ca_t}{Al_d}\right) + 1.30*10^{-8}SO_4{}^3 - 2.64*10^{-3}DOC^3 + 1.42pH$	45	0.39	0.110	Lakes, Rivers, EC Database*
MRS2Alt1		$Al_i = 7.86*10^1 - 1.18*10^4 Al_t{}^{-1} + 1.13*10^{-8}SO_4{}^3 - 1.62*10^{-1}DOC^3$	51	0.15	0.222	Lakes, Rivers, EC Database
MRS2Ald2		$Al_i = 1.32*10^2 + 3.57*10^{-6}Al_d{}^3 - 4.31*10^1\sqrt{DOC} + 4.19*10^{-2}T_a{}^2 - 2.64*10^{-1}pH^3 - 5.83*10^{-2}Dis^3$	85	0.04	0.679	Rivers
MRS2Alt2		$Al_i = 1.44*10^2 - 2.11*10^4 Al_t{}^{-1} + 1.47*10^{-8}SO_4{}^3 - 2.91*10^{-1}DOC^2 - 1.01*10^1\sqrt{Dis}$	69	0.09	0.513	Rivers, EC Database
MRS3Ald1	3	$Al_i = -1.48*10^2 - 8.71*10^{-4}Al_d{}^2 + 3.51*10^1 pH + 7.51DOC$	100	0.04	0.352	Lakes, Rivers, EC Database*
MRS3Alt1		$Al_i = 20.8 - 7.46\left(\frac{Al_t}{Ca_t}\right)^3 + 8.92\sqrt{DOC} - 115pH^{-1}$	99	0.09	0.603	Lakes, Rivers, EC Database*

3.5.2.2 Moose Pit Brook Al_i Equations

Al_i equations in MPB can be seasonally predicted for 2015 with R^2 between 62-94% (Table 3.6). For all 2015 MPB equations (spring/summer and fall), either Al_t or Al_d were included (Table 3.6). Equations had higher R^2 values when the Al_d parameter was included compared to the Al_t parameter for the spring/summer season; however, R^2 values did not vary between Al_t and Al_d for the fall equations. DOC and pH appear to be important parameters in predicting MPB Al_i, as they're each included in six of the eight equations (Table 3.6). The inclusion of discharge appears to increase the R^2 of the Al_i equations, as the 72% R^2 of MPBS2Ald1 and MPBS2Alt1 equations increased to 95% each for MPBS2Ald2 and MPBS2Alt2 (Table 3.6). Ca_t also appears to be an important parameter for fall Al_i prediction, as it appears in all four fall MPB equations (Table 3.6). All MPB Al_i equations had normal residuals (normality p-value > 0.05), and random distributions of residuals (Appendix F.2).

Table 3.6: Equations to predict Al_i for two seasons of MPB. Bolded equations are suggested for use on the Environment Canada (EC) 30-year database. #N indicates sampling points included in the creation of the equation, R^2 (%) indicates regression fit, p-value <0.05 are significant regressions at 95% using the Least Squares statistical test, Norm=Normality p-value, with p <0.05 indicating normal regressions, and Appl.=Possible applications for the equations. An asterisk indicates the requirement of a conversion before application to the EC Database.

Name	*Season*	*Equation*	*R^2 (%)*	*P-value*	*Norm.*	*Appl.*
MPBS1Ald1	1	$Al_i = -6.90 - 0.067 Al_d + 8.21*10^3 SO_4^{-1} + 1.60 DOC$	69	0.00	0.467	Rivers, Lakes, EC Database*
MPBS1Alt1		$Al_i = -2.10*10^1 - 2.28*10^{-6} Al_t^{\,3} + 1.04*10^4 SO_4^{-1} + 3.55 DOC$	62	0.01	0.290	Rivers, Lakes, EC Database
MPBS1Ald2		$Al_i = -1.65*10^2 + 1.48*10^{-6} Al_d^{\,3} - 1.42*10^1 Dis^2 + 7.90*10^2 pH^{-1}$	86	0.00	0.650	Rivers, EC Database*
MPBS1Alt2		$Al_i = -2.07*10^2 + 3.56*10^{-4} Al_t^{\,2} - 1.16*10^1 Dis^3 + 9.88*10^2 pH^{-1}$	82	0.00	0.725	Rivers, EC Database*
MPBS2Ald1	2	$Al_i = -1.81*10^1 - 9.01*10^{-1}\left(\frac{Ca_t}{Al_d}\right) + 8.34*10^{-4} DOC^3 + 2.00*10^2 pH^{-1}$	72	0.04	0.441	Lakes, Rivers, EC Database*
MPBS2Alt1		$Al_i = -2.03*10^1 - 7.20*10^{-1}\left(\frac{Ca_t}{Al_t}\right) + 8.19*10^{-4} DOC^3 + 2.05*10^2 pH^{-1}$	72	0.04	0.458	Lakes, Rivers, EC Database*
MPBS2Ald2		$Al_i = 4.20*10^1 + 3.98*10^1 \sqrt{\frac{Al_d}{Ca_t}} + 1.24*10^{-3} DOC^3 - 8.80 pH - 1.17*10^2 Dis^2$	94	0.04	0.689	Rivers, EC Database*
MPBS2Alt2		$Al_i = 4.62*10^1 + 4.00*10^1 \sqrt{\frac{Al_t}{Ca_t}} + 1.20*10^{-3} DOC^3 - 9.73 pH - 1.16*10^2 Dis^2$	94	0.04	0.956	Rivers, EC Database*
MPBS3	3	No Equations Available				

Seasonal- and river-specific $Al_{i\text{-}c}$ equations all included either pH, DOC, discharge, or a combination of the three parameters. MRS3Ald1, MPBS1Ald2 and MPBS1Alt2 solely used pH, DOC and discharge to predict $Al_{i\text{-}c}$ with an R^2 >80%. MRS1Alt1 also included pH, DOC and discharge; however, its R^2 was 22%, possibly due to the high variability in the spring/summer MR Al_t concentrations (56.3 µg/L standard deviation compared to the 30.4 µg/L standard deviation for MR spring/summer Al_d). The Al_i equation presented by Dennis and Clair (2012) also included Al_t, TOC and pH; however, the Al_i equation R^2 was 68% and equation was not river-specific. Although the Dennis and Clair Al_i equation has a higher R^2 than our MR fall season Ald1 and Alt1 equations, the $Al_{i\text{-}c}$ outputs may be more reliable when applied to MR, as we solely included data from MR to create the MRAld1 and MRAlt1 $Al_{i\text{-}c}$ equations. our study, all equations incorporated at least one of the pH, DOC, or discharge parameters; inclusion of other parameters (such as SO_4, Ca_t, and T_a) increased the R^2 of the $Al_{i\text{-}c}$ equations. The R^2 for MRS1Alt1 increased from 22% to to 42% when the T_a parameter was included. Although $Al_{i\text{-}c}$ can be predicted using pH, DOC, and discharge, it appears that the Ca_t, SO_4 and T_a parameters should also be considered when estimating $Al_{i\text{-}c}$.

Relationships between $Al_{i\text{-}c}$ and other river chemistry parameters are complex (Appendix E). I propose that the ratio of Al_i concentrations in rivers is primarily controlled by the total amount of Al available to speciate in rivers (indicated by Al_d and Al_t concentrations); however, the fractions of each Al_i species are driven by acidity (via pH or DOC) and temperature (Poleo, 1995). As DOC is a driver of Al_i in freshwaters (Hue et al., 1986, Driscroll, 1984), it makes sense that is included in almost all MR and MPB equations. pH is also commonly found in the $Al_{i\text{-}c}$ equations, and is known to affect Al_i via cation exchange and speciation (Robertson et al., 1999). The negative correlation between discharge and Al_i is found in all $Al_{i\text{-}c}$ equations that included the discharge parameter. The inverse relationship between Al_i and discharge supports the theory of Al_i dilution during high flow events (McKnight and Bencala, 1988); however, the dilution of Al_i concentrations does not agree with the findings of Campbell et al. (1992), where Al_i concentrations increased

with increased discharge in Quebec rivers during spring melt in 1986. There is a positive correlation between $Al_{i\text{-}c}$ and SO_4; Nordstrom (1892) reported that SO_4 concentrations control Al_t solubility via the formation of $Al_x[SO_4]_Y$ complexes. The role of Ca_t in the $Al_{i\text{-}c}$ equations is complex, as it appears in the equations as both a negative and a positive parameter; a positive correlation between Ca_t and Al_i concentrations may be due to the flushing of ions from soils (Figure 3.9). The inverse relationship between Ca_t and Al concentrations may be due to the cation exchange process in soils, as Schlesinger and Bernhardt (2013) reported that Ca, Na, and Mg ions are exchanged first and depleted before the mobilization and exchange of heavier cations, such as Al and Fe. Lawrence et al. (1995) observed this inverse relationship between Ca_t and exchangeable Al in freshwaters on the Whiteface Mountain, New York, where the Ca_t and Al concentrations were converted to masses per area to correct for the role of discharge.

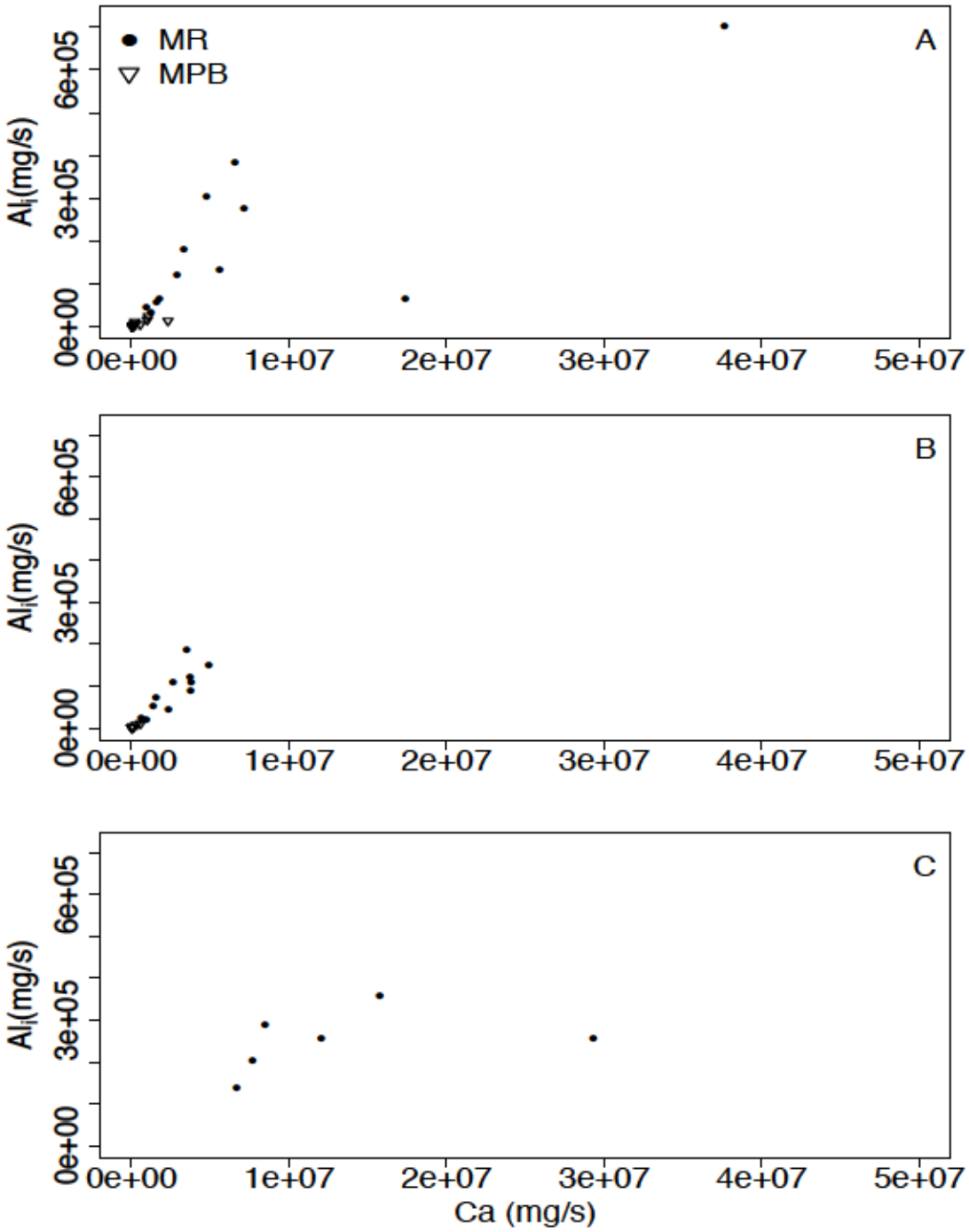

Figure 3.9: Mass exports of Ca_t and Al_i from MR and MPB for A) spring/summer (S1: April 1st-August 5th), B) fall (S2: August 12th-October 31st) and C) winter (S3: November 1st-March 31st).

3.5.2.3. Al_i Equation Validations and Extrapolation

$Al_{i\text{-}c}$ estimates do not consistently estimate $Al_{i\text{-}c}$ within 20% of the $Al_{i\text{-}direct}$ concentrations for their locations in season one, based on five monthly $Al_{i\text{-}direct}$ sampling events taken between April 28th, 2016 and July 14th, 2016 (which were not included in the calibration of the models; Table 3.7). Only 20% of the time could MR and MPB equations estimate $Al_{i\text{-}c}$ concentrations within 20% of $Al_{i\text{-}direct}$ (Table 3.7). The MRS1Alt1 overestimated Al_i concentrations, with a mean overestimation of 6.53 µg/L. The MPBS1Ald1 underestimated $Al_{i\text{-}direct}$ concentrations, with a mean underestimation of 4.29 µg/L (Table 3.7). Both equations provided $Al_{i\text{-}c}$ estimates within ±15 µg/L of the true $Al_{i\text{-}direct}$ values for their respective rivers; however, when MRS1Alt1 was extrapolated to the MPB site, the $Al_{i\text{-}c}$ concentrations underestimated $Al_{i\text{-}direct}$ values by an average of 11.5 µg/L, while the MPBS1Ald1 equation overestimated MR $Al_{i\text{-}direct}$ concentrations by an average of 21.2 µg/L (Table 3.7).

Table 3.7: 2016 $Al_{i\text{-}direct}$ samples, $Al_{i\text{-}c}$ concentrations calculated using the MRS1Alt1 and MPBS1Ald1 equations, the difference between the $Al_{i\text{-}c}$ and $Al_{i\text{-}direct}$ values, and whether the $Al_{i\text{-}c}$ concentrations are within 20% of the $Al_{i\text{-}direct}$ for MR and MPB.

River	$Al_{i\text{-}direct}$	$Al_{i\text{-}c}$		$Al_{i\text{-}c} - Al_{i\text{-}direct}$		Within 20% of $Al_{i\text{-}direct}$?	
		MRS1Alt1	MPBS1Ald1	MRS1Alt1	MPBS1Ald1	MRS1Alt1	MPBS1Ald1
MPB	14.0	18.52	5.29	4.52	-8.71	No	No
	20.0	38.72	16.20	18.72	-3.80	No	Yes
	14.0	44.05	18.18	30.05	4.18	No	No
	21.0	48.00	16.18	27.00	-4.82	No	No
	16.0	41.92	7.70	25.92	-8.30	No	No
MR	13.0	12.73	1.67	-0.27	-11.33	Yes	No
	12.0	18.29	2.40	6.29	-9.60	No	No
	12.0	19.26	0.18	7.26	-11.82	No	No
	16.0	21.25	0.20	5.25	-15.80	No	No
	8.0	22.10	-0.80	14.10	-8.80	No	No

The accuracy of MRS1Alt1 and MPBS1Ald1 $Al_{i\text{-}c}$ concentrations is reduced when extrapolated to other rivers across NS, possibly due to NS water chemistry data outside the range of observational data used for the creation of the MRS1Alt1 and MPBS1Ald1 equations (average overestimation by MRS1Alt1 of 3.5 µg/L for the

seven sites, and average underestimation by MPBS1Ald1 of -24.9 µg/L for the seven sites; Table 3.8). The MRS1Alt1 equation was capable of being within 20% of $Al_{i\text{-}direct}$ for 12 out of 36 sampling points from across NS (excluding MR). The MRS1Alt1 $Al_{i\text{-}c}$ equation accurately (within 20%) predicted 80% of the $Al_{i\text{-}direct}$ samples from BLB, 50% of the $Al_{i\text{-}direct}$ MB and CC samples and 40% of KB and LD $Al_{i\text{-}direct}$ samples (Table 3.8). The majority of MRS1Alt1 $Al_{i\text{-}c}$ estimates overestimated $Al_{i\text{-}direct}$ 2016 concentrations. The MPBS1Ald1 equation was only able to accurately (within 20%) predict one out of 36 $Al_{i\text{-}direct}$ concentrations across NS in 2016 (excluding MPB); MPBS1Ald1 accurately predicted 14% of PMB $Al_{i\text{-}direct}$ concentrations. The MPBS1Ald1 equation underestimated all 2016 $Al_{i\text{-}direct}$ samples from across NS.

Table 3.8: 2016 $Al_{i\text{-}direct}$ samples, $Al_{i\text{-}c}$ concentrations calculated using the MRS1Alt1 and MPBS1Ald1 equations, the difference between the $Al_{i\text{-}c}$ and $Al_{i\text{-}direct}$ values, and whether the $Al_{i\text{-}c}$ concentrations are within 20% of the $Al_{i\text{-}direct}$ for seven sites. There is a 14.1% error associated with $Al_{i\text{-}direct}$ concentrations.

River	$Al_{i\text{-}direct}$	$Al_{i\text{-}c}$		$Al_{i\text{-}c} - Al_{i\text{-}direct}$		Within 20% of $Al_{i\text{-}direct}$?	
		MRS1Alt1	MPBS1Ald1	MRS1Alt1	MPBS1Ald1	MRS1Alt1	MPBS1Ald1
PMB	2.0	26.96	5.76	24.96	3.76	No	No
	6.0	28.70	5.81	22.70	-0.19	No	Yes
	5.9	7.34	-0.77	1.44	-6.67	No	No
	35.0	22.09	7.07	-12.91	-27.93	No	No
	5.0	24.49	2.54	19.49	-2.46	No	No
	4.7	17.15	-1.12	12.45	-5.82	No	No
	10.3	23.60	-0.87	13.30	-11.17	No	No
MB	30.0	20.41	-7.69	-9.59	-37.69	No	No
	15.0	15.20	-5.41	0.20	-20.41	Yes	No
	27.0	25.26	-9.33	-1.74	-36.33	Yes	No
	40.0	22.58	-12.40	-17.42	-52.40	No	No
SKV	22.2	27.53	-5.32	5.33	-27.52	No	No
BLB	20.0	20.19	0.59	0.19	-19.41	Yes	No
	32.0	33.28	1.90	1.28	-30.10	Yes	No
	33.0	36.88	-3.68	3.88	-36.68	Yes	No
	26.0	37.08	-4.57	11.08	-30.57	No	No
	42.0	45.84	1.50	3.84	-40.50	Yes	No
CC	32.0	41.18	12.17	9.18	-19.83	No	No
	46.0	47.61	20.77	1.61	-25.23	Yes	No
	107.0	56.15	13.23	-50.85	-93.77	Yes	No
	53.0	64.29	39.06	11.29	-13.94	No	No
KB	14.0	23.84	0.03	9.84	-13.97	No	No
	20.0	28.30	4.41	8.30	-15.59	No	No
	38.0	32.62	0.05	-5.38	-37.95	Yes	No
	28.0	35.60	-0.57	7.60	-28.57	No	No
	41.0	45.52	7.42	4.52	-33.58	Yes	No
LD	19.0	16.17	3.04	-2.83	-15.96	Yes	No
	25.0	37.07	7.98	12.07	-17.02	No	No
	32.0	37.88	9.59	5.88	-22.41	Yes	No
	28.0	39.24	3.42	11.24	-24.58	No	No
	37.0	44.77	8.79	7.77	-28.21	No	No

3.5.3. Long-Term Al_i Estimations

3.5.3.3. Mersey River

The 2015 MR water samples' linear conversions of Al_d to Al_t, and lab pH to *in-situ* pH, are seasonally variable (Appendix D.1). The best R^2 for the best-fit line conversion

of Al_t to Al_d concentrations during fall 2015 is 83%; the spring/summer conversion has an R^2 of 8% and the winter conversion has a 26% R^2 value. The lab pH to *in-situ* pH linear conversions has R^2 values of 61%, 50% and 3% for spring/summer, fall and winter, respectively.

MR $Al_{i\text{-}c}$ seasonal trends vary in direction and rate from 1980-2014 (Appendix G.1, Figures 3.10 & 3.11). Only the MRS1Alt1, MRS2Ald1 and MRS3Alt1 $Al_{i\text{-}c}$ trends are analyzed for MR, as they provide the most reasonable $Al_{i\text{-}c}$ estimates ($Al_{i\text{-}c}$ first and third quarter estimates between 17.9 and 323.8 µg/L, respectively, when equations applied to EC MR database from 1980-2014) compared to the other seasonal MR $Al_{i\text{-}c}$ equations. The range of 17.9-323.8 µg/L for estimated $Al_{i\text{-}c}$ is consistent with the Al_i concentrations range of 1.0-200 µg/L across NS rivers in 2006 (Dennis and Clair, 2012). The MRAlt1 $Al_{i\text{-}c}$ estimates for spring/summer increase by $1.99*10^{-1}$ µg/L/year, with significance at 99% confirmed by both the SMK and LS statistical tests. The fall MRAld1 equation $Al_{i\text{-}c}$ estimates decrease significantly (at 99% confirmed by LS and SMK) by $1.52*10^{1}$ µg/L/year. The winter trend from MRS3Alt1 increases by $4.13*10^{-2}$ µg/L, significant at 99% according to the LS, but not significant according to the SMK. When the three seasonal estimates are combined, the overall $Al_{i\text{-}c}$ for MR is decreasing by 2.95 µg/L/year (Figure 3.8); the overall trend is significant at 99% and 95% for LS and SMK, respectively.

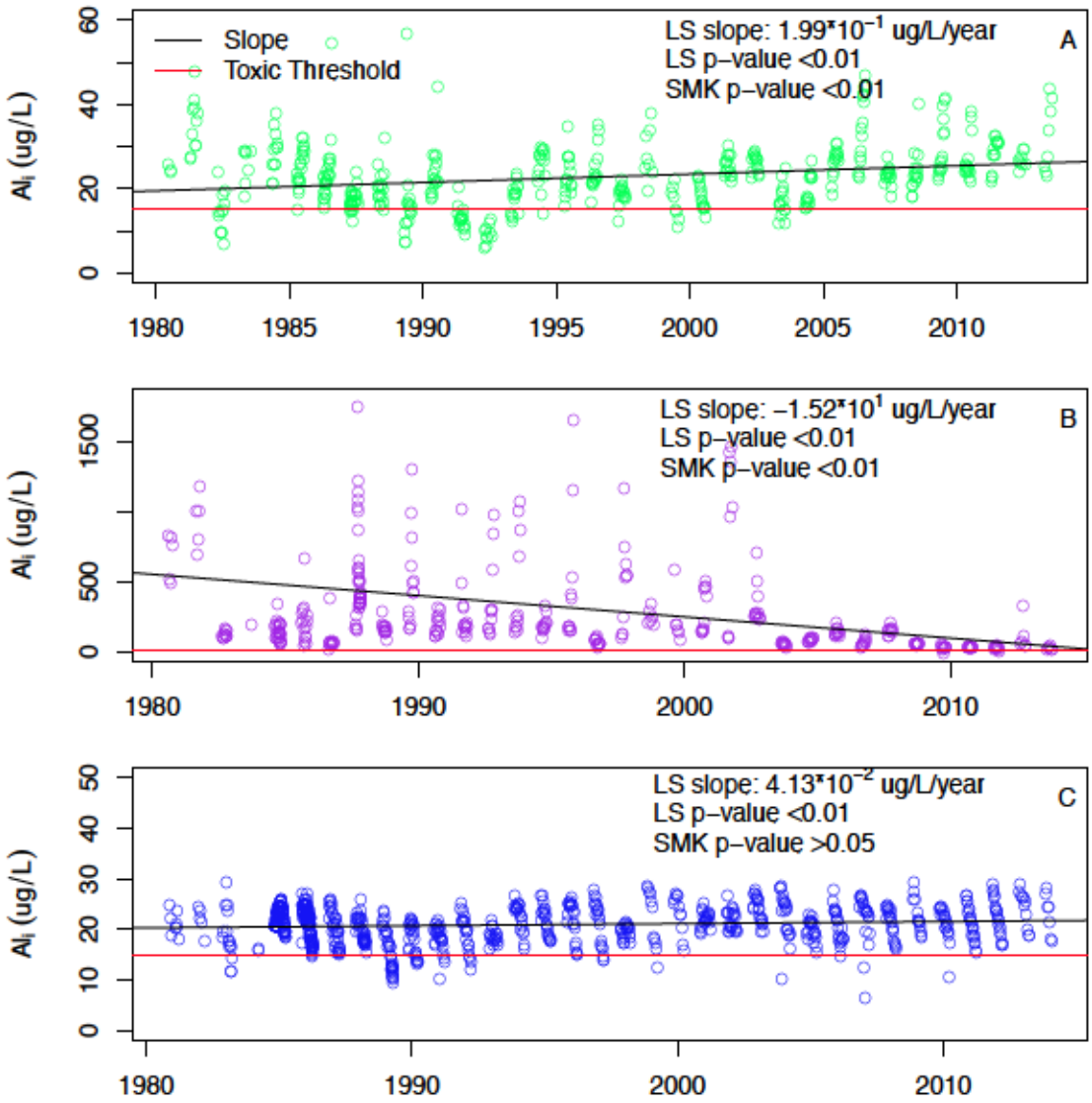

Figure 3.10: Best MR Al_i estimated time-series, with LS trends, and LS and SMK regression p-values for A) season one via MRS1Alt1, B) season two via MRS2Ald1, and C) season three via MRS3Alt1. The red line indicates the 15 µg/L Al_i toxic threshold for Atlantic salmon. Slope values measured using the Least Squares (LS) statistical method, with slope direction significance measured with the LS and Seasonal Mann Kendall (SMK) methods. Values for MRS2Ald1 not shown on graph are 8769.8 µg/L on Oct. 16th, 1980, 6112.5 µg/L on Oct. 24th, 2016, 2222.2 µg/L on Sept. 23rd, 1987, 2158.6 µg/L on Sept. 15th, 1997, 2185.4 µg/L on Sept. 24th, 2001, and 2340.8 µg/L on Oct. 22nd, 2001. Value for MRS3Alt1 not shown is -39.0 µg/L on Dec. 10th, 2002.

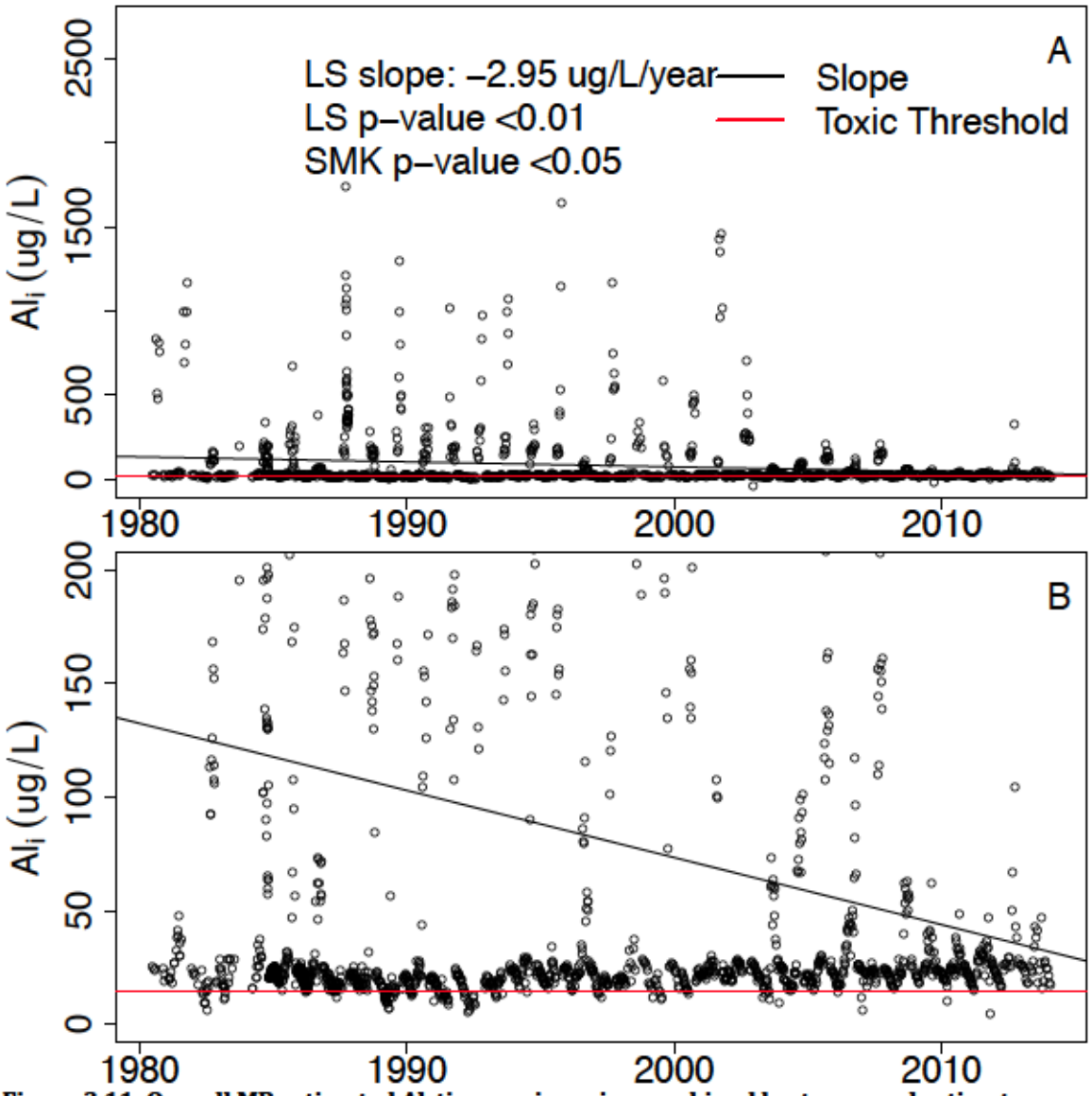

Figure 3.11: Overall MR estimated Al_i time-series using combined best seasonal estimates, with overall LS trend and LS and SMK regression p-values for A) $Al_{i\text{-}c}$ estimates below 2000 µg/L, and B) $Al_{i\text{-}c}$ estimates below 200 µg/L. The red line indicates the 15 µg/L Al_i toxic threshold for Atlantic salmon. Slope values measured using the Least Squares (LS) statistical method, with slope direction significance measured with the LS and Seasonal Mann Kendall (SMK) methods. Values not shown in "A" include -192.0 µg/L on Sept 29th, 1986, -39.0 µg/L on Dec 10th, 2002, -13.9 µg/L on Sept 21st, 2009, 8769.8 µg/L on Oct. 16th, 1980, 6112.5 µg/L on Oct. 24th, 2016, 2222.2 µg/L on Sept. 23rd, 1987, 2158.6 µg/L on Sept. 15th, 1997, 2185.4 µg/L on Sept. 24th, 2001, and 2340.8 µg/L on Oct. 22nd, 2001.

There is uncertainty in the trend slopes and directions for MRS1Alt1, MRS2Ald1, and MRS3Alt1 estimates due to extrapolation beyond the range of parameters used to create the $Al_{i\text{-}c}$ equations (Figure 3.12, Table 3.9). When data outside the parameter ranges for MRS1Alt1 and MRS2Ald1 are omitted, only two $Al_{i\text{-}c}$ values are estimated

for season one (20.9 µg/L and 25.8 µg/L), and one $Al_{i\text{-}c}$ value for season two (24.3 µg/L; Figure 3.12); the two $Al_{i\text{-}c}$ values for spring/summer and one value for fall in MR suggests that the range of parameters used to create the MRS1Alt1 and MRS2Ald1 equations does not include the majority of parameter variability in MR from 1980-2014 during the spring/summer and fall. It appears that pH is the limiting parameter for MRS1Alt1 estimates, as the S1Alt1 equation includes a range of pH which only accounts for 27% of EC pH values between 1980-2014 in spring/summer, while SO_4 is the limiting fall parameter for MRS2Ald1, as the range of SO_4 used to create the S2Ald1 equations accounts for 2.8% of the EC SO_4 concentrations. The season three $Al_{i\text{-}c}$ estimates within the MRS3Alt1 parameters' ranges produce a non-significant (based on LS and SMK) decreasing slope of $1.16*10^{-2}$ µg/L, the opposite direction of the estimated trend produced using all data.

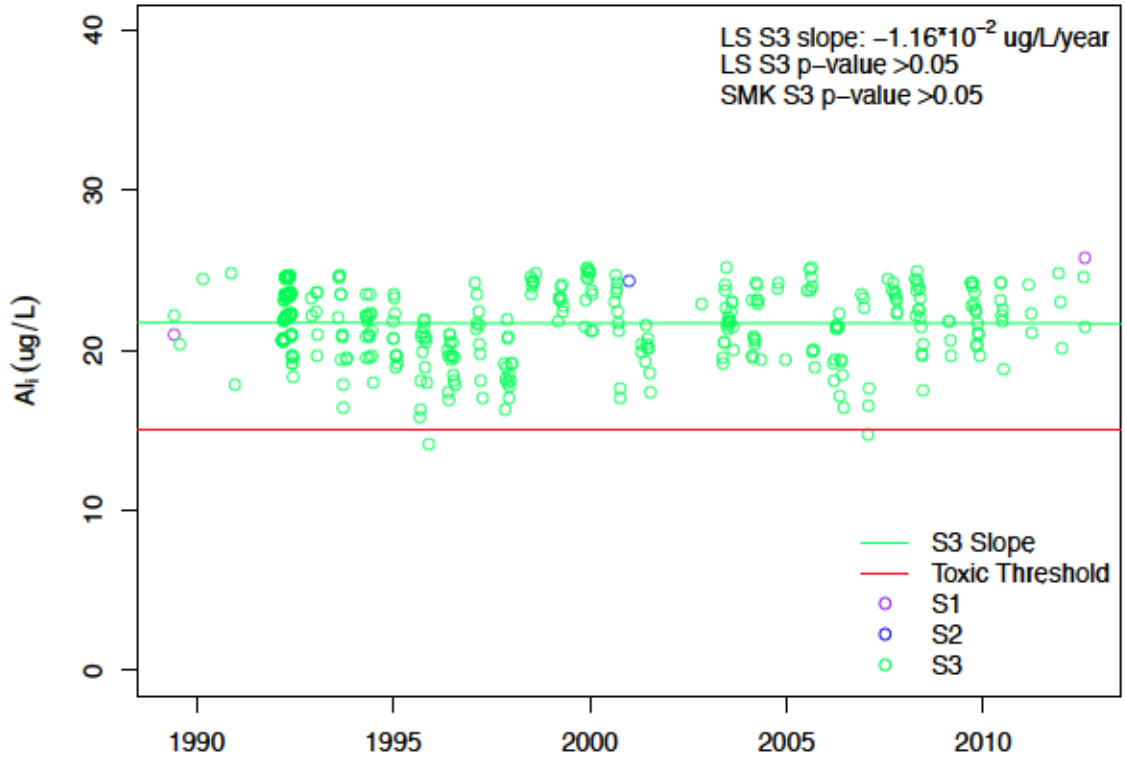

Figure 3.12: $Al_{i\text{-}c}$ estimates using MRS1Alt1, MRS2Ald1, and MRS3Alt1 equations, seasonal LS trend and LS and SMK regression p-values. The red line indicates the 15 µg/L Al_i toxic threshold for Atlantic salmon. Slope values measured using the Least Squares (LS) statistical method, with slope direction significance measured with the LS and Seasonal Mann Kendall (SMK) methods.

Table 3.9: Range of the observational data values used to generate the seasonal $Al_{i\text{-}c}$ equations for MR.

Equation	Season	Parameters	Range
MRS1Alt1	Spring/Summer	Al_t (µg/L)	154.0 – 335.0
		DOC (mg/L)	5.8 - 8.8
		pH	4.81 - 5.58
MRS2Ald1	Fall	Al_d (µg/L)	145.0 – 271.0
		DOC (mg/L)	6.5 - 12.5
		pH	4.18 - 5.20
		Ca_t (µg/L)	612.0 – 946.0
		SO_4 (µg/L)	776.0 – 1180.0
MRS3Alt1	Winter	Al_t (µg/L)	196.0 – 611.0
		DOC (mg/L)	6.12 - 14.4
		pH	3.71 - 3.93
		Ca_t (µg/L)	661.0 – 1480.0

The 20 most extreme $Al_{i\text{-}c}$ estimates (top 20 peaks) are correlated to TOC, SO_4 and Al_d from 1980-2014 for the MRS1Alt1, MRS2Ald1 and MRS3Alt1 equations (Appendix H.1). The MRS1Alt1 top 20 $Al_{i\text{-}c}$ peaks have a positive correlation to TOC (Appendix H.1). $Al_{i\text{-}direct}$ concentrations from 2015-2016 confirm the correlation with DOC (correlation of 67.2%), along with positive correlation with pH (correlation of 50.6%)(Appendix H.1). The top 20 S2MRAld1 $Al_{i\text{-}c}$ concentrations are positively correlated to SO_4 and Ca_t (Appendix H.1); $Al_{i\text{-}direct}$ concentrations have a better correlation with Ca_t (correlation of 64.5%) than with SO_4 (correlation of 42.5%; Appendix H.1); MRS3Alt1 $Al_{i\text{-}c}$ are positively correlated with TOC (Appendix H.1); the 2015-2016 $Al_{i\text{-}direct}$ and DOC concentrations are 67.8% correlated (Appendix H.1).

All equations (MRS2Ald1, MR combined $Al_{i\text{-}c}$ and non-extrapolated MRS2Ald1) project a decreasing trend in $Al_{i\text{-}c}$ between 1980 and 2014 in the MR (Figures 3.10B,

3.11 & 3.12). Estimated fall $Al_{i\text{-}c}$ concentrations are decreasing by $1.52*10^{1}$ µg/L/year in MR from 1980-2014; the decreasing fall $Al_{i\text{-}c}$ slope overpowers the increasing trends of spring/summer and winter, resulting in an overall decrease in $Al_{i\text{-}c}$ of $1.16*10^{-2}$ µg/L. The significant decreasing trends of both MRS2Ald1, and the combined MR seasons, are due to high extreme values at the beginning of the time sequence (8,769.8 and 6,112.5 µg/L on October 16th and 24th, 1980, respectively). When values greater than 100 µg/L are removed from MRS2Ald1 and the combined MR season $Al_{i\text{-}c}$ estimations, the $Al_{i\text{-}c}$ trend for MRS2Ald1 show significantly decreasing $Al_{i\text{-}c}$ concentrations ($-2.58*10^{-3}$ µg/L/year with 99% significance), while the trend of the combined seasonal $Al_{i\text{-}c}$ concentrations predicts significant $Al_{i\text{-}c}$ increases when the >100 µg/L outliers are removed ($5.21*10^{-4}$ µg/L/year at 99% significance). Due to the extreme values of $Al_{i\text{-}c}$ concentrations in 1980, the decreasing slope of MR fall form 1980-2014, using the MRS2Ald1 equation, may be an overestimation.

Due to the difference in $Al_{i\text{-}c}$ slopes by MRS3Alt1 for all data and in-range data, MR $Al_{i\text{-}c}$ equations provide unreliable trends when extrapolated beyond their parameters' ranges. Due to lack of data found within the ranges used for the MR equation parameters in seasons one and two (only 27% of the EC pH range covered in the MRS1Alt1 equation, and 2.8% of EC SO_4 included in the creation of the MRS2Ald1 equation), $Al_{i\text{-}c}$ trends have high uncertainties. In addition, the mean $Al_{i\text{-}c}$ concentration projected by MRS2Ald1 was $2.60*10^{2}$ µg/L; this appears to be an overestimation by the fall equation, as the projected $Al_{i\text{-}c}$ value when applied to range of observational data used to create the MRS2Ald1 equation was 24.3 µg/L (Figures 3.10B & 3.12). For the winter season, the $Al_{i\text{-}c}$ slope is $4.12*10^{-2}$ µg/L/year using all EC data; however, when only using in-range data, the winter slope changes to $-1.16*10^{-2}$ µg/L/year. Although the slope from the in-range data was not significant at 95%, the change from increasing to decreasing slopes for MRS3Alt1 suggests uncertainty associated with MR $Al_{i\text{-}c}$ trends during extrapolation; caution is required when applying the MR equations beyond their ranges.

3.5.3.4. Moose Pit Brook

Season-specific MPB linear equations are used to convert Al_d to Al_t, and lab pH to *in-situ* pH, based on the MPB 2015-2016 water chemistry data (Appendix D.2). The R^2 of the linear Al_t to Al_d model for MPB is 98% for spring/summer and fall in 2015. The R^2 for the linear lab pH to *in-situ* pH model is 44% in the spring/summer, and 36% in the fall. $Al_{i\text{-}c}$ trends are analyzed for MPBS1Ald1 and MPBS2Ald1, as their $Al_{i\text{-}c}$ estimates (first and third quarter $Al_{i\text{-}c}$ values between 6.4 and 48.7 µg/L, respectively) are within the 1.0-200 µg/L range of Al_i concentrations measured in SWNS by Dennis and Clair (2012). $Al_{i\text{-}c}$ trends are not analyzed for the other MPB equations due to unrealistic estimations (negative concentrations and extreme values >1000 µg/L).

Projections of MPB $Al_{i\text{-}c}$ concentrations show increasing $Al_{i\text{-}c}$ trends from 1983-2014 (Appendix G.2, Figures 3.13 & 3.14). The spring/summer trend is significantly (99% for LS and SMK) increasing by $3.09*10^{-1}$ µg/L/year, while fall is increasing (95% significance for LS and SMK) at $1.89*10^{-1}$ µg/L/year. When the $Al_{i\text{-}c}$ estimates are combined, the overall trend is increasing significantly by 99% (for LS and SMK) at $2.42*10^{-1}$ µg/L/year.

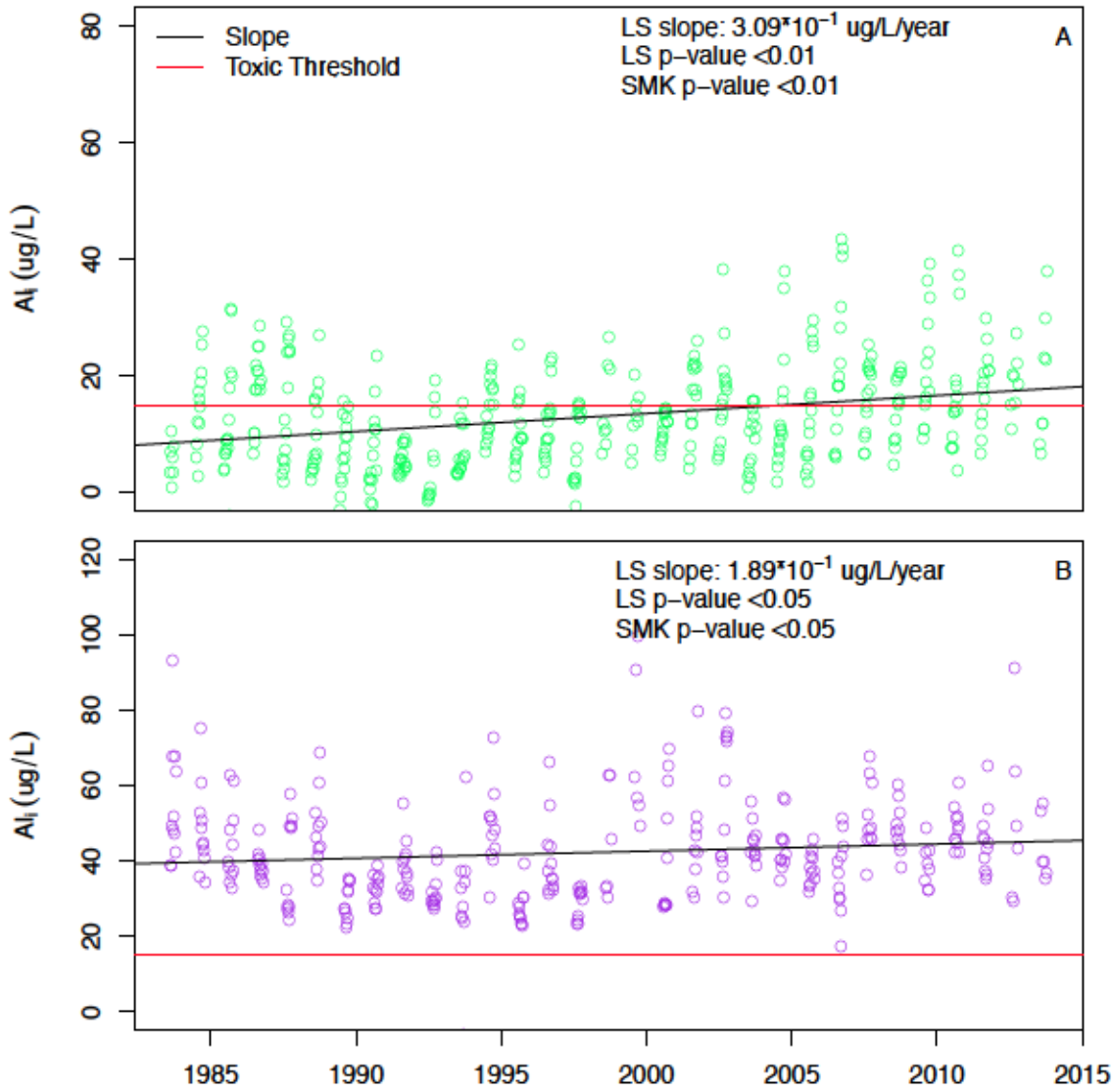

Figure 3.13: Best estimated Al_i trends, with LS trends and LS and SMK regression p-values for A) season one (MPBS1Ald1) and B) season two (MPBS2Ald1). The red line indicates the 15 µg/L Al_i toxic threshold for Atlantic salmon. Slope values measured using the Least Squares (LS) statistical method, with slope direction significance measured with the LS and Seasonal Mann Kendall (SMK) methods. Values on graph not shown for MPBS1Ald1 are -4.2 µg/L on July 1st, 1985, -3.2 µg/L on April 24th, 1989, -0.9 µg/L on May 1st, 1989, -1.7 µg/L on May 14h, 1990, -2.1 µg/L on June 4th, 1990, -1.4 µg/L on April 27th, 1992, -0.3 µg/L on May 4th, 1992, -1.2 µg/L on May 11th, 1992, -0.6 µg/L on May 19th, 1992, -0.1 µg/L on May 25th, 1992, and -2.5 µg/L on June 2nd, 1997. Value not shown for MPBS2Ald1 is -5.9 µg/L on Sept 20th, 1993.

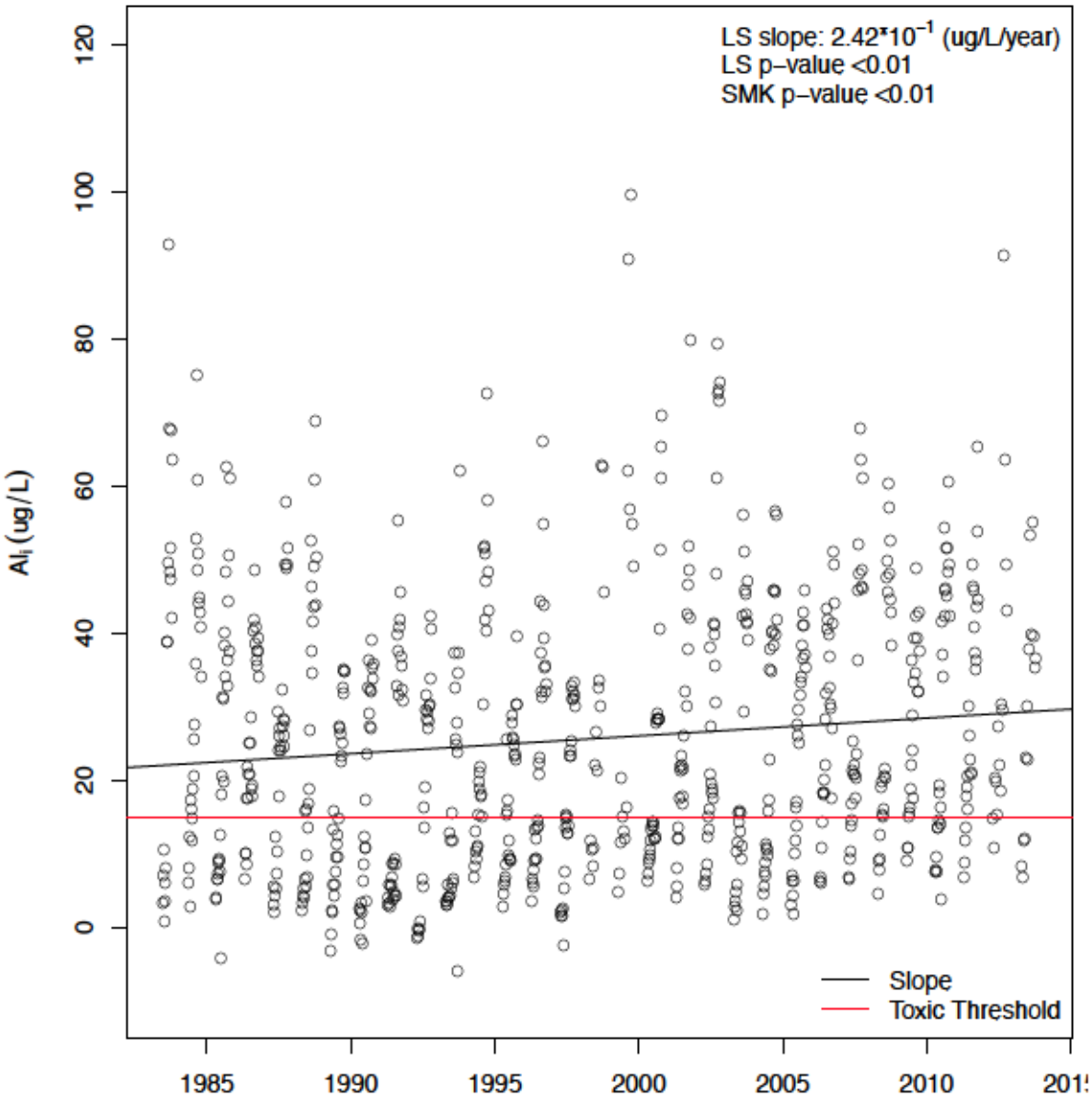

Figure 3.14: Overall MPB Al_i estimated time-series using best seasonal estimates, along with LS regression and LS and SMK regression p-values. The red line indicates the 15 µg/L Al_i toxic threshold for Atlantic salmon. Slope values measured using the Least Squares (LS) statistical method, with slope direction significance measured with the LS and Seasonal Mann Kendall (SMK) methods.

Constrained projections in MPB using the range of parameters used to create the MPB Al_i equations indicate significantly increasing $Al_{i\text{-}c}$ in the spring/summer and fall (Table 3.10, Figure 3.15). The $Al_{i\text{-}c}$ slopes for spring/summer and fall are $1.63*10^{-1}$ and $2.00*10^{-1}$ µg/L/year, respectively; both slopes are significant at 99% with the LS and SMK; trend directions are confirmed, with smaller slopes, using the in-range EC data (Figure 3.15). All $Al_{i\text{-}c}$ concentrations are above the toxic threshold

for season two (fall) from 1980-2014, while the 1980-2014 season one (spring/summer) trend projects increases in Al_{i-c} and the increased exceedance of the toxic threshold by Al_{i-c} values in the future. The application of the Dennis and Clair (2012) equation (referred to as 'TC' – Appendix G.1 and G.2) to the EC database based on spring/summer, fall and winter for MR and MPB also showed increasing Al_i trends in both rivers and all three seasons; however, the Al_i estimates from the TC equation were mostly negative values, which are impossible and reduce the reliability of the TC Al_i trends.

The increasing MPB Al_{i-c} trend is not consistent with the literature, as Al_i concentrations have decreased from 1992-2001 in New York streams (Burns et al., 2006) and in 20 of 22 European streams from 1988-2008 (Monteith et al., 2014). The increase of Al_i concentrations in two of the 22 European streams studied by Monteith et al. (2014) is attributed to increases in SO_4 or NO_3; conversely, declines in SO_4 concentrations have coincided with significant reductions in Al_i for streams in the Hubbard Brook Experimental Forest, New Hampshire, USA from 1982-1998 (Palmer and Driscoll, 2002). Our findings are not consistent with Monteith et al. (2014) and Palmer and Driscoll (2002), as Al_i increases in MPB from 1980-2014 are concurrent with decreases in acid deposition SO_4 concentrations (refer to Chapter 2.6.1); however, due to terminology and methodology inconsistencies (Table 3.1), we cannot say increasing Al_{i-c} in MPB contradicts these studies as the Al species analyzed may not be the same for each study.

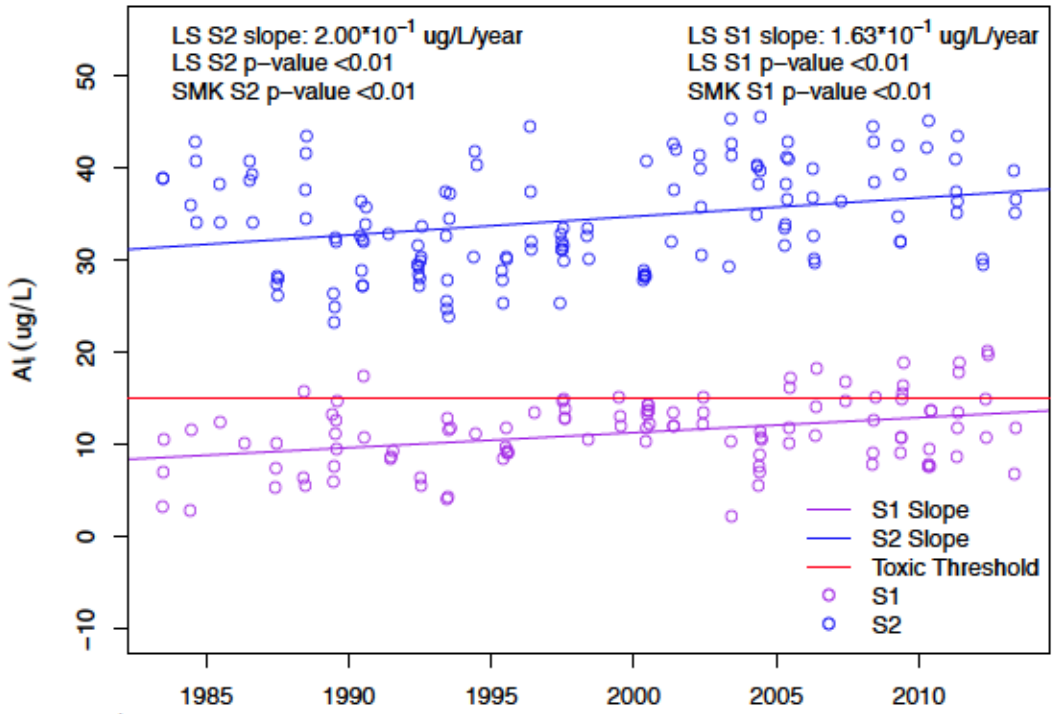

Figure 3.15: $Al_{i\text{-}c}$ estimates using MPBS1Ald1, and MPBS2Ald1 equations, seasonal LS trend and LS and SMK regression p-values. The red line indicates the 15 µg/L Al_i toxic threshold for Atlantic salmon. Slope values measured using the Least Squares (LS) statistical method, with slope direction significance measured with the LS and Seasonal Mann Kendall (SMK) methods.

Table 3.10: Range of the observational data values used to generate the seasonal $Al_{i\text{-}c}$ equations for MPB.

Equation	Season	Parameters	Range
MPBS1Ald1	Spring/Summer	Al_d (µg/L)	76.6 – 271.0
		DOC (mg/L)	4.3 – 19.0
		SO_4	322.0 – 1304
MPBS2Ald1	Fall	Al_d (µg/L)	196.0 – 434.0
		DOC (mg/L)	10.0 – 28.0
		Ca_t (µg/L)	715.0 – 1920.0
		pH	4.07 – 5.02

High TOC concentrations are correlated to the top 20 $Al_{i\text{-}c}$ peaks in MPB for MPBS1Ald1 and MPBS2Ald1, as all top 20 $Al_{i\text{-}c}$ peaks coincide with the highest TOC concentrations (Appendix H.2). The spring/summer top 20 $Al_{i\text{-}c}$ concentrations in MPB from 1980-2014 have a positive correlation with TOC and Al_d (Appendix H.2).

The 2015-2016 $Al_{i\text{-}direct}$ concentrations have a positive correlation with both DOC (correlation of 74.1%) and Al_d (correlation of 74.3%), and a negative correlation with SO_4 (correlation of -67.3%)(Appendix H.2). The fall $Al_{i\text{-}c}$ estimates from 1980-2014 in MPB have a positive correlation to TOC, Al_d and Ca_t(Appendix H.2); there is a negative correlation between $Al_{i\text{-}c}$ and pH(Appendix H.2). $Al_{i\text{-}direct}$ measurements in MPB during 2015-2016 show a positive correlation with DOC, Al_d and Ca_t (correlations of 80.4%, 72.6%, and 63.0%, respectively), and a negative correlation with pH (correlation of -69.9%)(Appendix H.2).

The significant decreasing fall trends, and overall trend of $Al_{i\text{-}c}$ concentrations in MR (Figures 3.10 & 3.11), and significantly increasing spring/summer and fall $Al_{i\text{-}c}$ concentrations in MPB (Figures 3.12, 3.13 & 3.14) suggest that $Al_{i\text{-}c}$ trends are watershed specific. I hypothesize that differences in catchment size and soil acidity control the predicted 1980-2014 $Al_{i\text{-}c}$ trends between MR and MPB. Lofgren et al. (2010) measured 114 Swedish streams in 2005 and found higher Al_i concentrations in smaller catchments (<500 ha) compared to larger catchments (>1000 ha) and attributed these differences to localized changes in podzolation processes, DOC, and groundwater flowpaths; our higher 2015/2016 $Al_{i\text{-}direct}$ concentrations in the MPB (17 km^2), compared to MR (291 km^2), confirm the role of catchment size and DOC on Al_i as presented by Lofgren et al. (2010). I hypothesize that the increases in $Al_{i\text{-}c}$ from 1980-2014 in MPB are due to increased DOC concentrations, as MPB 2015-2016 river DOC concentrations were higher (up to 30 mg/L) and pH values were lower (up to 5.0) compared to MR water samples (up to 15 mg/L of DOC and 6.0 for pH). The increased DOC concentrations in MPB may be increasing the acidity of MPB soils (Figure 3.5), allowing increased mobilization of Al and therefore, the increased projected $Al_{i\text{-}c}$ concentrations in MPB. Increases in DOC in the revised acidification recovery model (refer to Chapter 2.6.6) are concurrent with increases in Al_i concentrations.

The proportion of Al_i concentrations in MR and MPB that exceeds the toxic threshold varies seasonally (Figure 3.4). In both MR and MPB, Al_i levels were below the toxic

threshold during the 2015 and 2016 spring months (Figure 3.4). MR and MPB Al_i levels increase during the summer and fall months (Figure 3.4), a seasonal trend consistent with the summer peaks of Al species in soil waters in the Jizera Mountains, Czech Republic (Tejnecky et al., 2010). Tejnecky et al. attributed the increased Al_i to increased binding with DOC during the summer and early fall; however, in our data, there is a high uncertainty in the trends presented for the fall and winter in MR and MPB, as no data were collected during the fall and winter, 2016 to validate these equations.

Toxic concentrations of $Al_{i\text{-}direct}$ in the MR and MPB may be contributing to high mortality rates and the decline of the SWNS Atlantic salmon populations because $Al_{i\text{-}direct}$ concentrations have exceeded the 15 µg/L toxic threshold throughout 2015-2016 (Figure 3.4). Al_i concentrations are below the 15 µg/L toxic threshold during the spring (Figure 3.4); however, salmon spend several years growing in the rivers before smotification, therefore, they are exposed to the toxic concentrations of Al_i that occur during the summer, fall and winter months. Increases in estimated $Al_{i\text{-}c}$ concentrations are projected from 1980-2014 in the spring/summer and winter for MR, and spring/summer and fall for MPB (Figures 3.0 & 3.13). Increased $Al_{i\text{-}c}$ concentrations during spring/summer and winter in MR overlap with the smoltification stage of salmon; the non-toxic $Al_{i\text{-}c}$ concentrations may become toxic in the future, and $Al_{i\text{-}c}$ concentrations may become lethal if the increases continue. Although there $Al_{i\text{-}c}$ estimates are decreasing in the fall season of MR from 1980-2014 (Figure 3.10), the $Al_{i\text{-}c}$ concentrations still exceed the 15 µg/L threshold for 10% of the fall samples between 2010-2014 (compared to the 19% exceedance between 1980-1990; Figure 3.10), suggesting that future $Al_{i\text{-}direct}$ concentrations may decline, but may still be above the Al_i toxic threshold to Atlantic salmon if the $Al_{i\text{-}c}$ trends are similar to the $Al_{i\text{-}direct}$ concentrations in MR and MPB (Figure 3.10).

3.6.1. Al_i Estimation Uncertainties

Before applying the Al_i equations to the EC database, conversions of pH, Al_t-Al_d and TOC-DOC were required for several equations, increasing $Al_{i\text{-}c}$ trend uncertainties.

Low R^2 values increase the uncertainty in $Al_{i\text{-}c}$ equation outputs, as the conversion equation is based on a simple linear correlation and not representative of river chemical dynamics. Increased uncertainties in $Al_{i\text{-}c}$ may be due to the Al_t-Al_d conversions (R^2 between 7.8% in MRS1 and 98.1% in MPBS1); the oversimplified Al_t-Al_d correlation results in non-representative river water chemistry interactions, as the linear model does not incorporate more complex interactions (exponential, logarithmic, etc.). Conversions between lab and *in-situ* pH may cause $Al_{i\text{-}c}$ uncertainties due to similar reasons to the Al_t-Al_d conversion (lack of fit and linear model ignore more complex relationships). Increased sampling of pH and Al_t/Al_d concentrations in MR and MPB would be helpful to understand the chemical relationships in the rivers, which would allow us to apply a more complex, better-fit model for the conversions. The use of TOC as a proxy for DOC when estimating MR and MPB $Al_{i\text{-}c}$ trends may have resulted in an overestimation of $Al_{i\text{-}c}$ values, as TOC concentrations would include clays and large particles which would not be included in DOC concentrations, resulting in an artificially higher DOC value when applied to the MR and MPB $Al_{i\text{-}c}$ equations.

$Al_{i\text{-}c}$ equations validations suggest further sampling is required, as the equations have limited parameter ranges and have uncertainty in their outputs due to extrapolation (Figures 3.12 & 3.15). The equations have limited ranges due to the small sample numbers (<16 samples) used to create the equations (Tables 3.7 & 3.8). More samples in MR and MPB are necessary to increase the ranges and R^2 for MR and MPB $Al_{i\text{-}c}$ equations (I would recommend 30 samples be obtained for each season and river to ensure an accurate representation of water chemistry for each river and season); increased ranges would help increase how much the $Al_{i\text{-}c}$ equations cover the parameter ranges in the EC database from 1980-2014. More Al_i samples across NS, during all seasons, will help validate the equations for reasonable and reliable outputs.

3.6.2. Recommendations for Future Work

A clear definition and sampling method of Al_i is required for Al_i trend comparison (Table 3.1). Here we suggest a universal definition of Al_i to include all positive Al ions (Al^{3+}, $Al(OH)^{2+}$, and $Al(OH)_2^{1+}$ based on Poleo, 1995), and encourage the adoption of one method (in-field Al speciation, and the estimation of Al_i as the difference between Al_d and Al_o – based off Dennis and Clair, 2012) for Al_i sampling. A universal term and methodology will help encourage collaboration and remove uncertainties when comparing and calculating long-term trends of Al_i concentrations.

In order to improve the accuracy of $Al_{i\text{-}c}$ estimation, it would be beneficial if EC included filtered samples to their water-sampling program. In the application of MR and MPB equations to the EC database, the conversion from Al_t to Al_d adds uncertainty to the Al_i estimates (up to 92% error for the conversion in MRS3 from Al_t to Al_d), as clay particles were not considered and may affect the conversion (clay particles increase Al_t, which would result in the overestimation of Al_d).

pH and temperature would be more representative of river dynamics if *in-situ* monitoring was added to EC sampling techniques. The inclusion of *in-situ* data would remove the lab pH-*in-situ* pH conversion, reducing error in the MR and MPB $Al_{i\text{-}c}$ equations. In addition, *in-situ* temperature provides information on the dynamic of Al_i speciation in MR and MPB rivers.

To increase the accuracy and ability to extrapolate the MRS1Alt1, MRS2Ald1, MRS3Alt1, MPBS1Ald1, and MPBS2Ald1 equations, more Al_i sampling is required in MR and MPB. MR and MPB equations had limited samples to build the regressions ($N \leq 15$); samples are required for the winter season in MPB to create an $Al_{i\text{-}c}$ equation and estimate a long-term $Al_{i\text{-}c}$ trend. Further sampling is required at MR and MPB during the fall and winter seasons to validate the MRS1Alt1 and MPBS1Ald1 equations. With additional samples, parameter ranges of pH and DOC

in the MR and MPB $Al_{i\text{-}c}$ equations can be increased. pH values below 4.5 and greater than 5.5 are required to capture the relationship of Al speciation and pH. Samples with DOC concentrations >15 mg/L are required to capture the role of organic acidity and organic complexes on Al_i in all seasons, as all of our DOC data in MR and half of DOC data from MPB in 2015/2016 (Figure 3.5) were below the 10 mg/L throughout all season (Figure 3.5). In addition, the MRS1Alt1 and MPBS1Ald1 equations were only extrapolated to seven other sites (with <7 samples per site). More $Al_{i\text{-}direct}$ samples are required from sites across NS (not just SWNS and the ES) to understand what spatial characteristics are causing the spatial variation of Al_i (such as watershed size, vegetation coverage, and wetland coverage). More $Al_{i\text{-}direct}$ data is required from MR and MPB: in the spring to assess the threat of Al_i to Atlantic salmon, and in the summer to confirm the role of deep flow pathways on high Al_i concentrations. Increased sampling frequency of Al_i samples is suggested to capture river chemistry interactions for the diurnal cycle and during high-flow events. It would be beneficial to collect $Al_{i\text{-}direct}$ samples over several years, to confirm seasonal variations and the general direction of trends in MR and MPB.

$Al_{i\text{-}direct}$ concentrations pose a threat to aquatic health throughout the majority of the year (summer, fall and winter) because $Al_{i\text{-}direct}$ concentrations exceed the 15 µg/L toxic threshold for Atlantic salmon in the MR and MPB (Figure 3.4). Our data indicate that Al_i levels should be monitored to assess fish population losses related to acidification and toxic Al_i, as $Al_{i\text{-}direct}$ concentrations in MR and MPB from 2015-2016 exceeded the 15 µg/L toxic threshold, and Al_i is a known toxin to aquatic organisms. Liming mitigation strategies have been applied to regions of NS, by applying base cations to soils, to increase river pH, decrease Al_i concentrations, and increase the productivity of salmon habitats; monitoring Al_i concentrations during the application of lime is proposed, in order to help monitor the progress of salmon habitat restoration. It would be beneficial for future liming applications to include Al_i monitoring in the list of measured water chemicals to ensure enough lime has been applied to reduce Al_i concentrations below the toxic threshold. In addition, as Al_i affects other aquatic organisms, we advise that liming projects investigate the

negative effects and toxic thresholds for all species found within a catchment, not just Atlantic salmon.

3.7. Conclusion

Al, a toxin to aquatic organisms, is mobilized due to chronic acidification of soils. In NS, a region highly affected by acid deposition, Atlantic salmon populations have decreased by 88-99% in four rivers since the 1980s (Bowlby et al., 2013), concurrent with increases in Al concentrations in rivers (refer to Chapter 2). However, current concentrations and interannual trends of Al_i in NS are unknown. In addition, Al_i concentrations have not been validated in the literature, and are not tailored to NS-specific watershed characteristics (such as geology, acid deposition amounts, and base cation concentrations in soils). In this study, we investigated current concentrations of Al_i in 2015/2016, created Al_i regressions to predict Al_i concentrations in NS, and quantified interannual Al_i trends in two rivers in NS. We measured Al_i concentrations weekly in MR and MPB from 2015 to 2016, created season- and river-specific Al_i estimation equations and validated the equations using additional data from 2016 and extrapolated the equations to seven sites across NS.

Al_i concentrations in MR and MPB continuously exceeded the toxic threshold for salmon during the summer, fall and winter months between 2015 and 2016. Al_i concentrations are highest in the summer months for MR, and highest in the fall for MPB; Al_i concentrations peaked at 42 µg/L and 48 µg/L, respectively. Al_i summer and fall peaks coincide with peaks in DOC, while the low spring Al_i concentrations coincide with high flow due to spring melt, suggesting a dilution effect. McKnight and Bencala (1988) reported a dilution in Al concentrations in the Colorado Rockies, which supports our findings; however, the dilution effects in MR and MPB contradict the spring melt peak in Al_i concentrations recorded by Campbell et al. (1992). High Al_i concentrations during the summer suggest water flow paths through soils drive river Al_i concentrations (Sullivan et al., 1986, Cozzarelli et al., 1987). Winter Al_i concentrations do not agree with the literature, as the ratio of Al_i concentrations increases with decreased temperatures (Lydersen et al., 1990).

We created Al_i equations for MR and MPB, with R^2 up to 100%; however, small sample sizes limit the range of the equations. The spring/summer Al_i equation for MR, which uses Al_t as a parameter, has an R^2 of 22%; the spring/summer Al_i equation for MPB has an R^2 of 69%. During validation using five data points from the spring/summer 2016 for MR and MPB, the MRS2Alt1 and MPBS1Ald1 equations provided reasonable estimates (between 0-200 µg/L based on the range of Al_i concentrations measured in Atlantic Canada by Dennis and Clair, 2012). However, they could only estimate $Al_{i\text{-}c}$ concentrations within 20% of the true value for 20% of the samples. In addition, the spring/summer Al_i equations for MR and MPB were extrapolated to seven other sites across NS, with the MR equation overestimating values and MPB underestimating values.

Trends of Al_i in MR and MPB are seasonally-, and river-dependent. MR Al_i concentrations increased in the spring/summer and winter, and decreased in the fall from 1980-2014. MPB spring/summer and fall seasons showed increased Al_i concentrations from 1983-2014. When the seasonal trends of Al_i are combined, the overall Al_i trend in MR decreased from 1980-2014, while MPB Al_i increased from 1983-2014. When the MR and MPB equations are applied to EC data only within the range of values used to create the regressions, Al_i concentrations decreased in the winter; however, not enough EC data was within the range of values for the MR spring/summer and fall season equations, therefore no Al_i trends were calculated. Al_i concentrations decreased in the winter. In MPB, when applied to the ranges for parameters included to create the regression, both the spring/summer and fall seasons showed increasing trends.

$Al_{i\text{-}direct}$ concentrations may be a factor in the declines of Atlantic salmon populations in NS. As regional $Al_{i\text{-}direct}$ concentrations are above the toxic threshold, $Al_{i\text{-}direct}$ may be harming current salmon populations; expected increases in $Al_{i\text{-}direct}$ concentrations for the spring and summer months suggests $Al_{i\text{-}direct}$ may pose a greater threat to salmon populations in the near future. Mitigation strategies, such

as liming, should consider adding $Al_{i\text{-direct}}$ to the water chemistry sampling protocol, to ensure mitigation methods are addressing the toxic, indirect effect of acidification: Al_i.

Continued monitoring of Al_i concentrations in NS is recommended to increase knowledge of Al_i trends. Increased samples of Ali concentrations in MR and MPB are required during the winter season, and during high flow events, to understand how discharge and winter weather influences Al_i concentrations. In addition, winter samples are required in MPB to create an Al_i equation; samples are required during the fall and winter in MR and MPB to validate the Al_i equations. Additional samples would increase the range of values for parameters used to create the Al_i equations, and increase the accuracy and precision of parameter conversions. We recommend sampling Al_i concentrations in soils to investigate the source of the Al_i concentrations in NS rivers.

The exceedance of the toxic threshold by Al_i concentrations across NS in 2016 suggests diversity of life in NS is at risk. Al_i concentrations are above the toxic threshold for Atlantic salmon; however, Al_i is a known toxic to various aquatic species. If Al_i concentrations increase, few aquatic habitats may remain suitable to sustain life. Monitoring Al_i concentrations is required in chronically acidified regions where Al concentrations may be increasing, such as NS, to mitigate and prevent the loss of biodiversity.

Chapter 4 Conclusion

Acidification recovery coincides with Al decreases in Europe and North America; however, in regions with high concentration of organic acids, freshwaters are chronically acidified and chemical acidification recovery trends are less understood. As organic acids are known to reduce the recovery of stream pH, it is unclear whether regions with high DOC follow the same recovery stages as the classic model. In addition, as Al and Al_i trends have not been assessed in NS, it is unclear if Al_i is a factor in the declines of the Southern Uplands Atlantic salmon populations in NS since the 1980s. In this study, we monitored Al concentrations from 1980-2014 and measured Al_i concentrations from 2015-2016 in MR and MPB in SWNS to determine: are NS, DOC-rich freshwaters following the classic acidification recovery model, are flow, DOC and temperature correlated to changes in Al_t, are Al_i concentrations above the toxic threshold for Atlantic salmon, can Ali concentrations be predicted using an equation composed of DOC, pH and flow, and are Al_i concentrations increasing from 1980-2014?

Here we propose that NS rivers do not follow the classic acidification model, as Al_t concentrations are increasing from 1980-2014, a trend not consistent with the classic model. Following decreases in sulfate concentrations (refer to Chapter 2.6.1), MR and MPB have significant increases in Al_t and TOC concentrations, and significant decreases in base cation (Ca, Mg) concentrations from 1980-2014 (refer to Chapter 2.6.2); our findings suggest that chronic acidification has reduced NS soils' base cation saturation, with soil acidity maintained by organic acids from TOC resulting in increased mobilization of Al_t. Increases in Alt concentrations since the 1980s are recorded on 35.4% of 65 lakes and rivers analyzed across NS, suggesting that the divergence of acidification recovery due to increasing Al_t is a regional NS trend. Our results of increasing Al_t conflict with the decreases in Al recorded by Hruska et al. (2009), who projected acidification recovery with high DOC; we suggest that slow-weather bedrock is causing the divergence from the Hruska et al. findings due to

minimal soil base cation replenishment compared to the Hruska et al. watersheds. We propose a new acidification recovery model based on the >30-year water chemistry data from MR and MPB to account for the role of TOC concentrations on soil pH and Al_t (refer to Chapter 2.6.6).

Here we find that DOC, flow and temperature changes are correlated to changes in Al_t concentrations in NS from 1980-2014. Fall peaks in Alt concentrations for MR and MPB from 1980-2014 correspond to fall peaks in TOC and discharge. Increases in Al_t concentrations from the 1980-2003 to 2003-2014 period coincide with increases in TOC, discharge and air temperature (refer to Chapter 2.6.4). Climate change is influencing Al_t concentrations in high TOC regions, as increased temperatures have been linked with increased detritus decay and DOC production, which in turn, increases organic acidity and mobilizes Al, in addition, increased storms associated with climate change, represented by increased flow values between the 1980-2003 and 203-2014 periods, suggest that the increased frequency storms may be increasingly flushing cations (including Al) from soils.

Al_i concentrations are above the 15 μg/L toxic threshold for Atlantic salmon in NS during the summer, winter and fall 2015/2016 months. Al_i concentrations in MR reach 42 μg/L, which occur during the summer months, with concentrations up to 48 μg/L in MPB occurring during the fall months (refer to Chapter 3.5.1.1). The continuously higher DOC concentrations in MPB compared to MR during the summer, fall and winter months, suggests that MPB has higher concentrations of organic acids which may be mobilizing Al and increasing Al_i concentrations. The lowest concentrations of Al_i occur during the spring months for both MR and MPB, which coincide with spring melt. The dilution effect on Al_i concentrations we observed during the spring months in MR and MPB support dilution effects on Al recorded by McKnight and Bencala (1988); however, they contradict findings by Campbell et al., 1992, where Al_i concentrations rose with increased spring discharge. We hypothesize that shallow flow paths during high flow events in MR and MPB result in limited leaching of Al_i from the Al_i-poor shallow organic soil layers, as found

by Mulholland et al. (1981) and Sullivan et al. (1986). In addition, the high concentrations of Al_i in MR and MPB during the summer months disagree with Lydersen (1990), who found that Al_i ratios decrease with increased temperature. Toxic concentrations of Al_i appear to be a regional trend, as seven sites across NS, sampled during the spring and summer 2016, have Al_i concentrations exceeding the 15 µg/L threshold (refer to Chapter 3.5.1.2).

DOC, pH and flow parameters can predict Al_i concentrations in MR and MPB; however, more Al_i samples are required to improve the accuracy and validity of the equations. 90% of MR Ali equations required DOC as a parameter, with 20% incorporating the discharge parameter and 80% incorporating pH (refer to Chapter 3.5.2.1). In MPB, 75% of the spring/summer and fall Al_i equations incorporated DOC and/or pH, while 50% of the equations used the discharge parameter; however, due to lack of field data, no winter Al_i equation was created for MPB (refer to Chapter 3.5.2.2). The R^2 for MR and MPB Ali equations ranged from 22-100% and 62-94%, respectively. As the MR and MPB Ali equations were only created using 10-14 data points throughout 2015-2016, more Al_i samples are required to increase the accuracy of the equations, and to create a winter equation for MPB.

Our estimated $Al_{i\text{-}c}$ trends suggest Al_i trends from 1980-2014 are river- and season-dependent (refer to Chapter 3.5.3). Our $Al_{i\text{-}c}$ estimates are increasing in MR from 1980-2014 for the spring/summer and winter seasons, with a decreasing $Al_{i\text{-}c}$ trend during the fall. MPB $Al_{i\text{-}c}$ estimates show increasing Al_i concentrations from 1983-2014 for both the spring/summer and fall seasons. After applying our Al_i equations for the MR and MPB only to data within the parameter ranges used to create the Al_i equations, the MR spring/summer and fall estimates did not provide enough data to create any trends; however, the winter trend is decreasing, which suggests uncertainty in the winter MR Al_i equation due to extrapolation of the equation beyond its range. The MPB $Al_{i\text{-}c}$ estimates when applied to the range of data used to create the Al_i equations show significantly increasing Al_i. We suggest that more Al_i

samples from MR and MPB, in addition to Al_i samples across NS, are measured to increase the range of parameters in the Al_i equations and to validate the equations.

Our study shows the first reported case of increasing aluminum concentrations in DOC-rich rivers following decreased sulfate acid deposition. Increasing Al and Al_i concentrations in these rivers pose a threat to the diversity of life in these DOC-rich regions, as Al_i concentrations are expected to continue increasing if no mitigation strategies are applied. More research is needed on the drivers and different chemical conditions that control increases in Al_i concentrations, in order to understand the potential threat Al_i trends pose to Atlantic salmon populations, and other aquatic organisms.

References

Ashforth, D., & Yan, N. D. (2008). The interactive effects of calcium concentration and temperature on the survival and reproduction of daphnia pulex at high and low food concentrations. ***Limnology and Oceanography, 53***(2), 420.

Bache, B. (1985). Soil acidification and aluminium mobility. ***Soil use and Management, 1***(1), 10-13.

Baldigo, B., & Lawrence, G. (2000). Composition of fish communities in relation to stream acidification and habitat in the Neversink river, New York. ***Transactions of the American Fisheries Society, 129***(1), 60-76.

Bobba, A., & Lam, D. (1989). Application of hydrological model to acidified watersheds: A study on Mersey River and Moose Pit Brook, Nova Scotia. ***Water, Air, and Soil Pollution, 46***(1-4), 261-275.

Bowlby, H., Horsman, T., Mitchell, S., & Gibson, A. (2013). Recovery potential assessment for southern upland Atlantic salmon: Habitat requirements and availability, threats to populations, and feasibility of habitat restoration. ***DFO Canadian Science Advisory Secretariat Research Document, 6***

Bricker, O. P., & Rice, K. C. (1989). Acidic deposition to streams. ***Environmental Science & Technology***, ***23***(4), 379-385.

Burns, D. A., McHale, M. R., Driscoll, C. T., & Roy, K. M. (2006). Response of surface water chemistry to reduced levels of acid precipitation: Comparison of trends in two regions of New York, USA. ***Hydrological Processes, 20***(7), 1611-1627.

Butler, T. J., Likens, G. E., & Stunder, B. J. (2001). Regional-scale impacts of phase I of the clean air act amendments in the USA: The relation between emissions and concentrations, both wet and dry. ***Atmospheric Environment, 35***(6), 1015-1028.

Campbell, P. G., Hansen, H. J., Dubreuil, B., & Nelson, W. O. (1992). Geochemistry of Quebec north shore salmon rivers during snowmelt: Organic acid pulse and aluminum mobilization. ***Canadian Journal of Fisheries and Aquatic Sciences, 49***(9), 1938-1952.

Charles, D. F., Battarbee, R. W., Renberg, I., van Dam, H., & Smol, J. P. (1990). Paleoecological analysis of lake acidification trends in North America and Europe using diatoms and chrysophytes. ***Acidic precipitation*** (pp. 207-276) Springer.

Charles, D. F., Binford, M. W., Furlong, E. T., Hites, R. A., Mitchell, M. J., Norton, S. A., et al. (1990). Paleoecological investigation of recent lake acidification in the Adirondack mountains, NY. *Journal of Paleolimnology, 3*(3), 195-241.

Clair, T., Dennis, I., Vet, R., & Laudon, H. (2008). Long-term trends in catchment organic carbon and nitrogen exports from three acidified catchments in Nova Scotia, Canada. *Biogeochemistry, 87*(1), 83-97.

Clair, T. A., Dennis, I. F., Amiro, P. G., & Cosby, B. (2004). Past and future chemistry changes in acidified Nova Scotian Atlantic salmon (salmo salar) rivers: A dynamic modeling approach. *Canadian Journal of Fisheries and Aquatic Sciences, 61*(10), 1965-1975.

Clair, T. A., Dennis, I. F., Scruton, D. A., & Gilliss, M. (2007). Freshwater acidification research in Atlantic canada: A review of results and predictions for the future. *Environmental Reviews, 15*(NA), 153-167.

Clair, T. A., Dennis, I. F., & Vet, R. (2011). Water chemistry and dissolved organic carbon trends in lakes from Canada's Atlantic provinces: No recovery from acidification measured after 25 years of lake monitoring. *Canadian Journal of Fisheries and Aquatic Sciences, 68*(4), 663-674.

Clair, T. A., Ehrman, J. M., Ouellet, A. J., Brun, G., Lockerbie, D., & Ro, C. (2002). Changes in freshwater acidification trends in Canada's Atlantic provinces: 1983–1997. *Water, Air, and Soil Pollution, 135*(1-4), 335-354.

Clair, T. A., Pollock, T. L., Collins, P. V., & Kramer, J. R. (1992). How brown waters are influenced by acidification: The HUMEX lake case study. *Environment International, 18*(6), 589-596.

Cosby, B. J., Hornberger, G. M., Galloway, J. N., & Wright, R. E. (1985). Time scales of catchment acidification. A quantitative model for estimating freshwater acidification. *Environmental Science & Technology, 19*(12), 1144-1149.

Couture, S., Houle, D., & Gagnon, C. (2012). Increases of dissolved organic carbon in temperate and boreal lakes in Quebec, Canada. *Environmental Science and Pollution Research, 19*(2), 361-371.

Cozzarelli, I. M., Herman, J. S., & Parnell, R. A. (1987). The mobilization of aluminum in a natural soil system: Effects of hydrologic pathways. *Water Resources Research, 23*(5), 859-874.

Davies, J., Jenkins, A., Monteith, D., Evans, C., & Cooper, D. (2005). Trends in surface water chemistry of acidified UK freshwaters, 1988–2002. *Environmental Pollution, 137*(1), 27-39.

Davis, R. B., Anderson, D. S., & Berge, F. (1985). Palaeolimnological evidence that lake acidification is accompanied by loss of organic matter. ***Nature, 316***, 436-438.

De Wit, H. A., Mulder, J., Hindar, A., & Hole, L. (2007). Long-term increase in dissolved organic carbon in streamwaters in Norway is response to reduced acid deposition. ***Environmental Science & Technology, 41***(22), 7706-7713.

Dennis, I. F., & Clair, T. A. (2012). The distribution of dissolved aluminum in Atlantic salmon (salmo salar) rivers of Atlantic Canada and its potential effect on aquatic populations. ***Canadian Journal of Fisheries and Aquatic Sciences, 69***(7), 1174-1183.

Department of Natural Resources NS. (2005). ***Forest inventory NS - geographic information systems.*** http://novascotia.ca/natr/forestry/gis/dl_forestry.asp. Accessed August 20th, 2016.

Department of Natural Resources NS, Geoscience and Mines Branch. (2006). ***NS DEM version2.*** http://novascotia.ca/natr/MEB/download/mg/ofm/htm/disp_map_list.asp. Accessed August 20th, 2016.

Drever, J. I., & Vance, G. F. (1994). Role of soil organic acids in mineral weathering processes. ***Organic acids in geological processes*** (pp. 138-161) Springer.

Driscoll, C. T. (1984). A procedure for the fractionation of aqueous aluminum in dilute acidic waters. ***International Journal of Environmental Analytical Chemistry, 16***(4), 267-283.

Driscoll, C. T. (1985). Aluminum in acidic surface waters: Chemistry, transport, and effects. ***Environmental Health Perspectives, 63***, 93-104.

Driscoll, C. T., Baker, J. P., Bisogni, J. J., & Schofield, C. L. (1980). Effect of aluminium speciation on fish in dilute acidified waters.

Driscoll, C. T., Fuller, R. D., & Schecher, W. D. (1989). The role of organic acids in the acidification of surface waters in the Eastern US. ***Water, Air, and Soil Pollution, 43***(1-2), 21-40.

Driscoll, C.T., Lawrence, G.B., Bulger, A.J., Butler, T.J., Cronan, C.S., Eagar, C., Lambert, K.F., Likens, G.E., Stoddard, J.L. and Weathers, K.C., (2001). Acidic Deposition in the Northeastern United States: Sources and Inputs, Ecosystem Effects, and Management Strategies: The effects of acidic deposition in the northeastern United States include the acidification of soil and water, which stresses terrestrial and aquatic biota. ***BioScience, 51***(3): 180-198.

EPA. (1994). *"Method 200.8: Determination of trace elements in waters and wastes by inductively coupled plasma-mass spectrometry," revision 5.4.*

EPA. (1998). *"Method 6020A (SW-846): Inductively coupled plasma-mass spectrometry," revision 1.*

Erlandsson, M., Cory, N., Fölster, J., Köhler, S., Laudon, H., Weyhenmeyer, G. A., et al. (2011). Increasing dissolved organic carbon redefines the extent of surface water acidification and helps resolve a classic controversy. *Bioscience, 61*(8), 614-618.

Evans, C., Cullen, J., Alewell, C., Kopácek, J., Marchetto, A., Moldan, F., et al. (2001). Recovery from acidification in European surface waters. *Hydrology and Earth System Sciences Discussions, 5*(3), 283-298.

Evans, C., & Monteith, D. (2001). Chemical trends at lakes and streams in the UK acid waters monitoring network, 1988-2000: Evidence for recent recovery at a national scale. *Hydrology and Earth System Sciences, 5*(3), 351-366.

Evans, C., Monteith, D., & Cooper, D. (2005). Long-term increases in surface water dissolved organic carbon: Observations, possible causes and environmental impacts. *Environmental Pollution, 137*(1), 55-71.

Evans, C. D., Monteith, D. T., Reynolds, B., & Clark, J. M. (2008). Buffering of recovery from acidification by organic acids. *Science of the Total Environment, 404*(2), 316-325.

Exley, C., Chappell, J., & Birchall, J. (1991). A mechanism for acute aluminium toxicity in fish. *Journal of Theoretical Biology, 151*(3), 417-428.

Fernandez, I. J., Rustad, L. E., Norton, S. A., Kahl, J. S., & Cosby, B. J. (2003). Experimental acidification causes soil base-cation depletion at the Bear Brook watershed in maine. *Soil Science Society of America Journal, 67*(6), 1909-1919.

Freedman, B., & Clair, T. A. (1987). Ion mass balances and seasonal fluxes from four acidic brownwater streams in Nova Scotia. *Canadian Journal of Fisheries and Aquatic Sciences, 44*(3), 538-548.

Friedlingstein, P., Cox, P., Betts, R., Bopp, L., Von Bloh, W., Brovkin, V., Cadule, P., Doney, S., Eby, M., Fung, I. & Bala, G., (2006). Climate-carbon cycle feedback analysis: Results from the C4MIP model intercomparison. *Journal of Climate, 19*(14), 3337-3353.

Futter, M. N., Valinia, S., Löfgren, S., Köhler, S. J., & Fölster, J. (2014). Long-term trends in water chemistry of acid-sensitive swedish lakes show slow recovery from historic acidification. *Ambio, 43*(1), 77-90.

Galloway, J. N., Norton, S. A., & Church, M. R. (1983). Freshwater acidification from atmospheric deposition of sulfuric acid: A conceptual model. *Environmental Science & Technology*, *17*(11), 541A-545A.

Gilliam, F. S., & Adams, M. B. (1996). Wetfall deposition and precipitation chemistry for a central Appalachian forest. *Journal of the Air & Waste Management Association*, *46*(10), 978-984.

Ginn, B. K., Cumming, B. F., & Smol, J. P. (2007). Assessing pH changes since pre-industrial times in 51 low-alkalinity lakes in Nova Scotia, Canada. *Canadian Journal of Fisheries and Aquatic Sciences, 64*(8), 1043-1054.

Gorham, E., Underwood, J. K., Martini, F. B., & Ogden, J. G. (1986). Natural and anthropogenic causes of lake acidification in Nova Scotia. *Nature, 324*, 451-453.

Helliweli, S., Batley, G., Florence, T., & Lumsden, B. (1983). Speciation and toxicity of aluminium in a model fresh water. *Environmental Technology, 4*(3), 141-144.

Hesthagen, T., Fjellheim, A., Schartau, A. K., Wright, R. F., Saksgård, R., & Rosseland, B. O. (2011). Chemical and biological recovery of lake saudlandsvatn, a formerly highly acidified lake in southernmost Norway, in response to decreased acid deposition. *Science of the Total Environment, 409*(15), 2908-2916.

Hindar, A., Tørseth, K., Henriksen, A., & Orsolini, Y. (2004). The significance of the north atlantic oscillation (NAO) for sea-salt episodes and acidification-related effects in Norwegian rivers. *Environmental Science & Technology, 38*(1), 26-33.

Howells, G., Dalziel, T., Reader, J., & Solbe, J. (1990). EIFAC water quality criteria for european freshwater fish: Report on aluminium. *Chemistry and Ecology, 4*(3), 117-173.

Hruška, J., Krám, P., McDowell, W. H., & Oulehle, F. (2009). Increased dissolved organic carbon (DOC) in Central European streams is driven by reductions in ionic strength rather than climate change or decreasing acidity. *Environmental Science & Technology*, *43*(12), 4320-4326.

Hue, N., Craddock, G., & Adams, F. (1986). Effect of organic acids on aluminum toxicity in subsoils. *Soil Science Society of America Journal, 50*(1), 28-34.

Hurrell, J. W., & Deser, C. (2010). North Atlantic climate variability: the role of the North Atlantic Oscillation. *Journal of Marine Systems*, *79*(3), 231-244.

Jansen, B., Nierop, K. G., & Verstraten, J. M. (2003). Mobility of Fe (II), Fe (III) and Al in acidic forest soils mediated by dissolved organic matter: Influence of solution pH and metal/organic carbon ratios. *Geoderma, 113*(3), 323-340.

Jeffries, D. S., Clair, T. A., Couture, S., Dillon, P. J., Dupont, J., Keller, W., et al. (2003). Assessing the recovery of lakes in Southeastern Canada from the effects of acidic deposition. ***AMBIO: A Journal of the Human Environment, 32***(3), 176-182.

Josephson, D. C., Robinson, J. M., Chiotti, J., Jirka, K. J., & Kraft, C. E. (2014). Chemical and biological recovery from acid deposition within the Honnedaga Lake watershed, New York, USA. ***Environmental Monitoring and Assessment, 186***(7), 4391-4409.

Kerekes, J., Beauchamp, S., Tordon, R., Tremblay, C., & Pollock, T. (1986). Organic versus anthropogenic acidity in tributaries of the Kejimkujik watersheds in western Nova Scotia. ***Acidic precipitation*** (pp. 1219-1227) Springer.

Kingston, J. C., Birks, H. J. B., Uutala, A. J., Cumming, B. F., & Smol, J. P. (1992). Assessing trends in fishery resources and lake water aluminum from paleolimnological analyses of siliceous algae. ***Canadian Journal of Fisheries and Aquatic Sciences, 49***(1), 116-127.

Kopacek, J., Hejzlar, J., & Porcal, P. (2000). Seasonal patterns in chemistry of tributaries to plesne and certovo lakes in the 1998 hydrological year. ***Silva Gabreta,*** (4), 105-116.

Kopáček, J., Turek, J., Hejzlar, J., Kaňa, J., & Porcal, P. (2006). Element fluxes in watershed-lake ecosystems recovering from acidification: Čertovo lake, the bohemian forest, 2001–2005. ***Biologia, 61***(20), S413-S426.

Krám, P., Hruška, J., Driscoll, C. T., Johnson, C. E., & Oulehle, F. (2009). Long-term changes in aluminum fractions of drainage waters in two forest catchments with contrasting lithology. ***Journal of Inorganic Biochemistry, 103***(11), 1465-1472.

Kristensen, T., Åtland, Å., Rosten, T., Urke, H., & Rosseland, B. (2009). Important influent-water quality parameters at freshwater production sites in two salmon producing countries. ***Aquacultural Engineering, 41***(2), 53-59.

Kroglund, F., Rosseland, B. O., Teien, H. C., Salbu, B., Kristensen, T., & Finstad, B. (2007A). Water quality limits for Atlantic salmon (Salmo salar L.) exposed to short term reductions in pH and increased aluminum simulating episodes. ***Hydrology and Earth System Sciences Discussions, 4***(5), 3317-3355.

Kroglund, F., Finstad, B., Stefansson, S., Nilsen, T., Kristensen, T., Rosseland, B., et al. (2007B). Exposure to moderate acid water and aluminum reduces Atlantic salmon post-smolt survival. ***Aquaculture, 273***(2), 360-373.

Krug, E. C., & Frink, C. R. (1983). Acid rain on acid soil: A new perspective. ***Science (Washington), 217***(4610), 520-525.

Lacroix, G. L., & Townsend, D. R. (1987). Responses of juvenile Atlantic salmon (salmo salar) to episodic increases in acidity of Nova Scotia rivers. *Canadian Journal of Fisheries and Aquatic Sciences, 44*(8), 1475-1484.

Lacroix, G., Hood, D., Belfry, C., & Rand, T. (1990). Plasma electrolytes, gill aluminum content, and gill morphology of juvenile Atlantic salmon (salmo salar) and brook trout (salvelinus fontinalis) indigenous to acidic streams of Nova Scotia. *Canadian Journal of Zoology, 68*(6), 1270-1280.

Langan, S. J., & Wilson, M. (1992). Predicting the regional occurrence of acid surface waters in Scotland using an approach based on geology, soils and land use. *Journal of Hydrology, 138*(3-4), 515-528.

Larssen, T., & Carmichael, G. (2000). Acid rain and acidification in china: The importance of base cation deposition. *Environmental Pollution, 110*(1), 89-102.

Laudon, H., Clair, T. A., & Hemond, H. F. (2002). Long-term response in episodic acidification to declining SO_4^{2-} deposition in two streams in Nova Scotia. *Hydrology and Earth System Sciences Discussions, 6*(4), 773-781.

Lawrence, G. B., Burns, D. A., & Riva-Murray, K. (2016). A new look at liming as an approach to accelerate recovery from acidic deposition effects. *Science of the Total Environment, 562*, 35-46.

Lawrence, G. B., David, M. B., & Shortle, W. C. (1995). Aluminum mobilization as a mechanism for calcium depletion in organic forest soil horizons. *Nature, 378*, 162-165.

LaZerte, B. D. (1984). Forms of aqueous aluminum in acidified catchments of central Ontario: A methodological analysis. *Canadian Journal of Fisheries and Aquatic Sciences, 41*(5), 766-776.

Likens, G. E., Bormann, F. H., & Johnson, N. M. (1972). Acid rain. *Environment: Science and Policy for Sustainable Development, 14*(2), 33-40.

Likens, G. E., Butler, T. J., & Buso, D. C. (2001). Long-and short-term changes in sulfate deposition: Effects of the 1990 clean air act amendments. *Biogeochemistry, 52*(1), 1-11.

Löfgren, S., Cory, N., & Zetterberg, T. (2010). Aluminium concentrations in Swedish forest streams and co-variations with catchment characteristics. *Environmental Monitoring and Assessment, 166*(1-4), 609-624.

Lükewille, A., Jeffries, D., Raddum, G., Stoddard, J., & Traaen, T. (1997). *The Nine year report: Acidification of surface water in Europe and North America. Long-term Developements (1980s and 1990s)(ICP Waters report)*. Norsk institutt for vannforskning.

Lydersen, E. (1990). The solubility and hydrolysis of aqueous aluminium hydroxides in dilute fresh waters at different temperatures. *Hydrology Research, 21*(3), 195-204.

McHale, M. R., Burns, D. A., Lawrence, G. B., & Murdoch, P. S. (2007). Factors controlling soil water and stream water aluminum concentrations after a clearcut in a forested watershed with calcium-poor soils. *Biogeochemistry, 84*(3), 311-331.

McKnight, D., & Bencala, K. E. (1988). Diel variations in iron chemistry in an acidic stream in the Colorado Rocky Mountains, USA. *Arctic and Alpine Research,* , 492-500.

Menz, F. C., & Seip, H. M. (2004). Acid rain in Europe and the United States: An update. *Environmental Science & Policy, 7*(4), 253-265.

Monette, M. Y., & McCormick, S. D. (2008). Impacts of short-term acid and aluminum exposure on Atlantic salmon (Salmo salar) physiology: a direct comparison of parr and smolts. *Aquatic Toxicology, 86*(2), 216-226.

Monteith, D. T., Stoddard, J. L., Evans, C. D., de Wit, H. A., Forsius, M., Høgåsen, T., et al. (2007). Dissolved organic carbon trends resulting from changes in atmospheric deposition chemistry. *Nature, 450*(7169), 537-540.

Monteith, D., Evans, C., Henrys, P., Simpson, G., & Malcolm, I. (2014). Trends in the hydrochemistry of acid-sensitive surface waters in the UK 1988–2008. *Ecological Indicators, 37*, 287-303.

Climate Prediction Center Internet Team. (2012, January 10). North American Oscillation. *National Weather Service Climate Prediction Center.* http://www.cpc.ncep.noaa.gov/data/teledoc/nao.shtml Accessed on December 12th, 2016.

Neal, C., Smith, C. J., Walls, J., & Dunn, C. S. (1986). Major, minor and trace element mobility in the acidic upland forested catchment of the upper River Severn, Mid Wales. *Journal of the Geological Society, 143*(4), 635-648.

Nilsen, T. O., Ebbesson, L. O., Handeland, S. O., Kroglund, F., Finstad, B., Angotzi, A. R., & Stefansson, S.O. (2013). Atlantic salmon (salmo salar L.) smolts require more than two weeks to recover from acidic water and aluminium exposure. *Aquatic Toxicology, 142*, 33-44.

Nilsen, T. O., Ebbesson, L. O., Kverneland, O. G., Kroglund, F., Finstad, B., & Stefansson, S. O. (2010). Effects of acidic water and aluminum exposure on gill na , K - ATPase α-subunit isoforms, enzyme activity, physiology and return rates in Atlantic salmon (salmo salar L.). *Aquatic Toxicology, 97*(3), 250-259.

Nordstrom, D. K. (1982). The effect of sulfate on aluminum concentrations in natural waters: some stability relations in the system Al2O3-SO3-H2O at 298 K. *Geochimica et Cosmochimica Acta, 46*(4), 681-692.

Palmer, S. M., & Driscoll, C. T. (2002). Acidic deposition: Decline in mobilization of toxic aluminium. *Nature, 417*(6886), 242-243.

Peterson, R., Bourbonniere, R., Lacroix, G., Martin-Robichaud, D., Takats, P., & Brun, G. (1989). Responses of Atlantic salmon (salmo salar) alevins to dissolved organic carbon and dissolved aluminum at low pH. *Water, Air, and Soil Pollution, 46*(1-4), 399-413.

Poléo, A. B. (1995). Aluminium polymerization—a mechanism of acute toxicity of aqueous aluminium to fish. *Aquatic toxicology, 31*(4), 347-356.

Rencz, A., O'driscoll, N., Hall, G., Peron, T., Telmer, K., & Burgess, N. (2003). Spatial variation and correlations of mercury levels in the terrestrial and aquatic components of a wetland dominated ecosystem: Kejimkujik park, Nova Scotia, Canada. *Water, Air, and Soil Pollution, 143*(1-4), 271-288.

Robertson, G. P., Sollins, P., Ellis, B. G., & Lajtha, K. (1999). Exchangeable ions, pH, and cation exchange capacity. *Standard Soil Methods for Long-Term Ecological Research.Oxford University Press, New York,* , 106-114.

Rodushkin, I., Moiseenko, T., & Kudravsjeva, L. (1995). Aluminium in the surface waters of the Kola Peninsula, Russia. *Science of the Total Environment, 163*(1), 55-59.

Schlesigner, W. H., & and Bernhardt, E. S. (2013). *Biogeochemistry: An analysis of global change* Academic Press.

Seybold, C., Grossman, R., & Reinsch, T. (2005). Predicting cation exchange capacity for soil survey using linear models. *Soil Science Society of America Journal, 69*(3), 856-863.

Singh, A., & Agrawal, M. (2007). Acid rain and its ecological consequences. *Journal of Environmental Biology, 29*(1), 15.

Sjöstedt, C., Andrén, C., Fölster, J., & Gustafsson, J. P. (2013). Modelling of pH and inorganic aluminium after termination of liming in 3000 Swedish lakes. ***Applied Geochemistry, 35***, 221-229.

Skjelkvåle, B. L., Evans, C., Larssen, T., Hindar, A., & Raddum, G. G. (2003). Recovery from acidification in European surface waters: a view to the future. ***AMBIO: A Journal of the Human Environment, 32***(3), 170-175.

Skjelkvåle, B., Stoddard, J., Jeffries, D., Tørseth, K., Høgåsen, T., Bowman, J., et al. (2005). Regional scale evidence for improvements in surface water chemistry 1990–2001. ***Environmental Pollution, 137***(1), 165-176.

Stoddard, J. L., Jeffries, D., Lükewille, A., Clair, T., Dillon, P., Driscoll, C., et al. (1999). Regional trends in aquatic recovery from acidification in North America and Europe. ***Nature, 401***(6753), 575-578.

Strock, K. E., Nelson, S. J., Kahl, J. S., Saros, J. E., & McDowell, W. H. (2014). Decadal trends reveal recent acceleration in the rate of recovery from acidification in the Northeastern US. ***Environmental Science & Technology, 48***(9), 4681-4689.

Sullivan, T. J., Christophersen, N., Muniz, I. P., Seip, H. M., & Sullivan, P. D. (1986). Aqueous aluminium chemistry response to episodic increases in discharge. ***Nature***, ***323***(6086), 324-327.

Sullivan, T., Cosby, B., Driscoll, C., Charles, D., & Hemonds, H. (1996). Influence of organic acids on model projections of lake acidification. ***Water, Air, and Soil Pollution, 91***(3-4), 271-282.

Summers, P., & Whelpdale, D. (1976). Acid precipitation in Canada. ***Water, Air, and Soil Pollution, 6***(2-4), 447-455.

Tejnecký, V., Drábek, O., Borůvka, L., Nikodem, A., Kopáč, J., Vokurková, P., & Sebek, O. (2010). Seasonal variation of water extractable aluminium forms in acidified forest organic soils under different vegetation cover. ***Biogeochemistry, 101***(1-3), 151-163.

Thorstad, E. B., Uglem, I., Finstad, B., Kroglund, F., Einarsdottir, I. E., Kristensen, T., Diserud, O., Arechavala-Lopez, P., Mayer, I., Moore, A., & Nilsen R. (2013). Reduced marine survival of hatchery-reared Atlantic salmon post-smolts exposed to aluminium and moderate acidification in freshwater. ***Estuarine, Coastal and Shelf Science, 124***, 34-43.

Tipping, E. (1989). Acid-sensitive waters of the english lake district: A steady-state model of streamwater chemistry in the upper Duddon catchment. ***Environmental Pollution, 60***(3-4), 181-208.

Tipping, E., Rey-Castro, C., Bryan, S. E., & Hamilton-Taylor, J. (2002). Al (III) and Fe (III) binding by humic substances in freshwaters, and implications for trace metal speciation. *Geochimica Et Cosmochimica Acta, 66*(18), 3211-3224.

Underwood, B. E., Kruse, N. A., & Bowman, J. R. (2014). Long-term chemical and biological improvement in an acid mine drainage-impacted watershed. *Environmental Monitoring and Assessment, 186*(11), 7539-7553.

Walker, W., Cronan, C., & Bloom, P. (1990). Aluminum solubility in organic soil horizons from northern and southern forested watersheds. *Soil Science Society of America Journal, 54*(2), 369-374.

Wang, D., He, Y., Liang, J., Liu, P., & Zhuang, P. (2013). Distribution and source analysis of aluminum in rivers near Xi'an city, china. *Environmental Monitoring and Assessment, 185*(2), 1041-1053.

Warby, R. A., Johnson, C. E., & Driscoll, C. T. (2005). Chemical recovery of surface waters across the Northeastern United States from reduced inputs of acidic deposition: 1984-2001. *Environmental Science & Technology, 39*(17), 6548-6554.

Watt, W., Scott, C., & White, W. (1983). Evidence of acidification of some Nova Scotian rivers and its impact on Atlantic salmon, salmo salar. *Canadian Journal of Fisheries and Aquatic Sciences, 40*(4), 462-473.

Watt, W. D. (1986). The case for liming some Nova Scotia salmon rivers. *Acidic precipitation* (pp. 1829-1843) Springer.

Watt, W., Scott, C., Zamora, P., & White, W. (2000). Acid toxicity levels in Nova Scotian rivers have not declined in synchrony with the decline in sulfate levels. *Water, Air, and Soil Pollution, 118*(3-4), 203-229.

Wauer, G., & Teien, H. (2010). Risk of acute toxicity for fish during aluminium application to hardwater lakes. *Science of the Total Environment, 408*(19), 4020-4025.

Whitfield, C., Aherne, J., Watmough, S., Dillon, P., & Clair, T. (2006). Recovery from acidification in nova scotia: Temporal trends and critical loads for 20 headwater lakes. *Canadian Journal of Fisheries and Aquatic Sciences, 63*(7), 1504-1514.

Worrall, F., Burt, T., & Adamson, J. (2004). Can climate change explain increases in DOC flux from upland peat catchments? *Science of the Total Environment, 326*(1), 95-112.

Wright, R., Aherne, J., Bishop, K., Camarero, L., Cosby, B., Erlandsson, M., et al. (2006). Modelling the effect of climate change on recovery of acidified freshwaters: Relative sensitivity of individual processes in the MAGIC model. *Science of the Total Environment, 365*(1), 154-166.

Yanni, S., Keys, K., Meng, F., Yin, X., Clair, T., & Arp, P. A. (2000). Modelling hydrological conditions in the maritime forest region of South-Western Nova Scotia. *Hydrological Processes, 14*(2), 195-214.

You, S., Yin, Y., & Allen, H. E. (1999). Partitioning of organic matter in soils: Effects of pH and water/soil ratio. *Science of the Total Environment, 227*(2), 155-160.

Appendix A R-Scripts

A.1 Chapter 2 R-Scripts

R-scripts used to analyze and create all plots provided in Chapter 2 and the Appendix are available on DalSpace, at: http://dalspace.library.dal.ca/

A.2 Chapter 3 R-Scripts

R-scripts used to analyze and create all plots provided in Chapter 3 and the Appendix are available on DalSpace, at: http://dalspace.library.dal.ca/

Appendix B NS Lake and River Watershed Characteristics

Lake and river water chemistry data, and watershed characteristics (such as geology, coverage of wetlands and urban regions, etc.) from 1980-2014, measured by Environment Canada, used to calculate lake and river trends across Nova Scotia (refer to Chapter 2.6.2) are available on DalSpace, at: http://dalspace.library.dal.ca/

Appendix C 2015-2016 Field Data

River chemistry data collected throughout 2015 and 2016 by the Hydrology Research Group in Nova Scotia, used to analyze Al_i concentrations and create the Al_i predictive equations (refer to Chapters 3.5.1 & 3.5.2) on DalSpace, at: http://dalspace.library.dal.ca/

Appendix D Conversions

D.1 MR Conversions

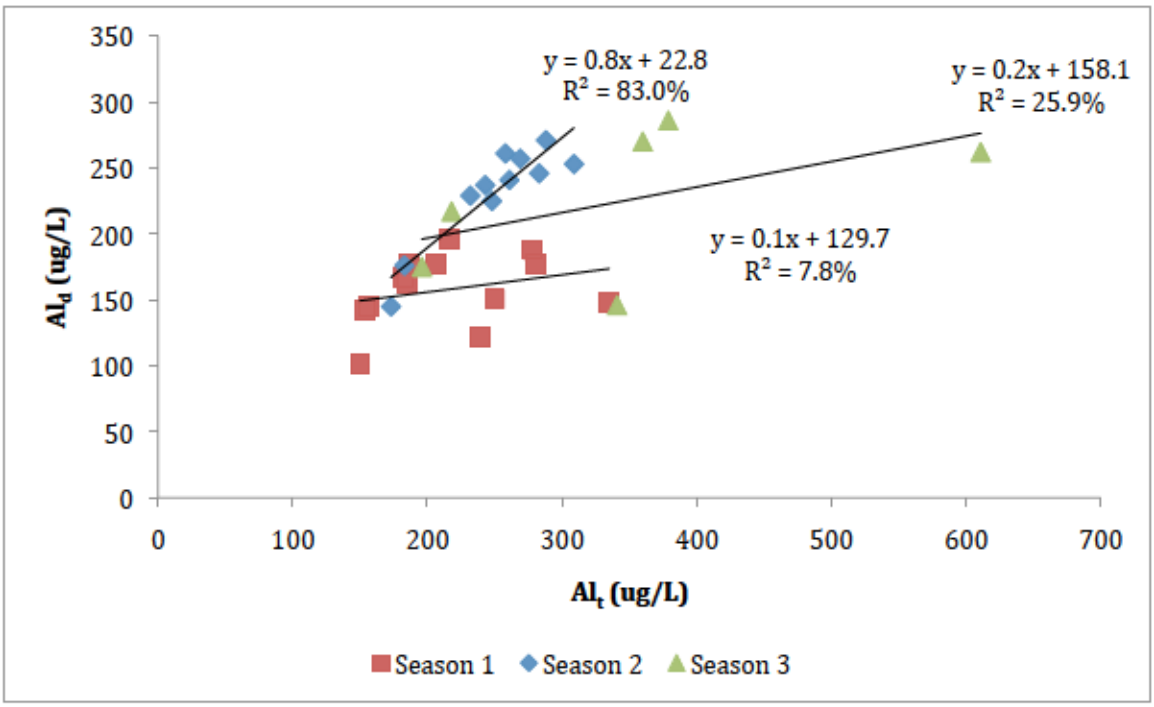

Figure D.1.1: Mersey River Al_d-Al_t correlation equations and linear regressions for three seasons. Samples were collected between April 22, 2016 and March 29th, 2016 from MR, stored during transit in ice for 2.5 hours, then stored in the Maxxam Analytics Laboratory fridge for 1-5 days before analysis. Lids were kept on the bottles until analysis. Season one refers to data collected between April 1st, 2015 and August 5th, 2015. Season two refers to data collected between August 12th, 2015 and October 31st, 2015. Season three refers to data collected between November 1st, 2015 and March 31st, 2016.

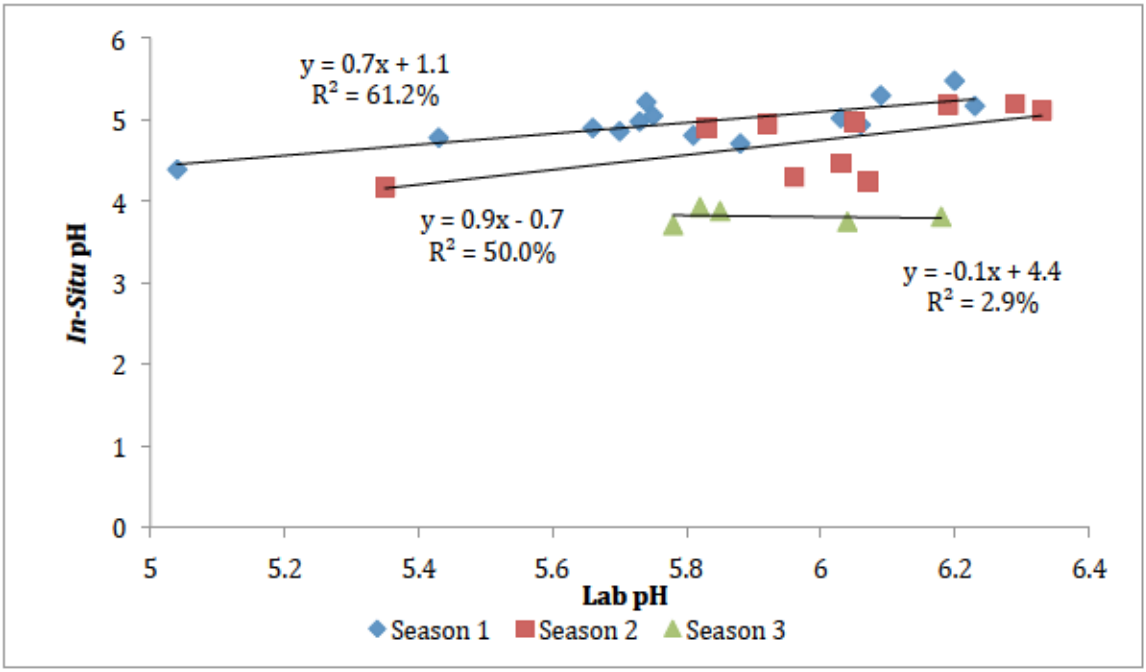

Figure D.1.2: Mersey River lab pH – *in-situ* pH correlation equations and linear regressions for three seasons. Samples were collected between April 22, 2016 and March 29th, 2016 from MR, with *in-situ* pH measured using the YSI sonde instrument. Samples were stored during transit in ice for 2.5 hours, then stored in the Maxxam Analytics Laboratory fridge for 1-5 days before analysis. Lids were kept on the bottles until analysis. Season one refers to data collected between April 1st, 2015 and August 5th, 2015. Season two refers to data collected between August 12th, 2015 and October 31st, 2015. Season three refers to data collected between November 1st, 2015 and March 31st, 2016.

D.2 MPB Conversions

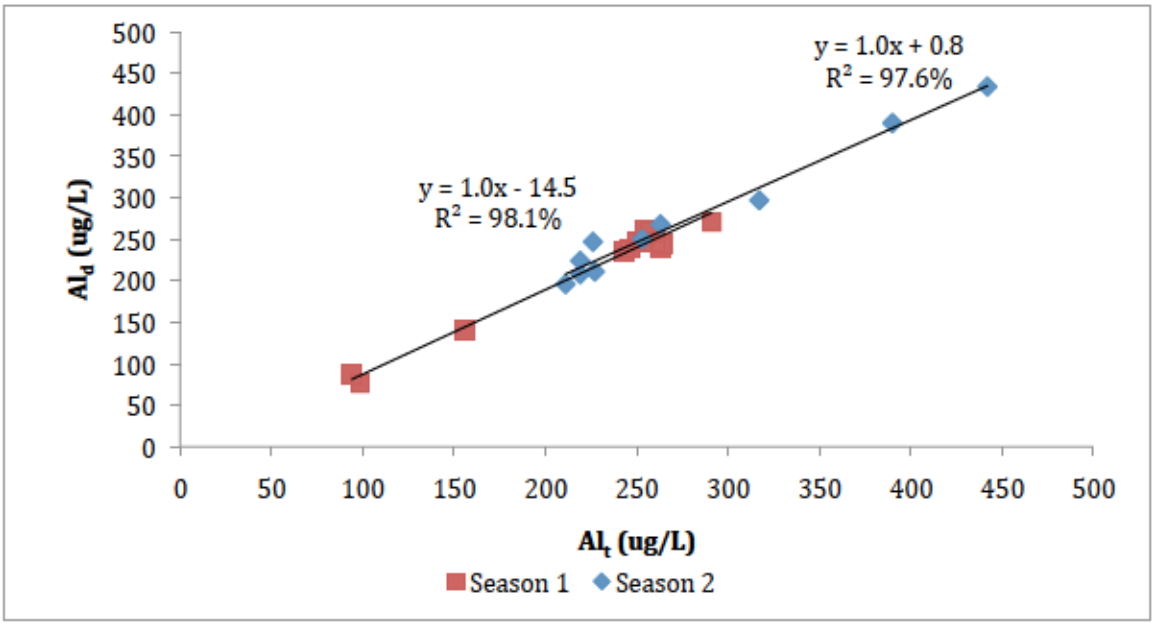

Figure D.2.1: Moose Pit Brook Al_d-Al_t correlation equations and linear regressions for two seasons. Samples were collected between April 22, 2016 and October 31st, 2015 from MPB, stored during transit in ice for 2.5 hours, then stored in the Maxxam Analytics Laboratory fridge for 1-5 days before analysis. Lids were kept on the bottles until analysis. Season one refers to data collected between April 1st, 2015 and August 5th, 2015. Season two refers to data collected between August 12th, 2015 and October 31st, 2015.

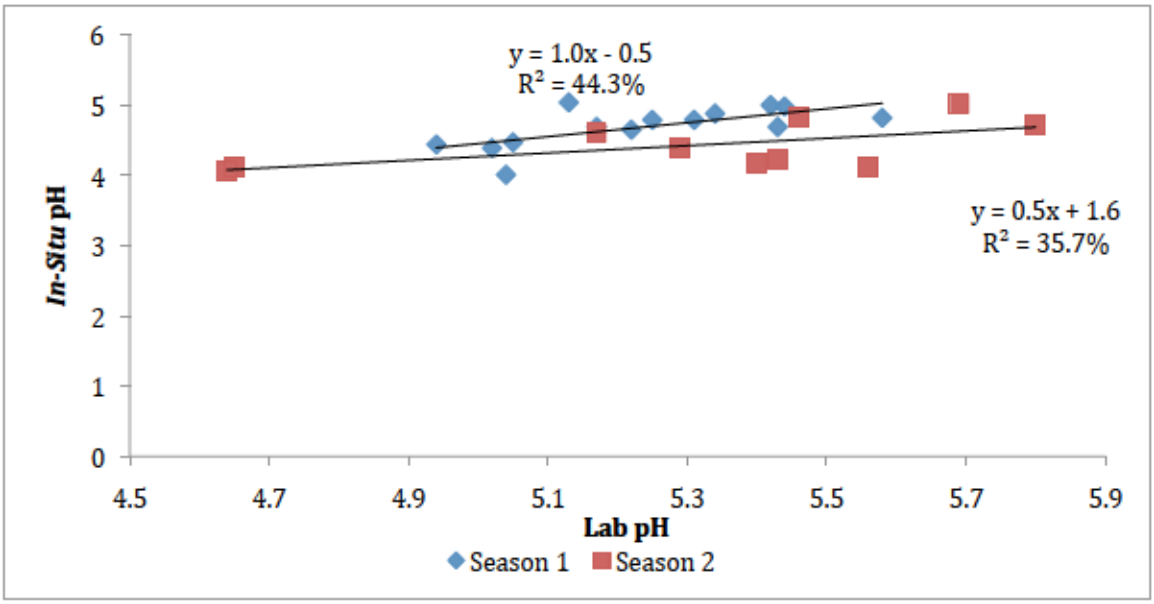

Figure D.2.2: Moose Pit Brook lab pH – *in-situ* pH correlation equations and linear regressions for two seasons. Samples were collected between April 22, 2016 and October 31st, 2015 from MPB, with *in-situ* pH measured using the YSI sonde instrument. Samples were stored during transit in ice for 2.5 hours, then stored in the Maxxam Analytics Laboratory fridge for 1-5 days before analysis. Lids were kept on the bottles until analysis. Season one refers to data collected between April 1st, 2015 and August 5th, 2015. Season two refers to data collected between August 12th, 2015 and October 31st, 2015.

Appendix E X-Y Scatterplots

E.1 Mersey River X-Y Scatterplots

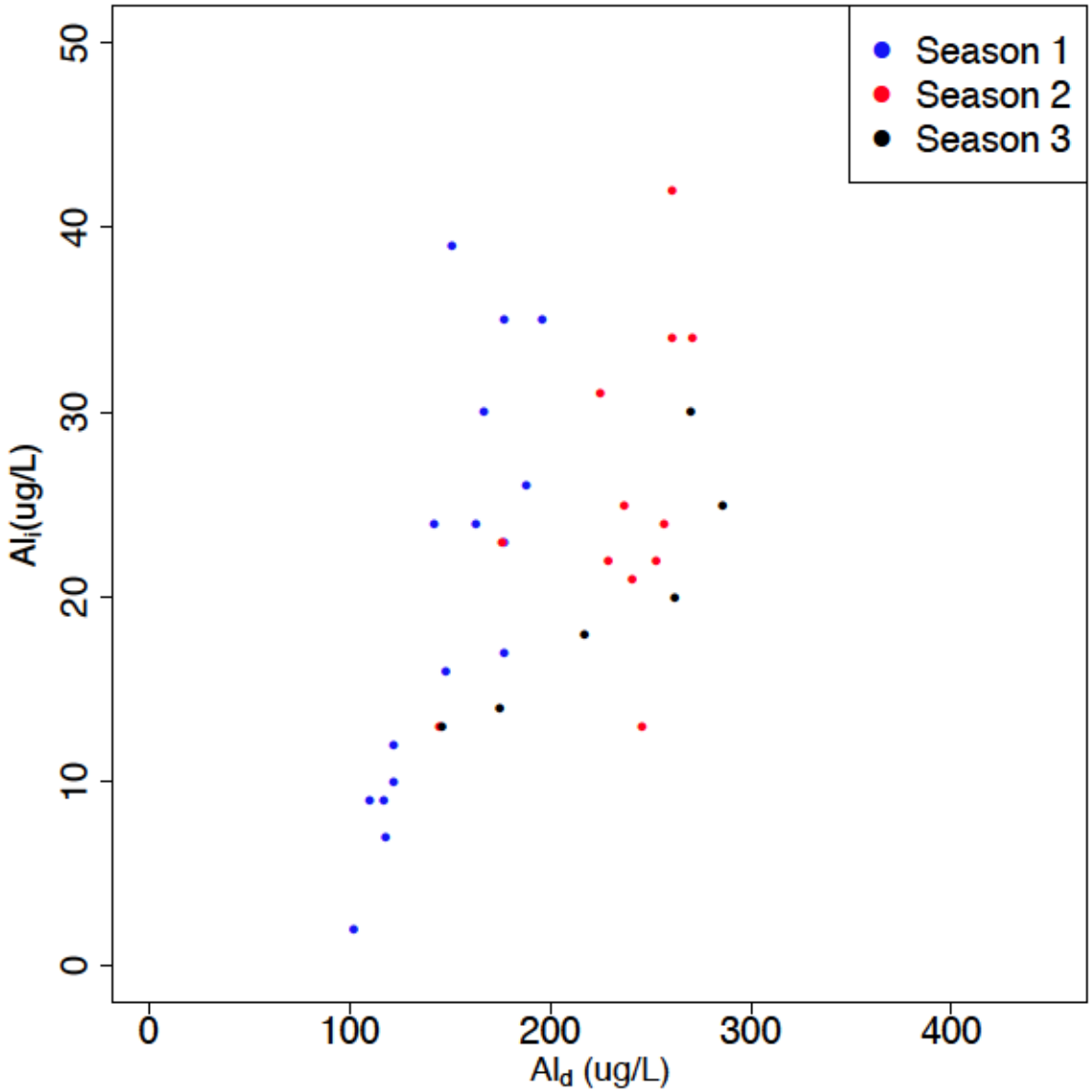

Figure E.1.1: Correlation of the $Al_{i\text{-direct}}$ concentrations with Al_d for three seasons throughout 2015-2016 in MR.

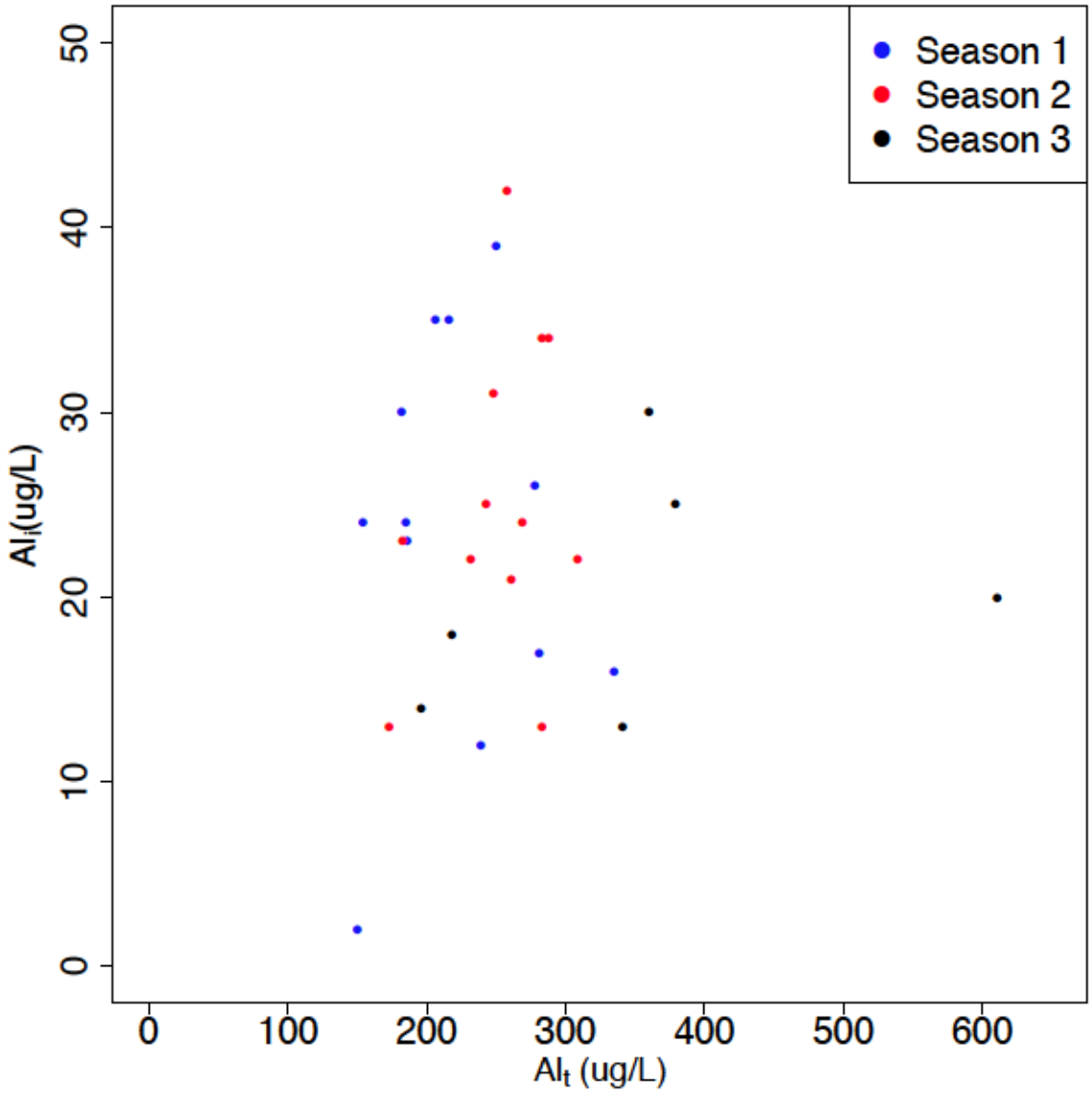

Figure E.1.2: Correlation of the $Al_{i\text{-direct}}$ concentrations with Al_t for three seasons throughout 2015-2016 in MR.

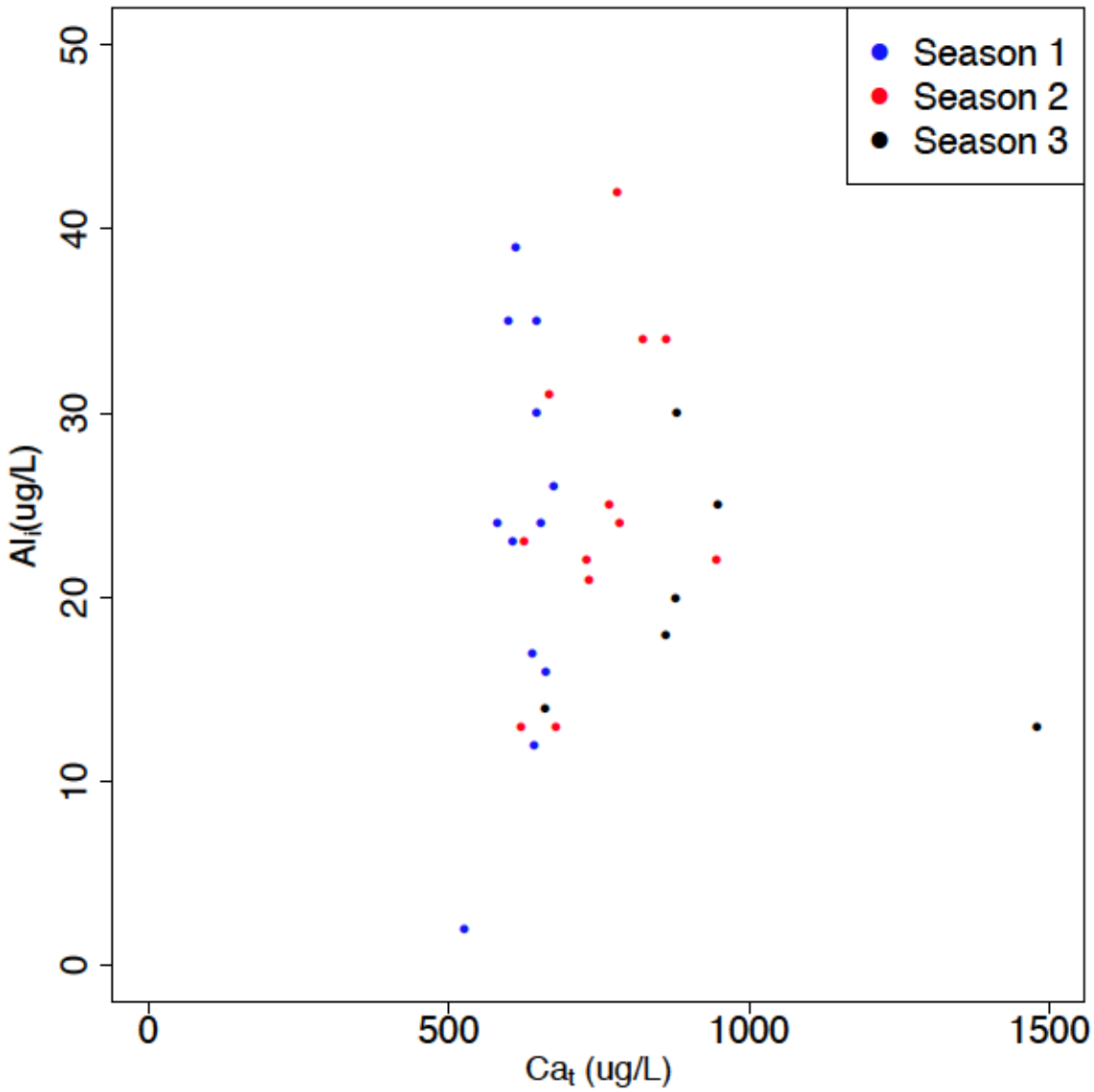

Figure E.1.3: Correlation of the $Al_{i\text{-direct}}$ concentrations with Ca_t for three seasons throughout 2015-2016 in MR.

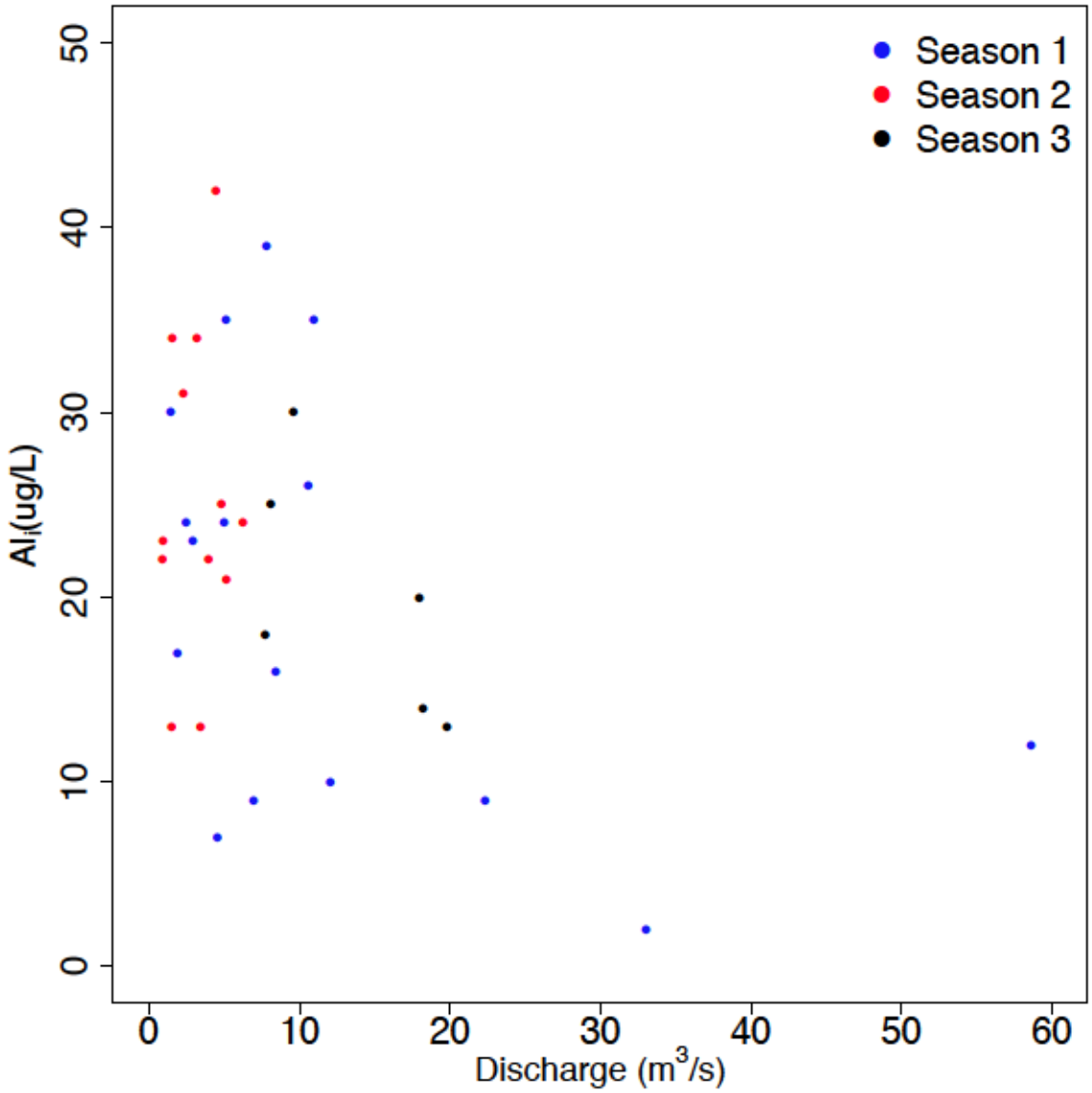

Figure E.1.4: Correlation of the $Al_{i\text{-direct}}$ concentrations with Discharge for three seasons throughout 2015-2016 in MR.

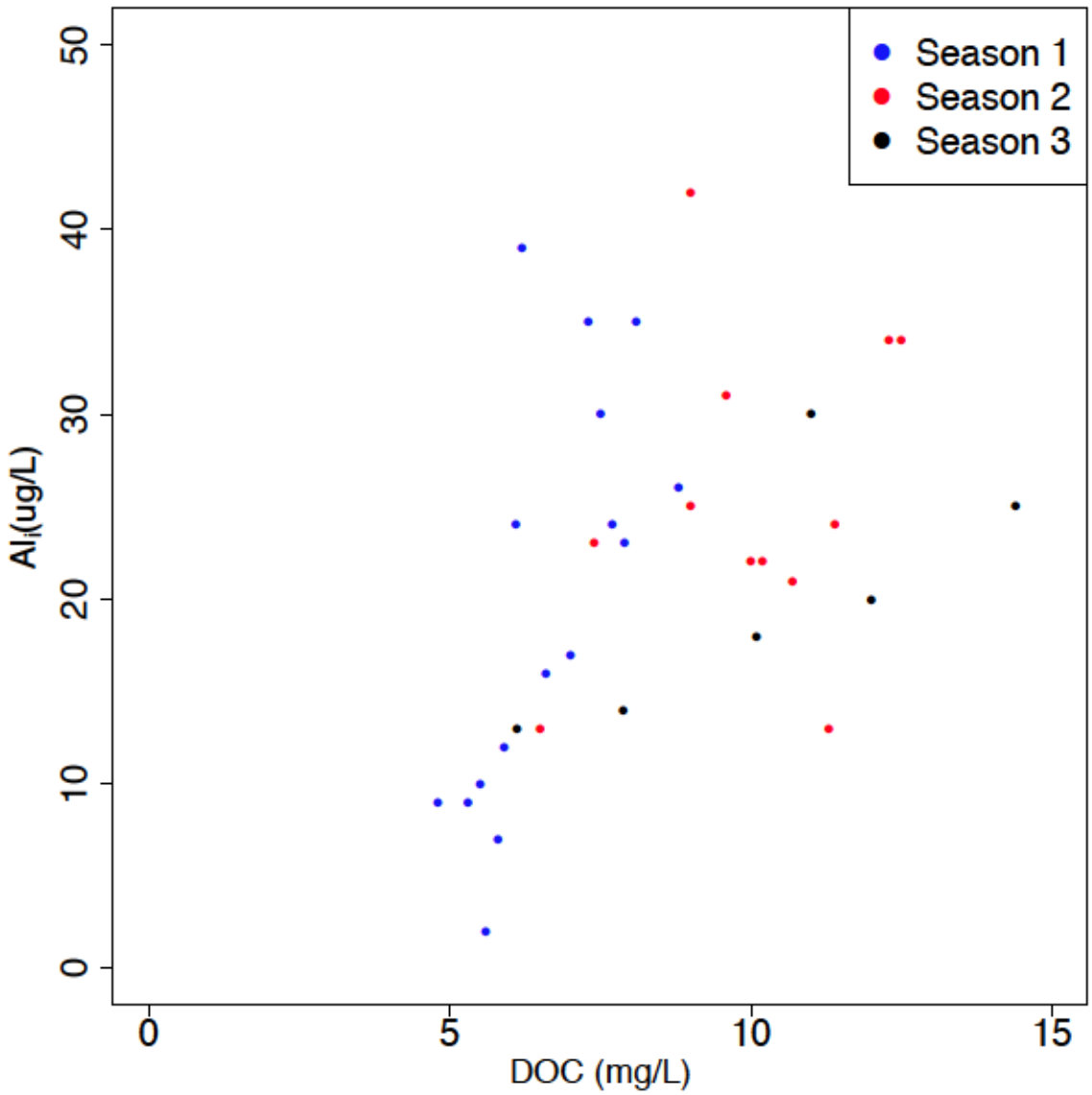

Figure E.1.5: Correlation of the $Al_{i\text{-direct}}$ concentrations with DOC for three seasons throughout 2015-2016 in MR.

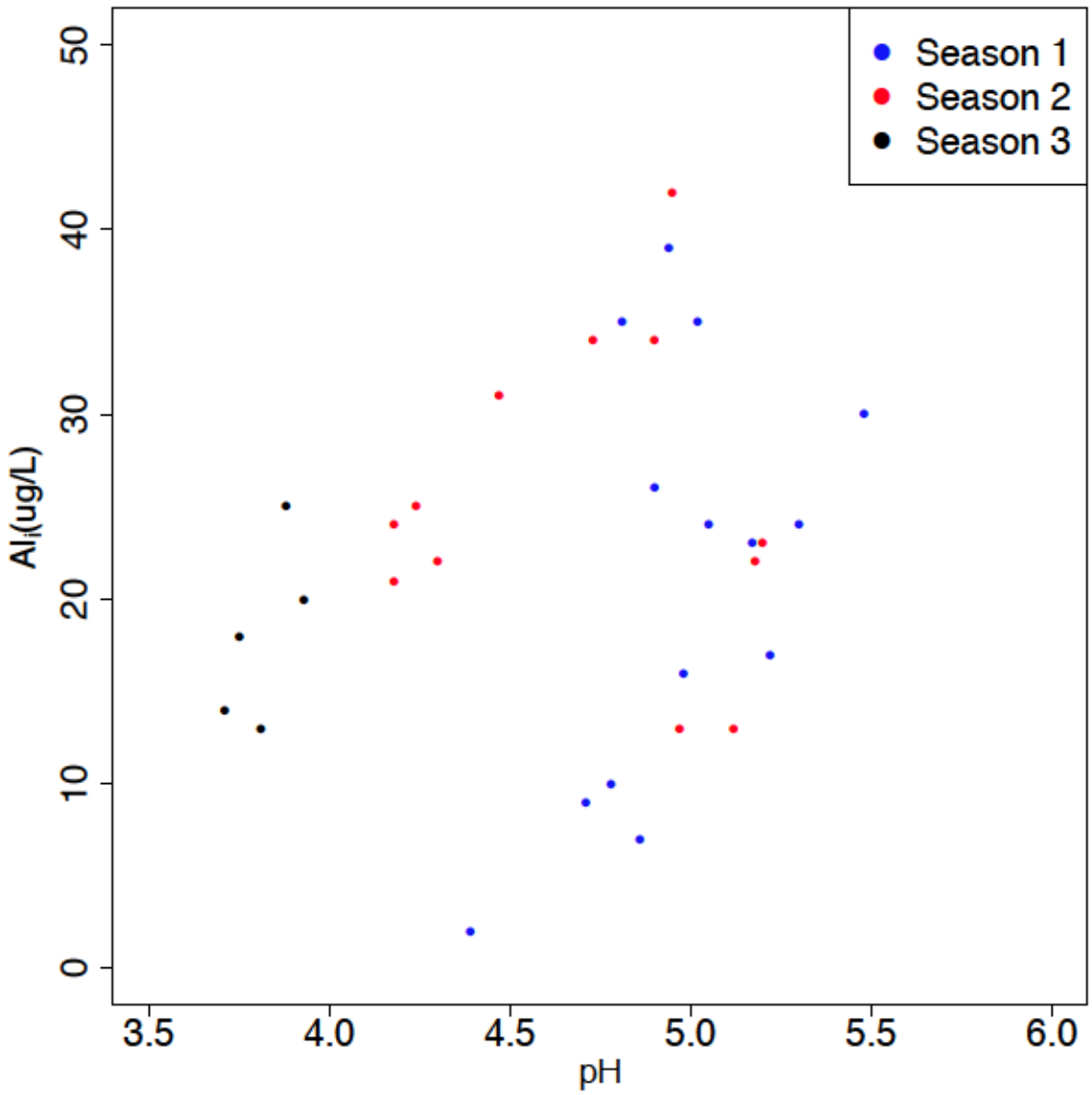

Figure E.1.6: Correlation of the $Al_{i\text{-direct}}$ concentrations with pH for three seasons throughout 2015-2016 in MR.

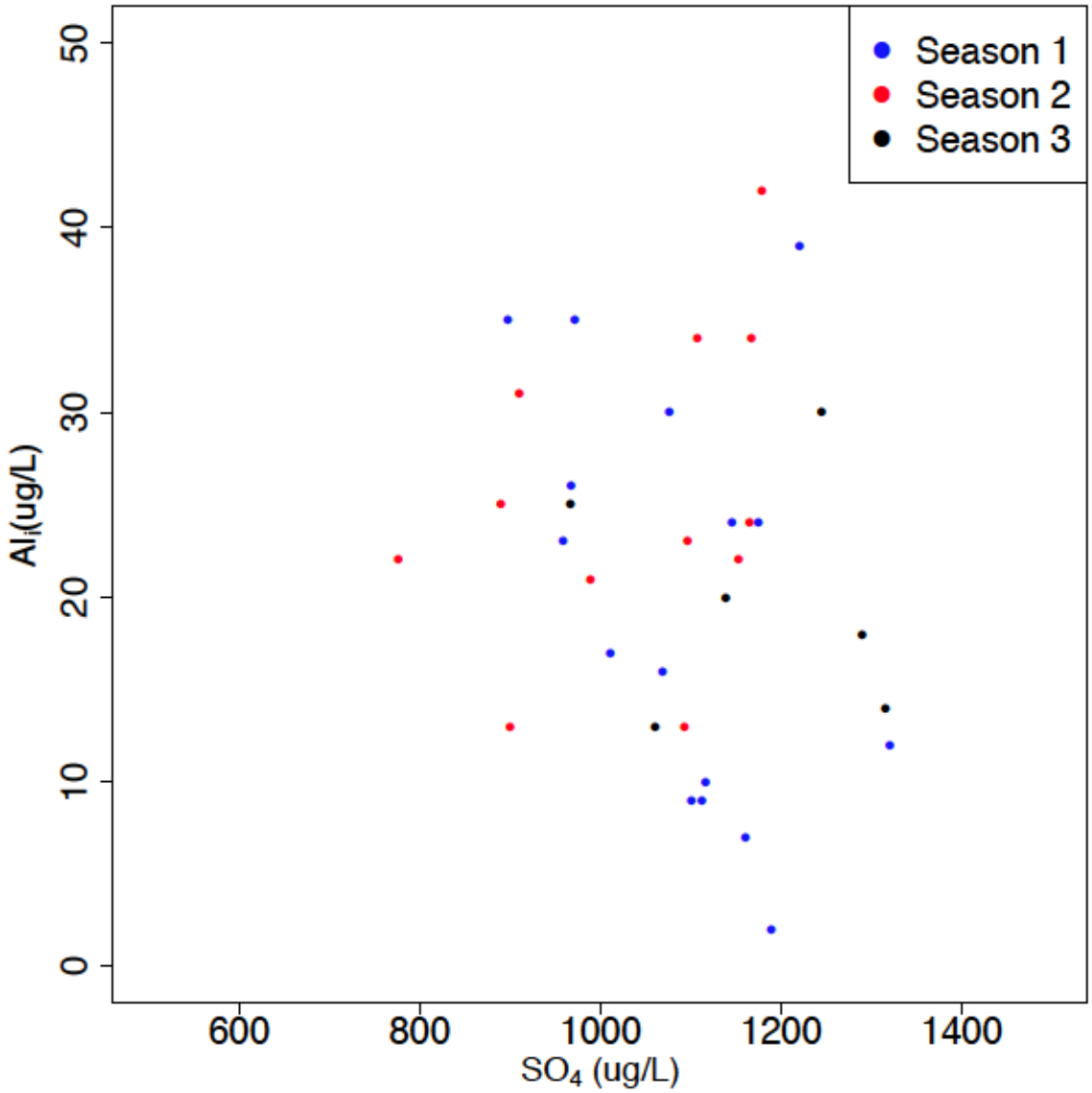

Figure E.1.7: Correlation of the $Al_{i\text{-direct}}$ concentrations with SO_4 for three seasons throughout 2015-2016 in MR.

E.2 Moose Pit X-Y Scatterplots

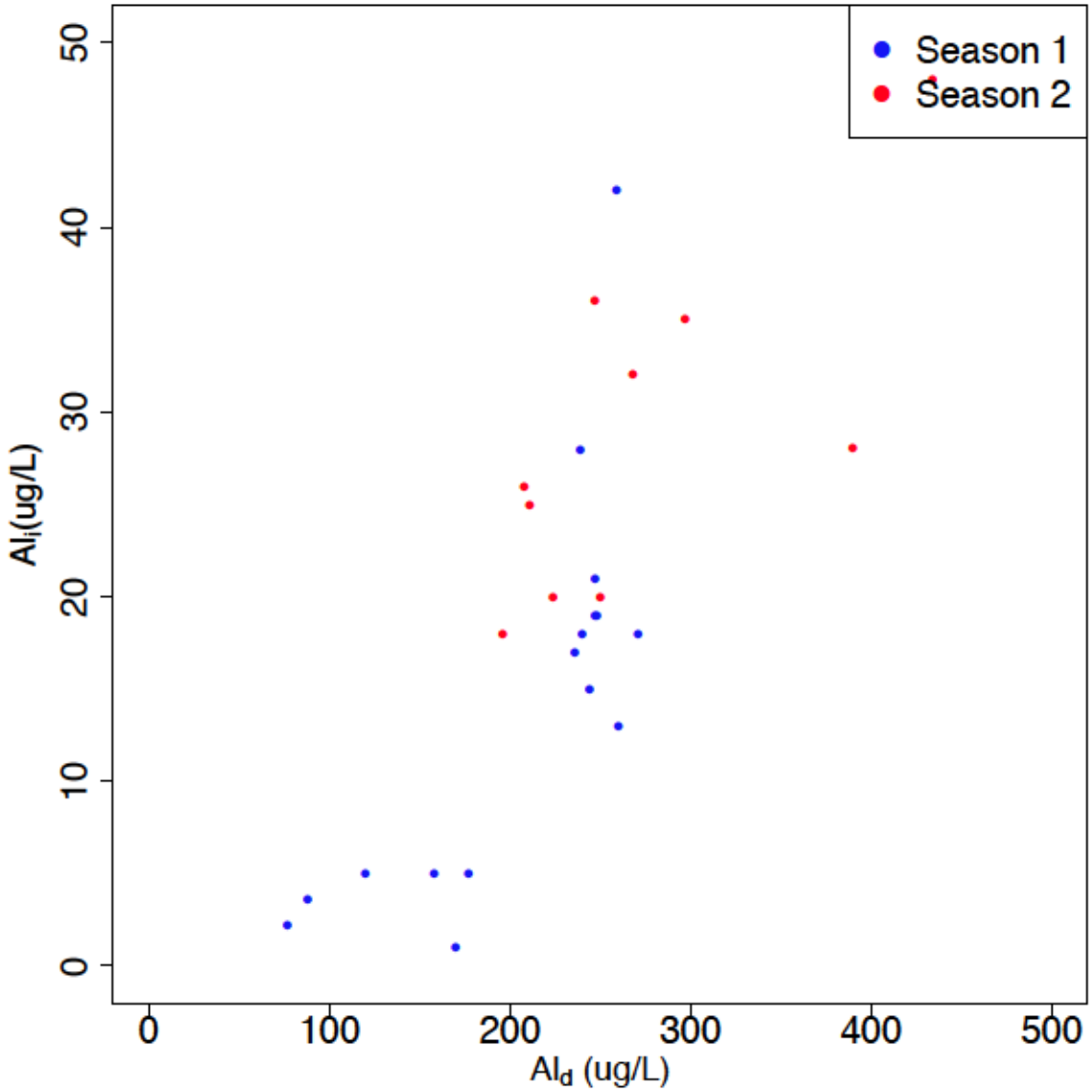

Figure E.2.1: Correlation of the $Al_{i\text{-direct}}$ concentrations with Al_d for two seasons throughout 2015-2016 in MPB.

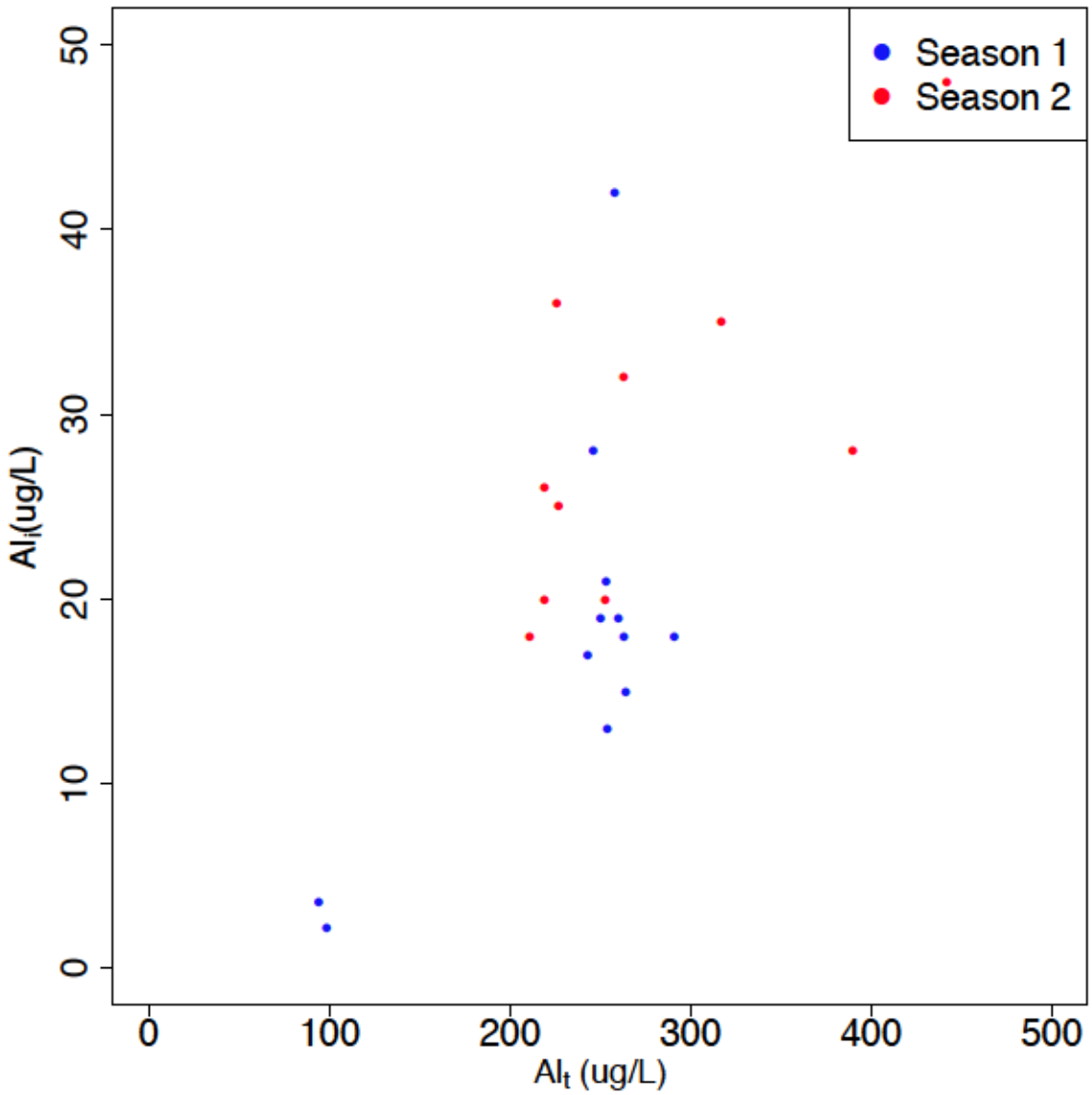

Figure E.2.2: Correlation of the $Al_{i\text{-direct}}$ concentrations with Al_t for two seasons throughout 2015-2016 in MPB.

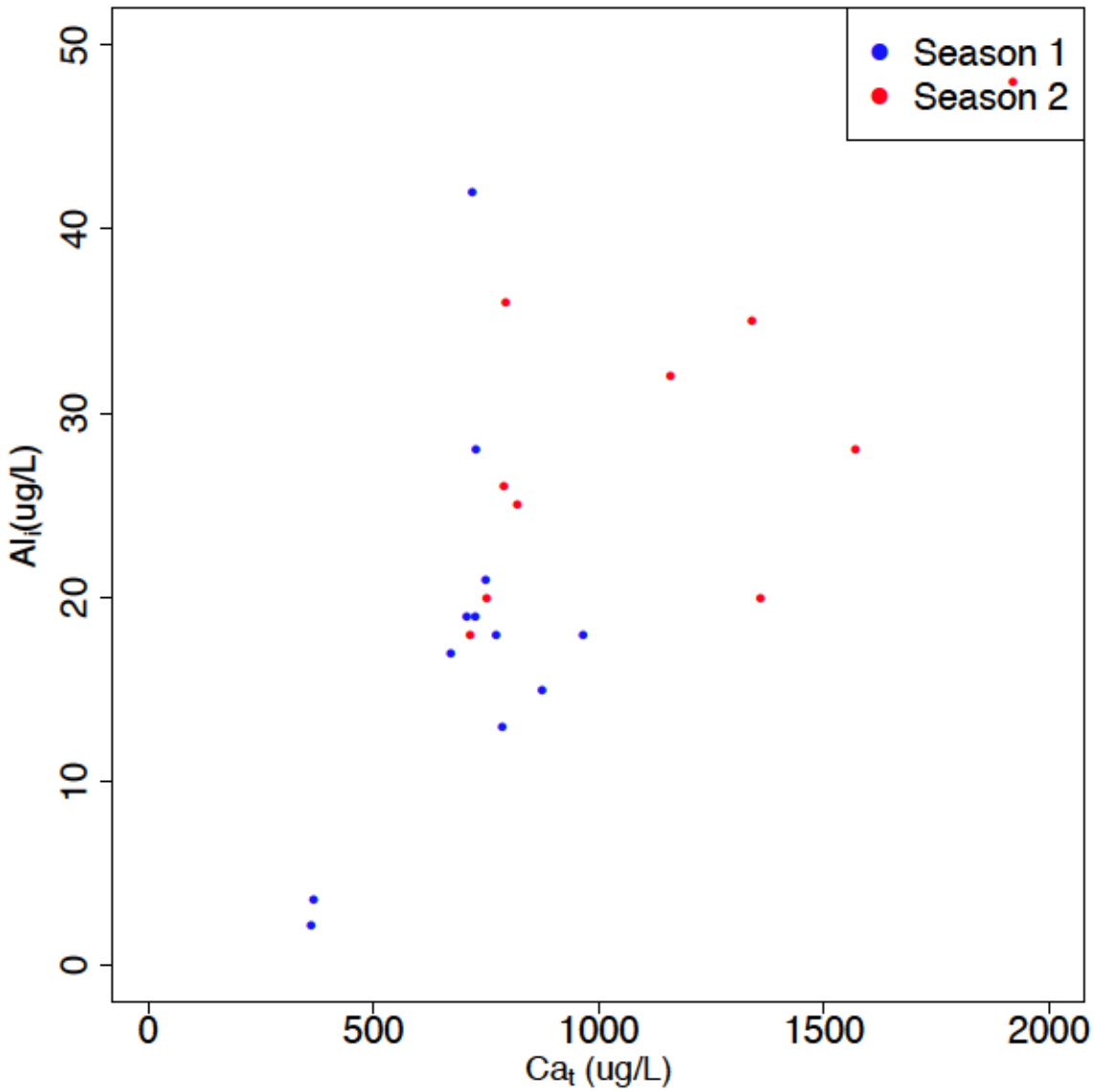

Figure E.2.3::Correlation of the $Al_{i\text{-direct}}$ concentrations with Ca_t for two seasons throughout 2015-2016 in MPB.

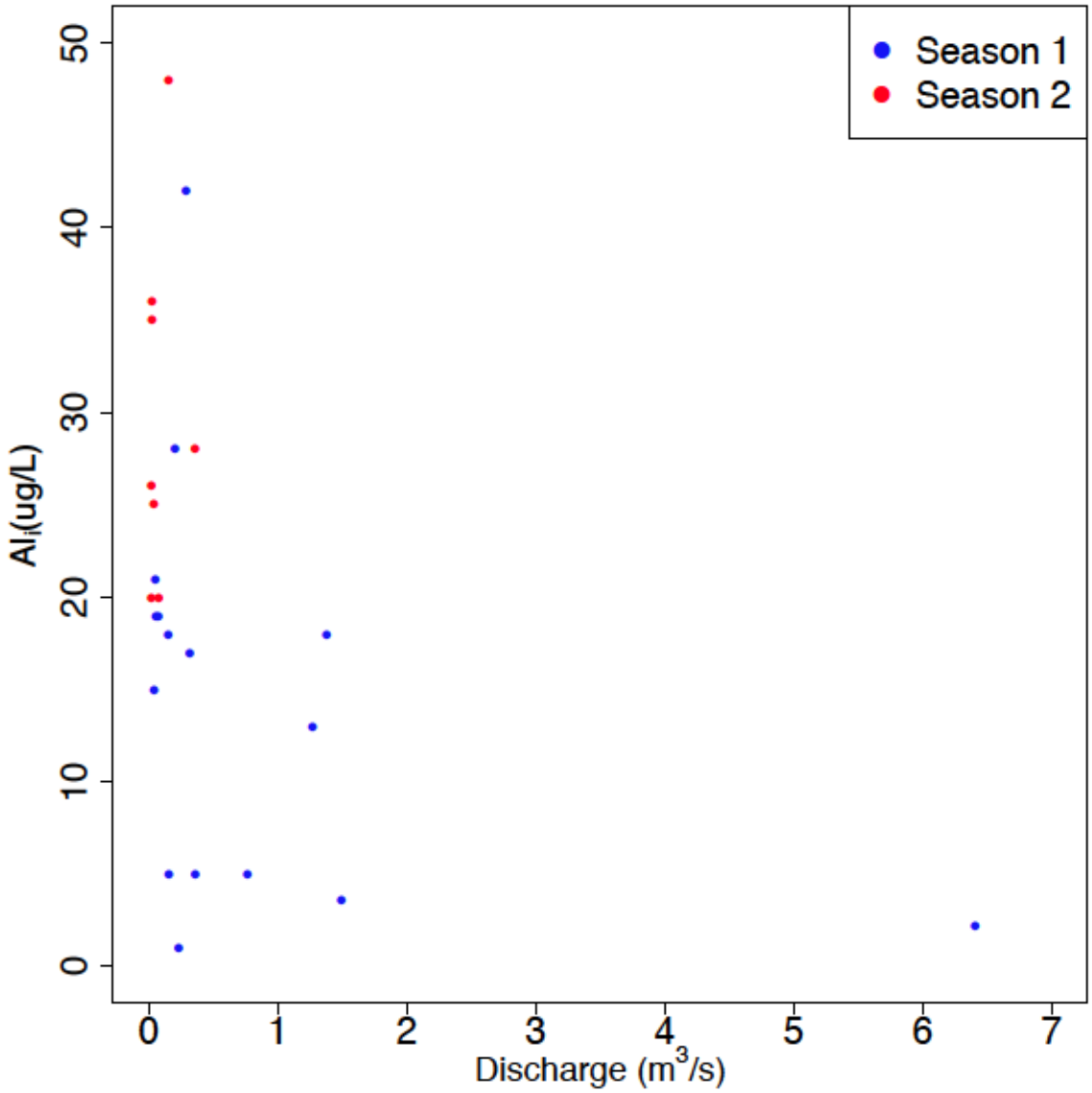

Figure E.2.4: Correlation of the $Al_{i\text{-direct}}$ concentrations with Discharge for two seasons throughout 2015-2016 in MPB.

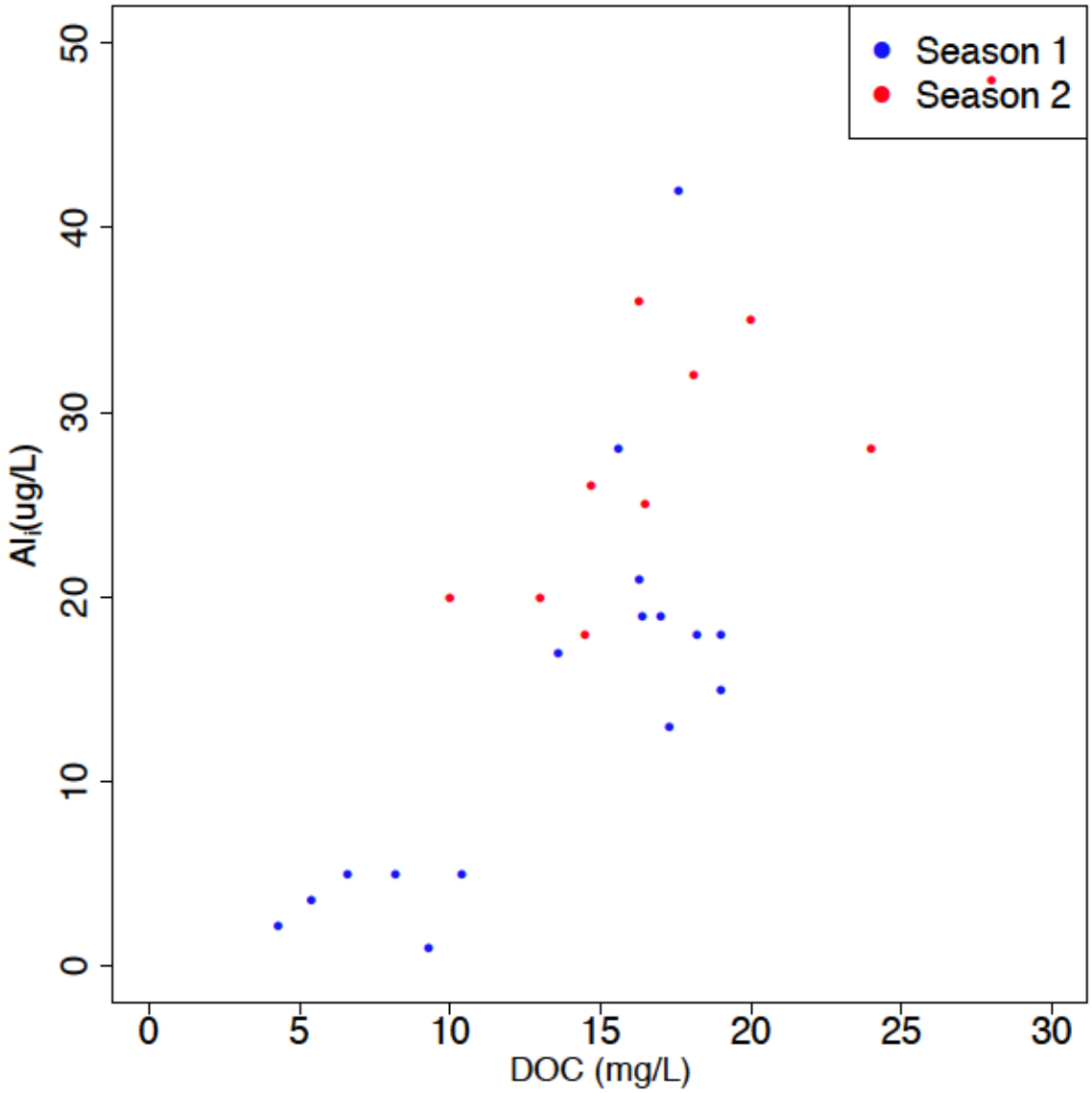

Figure E.2.5:Correlation of the $Al_{i\text{-direct}}$ concentrations with DOC for two seasons throughout 2015-2016 in MPB.

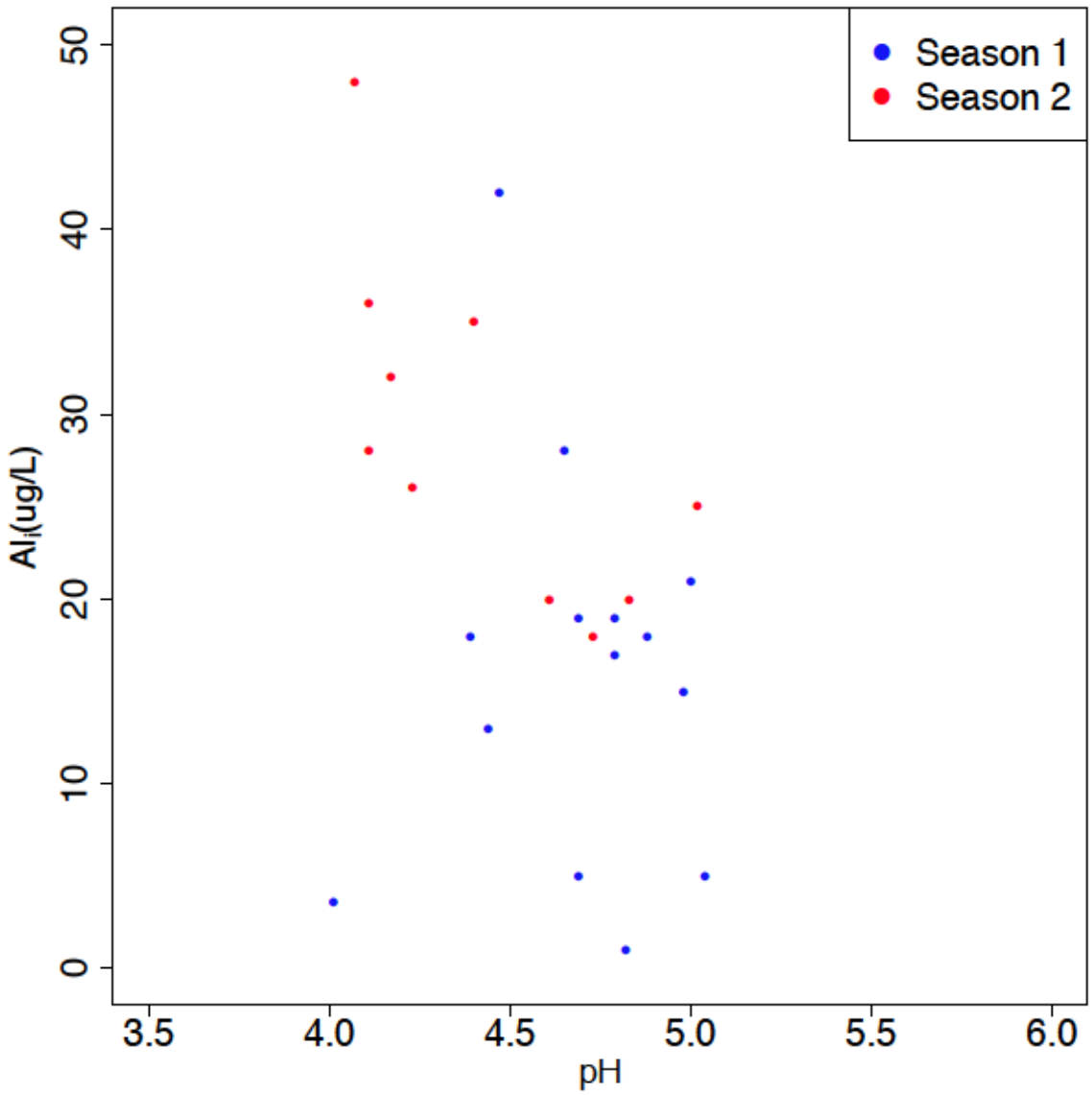

Figure E.2.6: Correlation of the $Al_{i\text{-direct}}$ concentrations with pH for two seasons throughout 2015-2016 in MPB.

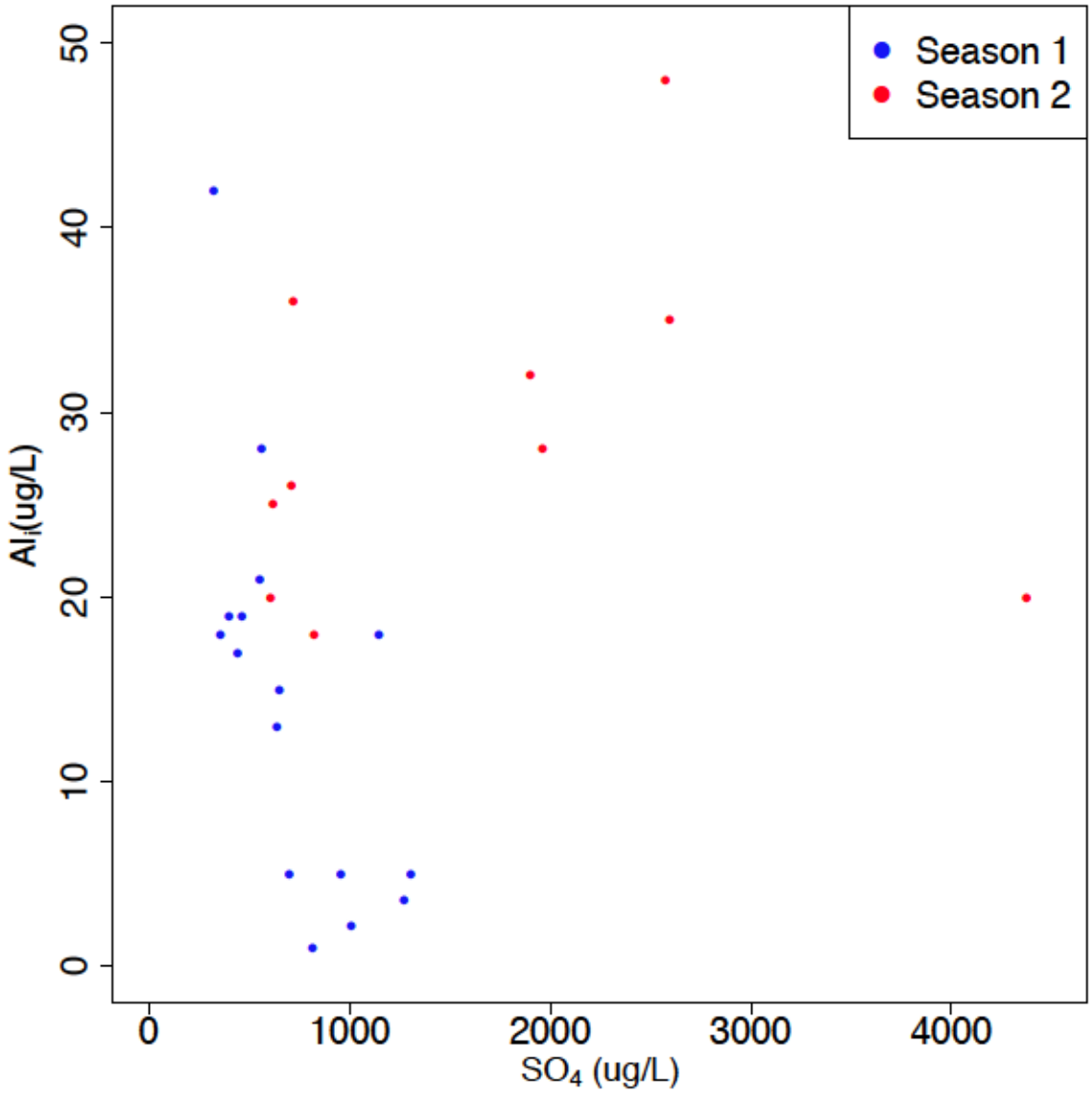

Figure E.2.7: Correlation of the $Al_{i\text{-direct}}$ concentrations with SO_4 for two seasons throughout 2015-2016 in MPB.

Appendix F Al_i Equation Residuals

F.1 Residuals for Mersey River Equations

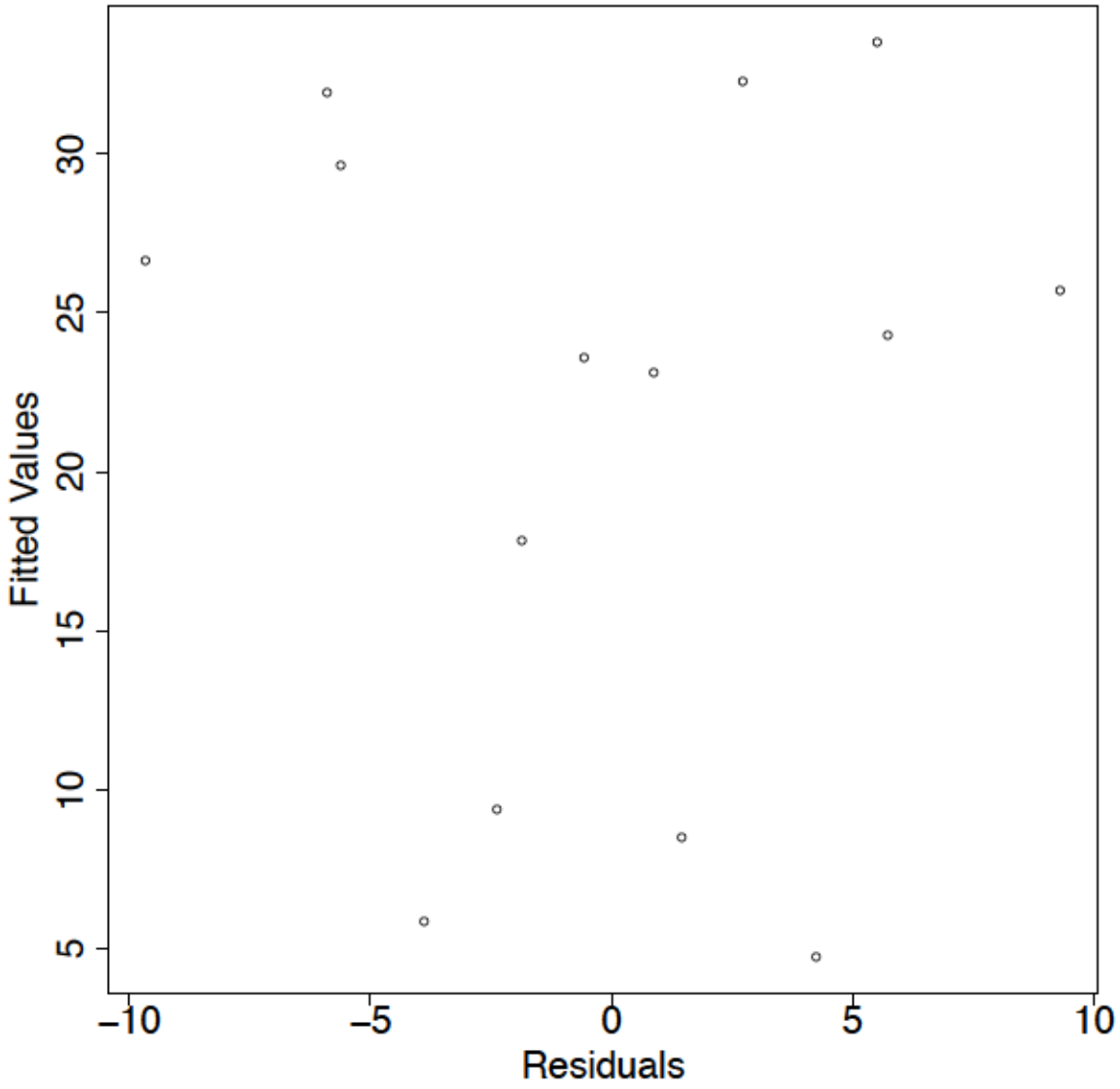

Figure F.1.1:Residuals for the MRS1Ald1 Al_i equation.

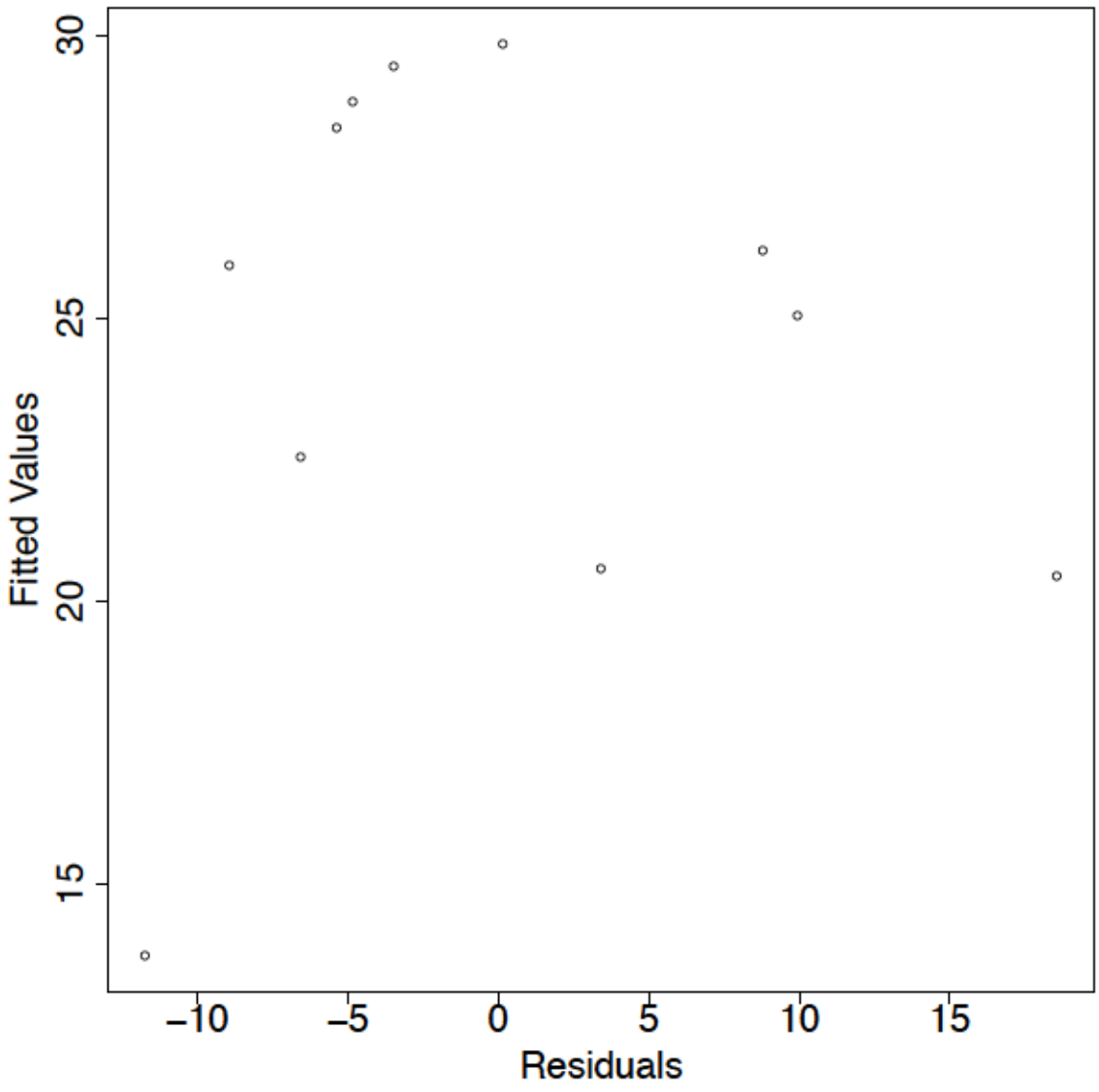

Figure F.1.2:Residuals for the MRS1Alt1 Al_i equation.

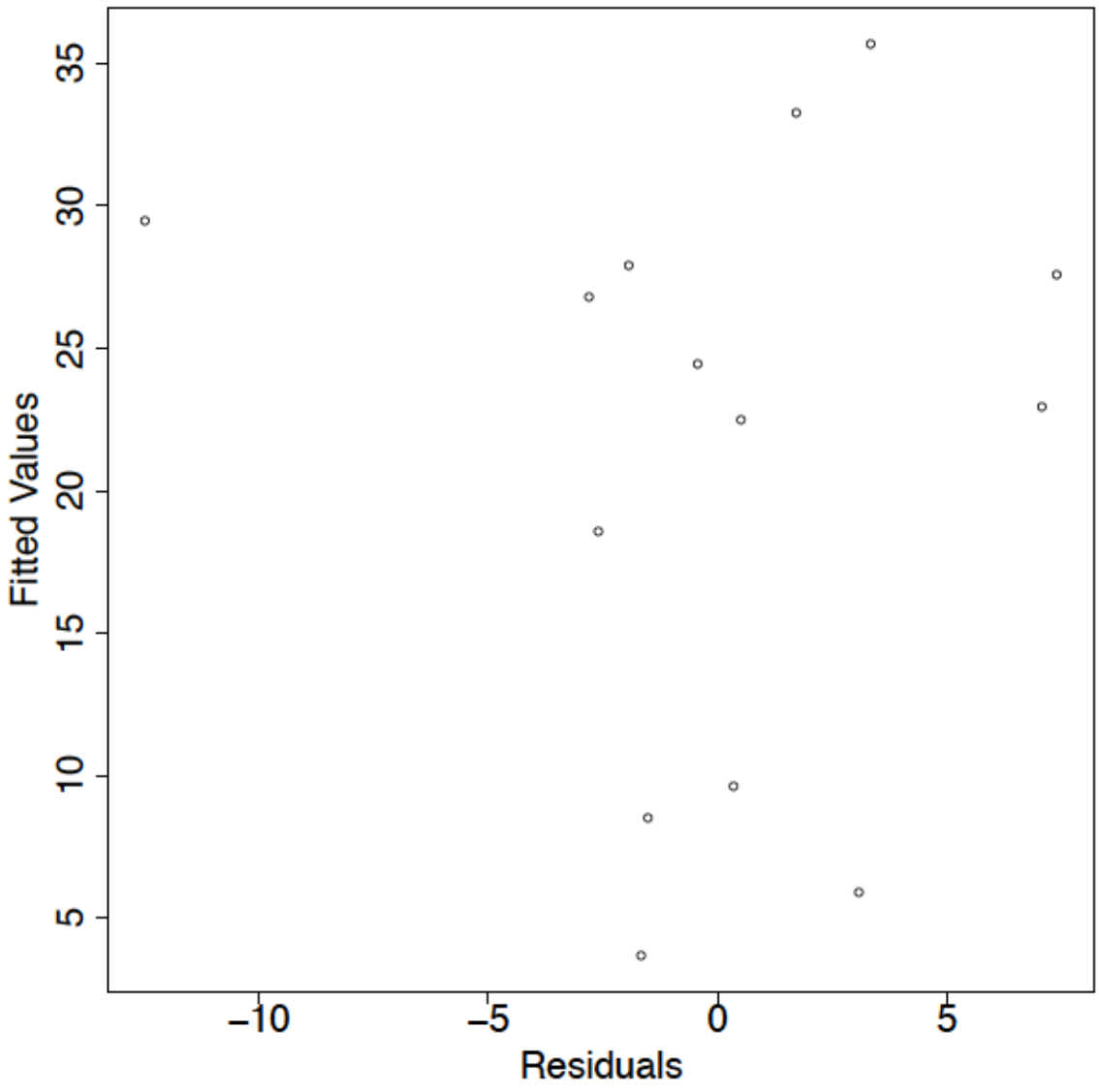

Figure F.1.3:Residuals for the MRS1Ald2 Al_i equation.

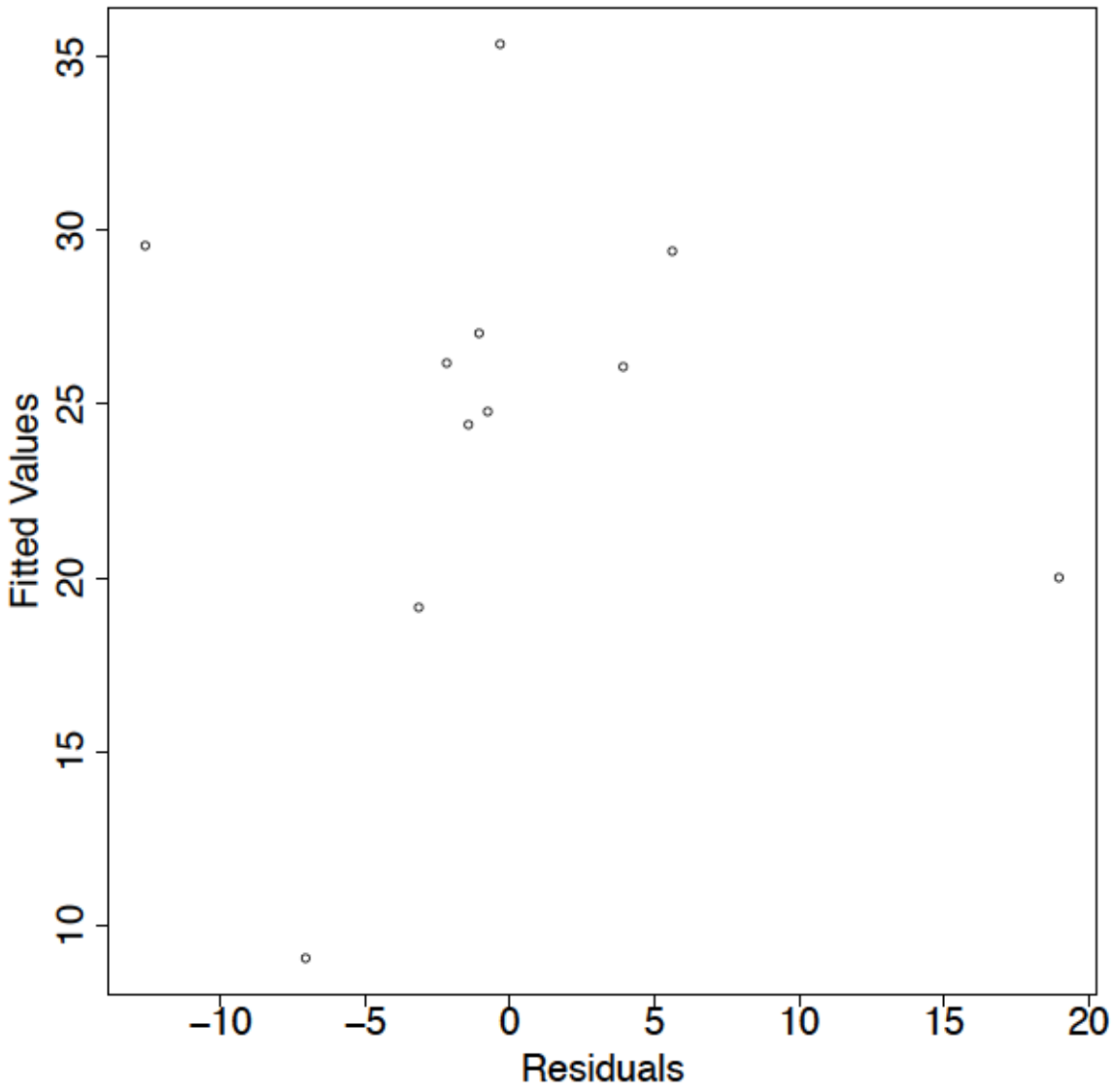

Figure F.1.4:Residuals for the MRS1Alt2 Al_i equation.

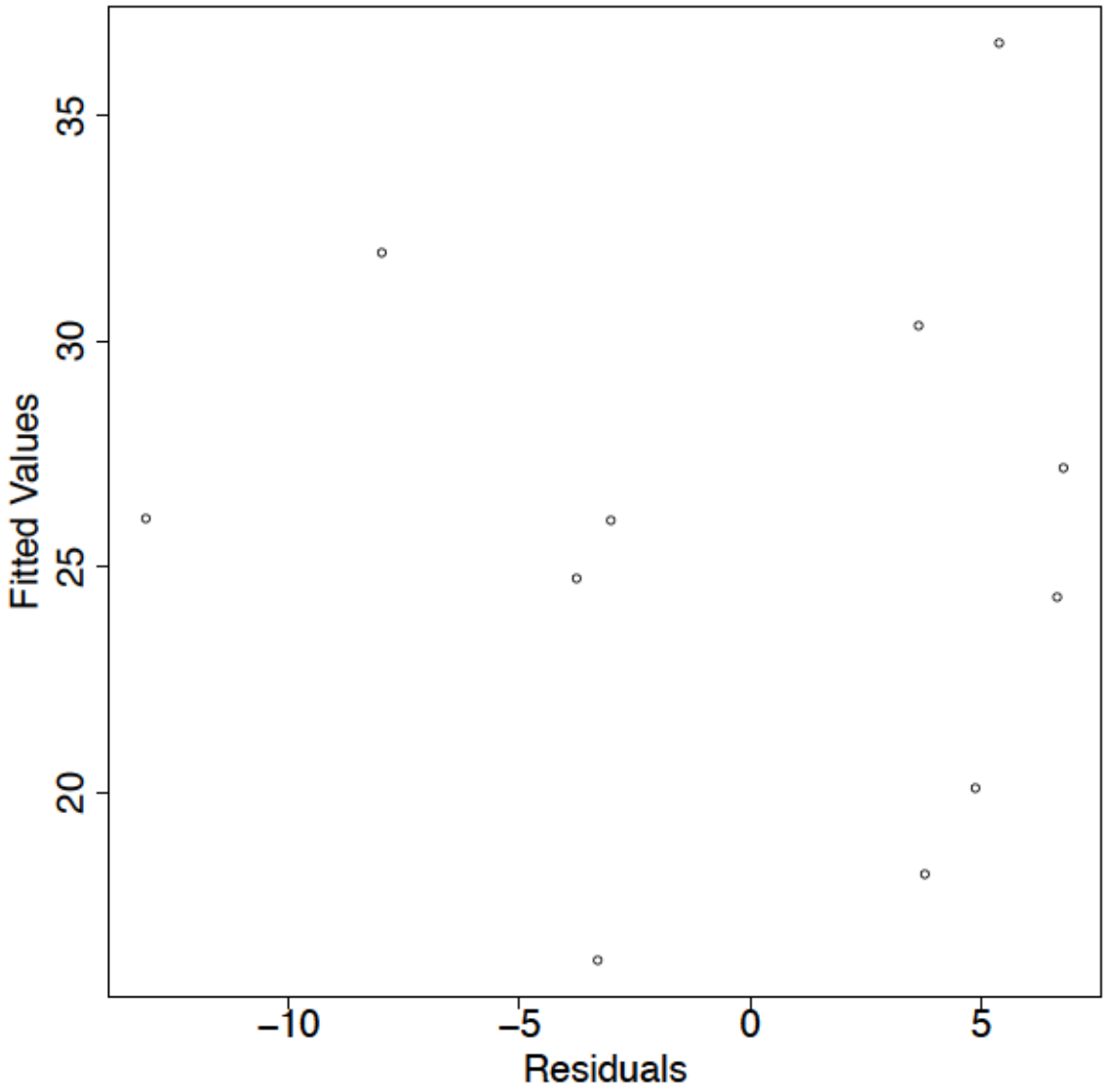

Figure F.1.5:Residuals for the MRS2Ald1 Al_i equation.

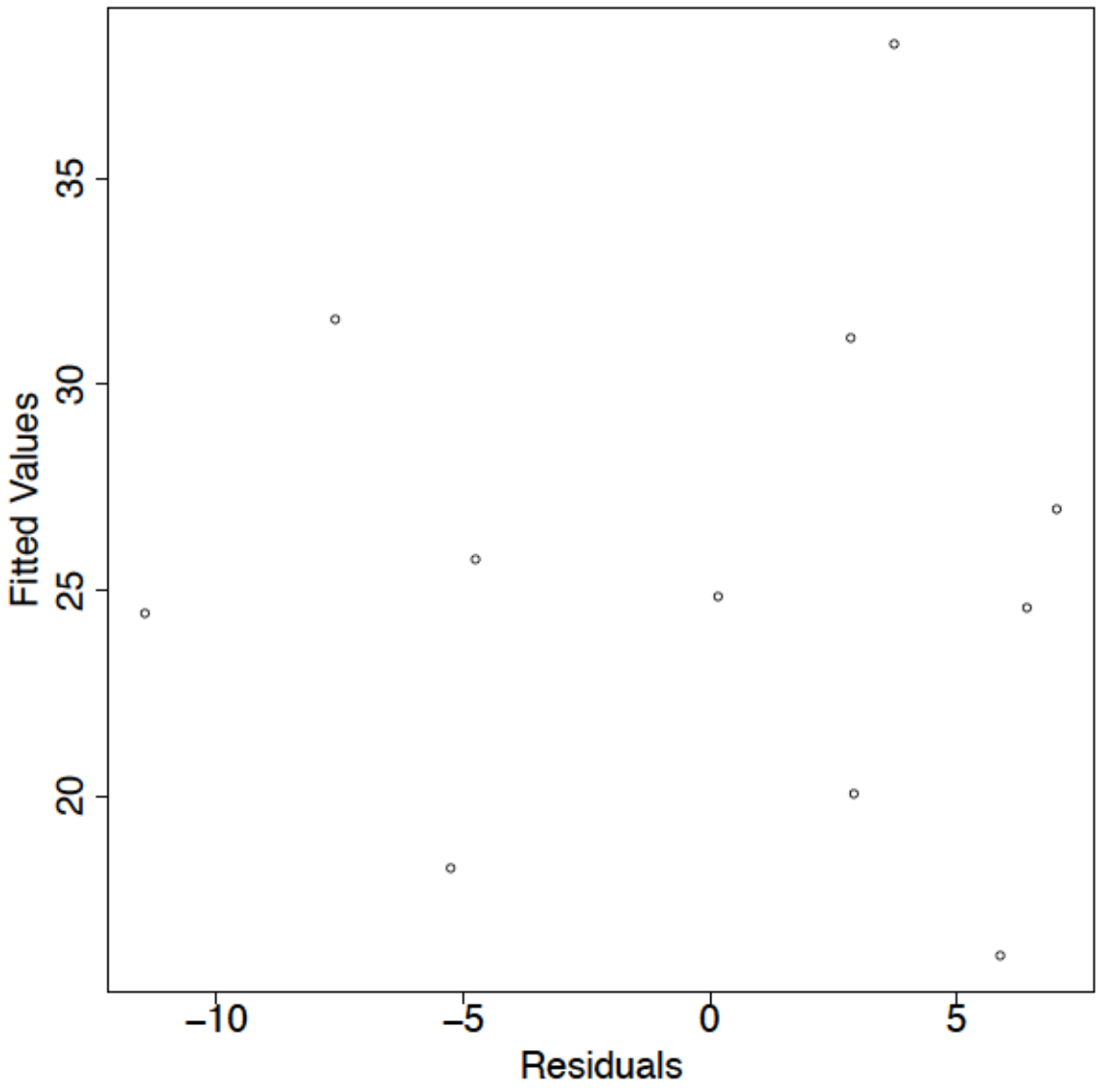

Figure F.1.6:Residuals for the MRS2Alt1 Al_i equation.

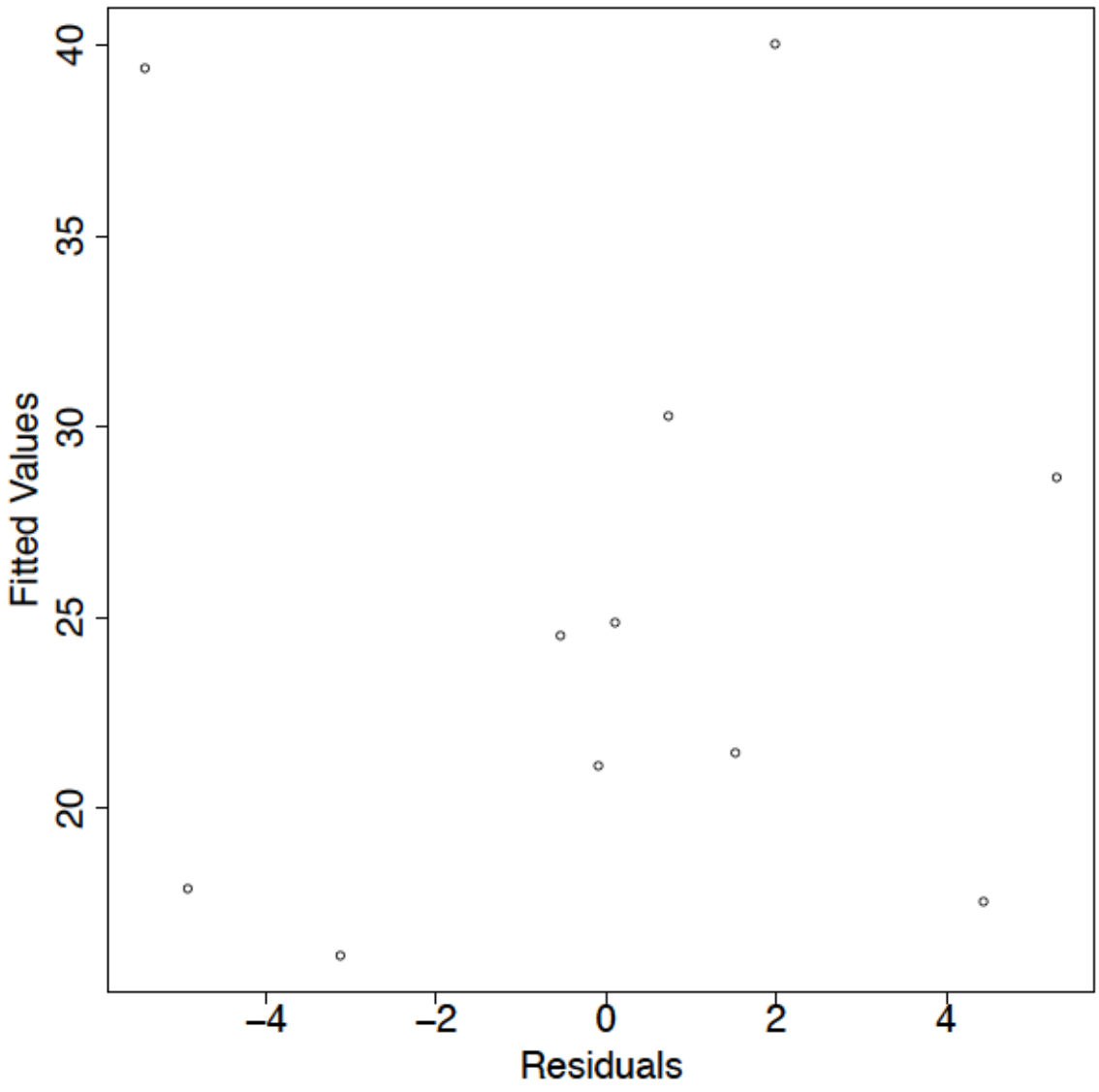

Figure F.1.7:Residuals for the MRS2Ald2 Al_i equation.

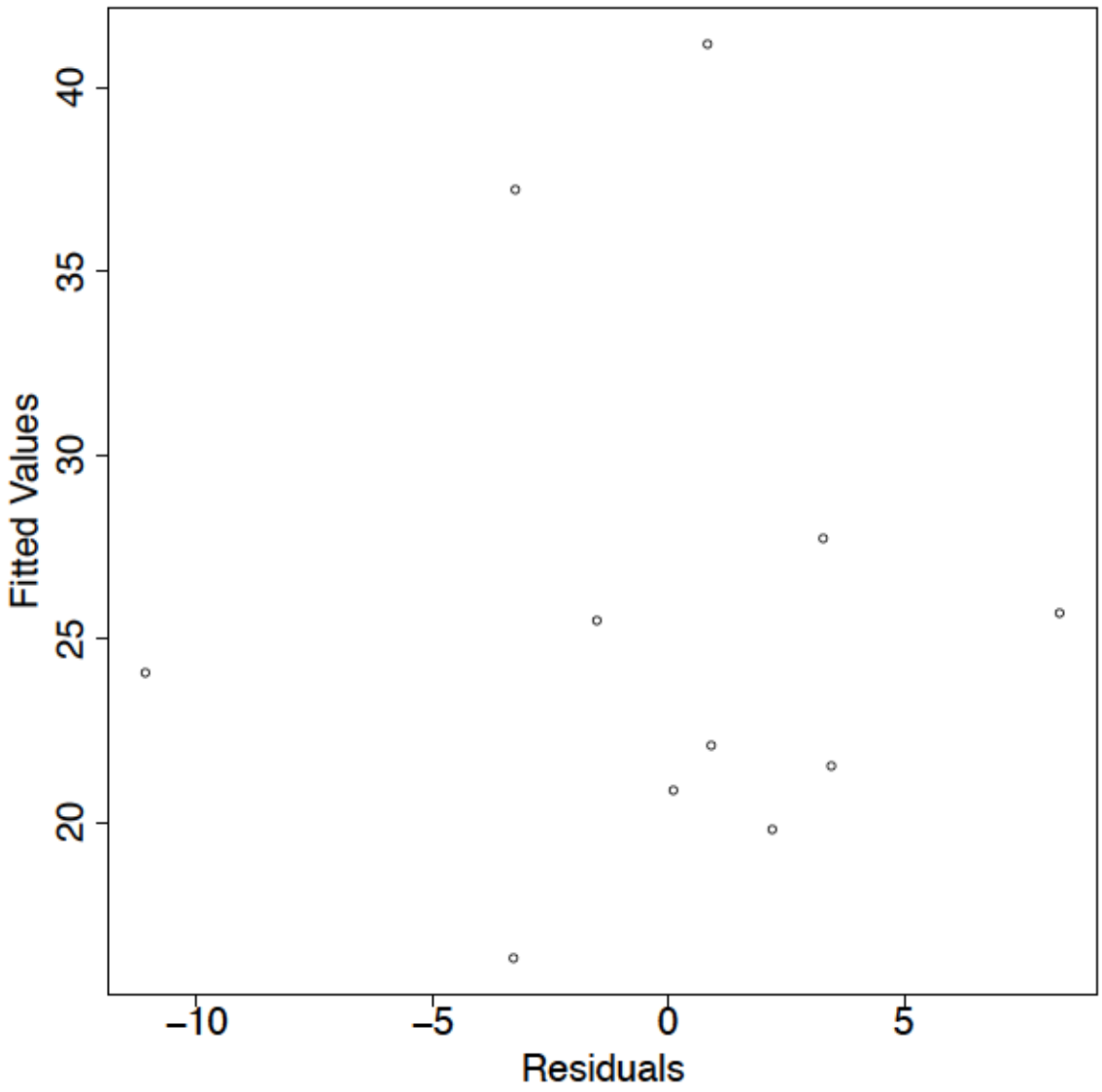

Figure F.1.8:Residuals for the MRS2Alt2 Al_i equation.

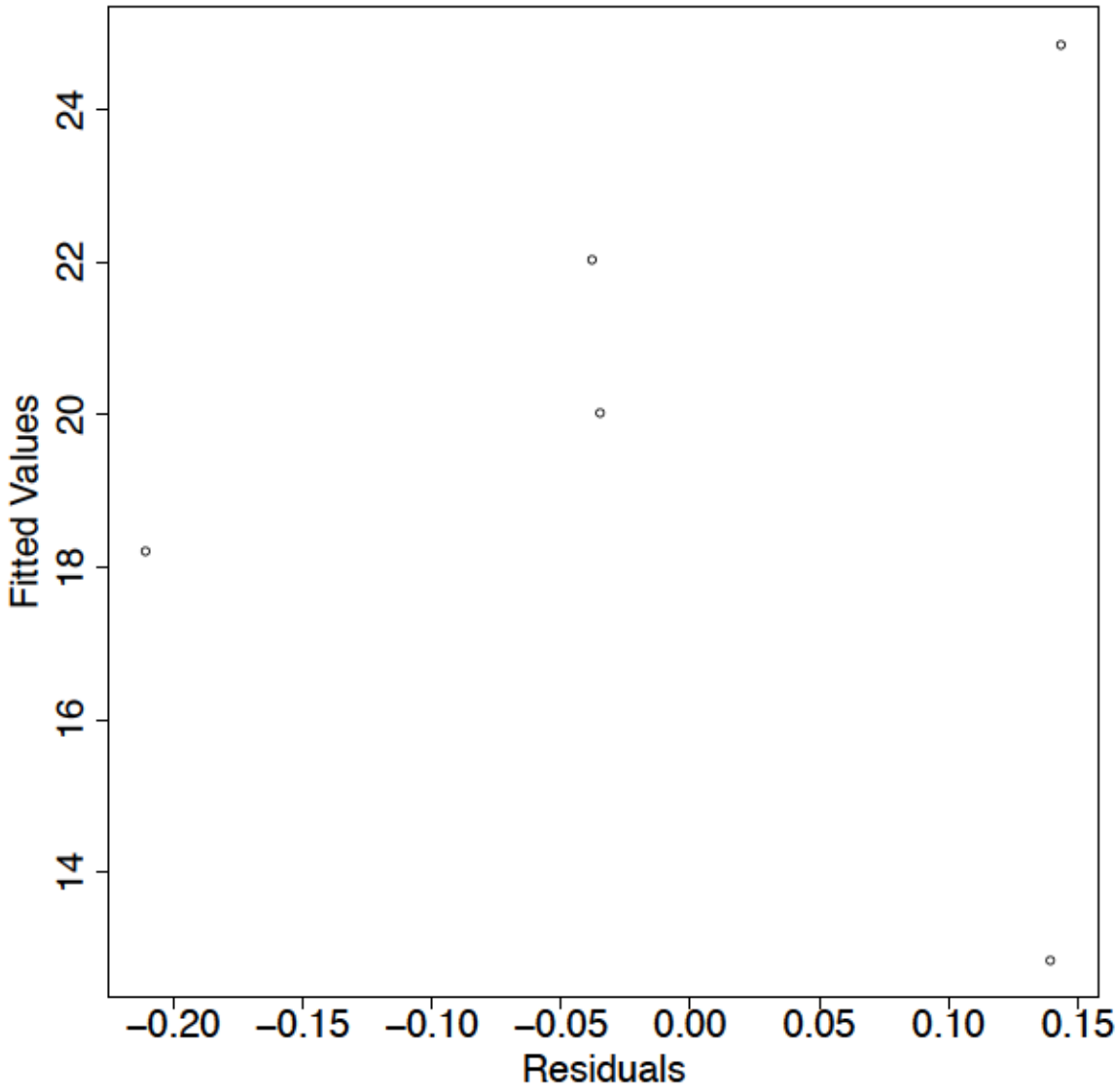

Figure F.1.9:Residuals for the MRS3Ald1 Al_i equation.

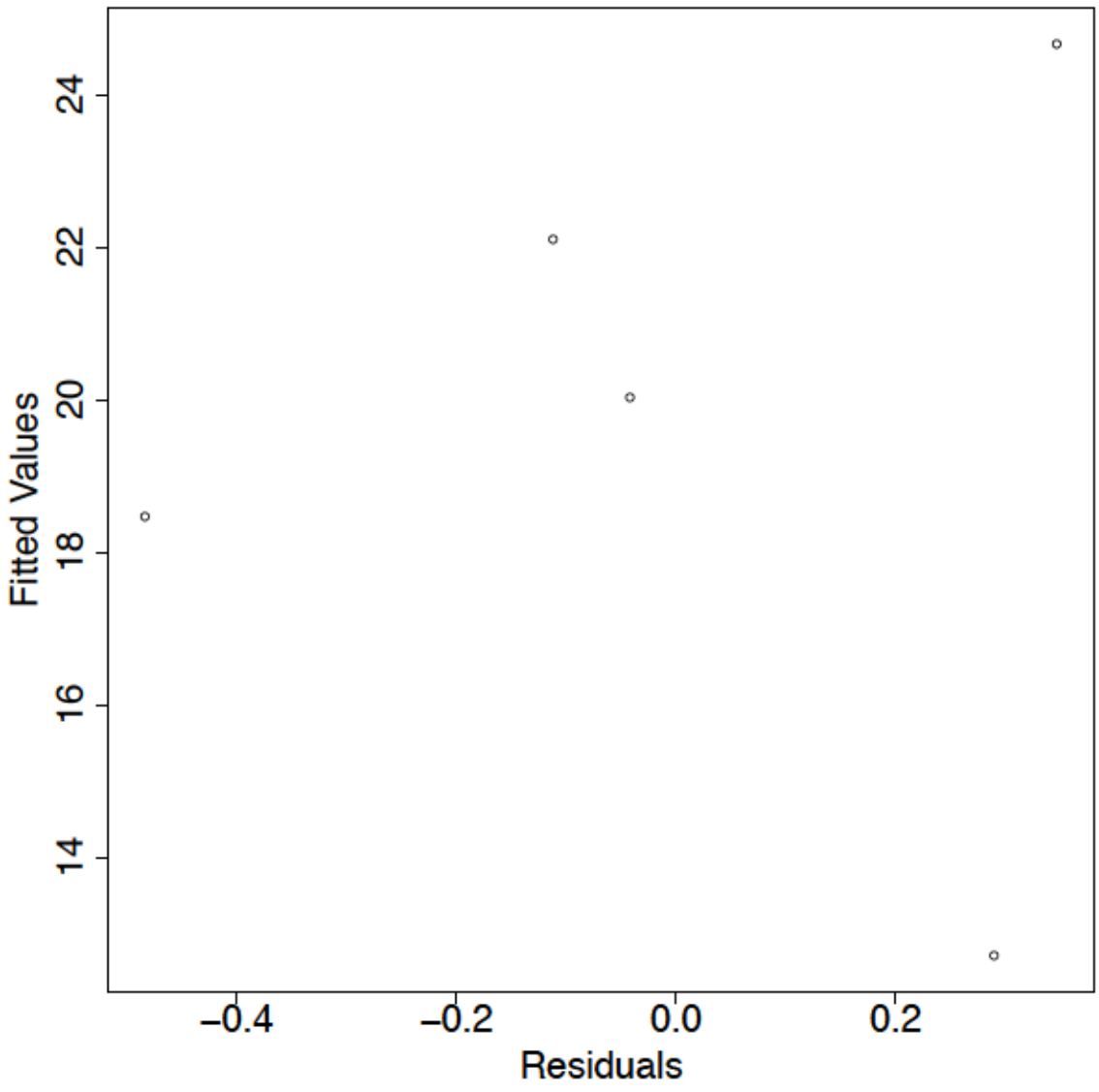

Figure F.1.10:Residuals for theMRS3Alt1 Al_i equation.

F.2 Residuals for Moose Pit Brook Equations

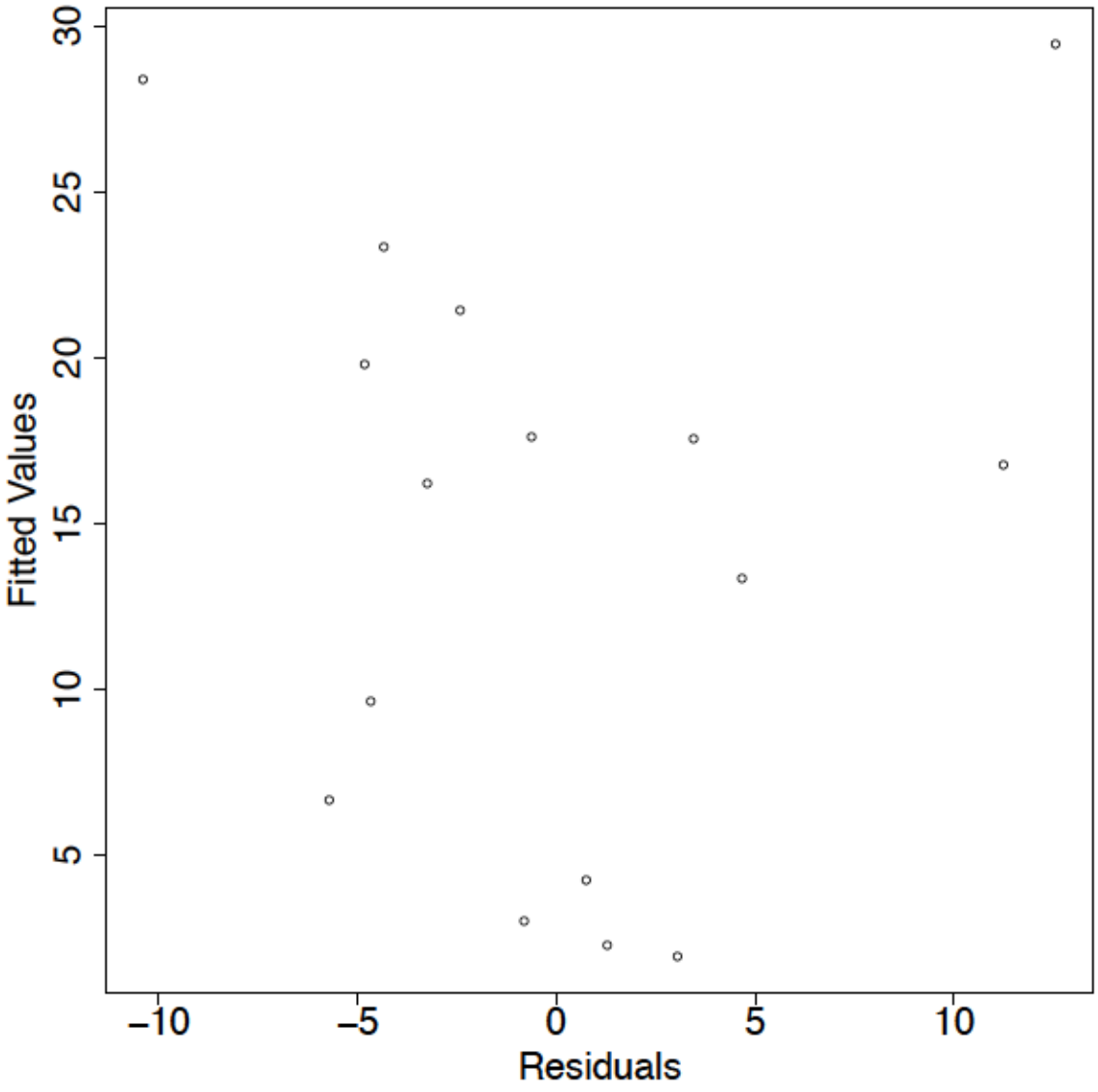

Figure F.2.1: Residuals for the MPBS1Ald1 Al_i equation.

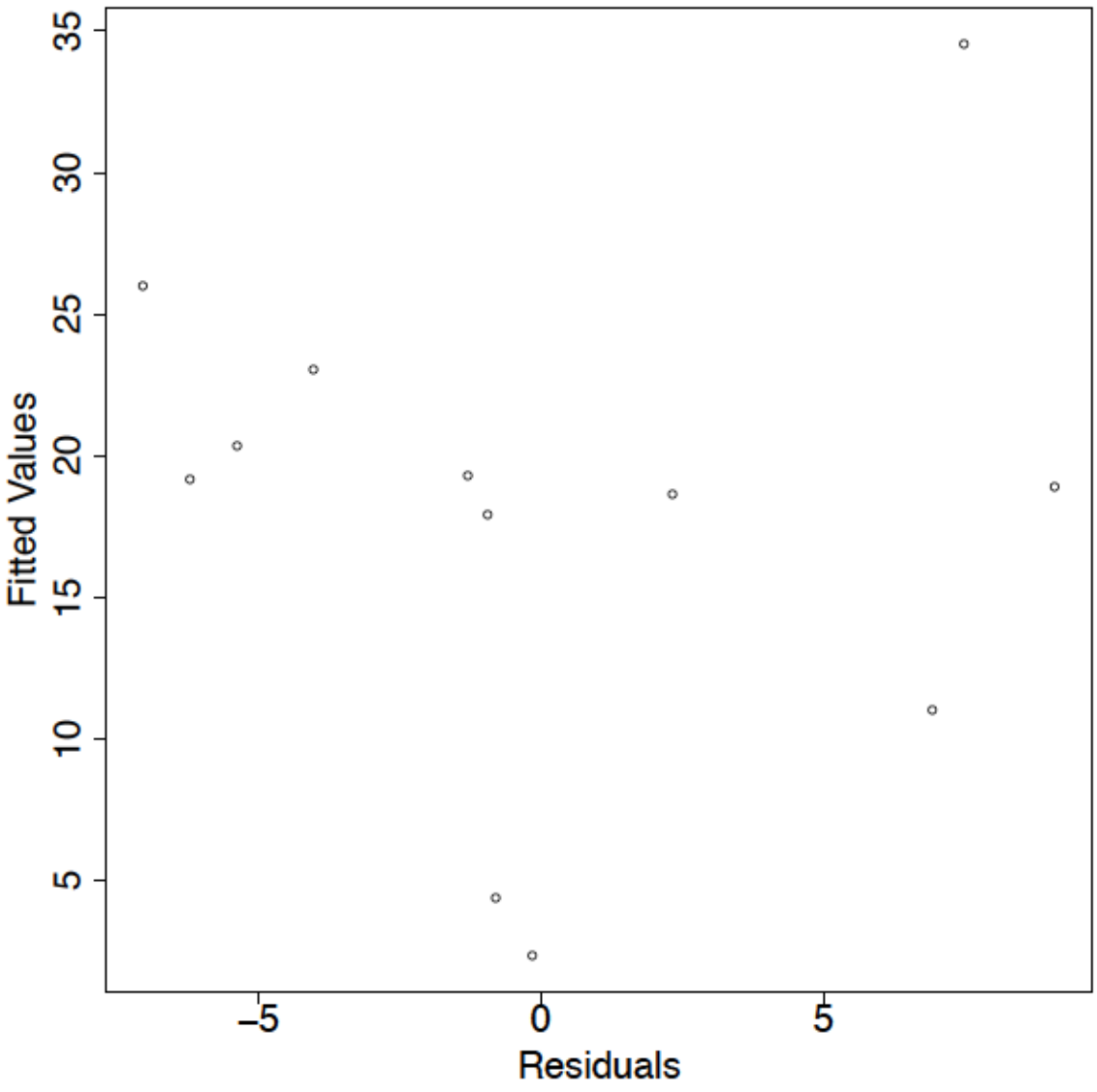

Figure F.2.2: Residuals for the MPBS1Alt1 Al_i equation.

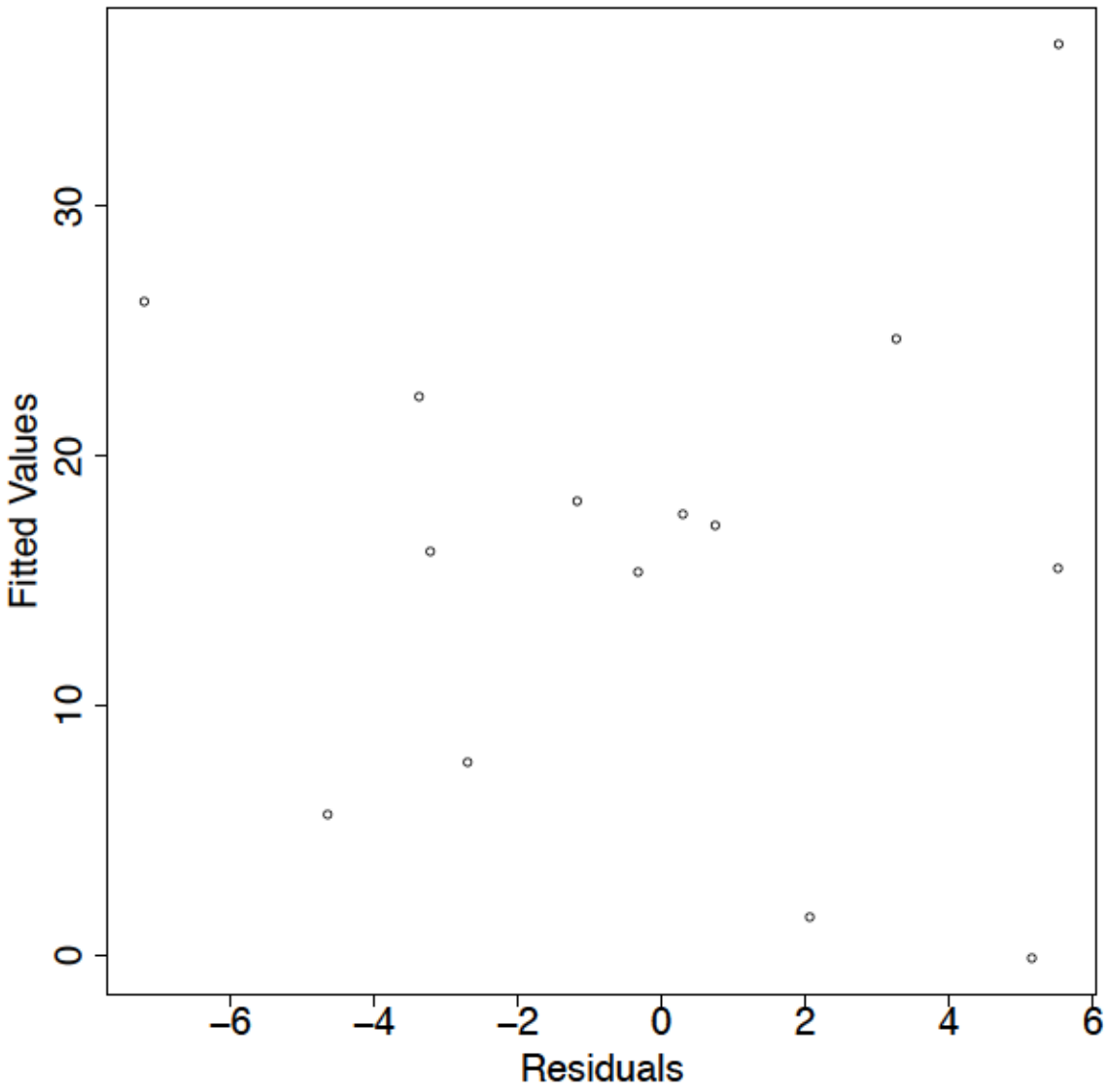

Figure F.2.3: Residuals for the MPBS1Ald2 Al_i equation.

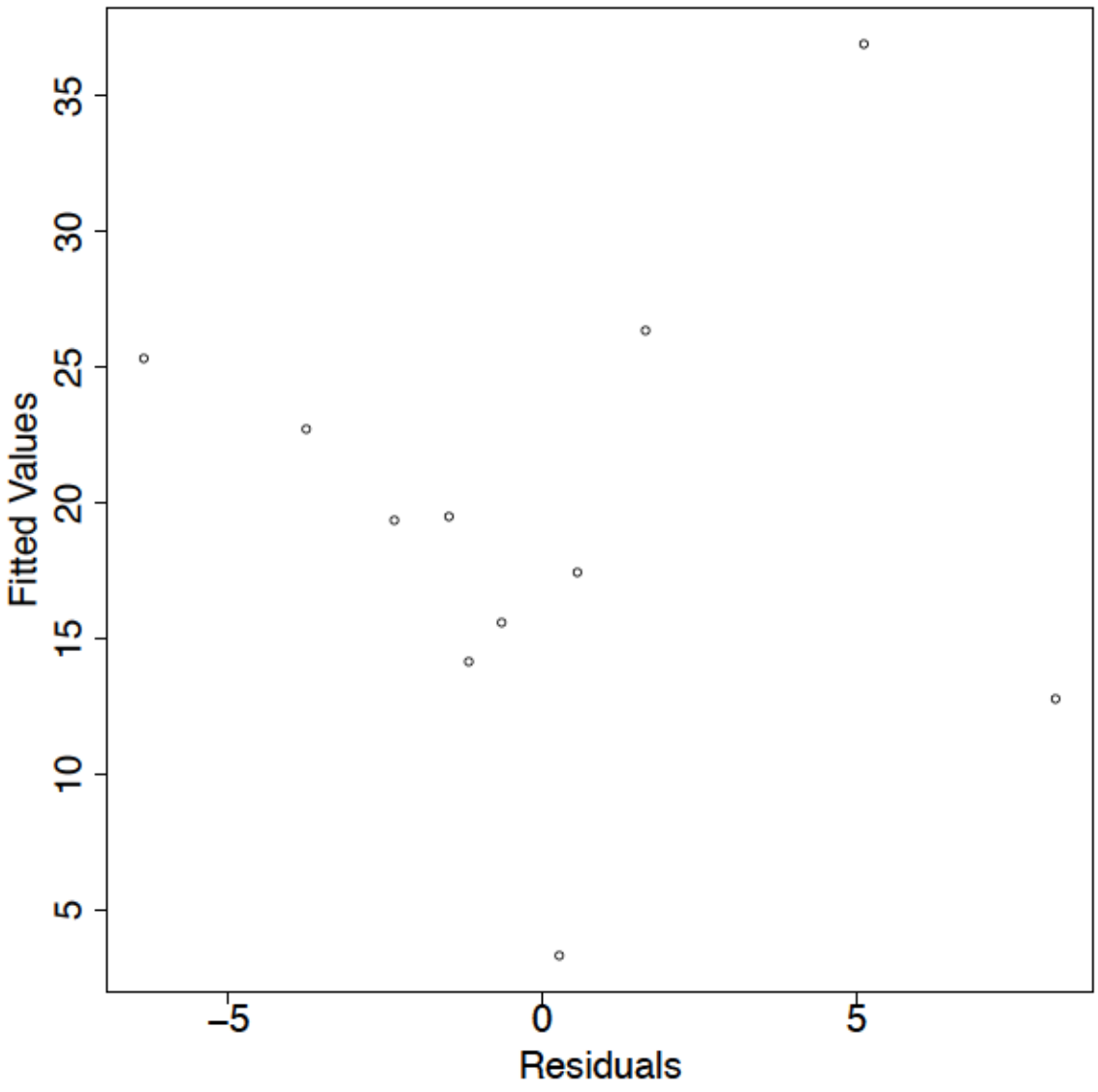

Figure F.2.4: Residuals for the MPBS1Alt2 Al_i equation.

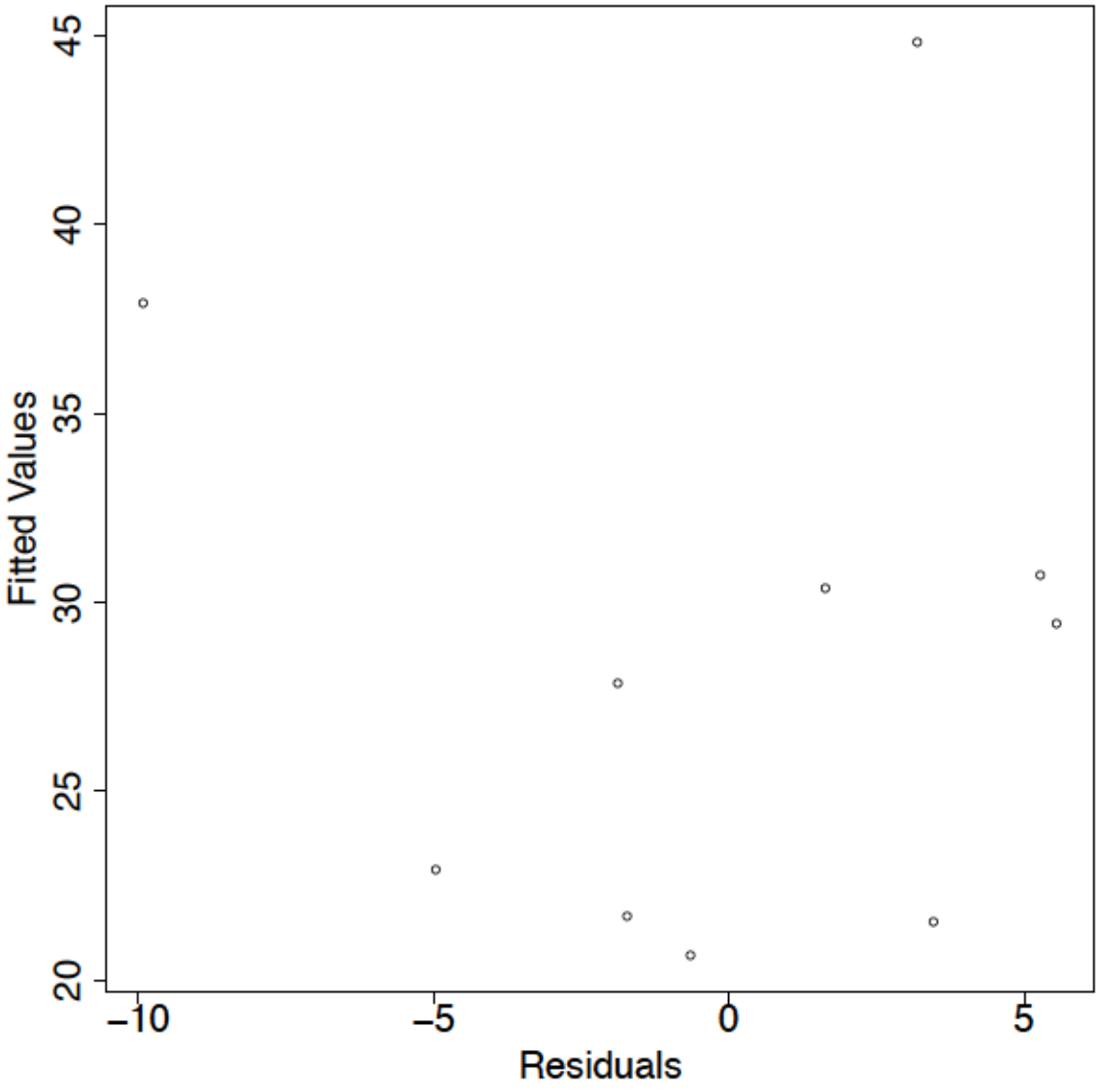

Figure F.2.5: Residuals for the MPBS2Ald1 Al_i equation.

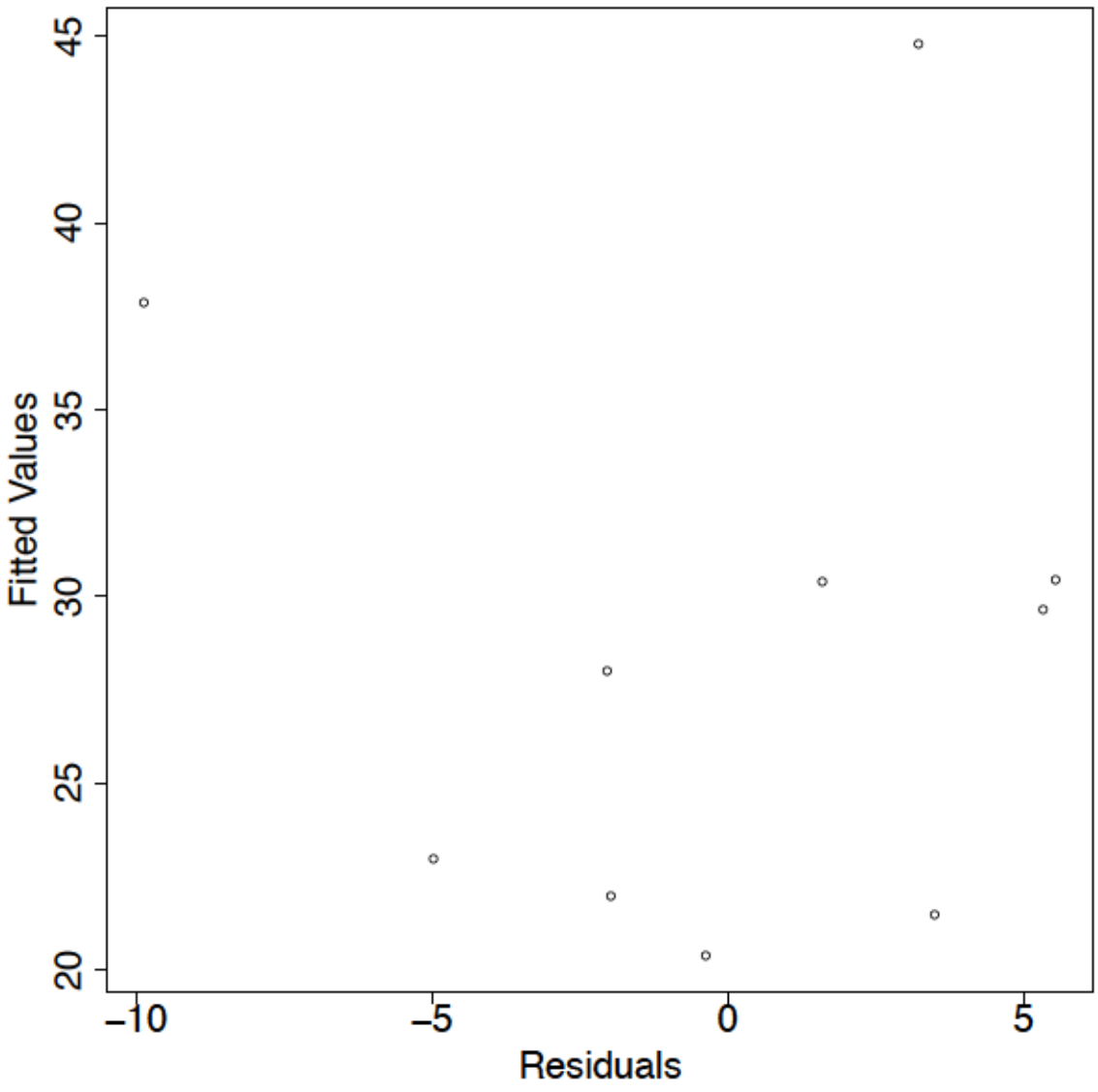

Figure F.2.6: Residuals for the MPBS2Alt1 Al_i equation.

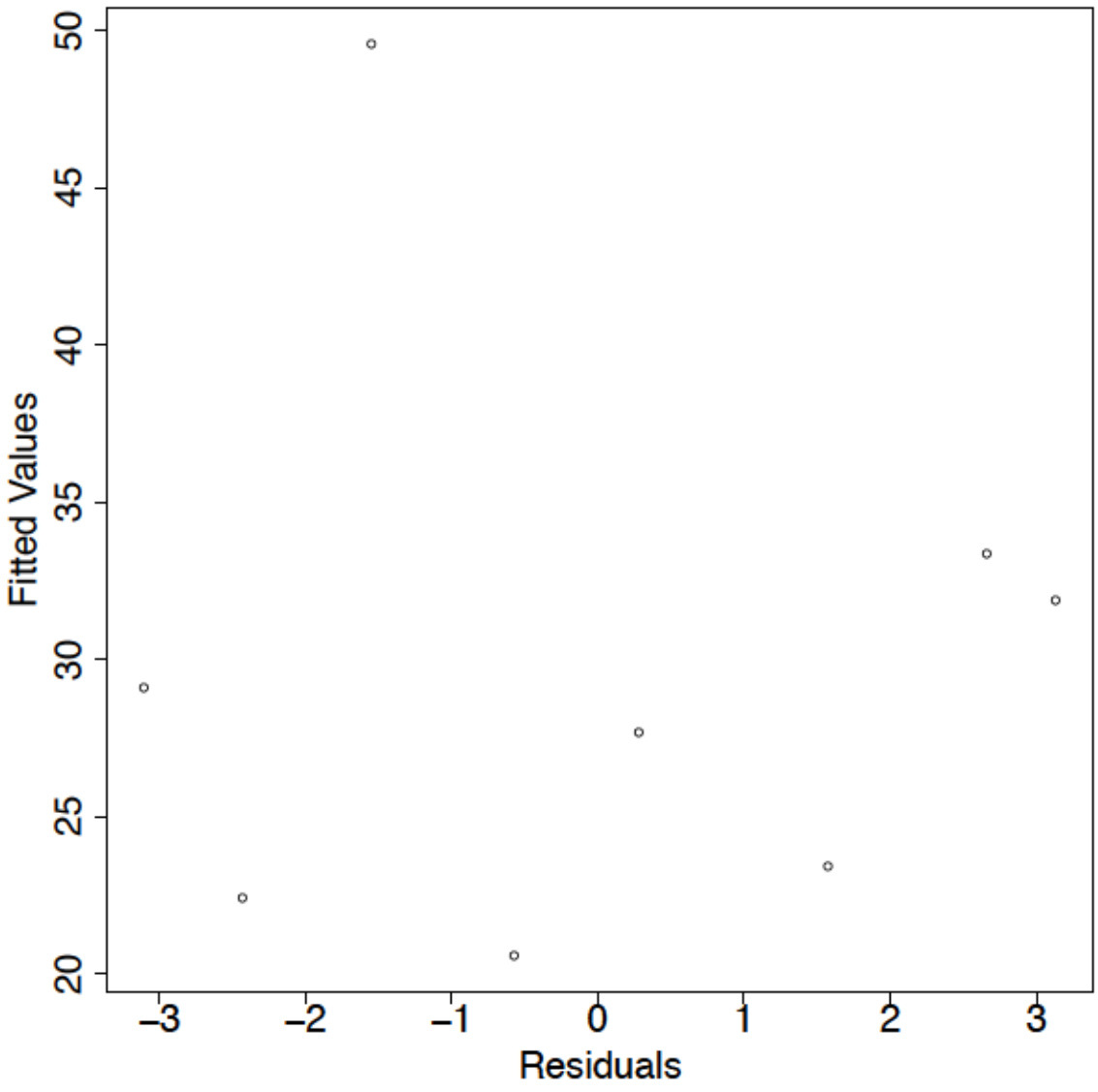

Figure F.2.7: Residuals for the MPBS2Ald2 Al_i equation.

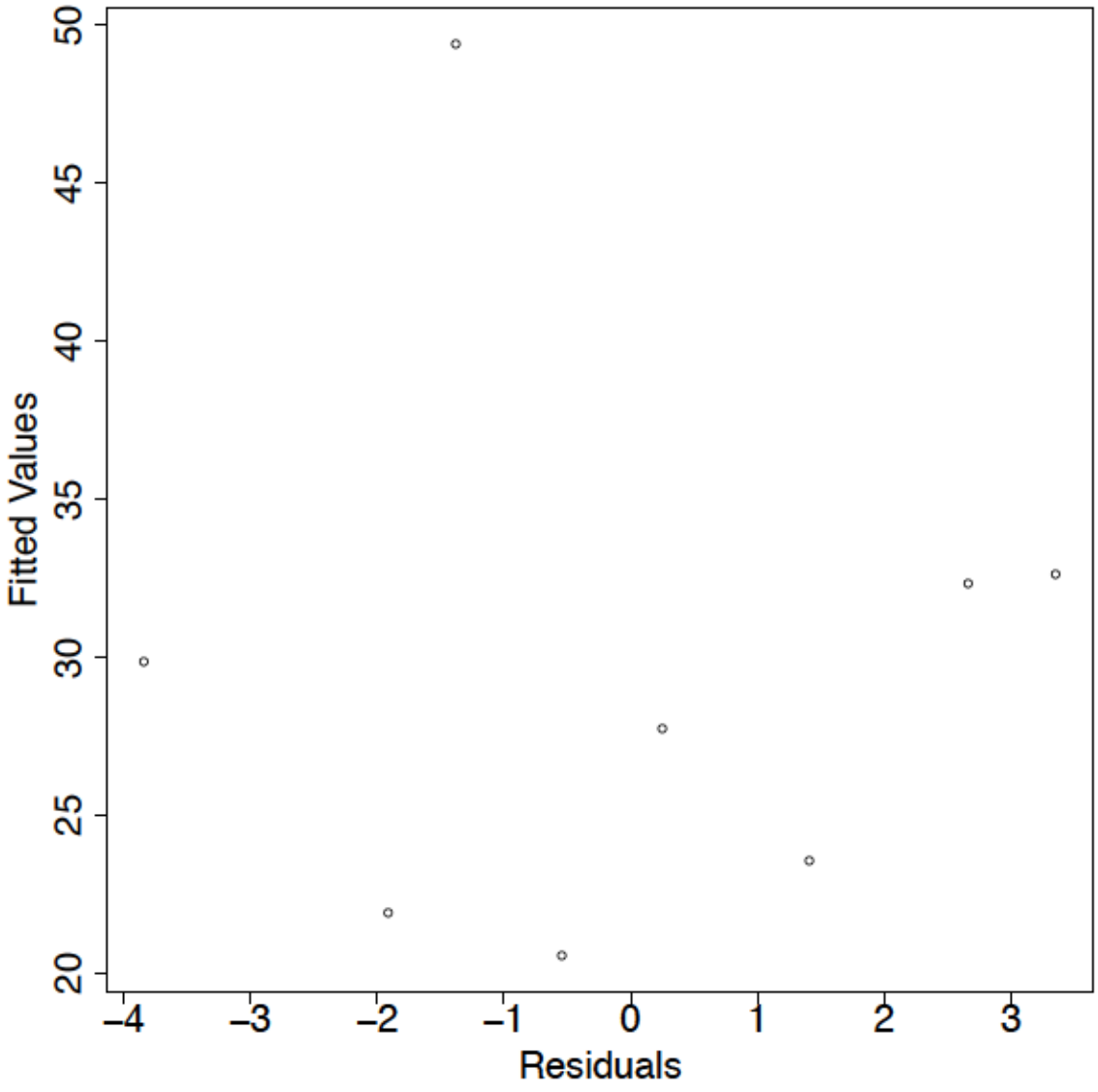

Figure F.2.8: Residuals for the MPBS2Alt2 Al_i equation.

Appendix G $Al_{i\text{-}c}$ Time-series

Here I present $Al_{i\text{-}c}$ estimates from 1980/1983-2014 using equations presented in Tables 3.5 and 3.6 that can be applied to the EC database; we compare the equation which include the Al_d parameter (Ald.1 and Ald.2), and the Al_t parameter (Alt.1 and Alt.2). We also compare $Al_{i\text{-}c}$ outputs to the Al_i equation presented by Dennis and Clair in 2012 (TC).

G.1 MR Time-series

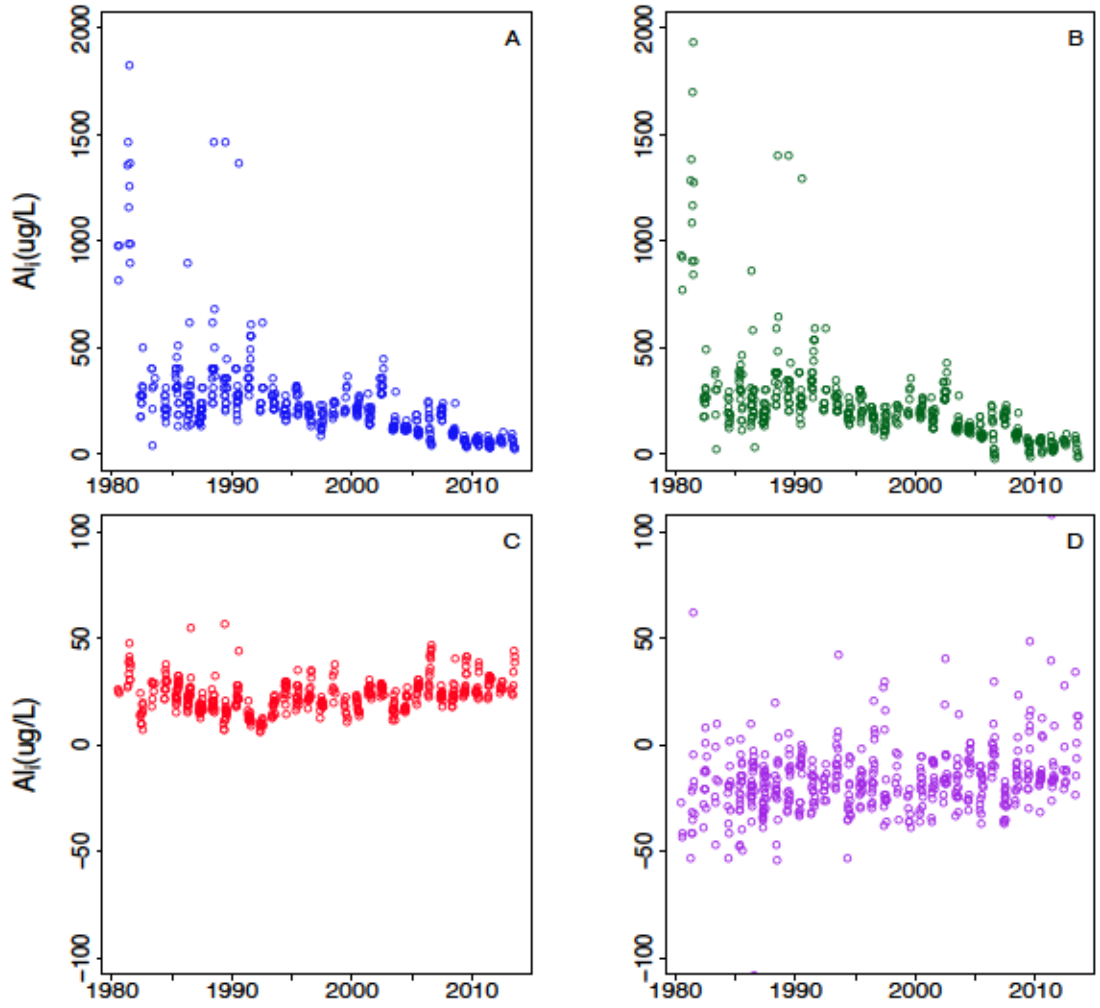

Figure G.1.1: A) MRS1Ald1, B) MRS1Ald2, C) MRS1Alt1 and D) TC $Al_{i\text{-}c}$ estimates for MR from 1980-2014 in season one (spring/summer: April 1st-August 5th). To see the overall trend of the Ali-c equation outputs, extreme values are not made visible in the figure. Values not shown for S1Ald1 are 2099.1 µg/L on June 23rd, 1981, 4976.4 µg/L on July 9th, 1981, and 2384.7 µg/L on May 30th, 1989. Values not shown for S1Ald2 are 4729.0 µg/L on July 9th, 1981, 2139.0 µg/L on May 30th, 1989, -6.3 µg/L on July 18th, 2006, -24.4 µg/L on July 26th, 2006, -9.7 µg/L on August 1st, 2006, -13.5 µg/L on August 1st, 2009, -19.2 µg/L on July 2nd, 2013, -12.5 on July 29th, 2013 and -1.1 on July 15th, 2015. Values not shown for S1TC are 107.6 µg/L on May 16th, 2011, -108.1 µg/L on July 29th, 1986, and -118.2 µg/L on May 30th, 1989.

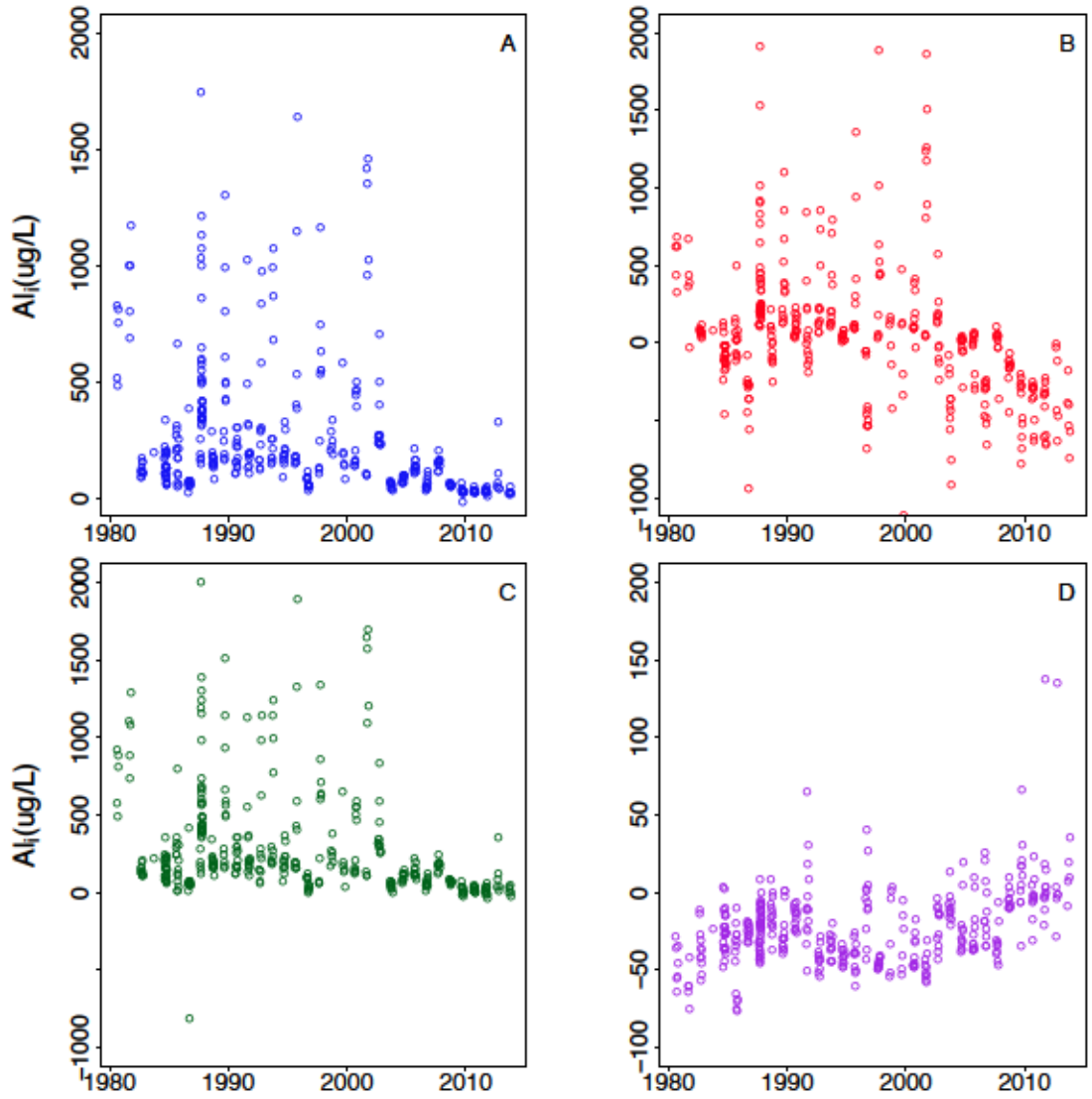

Figure G.1.2: A) MRS2Ald1, B) MRS2Alt1, C) MRS2Alt2 and D) TC $Al_{i\text{-}c}$ estimates for MR from 1980-2014 in season two (fall: August 12th-October 31st). To see the overall trend of the Ali-c equation outputs, extreme values are not made visible in the figure. Values not shown for S2Ald1 are 8769.8 µg/L on Oct 16th, 1980, 6112.5 µg/L on Oct 24th, 1980, 2222.2 µg/L on Sept 23rd, 1987, 2158.6 µg/L on Sept 15th, 1997, 2185.4 µg/L on Sept 24th, 2001, 2340.8 µg/L on Oct 22nd, 2001, -192.0 on Sept 29th, 1986 and -13.9 on Sept 21st, 2009. Values not shown for S2Alt1 are 7397.3 µg/L on Oct 16th, 1980, 4788.6 µg/L on Oct 24th, 1980, -2321.0 µg/L on Sept 13th, 1985, and -1118.4 µg/L on Oct 25th, 1999. Values not shown for S2Alt2 are 9988.9 µg/L on Oct 16th, 1980, 6951.3 µg/L on Oct 24th, 1980, 2542.6 µg/L on Sept 23rd, 1987, 2476.0 µg/L on Sept 15th, 1997, 2522.1 µg/L on Sept 24th, 2001, and 2702.1 µg/L on Oct 22nd, 2001. Values not shown for S2TC are 368.7 µg/L on Sept 24th, 2013, -122.8 µg/L on Sept 13th, 1985, and -139.0 µg/L on Sept 29th, 1986.

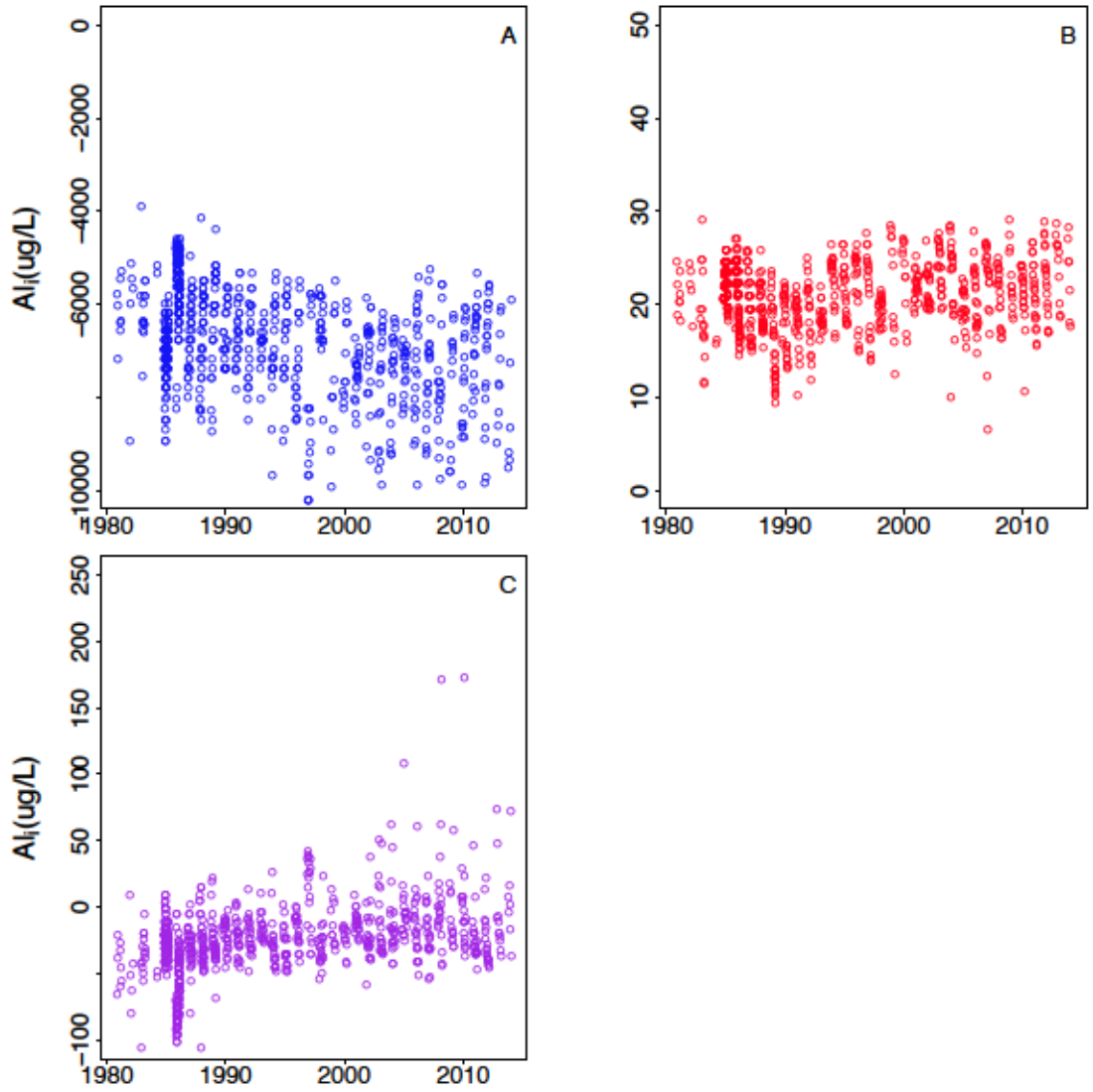

Figure G.1.3: A) MRS3Ald1, B) MRS3Alt1, and C) TC $Al_{i\text{-}c}$ estimates for MR from 1980-2014 in season three (winter: November 1st-March 31st). To see the overall trend of the Ali-c equation outputs, extreme values are not made visible in the figure. Values not shown for S1Ald1 are -10441.2 µg/L on Nov 4th, 1996, -10458.5 µg/L on Nov 18th, 1996, -10729.8 µg/L on Nov 25th, 1996, -10206.7 µg/L on Dec 2nd, 1996, -10197.3 µg/L on Dec 16th, 1996, -10204.4 µg/L on Dec 23rd, 1996, -11607.9 µg/L on Nov 25, 2002, -153337.6 µg/L on Dec 10th, 2002, -10532.9 µg/L on Jan 12th, 2004, -14006.4 µg/L on Dec 28th, 2004, -43427.7 µg/L on Jan 22nd, 2007, -10732.8 µg/L on jan 29th, 2008, -17668.3 µg/L on Feb 17th, 2008, -10518.5 µg/L on Feb 23rd, 2009, -18232.0 µg/L on Jan 25th, 2010, -11108.3 µg/L on Nov 15th, 2010, -13392.0 µg/L on Nov 5th, 2012, -11537.6 µg/L on Dec 4th, 2012 and -11246.3 µg/L on Jan 13h, 2014. Values not shown for S3Alt1 is -39.0 µg/L on Dec 10th, 2002. Values not shown for S3TC are 880.9 µg/L on Dec 10th, 2002, 412.8 µg/L on Jan 22nd, 2007, -105.6 µg/L on Nov 24th, 1982, -101.1 µg/L on Dec 10th, 1985, -101.5 µg/L on Dec 13th, 1985, and -105.9 µg/L on Dec 22nd, 1987.

G.2 MPB Time-series

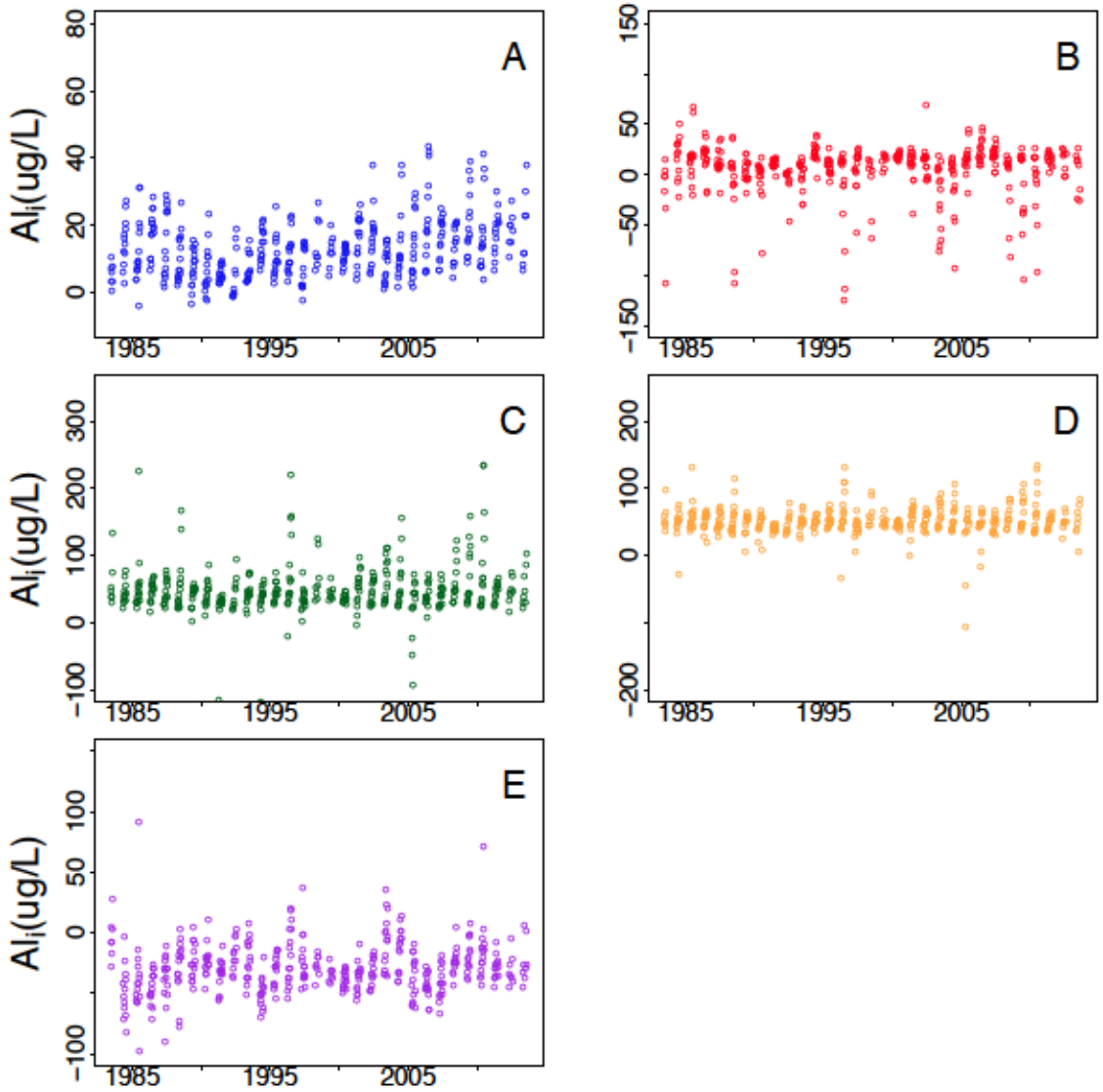

Figure G.2.1: A) MPBS1Ald1, B) MPBS1Alt1, C) MPBS1Ald2 and D) MPBS1Alt2, and E) TC $Al_{i\text{-}c}$ estimates for MPB from 1983-2014 in season one (spring/summer: April 1st-August 5th). To see the overall trend of the Ali-c equation outputs, extreme values are not made visible in the figure. Values not shown for S1Alt1 are -265.5 µg/L on July 1st, 1985, -194.6 µg/L on July 22nd, 1996, -256.6 µg/L on July 11th, 2010, and -185.6 µg/L on July 19th, 2010. Values not shown for S1Ald2 are -114.5 µg/L on April 22nd, 1991, -118.2 µg/L on May 9th, 1994, and -334.5 µg/L on May 24th, 2005. Values not shown for S1Alt2 are -334.5 µg/L on April 22nd, 1991, -363.7 µg/L on May 9th, 1994, -1509.4 µg/L on May 24th, 2005, and -246.9 µg/L on May 29th, 2005. Values not shown for S1TC are -122.6 µg/L on July 31st, 1985, and -164.1 µg/L on June 24th, 2002.

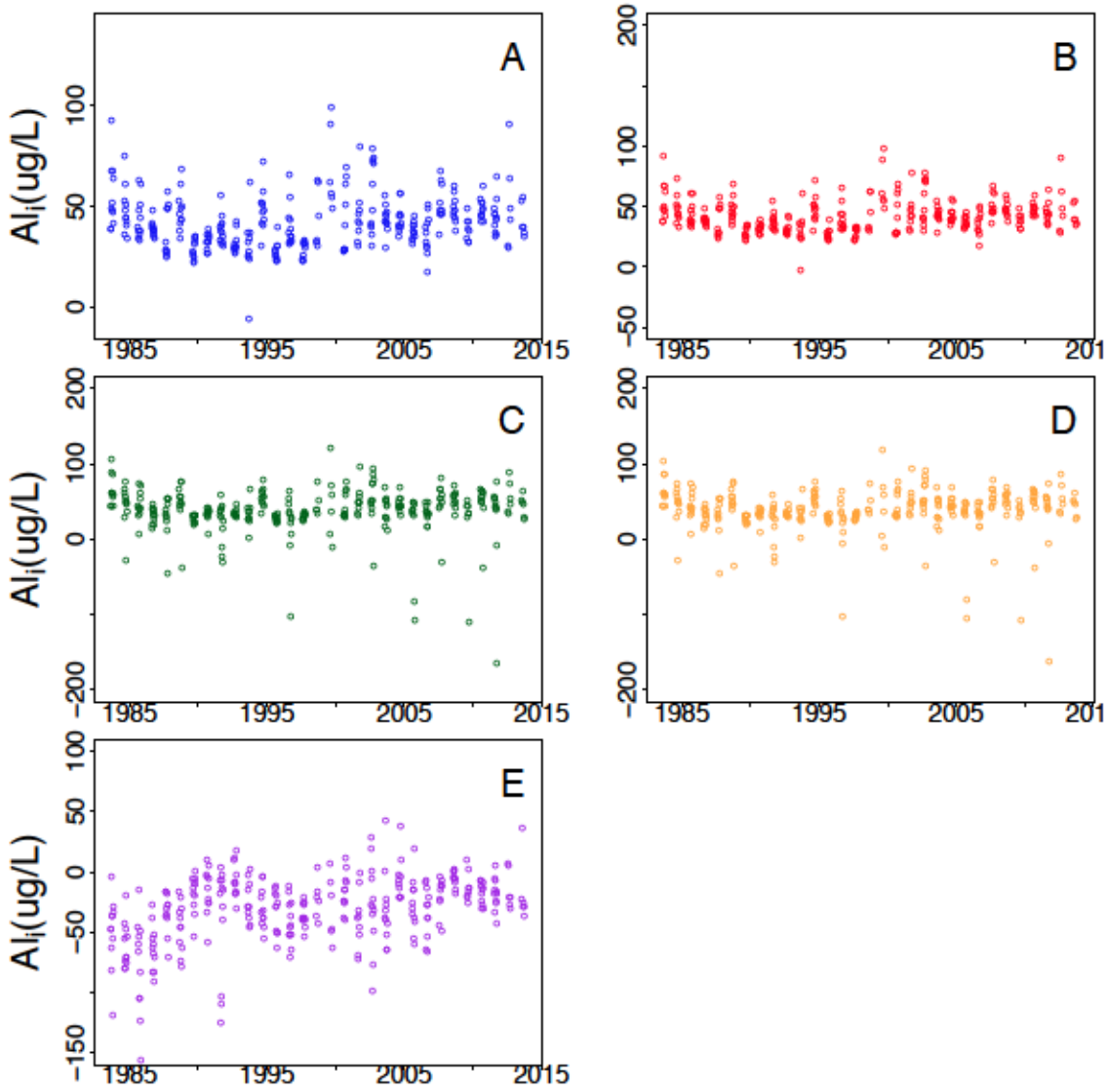

Figure G.2.2: A) MPBS2Ald1, B) MPBS2Alt1, C) MPBS2Ald2 and D) MPBS2Alt2, and E) TC $Al_{i\text{-}c}$ estimates for MPB from 1983-2014 in season two (fall: August 12th-October 31st). To see the overall trend of the Ali-c equation outputs, extreme values are not made visible in the figure. Values not shown for S2Ald2 are -536.2 ug/ on Sept 16th, 1996, -795.8 µg/L on Oct 12th, 1998, -1058.4 µg/L on Oct 12th, 2005 and -368.6 µg/L on Oct 6th, 2009. Values not shown for S2Alt2 are -531.3 µg/L on Sept 16th, 1996, -789.0 µg/L on Oct 12th, 1998, -1048.8 µg/L on Oct 12th, 2005, and -365.0 µg/L on Oct 6th, 2009. Value not shown for S2TC is -155.6 µg/L on Oct 21st, 1985.

Appendix H Extreme Outlier Correlations

H.1 MR Top 20 Extreme Correlations

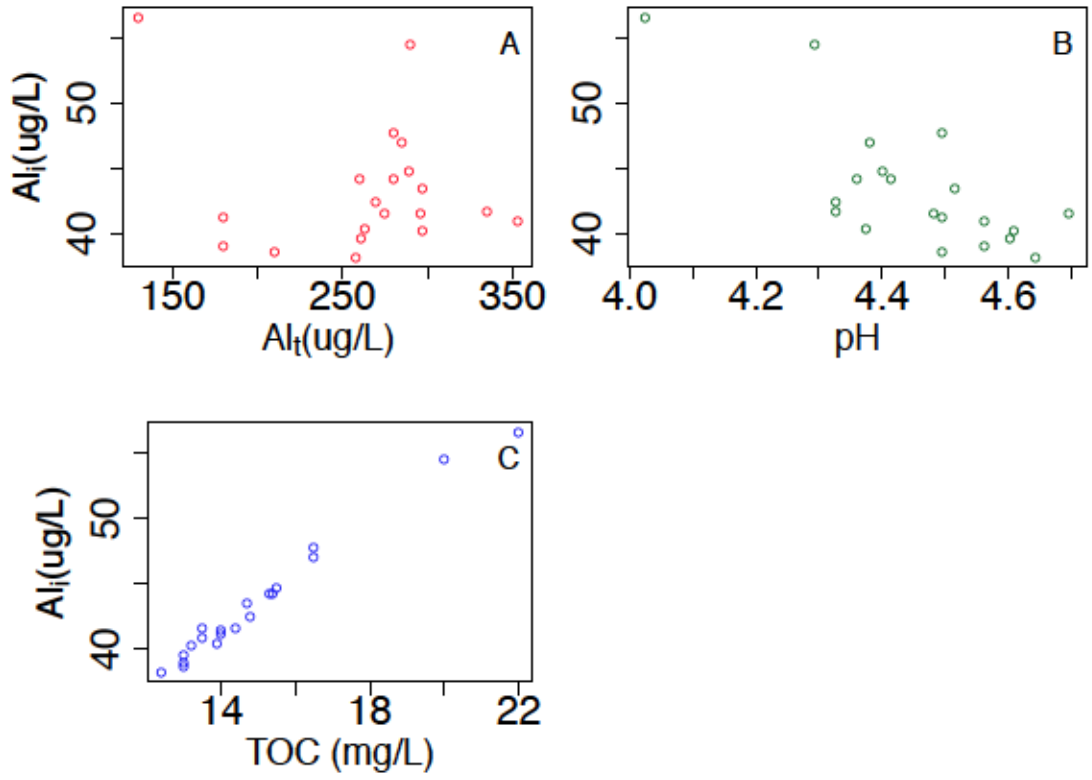

Figure H.1.1: Correlation of top twenty $Al_{i\text{-}c}$ with A) Al_t, B) pH, and C) TOC for MRS1Alt1.

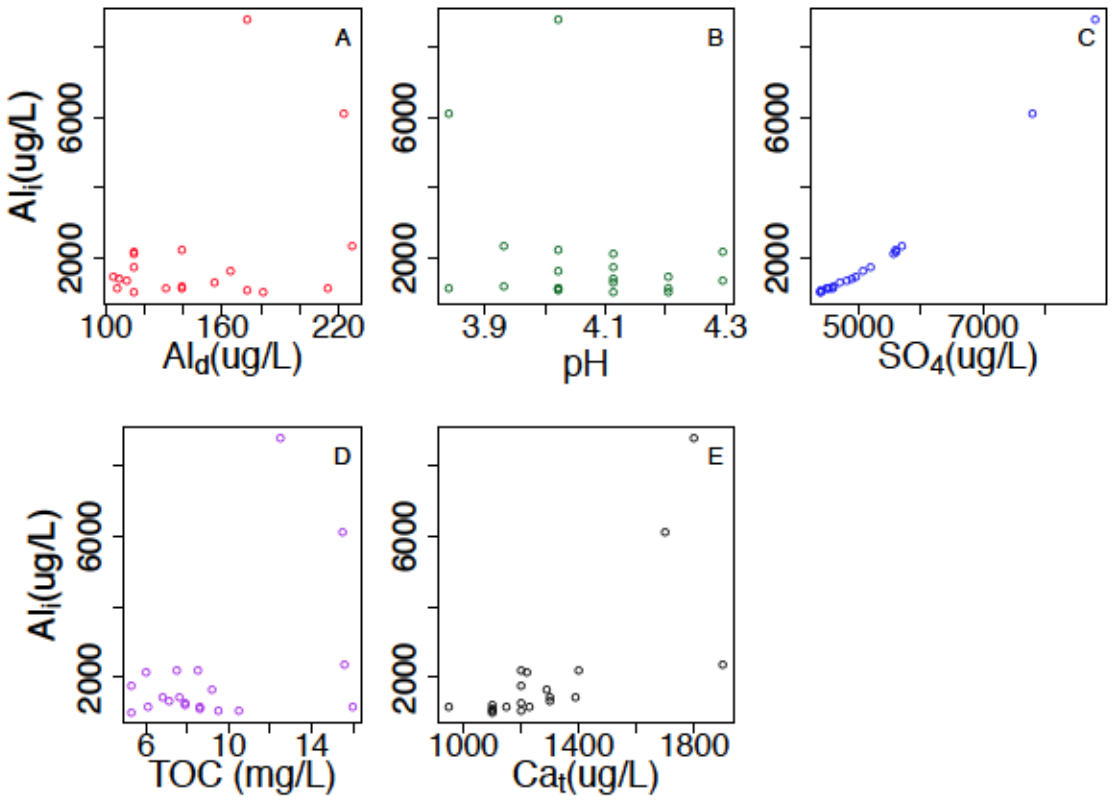

Figure H.1.2: Correlation of top twenty $Al_{i\text{-}c}$ with A) Al_d, B) pH, C) SO_4, D) TOC, and E) Ca_t for MRS2Ald1.

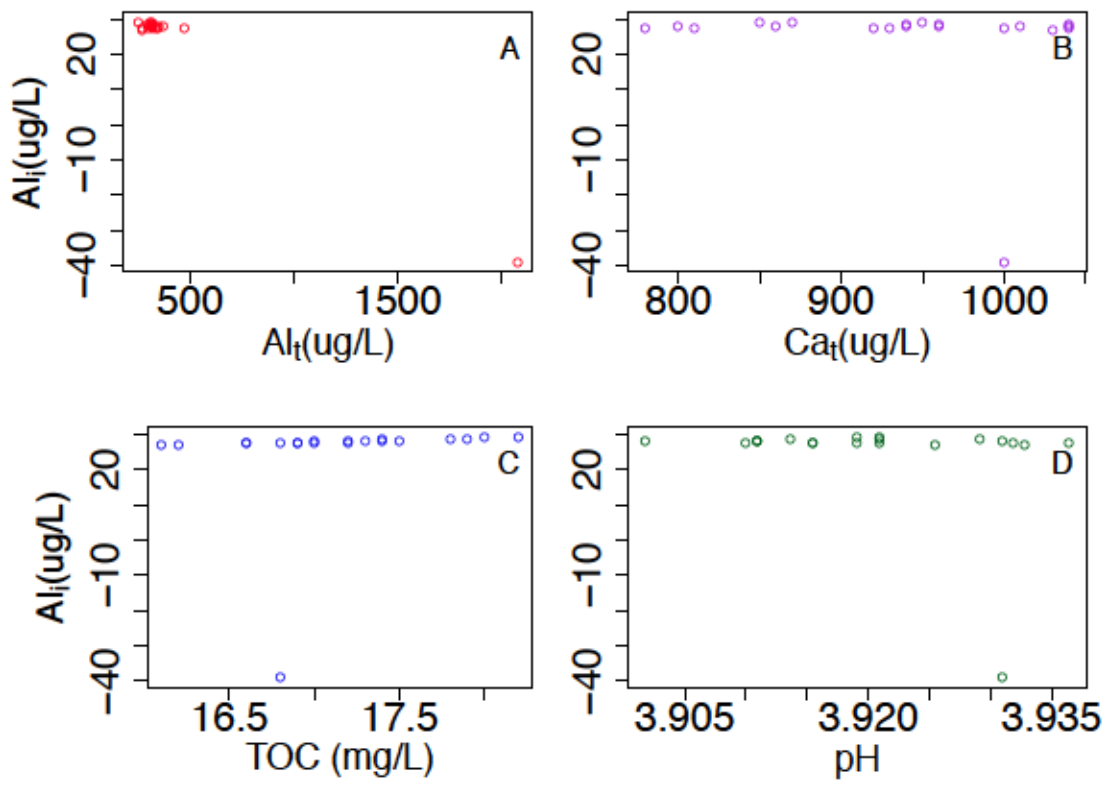

Figure H.1.3: Correlation of top twenty $Al_{i\text{-}c}$ with A) Al_t, B) Ca_t, C) TOC and D) pH for MRS3Alt1.

H.2 MPB Top 20 Extreme Correlations

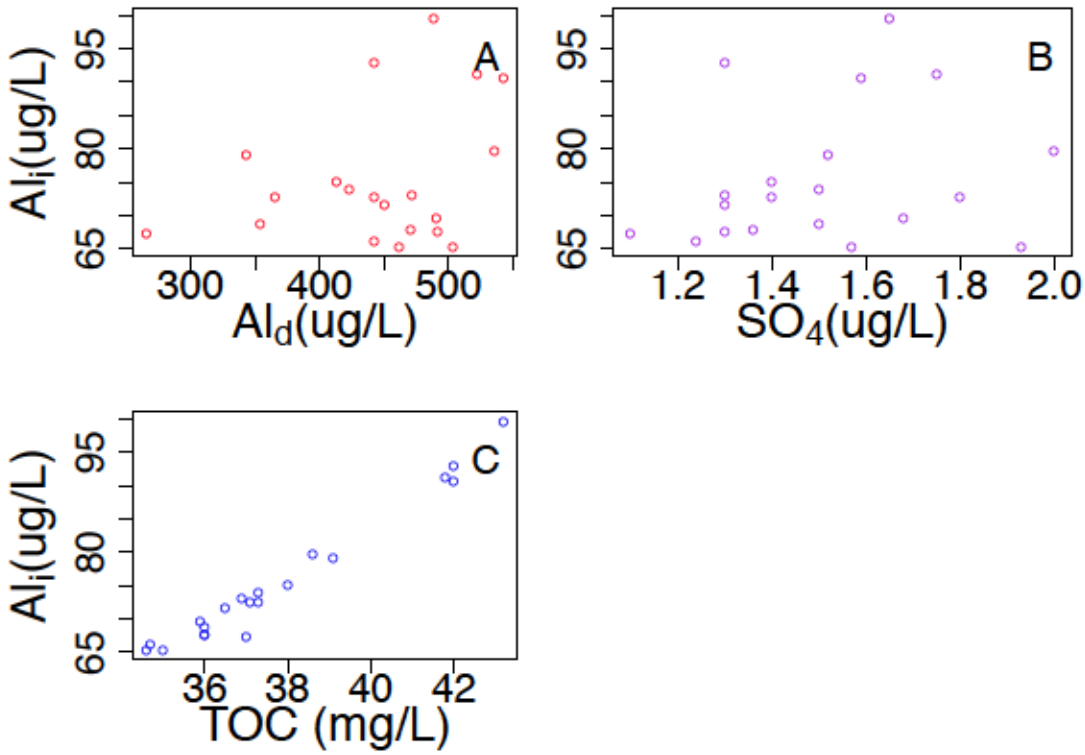

Figure H.2.1: Correlation of top twenty $Al_{i\text{-}c}$ with A) Al_d, B) SO_4, and C) TOC for MPBS1Ald1.

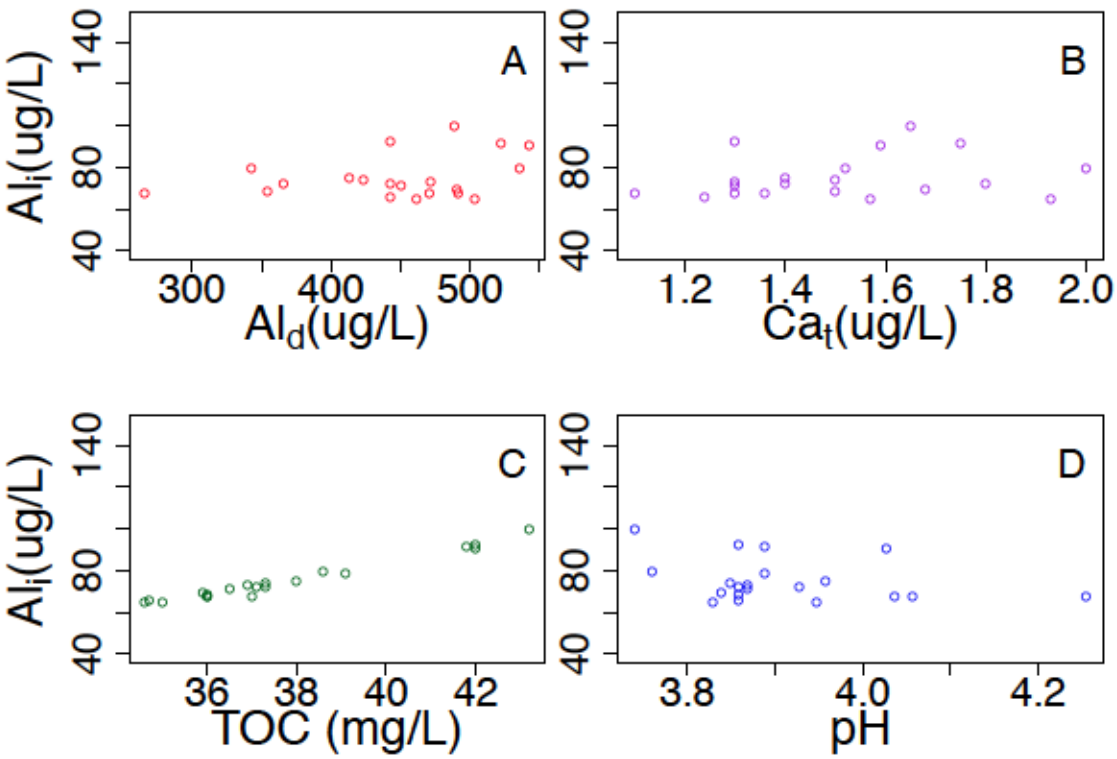

Figure H.2.2: Correlation of top twenty $Al_{i\text{-}c}$ with A) Al_d, B) Ca_t, C) TOC and D) pH for MPBS2Ald1.